# RESPONSE OF REINFORCED CONCRETE COLUMNS UNDER TEMPERATURE INDUCED TRANSIENT CREEP STRAIN

By

Saleh Mohammad Alogla

A DISSERTATION

Submitted to
Michigan State University
in partial fulfillment of the requirements
for the degree of

Civil Engineering—Doctor of Philosophy

2019

## ABSTRACT

RESPONSE OF REINFORCED CONCRETE COLUMNS UNDER TEMPERATURE INDUCED TRANSIENT CREEP STRAIN

By

Saleh Mohammad Alogla

Structural members experience significant creep deformations in later stages of fire exposure and are susceptible to failure due to temperature induced creep strains. Fire in a concrete structure can burn for several hours, and temperatures in concrete and reinforcing steel can exceed 500°C. At such temperatures, high levels of creep strains can develop in concrete and steel, especially in reinforced concrete columns. However, temperature induced creep strains are not fully accounted for in evaluating fire resistance of concrete members even through advanced analysis, and there is a lack of data on high-temperature creep strains for specific types of concrete.

To overcome current limitations, comprehensive experiments on evolution of transient creep strain are undertaken under various heating and loading regimes. Transient creep tests are conducted in the temperature range of 20°C to 750°C on four types of concrete; normal strength concrete, steel fiber reinforced concrete, high strength concrete, and high strength concrete with polypropylene fibers. The test variables include temperature, load level, rate of heating, strength of concrete and presence of fibers. Data from these tests indicate that transient creep strain constitutes a significant portion of the total strain developed during high-temperature exposure. Data also affirm that temperature range and stress level have significant influence on transient creep strain. However, rate of heating and presence of fibers have only a moderate influence on the extent of transient creep in concrete. Presence of steel fibers in normal strength concrete slightly reduce transient creep strain, while the presence of polypropylene fibers in high strength concrete leads to higher transient creep strain. Generated data from experiments is then utilized to

propose temperature and stress dependent creep strain relations for concrete. These transient creep strain relations can be implemented in fire resistance evaluation of concrete members.

To account for transient creep in undertaking fire resistance analysis of reinforced concrete (RC) columns, a three-dimensional finite element based numerical model is developed in ABAQUS. Temperature-induced creep strains in concrete and reinforcing steel are explicitly accounted for in this advanced analysis. The model also accounts for temperature induced degradation in concrete and reinforcing steel, and material and geometrical nonlinearities. The validity of the model is established by comparing fire response predictions generated from the model with measured response parameters in fire tests on RC columns. Results from the analysis clearly indicate that transient creep strain significantly influences the extent of deformations when the temperatures in concrete exceed 500°C for stress level of 40% or more, and this in turn influences fire resistance of RC columns.

The validated model is applied to assess the influence of transient creep on fire response of RC columns under different conditions, including different fire scenarios, load level, and number of exposed sides in a column. Results from the numerical studies clearly indicate that severe fire exposure induces higher creep strains in RC columns in much shorter duration than exposure to a standard building fire. Moreover, asymmetric thermal gradients resulting from two or three side fire exposure on a column, can increase transient creep effects and, thus, affect fire resistance. The extent of the developed transient creep in concrete columns under various scenarios of fire exposure is highly dependent on the type of concrete. Overall, results from the analysis infer that neglecting transient creep can lead to a lower prediction of deformations and, thus, overestimation of fire resistance in RC columns, particularly when subjected to severe fire exposure scenarios, with higher thermal gradients.

This Thesis is dedicated to Fatimah and Mohammad,
To my Parents and Siblings
To all Lives touched by fire

## ACKNOWLEDGMENTS

Thanks GOD (Alhamdulillah) for helping me through the hard times.

My sincere thanks are due in particular to my mentor during my Ph.D. study, Prof. Venkatesh Kodur for his valuable guidance and constant support in undertaking this Thesis. Special thanks are also due to the faculty members who served on my committee and helped me with their valuable advice. My sincere gratitude goes to Professors: Parviz Soroushian, Andre Benard, Roozbeh Dargazany and Weiyi Lu for joining my Ph.D. committee and helping me undertake the work presented in this Thesis.

I would like also to thank my wife, Fatimah, and my son, Mohammad, for their patience and support for me during my time at MSU. Appreciations are also due to my colleagues in the CEE department who shared their knowledge and experience with me during my Ph.D. research; including, Esam Aziz, Mohannad Nasser, Anuj Shakya, Amir Arablouei, Ankit Agrawal, Pratik Bhatt, Roya Solhmirzaei, Puneet Kumar, Srishti Banerji, and Svetha Venkatachari. My warm thanks are also due to the manager of the Civil Infrastructure Laboratory Mr. Siavosh Ravanbakhsh for his support, help, and friendship during the long and hard times in the laboratory. Special thanks are also due to the personnel in the Department of Civil and Environmental engineering particularly Laura Post, Laura Taylor, Margaret Conner and Baily Weber for their constant support for graduate students in the department. Thanks, are also due to my friends who were like a family for me during my time away from home (Saudi Arabia).

I wish also to acknowledge the support from Qassim University, Saudi Arabia, in the form of a Ph.D. fellowship to pursue my graduate studies at Michigan State University.

# TABLE OF CONTENTS

LIST OF TABLES

LIST OF FIGURES

# CHAPTER ONE

# 1. Introduction

## 1.1. Background

Fire represents a severe environmental condition when it occurs in a building and to mitigate its adverse effects on structural members, appropriate fire safety provisions are to be implemented in design and construction. The fire safety measures include active and passive fire protection systems with the aim of minimizing fire spread and its growth as well as enhancing fire resistance of structural members. Active fire protection systems are installed to control fire growth and include smoke detectors, sprinklers, and fire extinguishers and these get automatically activated once triggered by temperature rise or smoke. Passive fire protection systems, in contrast, relate to minimizing fire spread and its impact is achieved by protecting structural members as to withstand the temperature resulting in a fire. The ability of structural members to endure fire, however, is largely governed by the material performance which structural members are constructed of, namely: concrete, steel, timber, masonry, gypsum board, etc.

Concrete is widely used in building constructions due to its superior mechanical properties, including its high fire resistance, as compared to other materials. The high fire resistance properties of concrete are mainly due to its low thermal conductivity, high specific heat, and slower temperature-induced degradation in strength and elastic modulus. Due to these unique fire-resisting properties, structural members made of concrete possess the highest fire resistance (Kodur, 2014).

Recent fire incidents in concrete buildings, however, show that concrete structural members are prone to a certain level of damage under fire conditions, and in rare cases, partial or full collapse also resulted in these fire incidents. The failure of structural members occurs due to

loss of load carrying capacity and high levels of deflections (deformations). When sectional temperatures in concrete members reach above 500°C, much of these deformations result from effects of transient creep strain. Transient creep represents an additional strain in concrete which occurs during first time heating under constant load. With prolonged exposure to fire, temperatures in a concrete member increase to 600- 800°C range, which in turn induce high levels of transient creep strain in a concrete member. The effects of transient creep strain on the fire resistance of concrete structures have not been thoroughly examined in the literature, and a comprehensive understanding of this topic is critical to a realistic assessment of fire resistance of concrete structures.

## 1.2. Concrete under Elevated Temperatures

Concrete, as in the case of all construction materials, experiences deterioration when exposed to elevated temperatures. This deterioration is due to phase transformation mechanisms that occur in cement and aggregate at elevated temperatures, thermal incompatibility between aggregate and cement paste, and evaporation of different forms of moisture in concrete. These temperature-induced changes in microstructure cause deterioration in concrete properties leading to an adverse performance in the form of cracking, spalling, strength and stiffness degradation, that will produce loss of capacity and high level of deformations in a fire exposed concrete member. Therefore, degradation in properties of concrete is to be duly accounted for in evaluating fire performance of concrete structures.

Over the last few decades, significant research has been carried out to evaluate properties of concrete at elevated temperatures (Kodur, Dwaikat, and Dwaikat, 2008). Thermal, mechanical, and deformation properties of concrete at elevated temperatures, as well as various physical and

chemical changes occurring in concrete during exposure to high temperature, has been well studied (Georgali and Tsakiridis, 2005; Kodur, 2014; Lin, Lin, and Powers-Couche, 1996).

Thermal properties which determine temperature rise in a heated concrete member include thermal conductivity, specific heat, thermal diffusivity, and mass loss. For fire resistance analysis, thermal properties are needed to determine the temperature distribution in a concrete member. These thermal properties are variant with temperature.

Mechanical properties which influence the fire response of an RC member are compressive and tensile strength, modulus of elasticity, thermal expansion, and associated stress-strain response of both concrete and reinforcing steel. All these properties vary with temperature and also with type of concrete or steel. Mechanical response of concrete is best described by stress-strain curves of concrete at ambient or at elevated temperatures and to illustrate this, a set of stress-strain curves for different types of concrete is shown in Figure 1.1. In the figure, stress-strain curves of normal and high strength concretes are plotted for various temperatures. With incrementing temperature, strength degrades, however, higher softening of concrete results from rise in temperature with increased rupture strain.

In addition to thermal and mechanical properties, concrete members under certain fire exposure conditions experience spalling. This spalling results from pressure build up and restrained thermal dilatation (Kodur, 2014). Even though all concretes can experience spalling, concretes with high packing density such as high strength concrete (HSC) and ultra-high-performance concrete (UHPC) are more susceptible to spalling.

Further, concrete, under transient heating conditions experiences large level of temperature induced-deformations and this is primarily due to changes in microstructure and rapid loss of moisture. When temperature in concrete exceeds 500°C, these temperature-induced deformations

gets amplified by the effects of transient creep. Therefore, transient creep can constitute a significant portion of total strain in concrete and can govern the deformation levels in a fire exposed RC structural member (Colina and Sercombe, 2004; Khoury, Grainger, and Sullivan, 1985b). Therefore, the effect of transient creep has to be duly accounted in fire resistance evaluation of concrete members.

## 1.3. Temperature-Induced Creep in Concrete

Creep under ambient conditions (temperature) is a time-dependent deformation phenomenon that results in additional plastic deformation in a structural member which occurs under a sustained loading over a prolonged period. However, creep mechanics are different based on the material's microstructure and stress level in a member. For instance, creep in concrete has a different nature than that of metals or polymers. Creep of concrete at ambient temperature and humidity is defined as the additional time-dependent plastic strain which arises under a sustained load over a long period of service life (Bazant, 1975; 1995). At ambient conditions, creep in concrete originates near pores from the hydrated cement paste, which mainly consists of calcium silicate hydrates (C-S-H), through the process of hydration or solidification. This hydrated cement paste possesses four forms of water, namely: free "capillary" water, adsorbed water, interlayer water, and chemically bonded water. At ambient temperature, creep in concrete develops over a long period of time due to the slow process of cement hydration and loss of moisture, known as solidification of concrete (Bazant and Prasannan, 1989a; 1989b; Williamson, 1972). Although most of the creep deformation develops within the first year, concrete continues to creep for the rest of the service life of the structure. This creep is commonly referred to as classical, or basic creep. For a given stress level, the magnitude of creep in concrete varies depending on surrounding environmental conditions (i.e. humidity and temperature).

Creep strain, at high temperatures, however, develops at a much rapid rate depending on the stress level and temperature range. Such creep in concrete at high temperatures is typically classified as a steady-state creep or transient creep depending on the type of elevated temperature exposure. The creep that occurs under a steady-state of heating is classified accordingly as steady-state creep. On the other hand, creep strain that develops under a transient state of heating, such as under fire conditions, is classified as transient creep. This transient creep strain is also known as load-induced thermal strain or short-term creep.

Thus, creep at elevated temperatures is evaluated through two test methods. In the first test method, referred to as the steady-state approach, concrete is heated at a constant heating rate to a target temperature, and then the temperature is kept constant till steady-state is reached throughout the specimen. After reaching a steady-state, a specified load level is applied and maintained constant. The additive deformation, over thermal and mechanical deformations, resulting in the specimen is attributed to temperature induced creep in concrete. In the second method, referred to as the transient-state method, the concrete specimen is loaded to a pre-specified constant load, and then the temperature is raised at a constant rate to a target temperature. Additional deformation that results in concrete, over thermal and mechanical deformations, are taken as temperature-induced transient creep strain (Schneider, 1986).

Above 500°C, transient creep effects get amplified with the increase in temperature and stress level as shown in Figure 1.2 (Anderberg and Thelandersson, 1976; Schneider, 1986). At stress levels of less than 30%, concrete transient creep is insignificant until concrete above 500°C as in Figure 1.2. However, at stress levels of 50% and higher, transient creep strain can be a big part of the total strain of concrete at 400°C or above.

The mechanics of transient creep development are mainly related to moisture loss and its evaporation out of concrete. Moisture loss, in turn, is influenced by microstructural changes which take place in concrete under high-temperature exposure as listed in Table 1.1. These changes in microstructure occur in the main constituents of the concrete composite matrix; cement paste and aggregate. Further, thermal incompatibility between cement paste and aggregate also contribute to the evolution of transient creep in concrete when heated for first time. Under exposure to elevated temperatures, aggregate in concrete expand while the cement paste shrinks due to loss of moisture.

One of the first microstructural changes in concrete at elevated temperature is the decomposition of ettringite in the hydrated cement paste at around 80°C which has slight influence on transient creep in concrete. When temperatures in concrete exceed 100°C, a portion of free water in concrete starts to evaporate, and this phenomenon has little influence on transient creep. However, when temperatures in concrete reach about 300°C, adsorbed and interlayer C-S-H water and portion of the chemically bonded water from the C-S-H and sulfoaluminate hydrates start to evaporate (Mehta and Monteiro, 2006). Further increase in temperature of concrete to 500°C causes decomposition of calcium hydroxide and releases more moisture to evaporate. With this huge loss of moisture, pores (microstructure) within concrete collapse and the effect of transient creep strain becomes much more dominant at temperatures above 500°C leading to further deterioration of concrete (Anderberg and Thelandersson, 1976; Khoury, Grainger, and Sullivan, 1985a; Khoury et al., 1985b; Ulrich Schneider, 1986; Youssef and Moftah, 2007). When temperature reaches around 900°C, the C-S-H starts to completely decompose (Mehta and Monteiro, 2006).

Transient creep strain can form a significant portion of total strain in concrete at high temperatures and thus needs to be duly accounted for in fire resistance calculations in RC members.

A number of researchers proposed temperature dependent stress-strain relations for concrete considering the effect of transient creep strain (Anderberg and Thelandersson, 1976; Schneider, 1986; Li and Purkiss, 2005; Youssef and Moftah, 2007). These relations for total strain of concrete at high temperature contain an explicit term for transient creep strain which can be used separately to gauge the extent of creep in concrete. However, transient creep strain calculated from different creep models show considerable variation at different temperatures and stress levels. This variation is attributed to many factors including differences in concrete specimens and test conditions adopted in different experimental programs, data of which was used in developing creep models. There is no clear guidelines in the literature on the accuracy and reliability of transient creep models of concrete for use in fire resistance analysis (Kodur and Alogla, 2016). Therefore, comprehensive research for quantifying transient creep effects in different concrete types is needed.

## 1.4. Temperature-Induced Creep in Reinforcing Steel

Similar to concrete, reinforcing or prestressing steel present in concrete members can develop significant creep strains at elevated temperatures. Creep of steel at elevated temperatures is related to the movement of dislocations in the slip plane. At elevated temperatures, the vacancies in the crystalline structure start moving and cause dislocations to move faster to an adjacent slip plane, which increases the rate of creep dramatically (Kodur and Dwaikat, 2010). Typically creep in steel at ambient conditions is grouped under primary, secondary, and tertiary stages. In the primary stage, creep strain in steel increase at a gradual rate as compared to that in the secondary stage in which the rate of increase of creep strain is mostly constant. The tertiary stage is characterized by the exponential increase in creep strain due to necking of the steel coupon till failure through fracture. Progression of creep strain in steel is similar to concrete in which it

increases with stress level and temperature. At temperatures exceeding 600°C, creep strain in steel can be significant and can rapidly increase deformations in a structural member. The influence of high-temperature creep effects of steel reinforcement on deformation of RC structure is marginal since the area of reinforcing or prestressing steel is quite small as compared to the area of concrete in a cross-section. Furthermore, as reinforcing steel is embedded in concrete it takes a relatively long time to reach creep critical temperature.

## 1.5.Effect of Creep on Fire Resistance of Concrete Columns

Columns, as they are crucial from structural integrity consideration are required to sustain fire exposure for long duration. Fires in high-rise buildings can last for several hours before extinguished (Beitel and Iwankiw, 2005). Under such prolonged exposure to fire, temperatures within concrete can reach above 500°C resulting in the development of high levels of transient creep strain. Thus, transient creep strain needs to be properly accounted for in evaluating the response of concrete columns under fire conditions.

Fire resistance of concrete columns is currently mostly evaluated through prescriptive-based approaches as specified in ACI 216.1-14 (2014) or Eurocode 2 (2004). Current approaches for evaluating fire resistance do not fully account for transient creep effects. Further, stress-strain relations for concrete at elevated temperatures, as specified in ASCE manual (1992) and Eurocode 2 (2004), only account for partial transient creep strain. Thus, current calculation methods for evaluating fire resistance of concrete columns based on these stress-strain relations lack full extent of transient creep (Gernay and Franssen, 2012; Kodur and Alogla, 2016; Sadaoui and Khennane, 2009).

To illustrate the creep effects on the response of RC columns, data generated in a fire test can be used. Typical variation of sectional temperatures and axial deformations in the columns

with respect to fire exposure time is plotted in figures 1.3 and 1.4. With increase in fire exposure time, temperatures in concrete and reinforcing steel rise. As sectional temperatures increase, strength and elastic modulus of concrete and reinforcing steel decrease. Also, creep strains start to increase with temperature.

Variation of axial deformation with fire exposure time is plotted in Figure 1.4. In general, axial displacement response during fire exposure can be grouped under three main stages; expansion, steady-state, and creep. In the first stage, total deformation is mainly resulting from temperature-induced thermal expansion of constituent materials, concrete and steel, due to temperature rise. During this stage, concrete and reinforcing steel experience minimal material degradation due to lower sectional temperatures below 300°C in outer layers of concrete core and 400°C in rebars. Axial deformation gradually increases due to expansion of the column until it reaches to a point where expansion is fully developed.

In the second stage, thermal, mechanical, and transient creep strains contribute to axial deformation. This nearly steady-state response in this stage is attributed to counteracting of expansion effect from stiffness degradation in the column due to rise in sectional temperatures, as well as the development of effects of transient creep strain. In the third stage, axial displacement response is completely dominated by increasing transient creep strain and the high transient strains lead to transferring the deformation state from expansion to contraction. The contraction phase of the column continues until its failure. During this stage, cross-sectional temperatures (in concrete and rebar) in much of the section rises above 500°C and this produce high levels of creep strain, ultimately leading to “run-away” deformations and thus failure of the column.

To further illustrate the significant effect of transient creep strain on fire response of a concrete column, deformation in the above RC column is plotted to two cases, one with the

inclusion of creep effects, and the second without including the creep effects. These deformations were generated through Finite Element Analysis (FEA). The first case only included partial transient creep implicitly through Eurocode 2 stress-strain curves. In the second case, transient creep strain was accounted for explicitly. Both cases predictions of axial deformations are compared to measured axial displacement from fire test. The deformation response where transient creep is not explicitly accounted for follow measured deformation trend during test until failure of the column. At these stages, temperatures in most of the concrete section exceed 500°C and transient creep becomes dominant in axial displacement response.

The significant difference in axial deformation response between Case 1 and Case 2 is due to the role of transient creep strains. As can be seen, in Case 2, where transient creep strain is fully accounted for in analysis, predicted axial deformations match well with that measured during the test. Therefore, not accounting for transient creep in fire resistance analysis influences the predicted response and results in an unconservative estimation of failure time. The extent of transient creep developed during fire exposure is influenced by a number of factors such as temperature and stress levels, rates of heating, number of exposed faces, and concrete type. These factors are to be considered to determine the extent of transient creep strains in a fire exposed RC column.

## 1.6. Factors Influencing Transient Creep

The above-illustrated behavior of RC column is under standard fire exposure, certain levels of axial load and support conditions, and therefore represents an idealistic behavior. In practical situations, an RC column could encounter different fire scenarios, 1-, 2- or 3-side exposure, and different load levels. Further, the type of concrete used in columns can generate different levels of transient creep strain in concrete columns.

Exposure to severe fires, such as hydrocarbon fires, induce a rapid rate of heating and produce higher thermal gradients in concrete members. The extent of transient creep in a fire exposed concrete member mainly depends on cross-sectional temperatures in concrete and applied stress level on the member. Thus, type of fire exposure (i.e. low, moderate or severe intensity) influences the magnitude of transient creep deformations. Under moderate fire, such as standard fire, rate of heating and peak fire temperatures attained in a member are lower than what is experienced under severe fires, such as hydrocarbon or severe design fires. Thus, temperature range during fire exposure plays a key role in the development and extent of transient creep in concrete columns.

Stress level (i.e. ratio of applied load to the capacity of the column) applied on a column also influences the extent of transient creep effects in concrete columns. Transient creep at high temperatures is primarily a function of sectional temperature and stress levels as shown in Figure 1.2. At higher stress and temperature level, transient creep strain increases and constitutes a significant part of total strain in concrete. As applied load ratio to column capacity increases, the influence of transient creep in fire resistance analysis becomes more critical and needs to be considered. This is expected since transient creep magnitude increases with an increase in stress in concrete (See Figure 1.2). As stress increases, concrete is under more pressure to lose moisture with heat and pore gels are more susceptible to get crushed.

Furthermore, concrete columns are prone to exposure to fire from less than 4 faces depending on their location within a building. Exposure to fire on only 2, or 3 sides of the column could increase the effects of accounting for transient creep in fire resistance analysis. It is expected that under 2 and 3 side exposure the influence of transient creep will be higher due to differential temperature induced strains and stresses. These differential strain and stresses are resulting from

asymmetric thermal gradients instead of symmetric temperature distribution in the case of exposure from all four sides.

The extent of transient creep also depends on the type of concrete; normal strength (NSC), high strength (HSC), or fiber-reinforced concrete (Huismann, Weise, Meng, and Schneider, 2012; Khoury et al., 1985b; Tao, Liu, and Taerwe, 2013). These different concrete types possess different microstructure based on proportions of their mixed materials and aggregates. Concretes with high packing density such as high strength (HSC) and high-performance concretes (HPC) develop different magnitudes of transient creep than normal strength concrete (NSC). Further, under rapid rates of heating these high packing density concretes are prone to spalling at early stages of the fire before experiencing high levels of transient creep (Ali, O'Connor, and Abu-Tair, 2001; Dwaikat and Kodur, 2009; Kalifa, Menneteau, and Quenard, 2000; Ko, Ryu, and Noguchi, 2011). Transient creep, however, can be measured for high strength concrete with polypropylene fibers (HSC-PP) (Huismann et al., 2012; Wu et al., 2010). Addition of polypropylene fibers permit the escape of trapped vapor pressure inside concrete and minimize spalling (Han et al., 2005; Zeiml et al., 2006). Thus, accounting for transient creep can be more critical for columns cast with certain types of concrete than others.

## 1.7. Hypothesis

To overcome some of the current knowledge gaps with respect to transient creep in concrete, this study is developed based on the following hypothesis:

*"High-temperature transient creep can dominate the response of RC columns specifically when subjected to higher stress levels and severe fire exposure conditions, which in turn can govern the failure time in RC columns. Therefore, not accounting for transient creep in fire resistance analysis can lead to unconservative fire resistance predictions in RC columns."*

## 1.8. Objectives and Methodology

From the above discussion, it is evident that the current approaches of evaluating fire resistance of RC members, in general, do not take into account high-temperature (HT) transient creep. This is mainly due to the complexity associated with explicitly considering transient creep strain in fire resistance analysis. There are no standardized guidelines in the literature for accounting creep in fire resistance evaluation. Lack of experimental data and associated transient creep relations for modern types of concrete also hindering the incorporation of transient creep effects even in advanced fire resistance analysis of such concrete structures. Lack of such experimental data on transient creep strain is mainly due to the difficulty in isolating creep deformations at elevated temperatures. To overcome these limitations, the following are the key objectives addressed so as to improve understanding of high-temperature transient creep effect in fire exposed concrete structures;

- Carry out a state-of-the-art review on transient creep effects on fire response of concrete structures and identify knowledge gaps.
- Undertake high-temperature transient creep tests at material level to generate data pertaining to transient creep phenomenon in different types of concrete including normal strength concrete, fiber-reinforced concrete, and high strength concrete.
- Utilize data generated from high-temperature transient creep tests and develop empirical creep relations for different types of concrete.
- Develop a 3D finite element based numerical model to trace the response of RC columns subjected to fire, taking into account effects of high-temperature creep strain explicitly.
- Incorporate proposed creep relations into the numerical model to account for its influence in concrete columns under fire conditions.

- Validate the numerical model by comparing predictions from the developed finite element model to measured cross-sectional temperatures, axial displacement, and failure times in fire resistance tests on RC columns.
- Carry out parametric studies utilizing the validated model to quantify the influence of transient creep and associated factors on the response of RC columns under varying fire and loading conditions. Parameters include; fire severity, stress level, number of exposure sides, and type of concrete.

The above-stated objectives will be achieved by conducting creep experiments at the material level (concrete) and numerical studies at the structural level on RC columns. Data from the material level creep tests is utilized to quantify the extent of transient creep in concrete. Data from these transient creep experiments is then utilized to propose relations for uniaxial transient creep strain of NSC and HSC with and without fibers.

For numerical analysis, a numerical model is built in the general-purpose finite element program ABAQUS to trace the response of concrete columns under fire exposure through explicitly accounting for transient creep in fire resistance analysis. Transient creep proposed relations developed through creep experiments is incorporated into the numerical model to study the influence of creep effects on fire response of concrete columns.

The developed model is validated against published fire tests data available in the literature. Then this model is applied to study the influence of critical factors on the effect of transient creep on response of RC columns under fire conditions. Results from the parametric studies are then employed to highlight the effect of transient creep on RC columns and recommend guidelines to improve fire resistance analysis of RC column.

## 1.9.Layout

The research undertaken as part of this dissertation is presented in seven chapters. In Chapter 1, background information on the development of transient creep in concrete and its effect on fire performance of structural members is presented. In Chapter 2, a detailed state-of-the-art review relating to the treatment of transient creep in fire resistance design of reinforced concrete columns is presented and knowledge gaps relating to creep are identified. In Chapter 3, an experimental program designed to quantify and characterize transient creep in different types of concrete is laid out. Results from these tests are utilized to propose relations for transient creep strain of concrete and present a comparative transient creep strain of different concretes under different stress levels, temperature ranges, and rates of heating. In Chapter 4, a numerical element model to explicitly account for transient creep strains in tracing the response of concrete columns under fire conditions is developed. The validity of the numerical model is established in Chapter 4 by comparing fire response predicted from the model to that measured during fire tests performed on concrete columns. In Chapter 5, a set of parametric studies are performed utilizing the developed model to quantify the effect of transient creep on response of concrete columns under different conditions of fire exposure. These influencing conditions include stress level, fire scenario, and number of exposure sides. In Chapter 6, design guidelines for treatment of transient creep in fire resistance analysis and design is presented. Finally, conclusions and recommendations are summarized in Chapter 7.

Table 1.1 Changes in concrete's microstructure with rise in temperature

| Temperature, °C | Changes in Microstructure |
|---|---|
| 80 | Decomposition of ettringite |
| 100 | Evaporation of free "capillary" water out of concrete |
| 172 | Meltdown of polypropylene fibers (if added) |
| 300 | Loss of adsorbed, interlayer C-S-H water and chemically bounded water |
| 420 | Dissociation of $Ca(OH)_2$ into CaO and $H_2O$ |
| 500 | Progressive decomposition of C-S-H |
| 570 | Quartz phase transformation in some aggregate types |
| 650 | Decarburization of $CaCO_3$ into CaO and $CO_2$ |
| 700 | Decomposition of C-S-H into β-$C_2S$ (belite), βCS (wollastonite) and water |

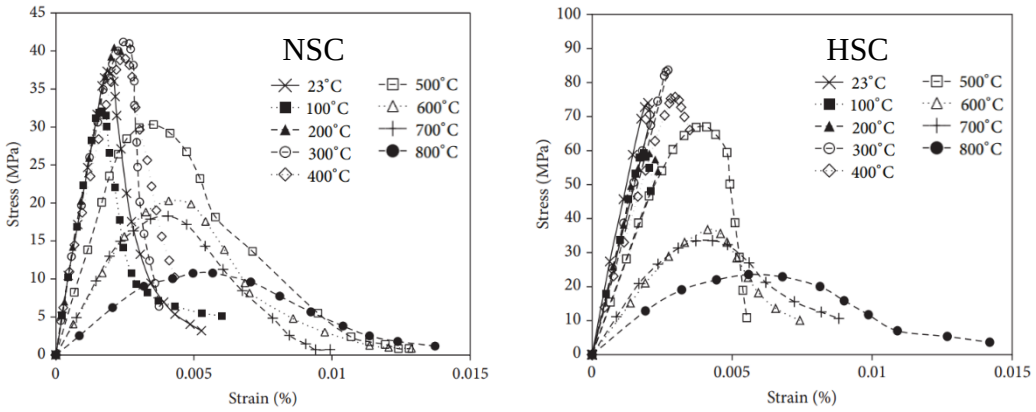


(a) HSC concrete (b) NSC concrete

Figure 1.1 Stress-strain of normal and high strength concretes at elevated temperatures (Kodur 2014)

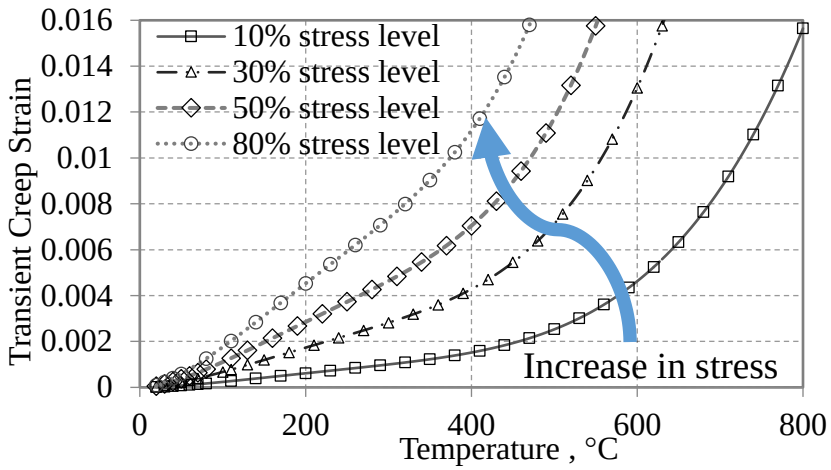


Figure 1.2 Effect of stress and temperature levels on transient creep strain of concrete

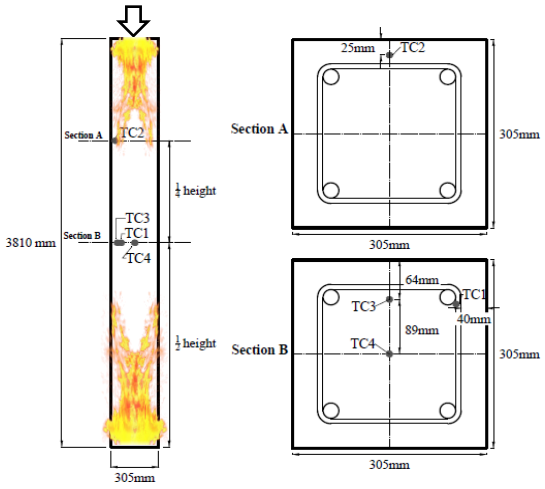


(a) Elevation and cross-sectional an RC column

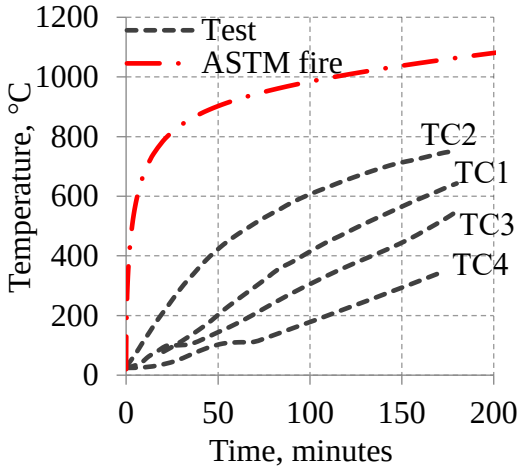


(b) Cross-sectional temperatures

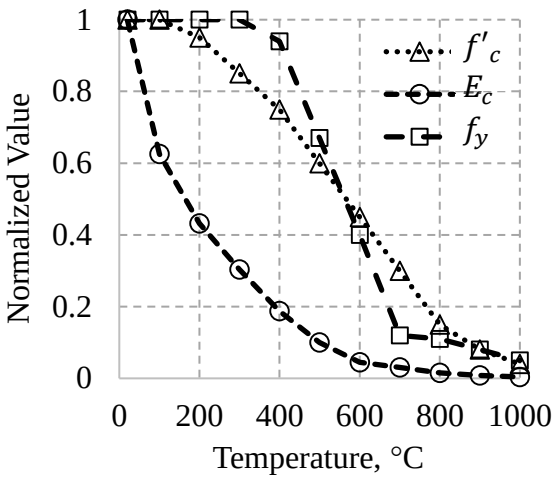


(b) Locations of thermocouples

Figure 1.3 Temperature evolution and material degradation of an RC column under fire exposure

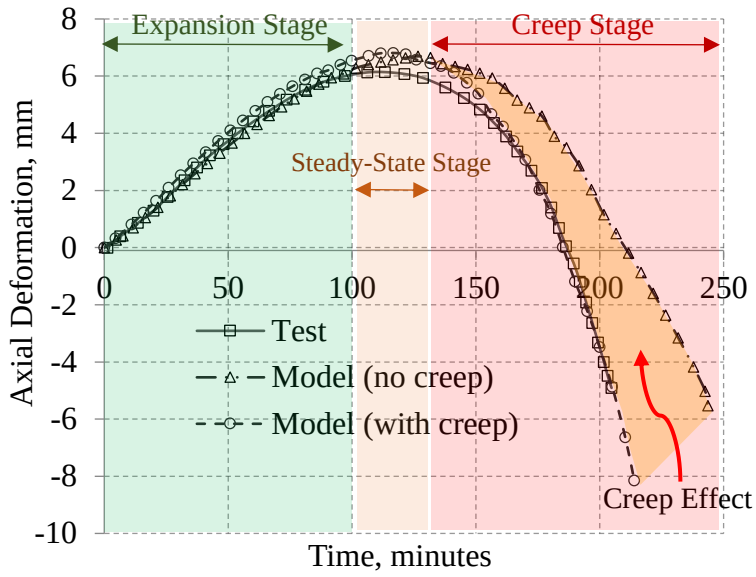


Figure 1.4 Illustration of axial displacement progression in a fire exposed concrete column with and without transient creep

# CHAPTER TWO

# 2. State-of-the-Art-Review

## 2.1. General

To mitigate adverse effects of fire exposure on concrete structures, a thorough understanding of the response of concrete members under fire is of essence. Over the past few decades, significant efforts have been made towards developing such an understanding of the behavior of concrete members under high-temperature exposure. However, previous studies on the fire resistance of RC structural members did not give due consideration to transient creep effects in concrete, which can dominate the deformation response at high temperatures (Gernay and Franssen, 2012; Kodur and Alogla, 2016; Sadaoui and Khennane, 2009; Schneider and Franssen, 2008). Currently, fire response of concrete members is evaluated through temperature dependent stress-strain relations. These relations only account for partial creep effects and therefore result in underestimation of deformations in concrete during fire (Kodur and Alogla, 2016). Further, neglecting full creep effects in fire resistance analysis can lead to overestimation of fire (Alogla and Kodur, 2018).

Most of the previous studies on creep effects focused on NSC only, without any consideration to different concrete types. Therefore, the existing relations for expressing transient creep in concrete are mostly for NSC, and limited relations are available for modern types of concretes. In reality, high-temperature creep is a function of microstructural changes and therefore can vary depending on the type of concrete mix.

To fully address the effect of transient creep in fire exposed concrete structures, developing creep properties of concrete at high temperatures is essential. In this chapter, reported studies on

thermal, mechanical, and deformation properties of concrete are reviewed. Then a detailed review on transient creep of concrete at high temperature is presented. Finally, a critical review on the behavior of RC columns, with a specific focus on the influence of transient creep, is provided.

## 2.2. Properties of Concrete at Elevated Temperatures

Concrete exhibit excellent thermal and mechanical properties at ambient and elevated temperatures; however concrete, like other materials, still experiences strength and stiffness degradation with rise in temperature (Kodur et al., 2008). Temperature-dependent properties which are essential for modeling the response of RC structures under fire conditions can be categorized as thermal, mechanical and deformation properties. Thermal properties of concrete are needed for determining the temperature distribution within a concrete member under fire exposure, while mechanical properties are required to evaluate the loss of strength and stiffness in a member with rise in temperature.

Deformation properties are also needed to evaluate the response of a concrete member. Significant levels of creep strain, grouped under deformation property, can develop in concrete at elevated temperature exposure, and this can alter the levels of deformations experienced in concrete structural members. These properties vary with temperature and also with the type of concrete (i.e. aggregate type, strength, and packing density of concrete). In addition to the above properties, spalling of concrete is another phenomenon that occurs in concrete members under fire conditions.

### 2.2.1. Thermal Properties of Concrete

When evaluating fire resistance of a structural member, it is important to accurately estimate the temperature distribution within the member. Temperatures progression within a concrete member is mainly dependent on key thermal properties: thermal conductivity, specific

heat, and density. Thermal properties of concrete at elevated temperatures are well documented for many types of concrete including NSC, HSC, and HPC (Kodur, 2014). Previous studies showed these thermal properties: thermal conductivity, specific heat, and density to be highly variable with temperature.

#### 2.2.1.1. Thermal Conductivity

Thermal conductivity is a measure of the degree at which a material conducts heat. It represents the flow of heat in a unit thickness of the material over a unit area when subjected to a temperature gradient between two sides of the material. The thermal conductivity of concrete (about 1.8 W/m.°C) is low as compared to other construction materials such as steel (which is 43 W/m.°C). For concrete, thermal conductivity can be measured based on either the "steady-state" or "transient" testing method (Bažant and Kaplan, 1996). However, the transient method is favored over the steady-state for measuring thermal conductivity due to the fact that the effect of variant heat flow within concrete can be captured (Shin et al., 2002).

The available data on thermal conductivity of concrete as a function of temperature is shown in Figure 2.1. Codes relations, as well as published data, were compiled to generate this figure (Kodur, 2014; Kodur et al., 2008). Thermal conductivity of concrete at room temperature ranges from 1.4 to 3.6 W/m.°C and decreases gradually with rise in temperature. The rate of decrease in thermal conductivity with rise in temperature is dependent on type of concrete and its mix properties. It can be seen in Figure 2.1 that the decrease in thermal conductivity with rise in temperature for normal and high strength concrete follows a nonlinear behavior. Considerable variation exists between the ASCE manual (carbonate aggregates) and Eurocode relations for thermal conductivity. Eurocode relation matches well with test data although some variation exists between predicted and measured data. The variation in reported test data is attributed to differences

in test methods, conditions, procedures, and measurement techniques. However, the range of compiled test data is bounded by the plotted tests upper and lower bounds in Figure 2.1. Also plotted in this Figure the upper and lower bounds specified as per Eurocode 2 for thermal conductivity of concrete with rise in temperature.

#### 2.2.1.2. Specific Heat

Specific heat represents the heat amount needed to raise the temperature of a unit mass of the material by one unit. Specific heat is often expressed in terms of heat (thermal) capacity which is the amount of heat required to raise the temperature of a unit volume of the material by one-unit temperature. The parameters influencing the specific heat of concrete are moisture content, aggregate type, and density. Specific heat of concrete takes into account both sensible heat and latent heat contributing to temperature change. Sensible heat is due to thermodynamic reactions with rise in temperature, whereas latent heat represents the absorbed or released heat during phases transition occurring in the material.

The available data on the specific heat of concrete as a function of temperature is shown in Figure 2.2. Specific heat for NSC and HSC is plotted along with generated data for specific heat from Eurocode and ASCE relations in Figure 2.2. The upper and lower bounds of reported tests in the literature are also plotted in this figure. Specific heat of concrete does not significantly vary with temperature. It is more influenced by the moisture changes and migration which occur in concrete with rise in temperature. These reactions start when free water evaporates at 100°C, followed by the dissociation of $Ca(OH)_2$ into CaO and $H_2O$ around 400-500°C. Finally, at temperatures around 600°C, the transformation of quartz in some aggregates affect specific heat of concrete. For carbonate or limestone aggregate concretes a peak in heat capacity is observed in temperatures between 600 - 800°C due to the endothermic reaction in the aggregate as shown in

Figure 2.2. This reaction results from decomposition of dolomite which absorbs a high amount of thermal energy. This peak in heat capacity helps in minimizing spalling and enhancing fire resistance (Kodur, 2014). Overall, concrete possesses excellent thermal properties as compared to other construction materials such as steel, and this help in enduring fire for prolonged durations.

#### 2.2.1.3. Mass Loss

The mass of concrete decreases with rise in temperature due to evaporation of moisture. The extent of mass loss is highly dependent on the type of aggregate used in the mix, siliceous or carbonate. Variation in mass of concrete with rise in temperature, compiled from previous studies, is plotted in Figure 2.3 for NSC for two types of aggregates: carbonate and siliceous.

Previous studies have shown that mass loss for both siliceous and carbonate aggregate concretes is minimal during first heating up to 600°C. Then an increase in mass loss occurs in concretes with carbonate aggregates due to the dissociation of dolomite at around 600°C (Kodur, 2014). Siliceous aggregate concrete undergoes a very minimal mass loss of less than 10% in 600-1000°C. Whereas carbonate aggregate concrete loses up to 30% of its mass in 600°C to 1000°C range.

### 2.2.2. Mechanical Properties of Concrete

A review of literature shows that significant efforts were directed towards studying the mechanical properties of concrete at elevated temperatures due to their crucial role in determining fire resistance of structural members. Therefore, high-temperature mechanical properties of concrete are well established in the literature. These properties mainly include compressive strength, elastic modulus, tensile strength, and compressive stress-strain curves of concrete at various temperatures (Kodur, 2014; Kodur et al., 2008). Typically, mechanical properties of concrete are measured through steady-state heating of a concrete specimen to a certain temperature

and then conducting strength test. The generated data for the temperature-dependent material property from such high-temperature tests can be then utilized to undertake fire resistance analysis numerically.

#### 2.2.2.1. Compressive Strength

The compressive strength of concrete is mainly affected by water-cement ratio, the transition zone between aggregate and cement paste, curing conditions, aggregate type and size, and admixtures (Mehta and Monteiro, 2006). In the early 1980s, the effect of pozzolans use in NSC to improve residual compressive strength at elevated temperatures for different water-cement ratios was studied (Carette, Painter, and Malhotra, 1982). The addition of fly ash and slag in NSC did not increase the residual compressive strength after exposure to elevated temperatures. The change in water-cement ratio in NSC also did not affect the residual compressive strength. In the 1990s, the effect of high temperature on compressive strength of NSC with and without steel fibers was first studied (Lie and Kodur, 1996). Compressive strength of steel fiber-reinforced concrete degrades faster with temperature than that of plain concrete.

Chan et al. (1999) studied the residual compressive of NSC and HSC concretes after high-temperature exposure. The study concluded that between 20-400°C only 10-15% of compressive strength is lost, and higher loss of compressive strength in concrete occurs between 400°C and 800°C. The significant loss in compressive strength in this temperature range is attributed to the decomposition of calcium silicate hydrate (C-S-H) gel and deterioration of cementing ability due to dehydration. When temperature exceeds 800°C, the residual strength is only a marginal percentage of strength at ambient conditions.

Lie et al. (2004) evaluated the residual mechanical properties of NSC and HSC experimentally at elevated temperatures. The influence of various parameters on mechanical

properties at elevated temperatures was studied in this study such as temperature, water content, specimen size, and strength. The study showed that compressive strength of HSC degrades even at temperature levels of 200°C, with loss of strength of up to 36% in the temperature range 200-400°C as compared to only 28% in NSC due to the dense and impermeable microstructure of HSC concrete. This study concluded that water content has a minimum effect on concrete compressive strength at elevated temperatures. Specimens with larger size experienced lower strength loss than smaller sized specimens.

Later in the early 2000s, researchers evaluated the mechanical properties of newer types of concrete such as HSC with polypropylene fibers and self-consolidating concrete (SCC) (Noumowe, 2005; Kosmas, 2007). SCC was found to show similar trends to NSC in terms of strength loss when exposed to elevated temperatures. However, SCC, similar to HSC, is prone to spalling when exposed to fire (at temperatures beyond 380°C) due to vapor build up in its impermeable microstructure.

Kim et. al. (2009) studied the variation in compressive strength of HSC with temperatures up to 700°C utilizing the stressed testing regime wherein specimens were subjected to 25% pre-load of the strength at room temperature during heating. Once target temperature is reached, the specimen is loaded to failure. It was concluded that with an increase in concrete strength, degradation in compressive strength at elevated temperature increases. In addition, the study showed that minimal strength was lost in HSC in temperatures between 100-400°C.

Khaliq and Kodur (2011a, b, 2012) studied the influence of temperature on mechanical properties (including compressive and residual strength) of high-strength concrete (HSC), self-consolidating concrete (SCC), and fly-ash concrete (FAC). The study showed that HSC, SCC and FAC experience higher degradation in compressive strength than NSC. For SCC, compressive

strength retention of up to 35% was reported at temperatures of 800°C. However, HSC and FAC experienced significant strength loss beyond 400°C of up to 70%. At a temperature of 800°C, HSC and FAC only retained about 15% of their strength at room temperature.

To summarize the influence of temperature on compressive strength of concrete, compiled test data combined with relations in Eurocode and ASCE for variation of compressive strength of NSC with temperature is plotted in Figure 2.4. Minimal degradation is experienced in compressive strength of NSC up to a temperature of 500°C. Then, compressive strength of NSC degrades rapidly after 500°C. The range of reported test data (shaded area in the figure) shows that concrete can lose up to 50% of its room temperature strength at temperatures around 600°C. At temperatures beyond 800°C, concrete loses most of its strength as shown by reported test data and Eurocode and ASCE relations.

Although HSC possesses superior compressive strength over NSC at room temperature, degradation in HSC compressive strength with temperature occurs at a faster rate than that in NSC. Degradation in compressive strength of HSC is plotted in Figure 2.5 for compiled test data and relations for different specified classes of HSC in Eurocode. Degradation in compressive strength of HSC is minimal up to 300°C. Beyond 400°C, reported test data and generated data from Eurocode relations show higher degradation in compressive strength of HSC. HSC loses more than 50% of its compressive strength by the time it attains 600°C and completely lose its strength at temperatures higher than 800°C.

#### 2.2.2.2. Tensile Strength

Tensile strength of concrete is measured in three ways: flexural tensile strength, direct tension strength, or splitting tensile strength. The test methods for evaluating tensile strength is as per standardized ASTM- C78 for the flexural tensile test, ASTM-C1583 for the direct tension test,

and ASTM-C496 for the splitting tensile test. At elevated temperatures, the same testing methods can be utilized to evaluate tensile strength of concrete.

A review of the literature shows that there is limited studies on the tensile strength of concrete at elevated temperatures, and most of the previous studies are conducted on cooled specimens after heating to a certain temperature (residual tests) (Khaliq and Kodur, 2011). Residual tensile strength, however, is not a good representation of tensile strength at hot state. Although tensile strength is often neglected in the design and analysis of concrete structures at ambient conditions, it is critical in controlling spalling in concrete members at elevated temperatures.

Carette et al. (1982) studied the influence of temperature on the residual tensile strength of NSC in 75-600°C temperature range after heating-cooling of the specimen. Based on splitting tensile strength tests, they reported that concrete loses up to 70% of its tensile strength at 600°C. The study concluded that water-cement ratio and aggregate type have the highest influence on residual tensile strength of NSC. Felicetti et al. (1996) studied the residual tensile strength of HSC in the temperature range 20-600°C utilizing the direct tension method. The study concluded that HSC concrete show similar behavior in residual tensile strength as that of NSC. Concrete softens significantly when exposed to elevated temperature which in turn greatly degrades its tensile strength.

Li et al. (2004) also studied residual tensile splitting strength of HSC (containing 27% fly ash) in the temperature range of 200-1000°C. The tested specimens were 100 mm cubes and retained about 50% of their splitting tensile strength at 800°C, and 16.9% at 1000°C. Chen and Liu (2004) studied residual splitting tensile strength of HSC with hybrid fiber reinforcement in the temperature range between 20-800°C. The study concluded that hybrid fiber reinforcement in HSC

(steel and polypropylene fibers) resulted in the retention of high tensile strength. Steel fibers mitigate cracks progression in concrete and confine expansion, while polypropylene fibers create micro-channels when melted which release trapped moisture vapor in concrete.

Khaliq and Kodur (2011) conducted a series of tensile strength tests on different concrete types including HSC, SCC, and fly-ash concrete (FAC). The tensile strength tests were carried out according to ASTM C496 (2004) specifications but at hot-state of the specimen. Thus, specimens were heated to target temperature then the test is conducted while the specimen is hot. The results showed that tensile strength of HSC and FAC degrades in similar trends as in NSC, with the lower degradation in FAC. SCC showed very low degradation in tensile strength at elevated temperatures as compared to HSC and FAC. When temperature in concrete exceed 400°C, HSC and FAC experienced significant degradation in splitting tensile strength due to development of severe microcracks in the concrete microstructure. However, SCC does not lose much of its tensile strength up to a temperature of 500°C (only 20% loss), then degradation starts to occur up to 800°C.

Overall, splitting tensile strength degrades with rise in temperature to below 20% of room temperature at 600°C strength. Figure 2.6. show compiled data on the tensile strength of concrete at elevated temperature from different codes of practice and previous studies (Kodur, 2014). The predicted tensile strength from codes relations and the range of reported test data (shaded area in the figure) clearly shows that tensile strength of NSC and HSC start degrading at very low temperatures (100-400°C). Beyond 500°C, tensile strength is marginal for both NSC and HSC as predicted by codes relations and reported test data.

#### 2.2.2.3. Elastic Modulus

The elastic modulus of concrete determines the stiffness of a concrete member at elevated temperature and can be evaluated utilizing the standardized method such as in ASTM -C469, after heating a concrete specimen to target temperature. Previous studies on the modulus of elasticity of concrete, $E_c$, showed that $E_c$ degrades with rise in temperature. At high-temperatures, disintegration in hydrated cement paste and breakage of chemical bonds in the cement paste microstructure reduces the elastic modulus. The extent of reduction in elastic modulus is dependent on moisture loss, high-temperature creep, and the type of aggregate present (Bažant and Kaplan, 1996). Disintegration of elastic modulus of concrete with rise in temperature is well established in the literature.

Castillo and Durrani (1990) conducted experiments to evaluate elastic modulus of NSC and HSC in the temperature range 20-800°C. The authors concluded that both NSC and HSC showed similar trends in elastic modulus variation with temperature with a minimum loss up to 400°C. Beyond 400°C concrete softens significantly until it losses most of its stiffness at temperatures between 600-800°C due to dehydration and bonds breakage. Bamonte and Gambarova (2010) tested HSC and SCC specimens (90 MPa strength) for elastic modulus at different temperatures ranging from 20-600°C. The study showed that the elastic modulus is much lower when concrete is tested at hot state than when elastic modulus is tested after cooling (residual test). In addition, they infer that HSC and SCC exhibit similar trends in elastic modulus deterioration with rise in temperature. Perrson (2004) conducted an extensive experimental study on residual elastic modulus of SCC at high temperatures ranging from 20-800°C and inferred that elastic modulus of SCC degrades faster than HSC with rise in temperature.

Reported test data for NSC and HSC, compiled by Kodur (2014) in Figure 2.7 along with EC2 relation for NSC show that degradation in elastic modulus with temperature is faster than that of compressive strength. The reported test data (shaded area in the figure) show that most of the degradation in elastic modulus occur beyond 400°C. At around 600°C, elastic modulus losses about 80% of its room temperature value for both NSC and HSC as can be seen in Figure 2.7 (Kodur, 2014). Beyond 600°C, concrete softens significantly, and elastic modulus is marginal as shown by reported test data. Proposed relations for both NSC and HSC assume a very low value for E beyond 600°C.

#### 2.2.2.4. Stress-Strain Response

At elevated temperature, the stress-strain response of concrete can be determined through two testing methods: steady-state, and transient. In the steady-state method, specimens are heated to target temperature, then loaded till failure. In contrast, the transient method includes simultaneous loading of the specimen and transient heating from room temperature to target temperature, then loading to failure. Most of the existing data on concrete stress-strain response were carried out according to the steady-state method. In the steady-state method, however, the specimen expands and losses most of its moisture under high-temperature exposure before being loaded to failure, thus, underestimating deformation, and is due to the fact transient creep effect is not being fully included. Under transient heating conditions, the deformation behavior of concrete is different from that under steady-state conditions in which transient creep strain form a significant portion of total strain in concrete. A review of existing studies on stress-strain response of concrete at elevated is presented in here and the effect of transient creep is discussed specifically in the next sections.

Castillo and Durrani (1990) evaluated the effect of transient heating on stress-strain response of both NSC and HSC under stressed and unstressed testing conditions in the temperature range between 20-800°C. It was found that temperature effect on stress-strain response of both NSC and HSC is similar. The values of strain at peak stress is very similar in the temperature range 100-200°C with a slight increase in temperature between 300-400°C. When temperatures exceed 500°C, however, strain at peak stress increases significantly with reduction in strength and elastic modulus. At 800°C, strain at peak stress was reported to be four times higher than that at room temperature.

Furumura et al. (1995) conducted compressive tests on cylindrical specimens to evaluate stress-strain response for both NSC and HSC, while the specimen is in hot state, and after heating. Data generated from this study showed that stress-strain behavior of HSC is quite different from NSC at elevated temperatures. For HSC, the behavior in stress-strain response is brittle up to 500°C, then the response in HSC becomes ductile beyond 500°C due to progression of temperature-induced internal microcracks and thermal incompatibility between cement paste and aggregate. Strain measured at peak stress during and after heating of the specimens increased significantly at temperature above 300-400°C. The study concluded that variation in HSC strength has a marginal influence on strain at peak stress value.

Felicetti et al. (1996) evaluated residual mechanical properties of heated HSC including stress-strain curves at elevated temperatures of 105, 250, 400, and 500°C. The strength of HSC was shown to decrease in the stress-strain response with increase in temperature. The strength decreased by 2.5% at 105°C, 25% at 250°C¸75% at 400°C, and 94% above 500°C. When temperatures exceed 500°C in concrete, residual strength was marginal or less than 10% in HSC.

Stress-strain response of concrete at elevated temperatures is similar to that at ambient conditions except that ultimate strength reduces and concrete become softer as temperatures rise. Due to reduced elastic modulus at elevated temperature there is increase in strain at a given stress level, as shown in Figure 2.8 for NSC. The descending branch of stress-strain response of concrete softens due to temperature induced plasticity and thus ultimate strain levels at failure increases. At temperature of 600$^{o}$C, for instance, ultimate strain can reach to more than double that experienced under ambient conditions. Both normal and high strength concrete exhibit similar response under compression but high strength concrete is more brittle with higher strength and lower undergone strains, as shown in Figure 2.9. As temperature increase, stress-strain response of HSC softens due to degradation in stiffness which results in higher strains at a given stress level. In HSC, the softening branch of the stress-strain response is hard to capture at low temperatures (100-300$^{o}$C) due to the brittle failure at peak stress which often results in breakdown of the specimen.

### 2.2.3. Temperature-Induced Spalling

Previous studies have shown that some concrete types are prone to spalling under certain fire exposure conditions. Higher strength concretes with dense microstructure and low permeability are more susceptible to spalling since these two properties prevent release of pore pressure resulting from trapped vapor in concrete microstructure. Once such accumulated vapor pressure exceeds the tensile strength of concrete, which also degrades with rise in temperature, spalling occurs. Previous studies on spalling of HSC showed that it is primarily influenced by concrete strength, permeability, density, moisture content, fire intensity, presence of fibers and dimensions of the specimens tested (Ali et al., 2001; Kalifa et al., 2000; Ko et al., 2011; Kodur and Mcgrath, 2003).

A review of the literature reveals that there are two major theories for the occurrence of spalling in concrete at elevated temperatures: i.e. pore pressure build-up, and brittle fracture. As per pore pressure theory, the permeability of concrete is the main controlling factor governing spalling. As concrete is heated, moisture starts to vaporize and accumulate within concrete leading to build-up of pore pressure. When this pore pressure exceeds tensile strength of concrete, concrete starts to disintegrate and chunks of concrete break away from structural members. This process can be explosive under some fire exposure scenarios (Kodur and Harmathy, 2002)

The second theory, brittle fracture, was proposed by Bazant (1997) in which the pore pressure induces thermal stresses that initiate cracking inside the heated surface. The flow of vapor pressure combined with moisture from adjacent concrete start filling the thermal stress induced cracks. When no additional water is flowing to fill up the crack, the pore pressure decreases while the crack widens until spalling occurs. In this theory vapor pressure initiates the crack but does not induce explosion or widen the crack, thus, spalling is assumed to be partially induced by thermal stresses. Furthermore, the theory is consistent with the results of heating treatment to minimize spalling in pre-dried concrete, and also agrees with high levels of pore pressure and spalling in wet concrete.

Although exact mechanisms for spalling are not well defined, spalling behavior in concrete structural members is well studied in the literature with a good number of experimental studies on both the material and the structural level. At the material level, limited researches were directed towards measuring pore pressure and investigating the effect of thermal stresses. Kalifa et al. (2001) measured vapor pressure in high-performance concrete (HPC) specimens (slabs of $30\times30\times12$ $cm^3$) with and without different dosages of polypropylene fibers (0 to 3 $kg/m^3$) when concrete is heated from one side at 5 °C/min up to 600°C. The study showed that vapor pressure

in HPC specimens reduces following the melting and evaporation of added polypropylene fibers even at lower dosages of PP fibers. Furthermore, the study concluded that addition of polypropylene fibers in concrete facilitate release of moisture from concrete and mitigate spalling in concrete under high-temperature exposure.

Hertz (2003) carried out tests to investigate the thermal stresses influence on fire-induced spalling in high-packing density concrete. The specimens were prisms of 600×600×20 mm and were heated in a selected area of 200×200 mm at the center of one side. The study showed that concrete types containing pozzolans such as silica fume are more prone to spalling when moisture content is less than 3%. This is mainly due to the dense microstructure of concrete when pozzolans are added to concrete to improve its durability and strength. Most of the reported spalling in this study occurred at temperatures around 374°C, at which most of the water in concrete was converted into vapor.

### 2.2.4. Deformation Properties of Concrete

Concrete undergoes temperature induced deformation when exposed to high temperature. These temperature-induced deformations, grouped under expansion and creep, influence the structural response of concrete members under fire conditions. The expansion and creep strain depend on many factors including strength of concrete, aggregate type, moisture content, and level of stress and temperature.

#### 2.2.4.1. Free Thermal Expansion in Concrete

Thermal strain is the increase (expansion) or decrease (shrinkage) of a unit length of a material when temperature is raised by one degree. The coefficient of thermal expansion represents the percentage change in length of the material per degree rise in temperature. A positive value of thermal strain is treated as expansion, while negative thermal strain is taken as shrinkage or

shortening of the specimen. The extent of thermal strain is highly affected by temperature level, water content, and aggregate type. Thermal strain of concrete and its variation with temperature have been well established in the literature for different types of concrete (Kodur, 2014).

Previous studies focused on studying thermal strain in different concretes including NSC, HSC, HPC, and other fiber-reinforced concrete types (Khaliq, 2012; Kodur, 2014). Figure 2.10 shows the variation in thermal strain of concrete with rise in temperature based on codes (ASCE, 1992; Eurocode 2, 2004) together with compiled data from experimental studies for NSC. The data presented in this figure is based on two types of aggregate; siliceous and carbonate and upper and lower bounds for test data are plotted in the figure accordingly. Thermal strain increases from zero at room temperature to around 1.3% at temperatures of 700°C and then remain almost constant up to 1000°C. The significant increase in thermal strain result from expansion of both aggregate and cement paste. However, the extent of free thermal expansion is also affected by moisture content, dehydration, shrinkage, and microcracking caused by temperature-induced thermal stresses (Kodur, 2014).

Previous studies have shown that strength of concrete and addition of fibers in concrete influence level of thermal expansion in concrete (Kodur, 2014; Kodur and Sultan, 2003; Lie and Kodur, 1996). Thermal strain in NSC increases in the range between 20°C to 600°C then the rate of increase in thermal strain reduces up to temperatures around 800°C due to loss of chemically bound water in the cement hydrates. However, the rate of thermal expansion increases after 800°C due to excessive softening of concrete and significant micro-cracking development (Fu et al., 2004). Other types of concrete including HSC and HPCs experience similar thermal strain trends as in NSC but with different extent of experienced thermal strain.

#### 2.2.4.2. Evolution of High-temperature Creep in Concrete

Creep phenomenon at room temperature in concrete was first reported by Hatt (1907) at Purdue University. Although creep has been studied since then, fundamental understanding on this phenomenon in concrete still far from clear. The first major advances in creep research started to flourish in the 1930s and 1940s due to the spread of long-span arches and the invention of prestressed concrete (Bažant and Jirásek, 2018). Design of long-span arches needed careful consideration of creep deformations, as was the case in prestressed concrete members where prestressing force losses in the strands are highly influenced by creep. In the 1950s, another impetus was handed over to creep research with the invention of double cantilever method for the segmental erection of long-span bridges constructed with prestressed concrete box girders (Bažant and Jirásek, 2018). This technique for construction prestressed box-girders required detailed analysis of creep deformations over both the construction time period and the span of service life. These aspects encouraged researches to evaluate creep properties in concrete and its implications on design and response of concrete structures.

High-temperature (HT) creep of concrete was often overlooked till the 1960s and 1970s when the spurt of research in behavior of nuclear reactor vessels constructed with prestressed concrete started. The extreme hazard imposed by nuclear power plants called for a comprehensive understanding of concrete behavior when in operating mode. Further, in the 1980s, research was expanded to study the response of concrete in these reactor vessels under hypothetical accidental breakdown in their cooling systems in which the temperature rise dramatically in concrete and transient creep dominate the response (Khoury et al., 1985a). Since then, HT creep has been of interest to concrete researchers from different disciplines.

With advancements in structural fire safety, few researches focused on studying the effect of high-temperature creep on fire response of concrete members. Creep at elevated temperatures are grouped under two types; steady-state creep and transient creep, depending on prevailing heating conditions. Figure 2.11 shows the two testing methods utilized to generate these two types of creep. Steady-state creep is analogous to basic creep at room temperature but measured at a selected high temperature for a certain duration (i.e. 100°C, 200°C, 300°C etc). This steady-state creep has time as the variant parameter, but the temperature is constant. Transient creep, at elevated temperature, occurs only at the first-time heating in which temperature is varying with time, although this is over minutes, rather than years as in the case of creep at room temperature.

#### 2.2.4.3. High-temperature Creep of Concrete

Creep is the additional time-dependent plastic deformation which arises in concrete under a sustained constant load over a prolonged period of time and its rate increases with rise in temperature. Creep phenomenon in concrete (cementitious materials) is different in nature from creep of other materials such as metals or polymers.

At ambient temperatures, creep strain in concrete develops over a long period of time due to the slow process of cement hydration and loss of moisture, known as solidification of concrete (Bazant and Prasannan, 1989a, 1989b; Williamson, 1972). Although much of the creep strain occurs within the first year, concrete continues to creep for the remaining years of service life of the structure. This creep is commonly referred to as classical, or basic creep. Typical variation of reported creep strain in concrete with time at ambient temperature is shown in Figure 2.12. With increase in time (years), concrete under loading experience creep strain at a rising rate at the beginning. Then the rate of creep in concrete reduces to a near plateau response in the development

of creep with time. Some portion of the creep strain is recoverable over time upon unloading but most of the developed creep is permanent (plastic).

Creep effects are to be incorporated in evaluating deformations in a member both under serviceability and safety limit states. Most common skeletal concrete structures are not highly affected by creep deformations, and thus, designers often neglect its effect at ambient temperature. Yet, creep in highly loaded structures can be a dominant factor in design and can lead to excessive deformations in concrete structures. Creep of concrete can cause as adverse of effects as differential column shortening over long-term in high-rise buildings. Creep also promote cracking of concrete which promotes ingress of moisture into concrete and results in corrosion of reinforcement. Overall, previous studies have shown that creep of concrete at ambient temperatures is important in certain applications depending on the conditions (stress level, time) of the structure (Bažant and Jirásek, 2018).

High-temperature (HT) creep occurs when concrete is subjected to combined effects of sustained loading and temperatures in the range of 20-800°C. Steady-state creep is the one that occurs under constant temperature level and stress over a time period (minutes). This is analogues to creep at ambient conditions in which the varying parameter is only time and the rest of influencing factors on creep remain constant (i.e. stress and high-temperature level). At elevated temperatures, creep originates near pores from the hydrated cement paste which mainly consists of calcium silicate hydrates (C-S-H). Hydrated cement paste contains four forms of moisture, namely: free “capillary” water, adsorbed water, interlayer water, and chemically bonded water. With rise in temperature, higher loss in moisture arises from disassociation of interlayer water and chemically bounded water, which in turn intensifies creep in concrete.

Previous studies have shown that high-temperature creep of concrete at steady-state heating (constant temperature) is much higher than basic creep experienced at ambient temperature (Bazant, Cusatis, and Cedolin, 2004; Gillen, 1981; Gross, 1975; Nasser and Lohtia, 1971; Nasser and Neville, 1965). As shown in Figure 2.13, steady-state creep strain at 500°C can be much higher than steady-state creep undergone under 100°C.

Nasser and Neville (1965) study was one of the first studies on high temperature creep on concrete. They concluded that creep behavior at elevated temperatures is an amplified version of the behavior at room temperature. The study showed that creep is mainly affected by stress level and reported a maximum in creep in the temperature range between 50 to 70°C. Later, Gross (1975) at Imperial College, UK, tested concrete for creep at various stress levels and temperatures up to 450°C utilizing the steady-state method. Data from this study showed that at temperatures of 450°C concrete experienced 10 times higher creep strain than what is measured at room temperature during a period of one week.

#### 2.2.4.4. Drawbacks and limitations

Creep strains obtained from the steady-state procedure (constant stress and temperature) are not representative of the concrete response under fire conditions. Under realistic fire exposure conditions, structural elements can experience variant temperature and stress levels depending on many factors, and thus, non-uniform distribution of temperature is always present within a concrete member. Thus, researchers like Malhotra (1982) suggested the use of transient testing method over short-duration to evaluate transient creep. This transient creep is more suitable to characterize creep under fire scenarios since concrete in structural members is subjected to combined effects of loading and temperature rise. In this method, all experienced deformations including transient

creep strain are accounted for (Anderberg and Thelandersson, 1976; Khoury et al., 1985a; Schneider, 1986; Terro, 1998).

## 2.3. Transient Creep of Concrete

### 2.3.1. Definition

Transient creep strain is defined as irrecoverable experienced strain under constant load (after loading) and gradual rise in temperature. Transient creep occurs at first-time heating of concrete due to loss of moisture and physio-chemical changes which take place within the cement paste with temperature rise (Colina and Sercombe, 2004; Huismann et al., 2012; Khoury et al., 1985b). This transient creep strain is also known as, transitional thermal strain or load-induced thermal strain, and was first reported properly by Johansen and Best, (JOHANSEN and BEST, 1962). In the last three decades, several researchers have studied creep effects under simultaneous loading and transient heating conditions (Anderberg and Thelandersson, 1976; Colina and Sercombe, 2004; Hassen and Colina, 2006; Huismann et al., 2012; Khoury et al., 1985a; Schneider, 1988; Thienel and Rostasy, 1996).

### 2.3.2. Transient Creep Experiments and Associated Models

As discussed earlier, transient creep strain of concrete form a significant portion of total strain at high temperatures and thus needs to be fully accounted for in fire resistance analysis. This led a number of researchers to undertake experiments on creep effects under transient heating conditions and propose temperature dependent stress-strain relations for concrete considering the effect of transient creep strain (Anderberg and Thelandersson, 1976; Kodur et al., 2008; Li and Purkiss, 2005; Schneider, 1986; Youssef and Moftah, 2007). Many of these relations are based on data generated on normal strength concrete and only limited data and relations are other types of concrete (Huismann et al., 2012; Kodur et al., 2008; Tao et al., 2013).

#### 2.3.2.1. Experiments and Associated Models by Anderberg and Thelandersson

Anderberg and Thelandersson (1976) performed a set of deformation property tests on concrete cylinders. These experiments studied a number of combinations of stress level and temperature range; heating to failure at constant stress, loading to failure at constant temperature, and creep at constant temperature. Based on the tests, they plotted uniaxial deformation of concrete under transient heating as a function of temperatures as shown in Figure 2.14. Under transient heating conditions, total strain of concrete varies with temperature and is highly dependent on the applied stress level. With increase in temperature and stress level, higher strain gets developed in concrete. Most of this total strain at elevated temperature is attributed to transient creep strain. Using data from tests, Anderberg and Thelandersson (1976) proposed a theoretical material model for the mechanical behavior of concrete under compression and transient heating.

In the proposed model, the total strain of concrete comprises four strain components namely; thermal, mechanical, creep, and transient strains. Creep strain in this model is based on steady-state tests and measured at constant stress and constant temperature. The classical steady-state creep strain ($\varepsilon_{cr}$) is expressed as a function of stress level, temperature, and time, and is given as:

$$\varepsilon_{cr}(\sigma, T, t) = -0.00053\left(\frac{\sigma}{f'_{cT}}\right)\left(\frac{t}{180}\right)^{0.5} e^{0.00304(T-20)} \quad \text{.....[2.1]}$$

where, $t$, represents time in minutes, $T$ is temperature in °C, $\sigma$ is stress, and $f'_{cT}$ is concrete strength at temperature, $T$. Creep strain can be calculated for a given stress level and temperature. For variant combinations of stress and temperatures with time, creep of concrete can be evaluated based on an accumulative approach using strain hardening principle. Assuming stress, $\sigma_i$ , temperature, $T_i$ , and accumulated creep strain, $\varepsilon_{cr,i}$ , are known at time $t_i$, then $\varepsilon_{cr,i+1}$, at time $t_{i+1}$ can be determined as shown in Figure 2.15.

The transient strain ($\varepsilon_{tr}$), which is more representative under fire exposure conditions, is evaluated as:

$$\varepsilon_{tr} = -k_{tr}\left(\frac{\sigma}{f'_c}\right)\cdot\varepsilon_{th} \qquad for\ T \le 550^oC \quad \text{[2.2]}$$

$$\frac{\partial\varepsilon_{tr}}{\partial T} = -0.0001\cdot\left(\frac{\sigma}{f'_c}\right) \qquad for\ T \ge 550^oC \quad \text{[2.3]}$$

where $k_{tr}$ is a dimensionless constant specified by Anderberg and Thelandersson (Anderberg and Thelandersson, 1976), $\varepsilon_{th}$ is thermal strain, and $f'_c$ is concrete strength at ambient temperature. The variation of transient strain with temperature and stress level based on this model is plotted in Figure 2.16. As the temperature and stress level increase, transient strain also increases.

#### 2.3.2.2. Transient Creep Experiments by Khoury et. al.

Khoury et al. (1985) conducted experiments on concrete and cement paste to quantify transient creep strain of concrete and characterize its behavior under heating and cooling. The test variables included four concrete mixtures which are selected to represent concrete used in nuclear reactor vessels. In these experiments, several factors were considered including age of concrete, 1 and 9 years, initial moisture condition, stress level, different rate of heating, and different aggregate-based concretes. The total strain under transient heating and loading were divided into free thermal strain, FTS, instantaneous stress-related strain, and load induced thermal strain, LITS.

The experimental program provided much needed data on transient creep of concrete during heating and cooling phases. This study showed that transient creep is irrelevant to age of concrete. However, the type of concretes used in these experiments are mostly NSC and not representative of current concrete types including fiber reinforced concretes and high strength concrete. The studied stress levels were 10, 20 and 30% which are considered low for typical concrete members in buildings and infrastructure. Two heating rates were considered to simulate the breakdown of

the cooling system of nuclear reactor vessels; 0.2 °C/min and 1 °C/min. These heating rates are also low compared to what is experienced under fire conditions.

#### 2.3.2.3. Transient Creep Experiments by Huismann et. al.

Huismann et. al. (2012) conducted an experimental study on transient strain of high strength concrete under heating up to 750°C and studied the impact of polypropylene fibers. In this study, the total strain of concrete under transient heating conditions is divided into two components only: free thermal strain and mechanical strain. Thus, transient strain is assumed to be included within mechanical strain in this case. The study concluded that polypropylene fibers enable easier moisture flow of free and physical bound water out of concrete when fibers melt. This faster moisture migration induces drying shrinkage which counteracts expansion in temperatures between 200°C-250°C. Thus, it is reported that HSC with PP fibers undergo higher transient creep than HSC without PP fibers.

#### 2.3.2.4. Transient Creep Experiments by Tao et. al.

Tao et. al. (2013) conducted a series of experiments to study the deformation properties of loaded high strength self-consolidating concrete, SCC, specimens under fire conditions for temperatures up to 700°C. SCC cylinders of 150 mm by 300mm were cast from three SCC mixtures of two strength grades C30 and C60. The specimens were demolded one day after casting and kept in a curing room with 90% relative humidity for 28 days then moved to ambient temperature for 90 days before testing. Different parameters affecting transient strain of SCC are studied such as temperature level, heating rate, stress level, strength of SCC, and content of PP fibers. These experiments concluded that temperature and stress level have significant influence on transient creep strain. As temperature and stress level increase, transient creep increases. No clear conclusions were drawn on the effect of heating rate on transient strain. Similar to previous

studies, these experiments showed that SCC with PP fibers exhibited higher transient strain than SCC without PP fibers.

#### 2.3.2.5. Experiments and Associated Models by Wu et. al.

Wu et. al. (2010) conducted an experimental study to examine high-temperature creep of HSC with polypropylene fibers (HSC-PP) under different combinations of stress and temperature. Among the selected combinations is transient heating under constant load in which transient creep strain was measured for HSC-PP up to temperatures of 700°C. The results showed that HSC-PP experience higher transient creep than conventional concrete specifically at high temperatures exceeding 500°C. This is mainly due to differences in physio-chemical reactions occurring at elevated temperatures in HSC and NSC. Further, the evaporation of polypropylene fibers promotes higher moisture loss and in turn increase experienced transient creep strain.

Based on the generated transient creep strain data for HSC-PP, Wu et. al (2010) proposed the following equation to estimate transient creep strain in HSC-PP:

$$\varepsilon_{tr} = \begin{cases} 1.2256\left(\frac{\sigma}{f_c}\right) \times \left[\left(\frac{T-20}{100}\right) \times \left(\frac{T}{100} + 0.4110\right)\right] \times 10^{-3} & 20℃ \leq T < 220℃ \\ \left(\frac{\sigma}{f_c}\right) \times \left[6.4 + 1.3366\left(\frac{T-220}{100}\right) \times \left(\frac{T}{100} - 1.1766\right)\right] \times 10^{-3} & T \geq 220℃ \end{cases} \quad [2.4]$$

where $\left(\frac{\sigma}{f_c}\right)$ represent the stress level (applied stress divided by strength of concrete) and $T$ is the temperature in Celsius.

#### 2.3.2.6. Transient Creep Model by Schneider

Schneider (1986), based on experimental data reported in literature, expressed total strain in concrete at high temperatures to be comprised of three components; thermal, mechanical, and transient creep strains. This transient creep strain ($\varepsilon_{cr} + \varepsilon_{tr}$) is expressed as a function of stress ($\sigma$), elastic modulus ($E$) temperature ($T$) and initial stress state ($f_{ci}$) in concrete before heating and is given as:

$$(\varepsilon_{cr} + \varepsilon_{tr}) = \frac{\Phi}{g} \cdot \frac{\sigma}{E} \quad \text{.....[2.5]}$$

where $\Phi$ is an empirical function to account for stress and temperature effects through the function $\varphi$, as follow:

$$\Phi(\sigma, T) = \begin{cases} g\varphi + \frac{\sigma}{f'_c} \cdot \frac{T-20}{100}, & \frac{\sigma}{f'_{cT}} \leq 0.3 \\ g\varphi + \frac{0.3(T-20)}{100}, & \frac{\sigma}{f'_{cT}} > 0.3 \end{cases} \quad \text{.....[2.6]}$$

$$\varphi = C_1 \cdot tanh[\gamma_\omega \cdot (T-20)] + C_2 \cdot tanh[\gamma_0 \cdot (T - T_g)] + C_3 \quad \text{.....[2.7]}$$

The function, $g$, accounts for the increase in initial tangent modulus due to pre-applied stress, $f_{ci}$, and is given as:

$$g(f_{ci}, T) = \begin{cases} 1 + \frac{f_{ci}}{f'_c} \cdot \frac{T-20}{100}, & \frac{f_{ci}}{f'_c} \leq 0.3 \\ 1 + \frac{0.3(T-20)}{100}, & \frac{f_{ci}}{f'_c} > 0.3 \end{cases} \quad \text{.....[2.8]}$$

and the symbols $\gamma_0$, $C_1$, $C_2$, and $C_3$ are constants defined by Schneider (1986) for different types of concrete and aggregate (1986). The symbol $\gamma_\omega$ represents a function which considers moisture content effect and is given as:

$$\gamma_\omega = (0.3\omega + 2.2) \times 10^{-3} \quad \text{.....[2.9]}$$

where $\omega$ represents moisture content in concrete. The variation of transient creep strain with temperature and stress based on the above model is plotted in Figure 2.16.

#### 2.3.2.7. Transient Creep Model by Diederich

Diererichs cited in (Li and Purkiss, 2005) proposed a model for total strain in concrete at high temperatures as the sum of mechanical, thermal, and transient creep strains. The transient creep strain ($\varepsilon_{cr}$ + $\varepsilon_{tr}$) is expressed as a function of stress level and temperature and is given as:

$$(\varepsilon_{cr} + \varepsilon_{tr}) = \frac{\sigma}{f'_c} \cdot f(T) \quad \text{.....[2.10]}$$

$$f(T) = 3.3 \times 10^{-10}(T-20)^3 - 1.72 \times 10^{-7}(T-20)^2 + 0.0412 \times 10^{-3}(T-20) \text{....[2.11]}$$

where *f(T)* is an empirical function proposed by fitting experimental results provided by Diederichs (Li and Purkiss, 2005; Youssef and Moftah, 2007). The prediction of Diederichs's model of transient creep strain at different temperatures is shown in Figure 2.16.

#### 2.3.2.8. Transient Creep Model by Terro

Terro (1998) expressed total strain in concrete as the sum of free thermal strain, (FTS), instantaneous stress-related strain and load induced thermal strain, (LITS), and this model was derived based on the experimental data generated by Khoury et al. (Khoury, Dias, and Sullivan, 1986; Khoury et al., 1985a). The model assumes that the mechanical strain is comprised of the elastic strain and therefore, separating FTS and mechanical strain from the total concrete strain gives LITS. This LITS includes creep and transient strains ($\varepsilon_{cr} + \varepsilon_{tr}$) and is given as:

$$LITS = (\varepsilon_{cr} + \varepsilon_{tr}) = \varepsilon_{0.3} \cdot \left(0.032 + 3.226 \frac{\sigma}{f'_c}\right) \quad \text{.....[2.12]}$$

where ($\sigma / f'_c$) should not be taken more than 0.3 $f'_c$. Terro's equation accounts for the effect of volume fraction of aggregates on transient creep strain (Youssef and Moftah, 2007). The term $\varepsilon_{0.3}$ in the equation represents the value of transient creep strain at a stress level of 0.3 $f'_c$ and is estimated through two sets of relations for two specific type of concretes, namely, carbonate and lightweight aggregate concrete (Eq. 2.13); and siliceous aggregate concrete (Eq. 2.14)

$$\varepsilon_{0.3} = -43.87 \times 10^{-6} + 2.73 \times 10^{-8} \cdot T + 6.35 \times 10^{-8} \cdot T^2 - 2.19 \times 10^{-10} \cdot T^3 + 2.77 \times 10^{-13} \cdot T^4 \quad \text{.....[2.13]}$$

$$\varepsilon_{0.3} = -1625.78 \times 10^{-6} + 58.03 \times 10^{-6} \cdot T - 0.6364 \times 10^{-6} \cdot T^2 - 3.6112 \times 10^{-9} \cdot T^3 - 9.2796 \times 10^{-12} \cdot T^4 + 8.806 \times 10^{-15} \cdot T^5 \text{.....[2.14]}$$

The transient creep strain in carbonate aggregate concrete, as obtained from Terro's model, is plotted for variant temperatures and stress levels in Figure 2.16. It should be noted that all these equations are based on concrete with aggregate volume fraction of 65%. For any other aggregate

volume fractions, $V_a$ , the following adjustments are to be made to evaluate transient creep strain (Terro, 1991)

$$(\varepsilon_{cr} + \varepsilon_{tr})_{V_a} = (\varepsilon_{cr} + \varepsilon_{tr})_{65\%} \cdot \frac{V_a}{0.65} \quad \text{.....[2.15]}$$

#### 2.3.2.9. Transient Creep Model by Nilsen et. al.

Nielsen et al. (2002) proposed a model for transient creep strain in concrete by modifying Anderberg and Thelandersson's (1976) transient strain relation. The model assumes that transient strain is linearly proportional to temperature instead of thermal strain, and is extended to cover the full temperature range from 20°C to 800°C (Nielsen et al., 2002; Youssef and Moftah, 2007) as:

$$\varepsilon_{tr} = 0.000038 \cdot \left(\frac{\sigma}{f'_c}\right) \cdot T \quad \text{.....[2.16]}$$

Although transient creep in this relation follows a linear trend, it is simplified in form and correlates well with experimental results for temperatures below 500°C (Youssef and Moftah, 2007). The transient strain predicted from this model increases with temperature and stress level as shown in Figure 2.16.

#### 2.3.2.10. Drawbacks and Limitations

As shown in Figure 2.16, the presented transient creep strain in concrete from different models show considerable variation at different temperatures and stress levels. This variation is attributed to many factors including differences in concrete specimens and test conditions adopted in different experimental programs, data of which was used in developing creep models. The differences in test specimens and conditions are due to the lack of a standardized testing method to conduct transient creep tests in ASTM and the limited recommendations in RILEM. Since Eurocode 2 stress-strain response at elevated temperature only considers partial creep effects, the use of such transient creep models in fire resistance analysis of concrete members can be critical.

However, there are no clear guidelines in the literature on the accuracy and reliability of concrete transient creep models to use in fire resistance analysis. Further, transient creep strain of concrete for specific types of concrete such as, high strength concrete and fiber-reinforced concrete is not well characterized and quantified.

## 2.4. High-Temperature Creep in Reinforcing Steel

### 2.4.1. General

Reinforcing and prestressing steel present in concrete members can develop significant creep strains at elevated temperatures. This creep in steel at elevated temperatures is mainly due to the movement of dislocations in the slip plane. At high temperatures, the vacancies in the crystalline structure start moving and cause dislocations to move faster to an adjacent slip plane, which increases the rate of creep dramatically (Kodur and Dwaikat, 2010). Typically creep in steel, under constant temperature and stress level, is grouped under primary, secondary, and tertiary stages as shown in Figure 2.17. In the primary stage, creep strain in steel increase at a gradual rate as compared to that in secondary stage in which the rate of creep increase is mostly constant. The tertiary stage is characterized by the exponential increase in creep due to necking of the steel coupon till failure by fracture. Creep progression in steel is similar to concrete in which it increases with stress level and temperature. Generally, for metals, creep strain reaches a critical level at temperature above 40% of the melting point (0.4 $T_m$). For steel, creep can be significant when temperatures exceed 500°C and can rapidly increase deformations in a structural member.

Since the area of reinforcing or prestressing steel is quite small as compared to area of concrete in a cross-section, the influence of high-temperature creep effects of steel reinforcement on the deformation response of RC structures is only marginal. Furthermore, as reinforcing steel is embedded in concrete it takes relatively longer times to reach creep critical temperatures and

develop high creep strain during fire exposure on reinforced concrete members. Due to these reasons, previous studies on HT creep in steel were mainly carried out to study the fire response of steel structural members since they are susceptible to high levels of creep at later stages of fire exposure. In this literature review, the reported studies on HT creep in steel is primarily based on tests conducted on steel coupons prepared from different grades used in structural steel members. The creep mechanisms of steel, however, are very similar in reinforcing steel and structural steel.

### 2.4.2. Previous studies

At room temperature, creep strain in steel is negligible especially for high-strength steels which typically are subjected to stresses well below their yield stress (Cheng et al., 2000). However, under high-temperature exposure, steel has been shown to undergo high levels of creep, which eventually leads to failure (Kodur and Aziz, 2015). The extent of this HT creep in steel depends mainly on material properties of steel, exposure temperature, stress level, and time of exposure. Similar to concrete, HT creep tests are typically conducted on steel coupons of certain grade according to two testing methods, steady-state and transient. Due to the complexity of conducting such HT creep tests, limited creep data for steel is available in the literature (Harmathy and Stanzak, 1970; Kodur and Aziz, 2015; Morovat et al., 2012). Most of these studies were conducted on structural steel and no notable studies were specific to reinforcing steel.

Harmathy and Stanzak (1970) conducted one of the early studies on high temperature creep of ASTM A36 structural steel and ASTM A421 steel for prestressing strands which are extensively used in built infrastructure. The creep tests were conducted to determine the creep parameters required to predict creep behavior for studied steel grades for temperatures up to 700°C. The study showed that tested steel grades undergo considerable creep strain at elevated temperatures. Further,

the model proposed by Harmathy (1967) was compared against generated creep data and was fairly aggregable for all three tested steel types.

Brinc et al., (2009) conducted a set of creep tests on stainless steel (AISI 316Ti) at various stress and temperature levels ranging from 400 to 700°C. Stress levels in this study ranged from 25% to 90% of the yield stress at room temperature. Results of this study indicated that AISI 316Ti steel can endure exposure to elevated temperatures when stress level is low. The study also showed that HT creep in steel is not significant at temperatures below 600°C when stress levels are not high. Later, Brinc et al., (2011) studied HT creep of another steel type, high strength low-alloy ASTM A618 steel. Creep testes for ASTM A618 steel were conducted at three selected target temperatures (400°C, 500°C, and 600°C) and various stress levels ranging from 33% to 77% of the yield stress at room temperature. Results of this study showed that HT creep is not critical at temperatures of 400°C and 500°C, when stress levels are lower than 50% and 40% of ambient yield stress, respectively.

Morovat et al., (2012) conducted tests to assess HT creep behavior in ASTM A992 grade structural steel. Test specimens were cut from web and flange plates of W4x13 and W30x99 wide-flange sections. The creep experiments were performed at temperatures ranging from 400°C-700°C and stress levels ranging from 50%-90% of the yield stress at room temperatures. Experimental creep data from this study for HT creep were compared to Harmathy's (1967) creep model. The study showed that ASTM A992 steel experience high levels of creep when exposed to elevated temperatures.

Kodur and Aziz (2014) experimentally studied HT creep deformation of high-strength low-alloy ASTM A572 steel in the temperature range between 400°C-800°C and under various stress levels. Specimens (coupons) were cut from ASTM A572 Gr. 50 steel sheets and tested in a custom-

built load-heating furnace equipment according to the steady-state method. Results from this study showed the HT creep to be primarily a function of stress level and temperature in which it becomes critical at stress levels above 50% and temperatures higher than 500°C.

### 2.4.3. Drawbacks and Limitations

The above review on HT creep in steel shows that very limited experiments have been conducted on creep of steel at elevated temperatures. Further, almost all of HT creep tests are conducted on structural steel and limited studies exist on reinforcing or prestressing steel. The carried out high-temperature creep tests on steel are also limited to specific stress levels and temperature ranges and many other combinations of stress and temperature are yet to be tested. Most of the available data on high-temperature creep of steel is based on exposure to a selected temperature and measurement of creep strains occurring at that selected temperature for a given stress level. High-temperature creep, thus, was not measured under transient heating conditions and simultaneous loading which relates more to the case of fire exposure on reinforced concrete members.

## 2.5. Behavior of RC Columns under Fire Exposure

Behavior of RC columns under fire conditions is well established and the influence of factors such as stress level, concrete type, restraint conditions, and constituent materials properties are well studied through fire tests and numerical models. Results from fire tests and numerical studies were also utilized in developing current codal provisions for fire resistance evaluation of RC columns. Codes of practice such as EC2 (2004) and ACI 216.1 (2014) provide prescriptive approaches and performance-based methods for fire design of RC columns, and determination of fire resistance. However, transient creep in provisions of fire resistance analysis in codes of practice still not fully accounted for.

Most of the experimental studies on behavior of RC columns were carried under standard fire conditions such as ASTM-E119 (2014). Thus, very limited experimental data is available in literature on deformation response of concrete columns under severe fire exposure. Further, lack of reliable creep models specific to high rates of heating, that represent severe fires, limited studies on the effect of transient creep strain under severe fires. In the following sections, several experimental and numerical studies conducted on behavior of RC columns under fire are discussed. Moreover, numerical studies targeting the effect of transient creep on RC columns under fire are summarized.

### 2.5.1. Fire Resistance Tests on RC Columns

Fire resistance of RC columns was mostly evaluated in the past through fire tests under standard fire conditions. A number of test programs were carried out to study the performance of RC column under fire in the past three decades (Aldea, Franssen, and Dotreppe, 1997; Ali et al., 2001; Ali et al., 2004; Benmarce and Guenfoud, 2015; Franssen and Dotreppe, 2003; Kodur et al., 2001; Kodur et al., 2003; Kodur and Mcgrath, 2003; Lie et al., 1984). These tests were conducted to generate fire resistance data for columns of specific characteristics. Moreover, the generated data from fire tests is implemented for verification of computer models for fire resistance analysis of RC columns. These tests were also intended to investigate the influence of different parameters on fire resistance of RC columns. In the following presented summaries of fire tests in the literature, the relevance of the study to axial displacement and transient creep will be highlighted.

Lie and Woolerton (1988) conducted fire tests on 41 RC columns under standard fire exposure to study the effect of different parameters including shape of cross-section, cover thickness, reinforcement, aggregate type, load level, and eccentricity. They concluded that carbonaceous aggregate enhances the fire resistance of RC columns and that heavy reinforced

columns attained higher fire resistance. The reported axial displacement response from these fire tests showed that at later stages of the response columns contract significantly before failure.

Franssen and Dotreppe (2003) tested four circular RC column to examine the influence of circular cross sections on the fire response of RC columns. They concluded based on the fire test observation and analyses of test data that the circular shape doesn't affect the occurrence of spalling, the diameter size of longitudinal reinforcement showed no significant effect on surface spalling, and that increased load level lead to reduced fire resistance. The axial displacement and deformation in these circular columns during fire exposure was not reported since the objective was to investigate the effect of circular column shape on spalling occurrence.

Kodur et. al. (2001) carried out a comprehensive experimental study on a large number of RC columns to develop fire resistance guidelines for HSC columns. Several variables were considered in the experimental program including column dimensions, concrete strength, aggregate type, tie configuration, fiber reinforcement, fire scenarios, load intensity and eccentricity of loading. The study quantified the influence of many factors on fire resistance and developed guidelines some of which have been incorporated in ACI 216.1 (2014) for improving fire performance of HSC columns. The main findings of this study included that columns with concrete strength of 70 MPa and higher are more susceptible to spalling. Further, higher moisture content and packing density in concrete increase the chance of spalling occurrence. Another finding is that larger cross-section columns are more prone to explosive spalling. And, columns with carbonate aggregate-based concrete had higher fire resistance and better spalling resistance than columns constructed from siliceous aggregate based concrete. The reported axial displacement showed that HSC columns undergo lower deformation under fire exposure than NSC columns. This implicitly

indicates that the effect of transient creep can be lower in HSC columns, and that concrete with high strength may experience lower transient creep than NSC.

Benmarce and Guenfoud (2015) studied fire behavior of HSC columns through carrying out fire tests on 12 HSC columns. These fire tests examined different parameters influence on fire resistance of HSC columns including load level, restraint ratio, and heating rate. It was concluded from these tests that increase in load level reduce failure time of HSC columns. Further, imposing a restraint on the axial expansion of HSC column, reduced forces generated in the column, and consequently, reduced failure time. Another finding was that maximum axial displacement during fire exposure is independent of the rate of heating and more influenced by load level. However, the rate at which axial displacement occurred is highly affected by the rate of heating. Failure time of the tested columns under low heating rate is nearly twice as failure time under high heating rate for similar conditions of restraint and load level. This study although was not intended to shed some lights on transient creep showed evidence that transient creep is affected by the rate of heating. The progression of axial displacement and contraction rate towards failure of the column was higher with high rates of heating.

Previous experimental studies on fire response of concrete columns have investigated the effect of various parameters on fire performance of RC columns including, column size and shape, type of concrete, load intensity, tie configuration, presence of fibers, and strength of concrete etc. Fire resistance tests also showed that columns fabricated with NSC possess higher fire resistance than HSC columns, and undergo higher axial displacement (Kodur and McGrath, 2003; Raut and Kodur, 2011). Fire intensity and the rate of heating also affects fire resistance of RC columns and control the extent of undergone deformations.

The studies which reported axial displacement measurement showed that a rapid contraction in axial displacement occurs just prior to failure. Transient creep strain is the main cause of this contraction in axial displacement towards failure. To illustrate this, Figure 2.18 shows the response in axial displacement of an RC column under fire exposure together with cross-sectional temperatures and developed transient creep in concrete. As shown in Figure 2.18 - (a), temperatures in the column increase with time under fire exposure. As temperatures increase in the column, the extent of developed transient creep increase dramatically (Figure 2.18 – (b)). When temperatures in the column core exceed 500°C, a rapid contraction occur in the axial displacement due to transient creep (Figure 2.18 - (c)). The transient creep in this figure is under 50% stress level, however, as applied load increases relative to capacity, the extent of experienced deformations increases.

### 2.5.2. Numerical Studies with and without Transient Creep Effects

Number of numerical and analytical studies have been performed on fire resistance analysis of RC columns. However, very limited numerical studies are available on the effect of transient creep strain on response of RC columns under fire conditions. Many of the early numerical models were limited to sectional analysis in which the mid-height is generalized for the whole column, and are purely based on codes stress-strain relations (Lie, 1993; Lie and Celikkol, 1991). These stress-strain relations implicitly account for partial transient creep.

Franssen et al. (1990) created a computer program, SAFIR, which can be utilized to analyze and simulate deformation response of RC columns. SAFIR program (2017) then has been utilized by many researchers to understand RC columns response. Gernay and Franssen (2012) later utilized SAFIR to account for transient creep in analysis of RC columns through modifying the Eurocode concrete material model. The study had two objectives. First, to show the capabilities

and limitations of concrete high-temperature uniaxial constitutive laws for modeling the thermo-mechanical response of concrete members under fire. Second, to propose a new formulation for concrete strain at elevated temperatures that accounts for transient strain explicitly. In the study, strain of concrete at high temperature was compared based on both the implicit and explicit models. Figure 2.19 shows strain components of concrete based on implicit and explicit consideration of transient creep. As part of the study, the explicit formulation was applied to study columns response utilizing SAFIR. The results showed that transient creep is underestimated in Eurocode stress-strain relations, and that Eurocode stress-strain relations are not accurate when used for tracing the response of RC columns under natural fire exposure (i.e. fire with cooling phase). The results showed that implicit models miscapture the actual unloading stiffness properly, while, the proposed explicit formulation of transient creep in constitutive models provided a supplementary accuracy in modelling the response of concrete columns. They recommended utilizing the explicit model during the cooling phase of the fire since it can capture the irreversibility of transient creep strain. Finally, the study concluded that transient creep highly affects the response at later stages of fire exposure in RC columns.

Bratina et al. (2005) developed a two-step finite element formulation for thermo-mechanical non-linear analysis of RC columns response under fire. The purpose of the study was to discuss numerical modeling of RC columns in fire based on their model as compared to Eurocode 2 procedure of evaluating columns fire resistance. A new strain-based formulation was assumed in the model which accounts for transient creep explicitly. Results from the numerical model were compared to measurements from full-scale tests on concrete columns. The results of this method showed that Eurocode 2 stress-strain relations (implicitly considers transient creep) might be non-conservative in estimating fire resistance of RC columns.

Sadaoui and Khennane (2009) studied the effect of transient creep on response of concrete columns. A numerical model was developed that considers transient creep explicitly in fire resistance analysis of concrete columns. The study compared implicit and explicit results from the model on response of concrete columns under fire. It was found that transient creep induces an additional compressive stress on the column which in turn magnifies bending moment and contributes to governing failure.

The above brief review shows that effects of transient creep strain on RC columns under different fire scenarios and number of exposure sides has not been well established. In fact, few numerical studies are focused on accounting for transient creep strain explicitly in fire resistance analysis of RC columns but under standard fire conditions (Alogla and Kodur, 2018; Gernay and Franssen, 2012; Gernay and Franssen, 2011; Kodur and Alogla, 2016; Sadaoui and Khennane, 2009). These studies have shown that accounting for transient creep explicitly in fire resistance analysis results in more precise response of RC column and accurate conservative fire resistance times. Previous research has also inferred that transient creep has only marginal effect on fire resistance of RC beams (Gao et al., 2013; Sadaoui and Khennane, 2012), and that it does not alter the predicted response significantly as in columns since columns are under compressive state of loading. Another case where transient creep can have dominant influence on fire resistance is in post-tensioned concrete slabs where creep effects can reduce tendon stresses and deflections (Wei et al., 2016).

### 2.5.3. Limitations and Drawbacks

Fire tests on RC columns were conducted to generate fire resistance data which can be implemented for verification of computer models for fire resistance analysis of RC columns. Fire tests were also intended to investigate the influence of different parameters on fire resistance of

RC columns. However, transient creep is rarely examined in fire tests of RC columns. Transient creep influences the response of RC columns at later stages of fire exposure when cross-section temperatures are at their peak. The previously conducted fire tests implicitly showed evidence, in reported axial displacements, that transient creep governs the response. RC columns at later stages of fire, just before failure, experience rapid contraction in axial displacement caused mainly by transient creep. However, transient creep is often ignored in explaining this contraction of RC columns before failure, and this contraction is completely attributed to degradation in constituent materials strength and stiffness.

The previous numerical studies on effect of transient creep strain on RC columns under fire utilized different theoretical creep relations, which resulted in variation in the quantification of HT transient creep, and, consequently the predicted deformation response (Bratina et al., 2005; Huang and Burgess, 2012; Sadaoui and Khennane, 2009). Nevertheless, most studies inferred that not accounting for transient creep strains in RC columns can lead to underestimation of deformations at the later stages of fire exposure, and un-conservative fire resistance predictions that can reach to half an hour in some cases (Gernay, 2011; Huang and Burgess, 2012; Kodur and Alogla, 2016; Sadaoui and Khennane, 2009). However, the magnitude of transient creep impact on RC columns is still not well established. Influence of exposure to different fire scenarios on the extent of transient creep strain has not been discussed in the literature. Further, no studies available on the effects of number of exposure sides and biaxial bending resulting from eccentricity and thermal gradients and how that manifest transient creep influence in RC columns.

## 2.6. Codal Provisions for High-Temperature Creep

Building codes and national standards such as ACI 216.1 and Eurocode 2 provide users with specifications for evaluating fire resistance of concrete structural members. In the United

States, prescriptive-based design is provided for fire resistance of RC columns in ACI 216.1 (2014) standard which is solely dependent on concrete cover thickness and minimum column dimensions required for achieving a selected fire resistance. In Europe, Eurocode 2, Part 1-2 (2004), provides simplified empirical equations for calculating fire resistance of RC columns based on minimum dimensions, cover thickness, stress level, and reinforcement ratio.

Transient creep strain is accounted for partially and implicitly in stress-strain relations of ASCE (1992), structural fire protection manual and Eurocode 2, Part 1-2, (2004), structural fire design of concrete structures. In fact, Eurocode 2 (2004) specifically states that "creep effects are not explicitly considered" in the stress-strain relations of concrete, and recommends to explicitly account for it in carrying out advanced fire resistance analysis of RC structures. Only implicit consideration of transient creep underestimates deformations in concrete at elevated temperatures. ACI 216.1 (2014) and other codes do not specifically account for transient creep strain in evaluating fire resistance of concrete members.

It has been shown in previous studies that in advanced fire resistance calculations to assess fire resistance of RC columns, utilizing implicit consideration of transient creep in codal stress-strain relations can result in lower estimated deformations and unconservative failure times (Alogla and Kodur, 2018; Gernay and Franssen, 2011; Kodur and Alogla, 2016; Sadaoui and Khennane, 2009). When RC columns are exposed to transient heating state, such as fire, special consideration should be directed to transient creep particularly at temperatures exceeding 500°C.

## 2.7. Knowledge Gaps

The state-of-the-art review presented in this chapter clearly indicates that there is a lack of reliable information and material models for high-temperature transient creep effects. The creep effects can dominate the response of RC members, specifically at later stages of fire. There is large

variability in the existing relations for transient creep strain of concrete, and this is due to test data derived from different test procedures and test conditions. Moreover, the effect of transient creep strain on RC columns is not well established. Most of fire resistance analyses on the response of RC columns in the literature are performed without specifically accounting for transient creep strain, which is shown recently to be a critical factor in determining failure of an RC column. The following are the key gaps in the literature with regards to transient creep effects in concrete at elevated temperatures:

- There is a lack of experimental data and associated transient creep strain models for newer concrete types, including HSC and fiber reinforced concrete.
- Limited data is available on the effect of key factors, such as high-stress levels and different heating rates, on the magnitude of transient creep strain.
- Transient creep is not fully accounted in current fire resistance analysis approaches on RC columns.
- Transient creep strain influence on RC column under fire exposure is not well established for different conditions of stress level, varying fire scenarios, heating rate and uneven fire exposure from 1-, 2-, or 3 faces.

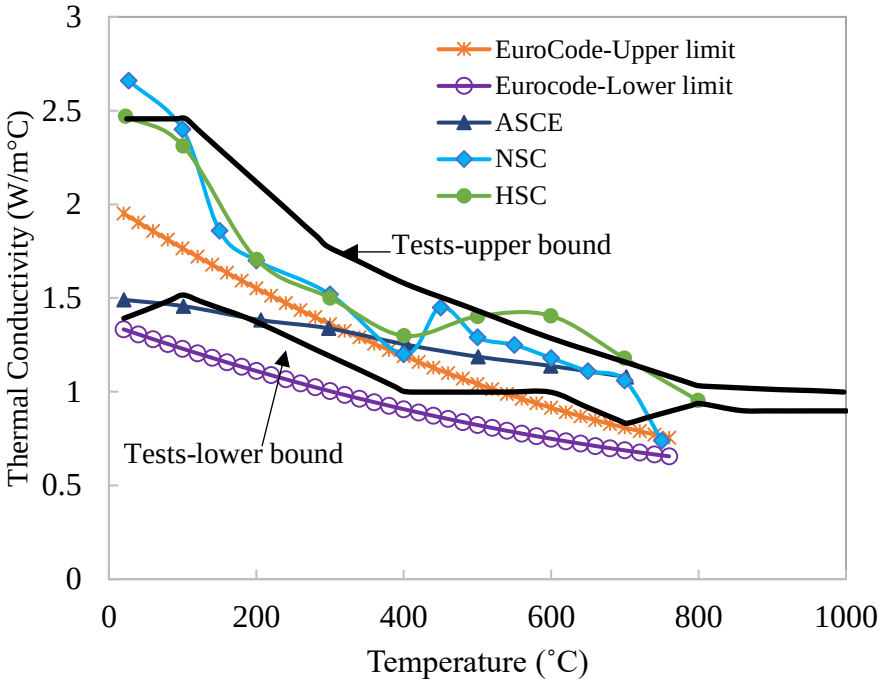


Figure 2.1 Variation of thermal conductivity in concrete with rise in temperature

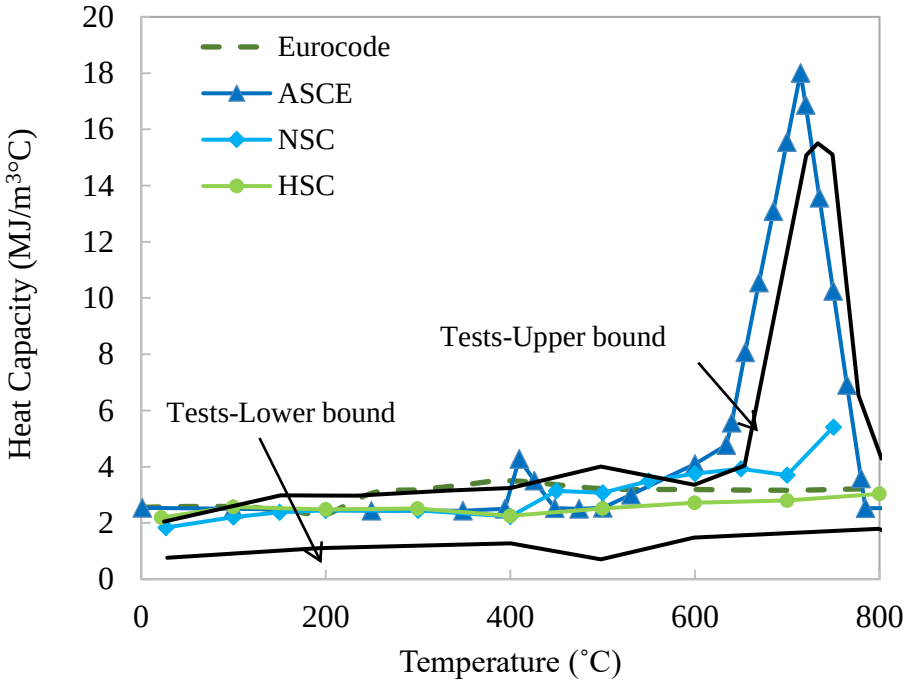


Figure 2.2 Variation of concrete heat capacity with rise in temperature

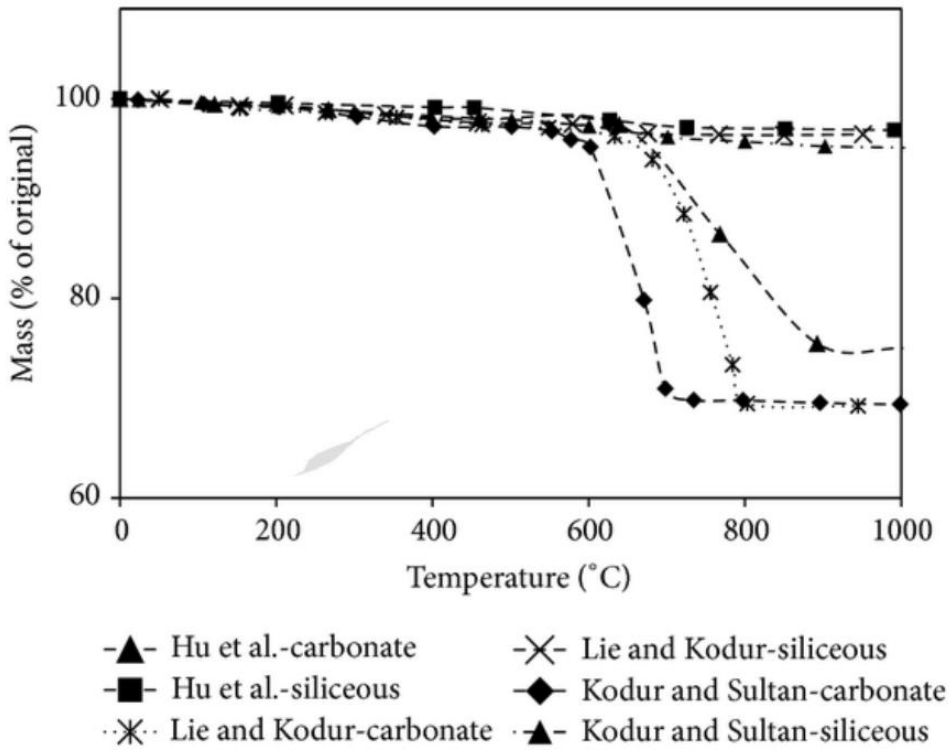


Figure 2.3 Variation in mass loss of concrete with rise in temperature (Kodur, 2014)

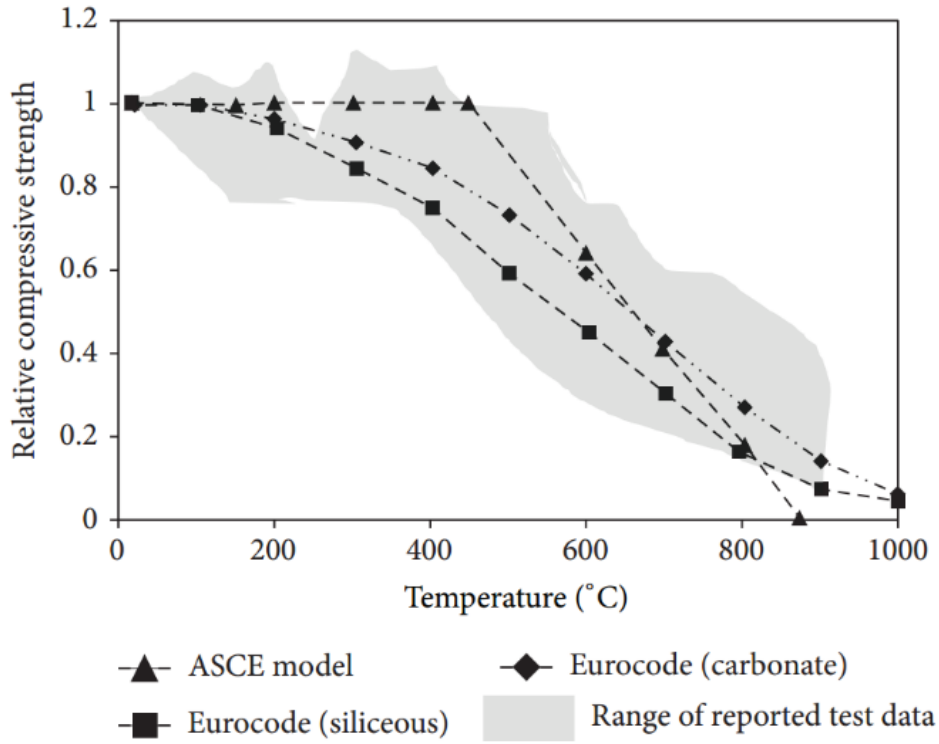


Figure 2.4 Variation of compressive strength with temperature for NSC (Kodur, 2014)

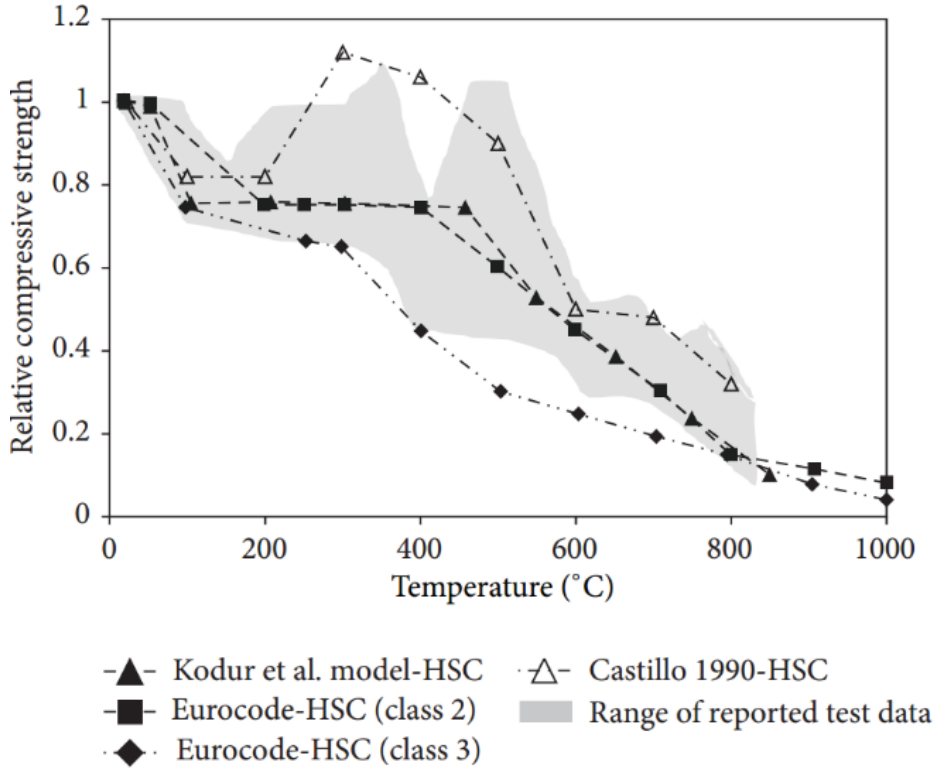


Figure 2.5 Variation of compressive strength with temperature for HSC (Kodur, 2014)

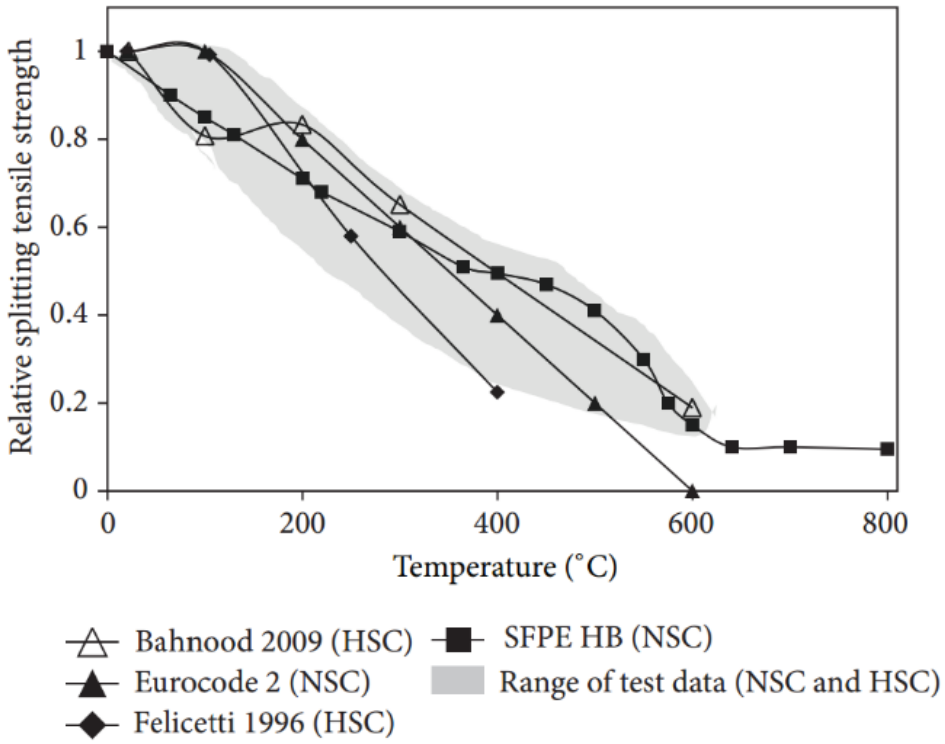


Figure 2.6 Variation of tensile strength of concrete with rise in temperature (Kodur, 2014)

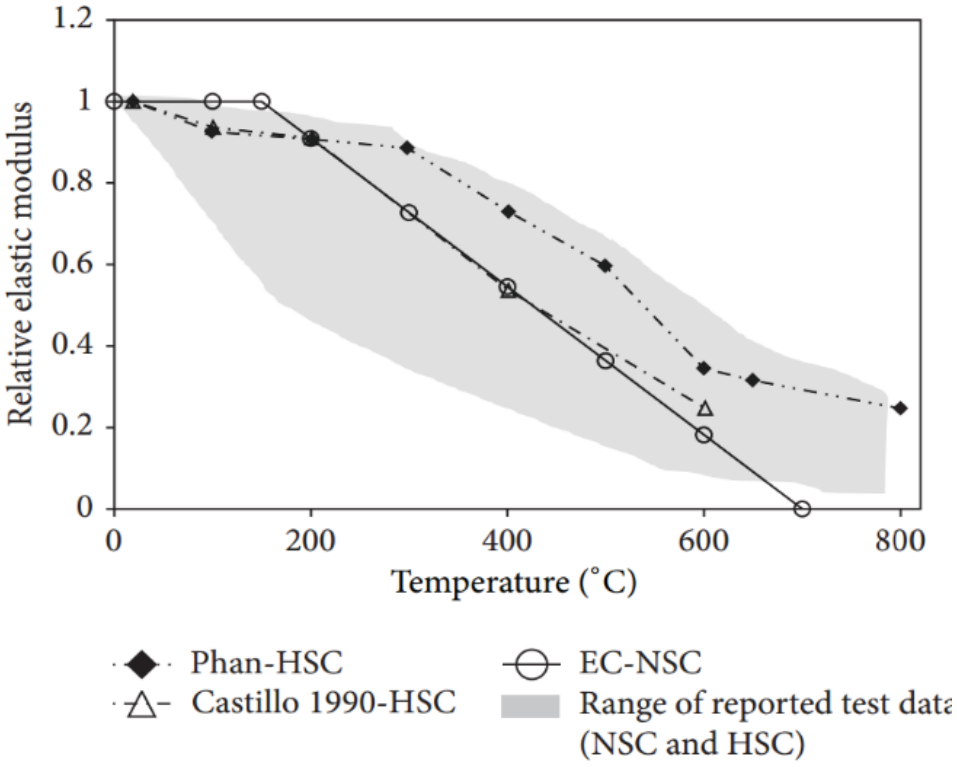


Figure 2.7 Variation of elastic modulus of concrete with rise in temperature (Kodur, 2014)

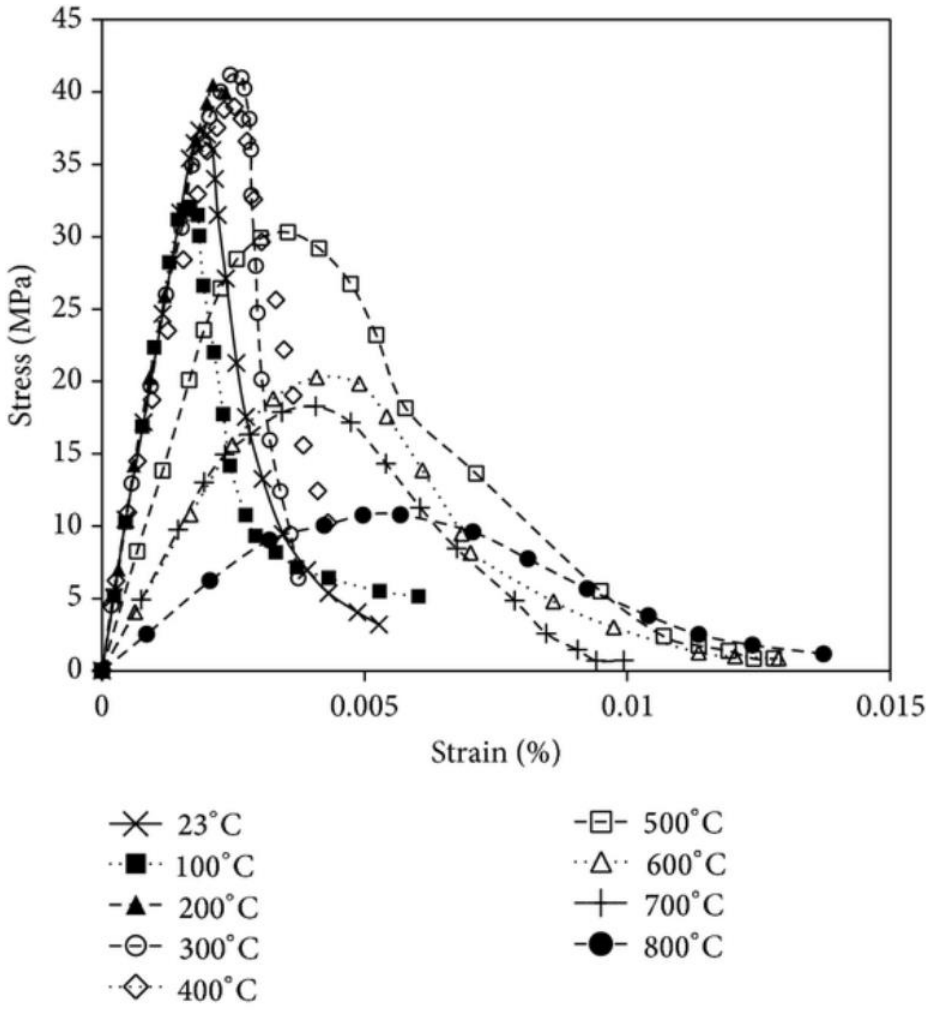


Figure 2.8 Stress-strain response of NSC at elevated temperatures (Kodur, 2014)

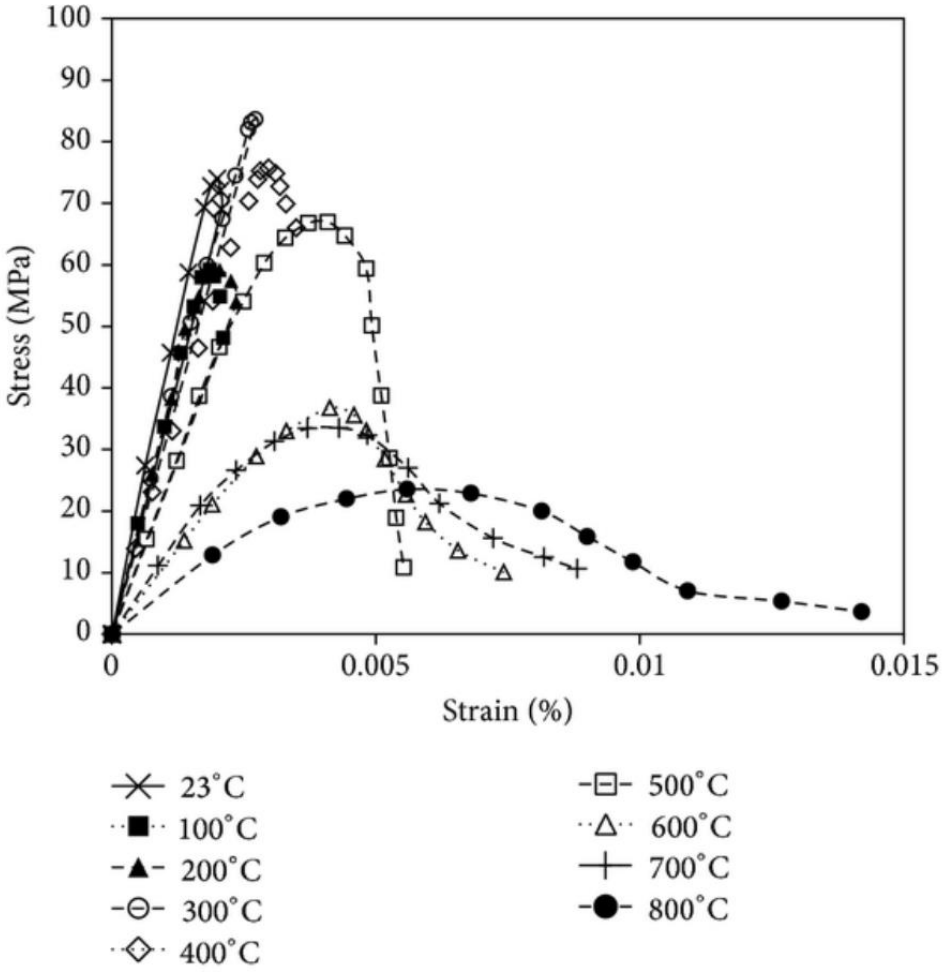


Figure 2.9 Stress-strain response of HSC at elevated temperatures (Kodur, 2014)

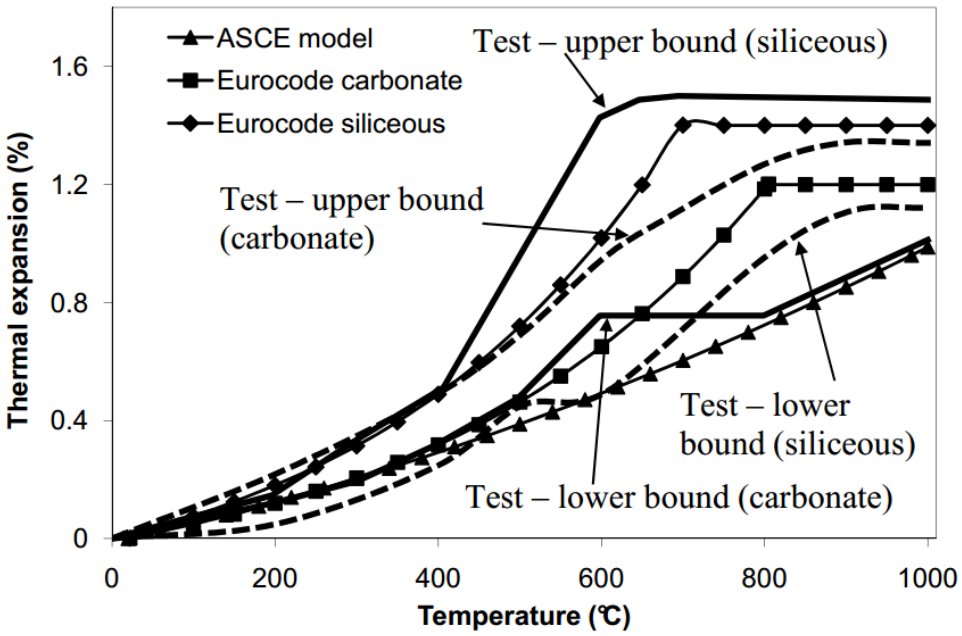


Figure 2.10 Variation in thermal expansion of concrete with rise in temperature (Khaliq, 2012)

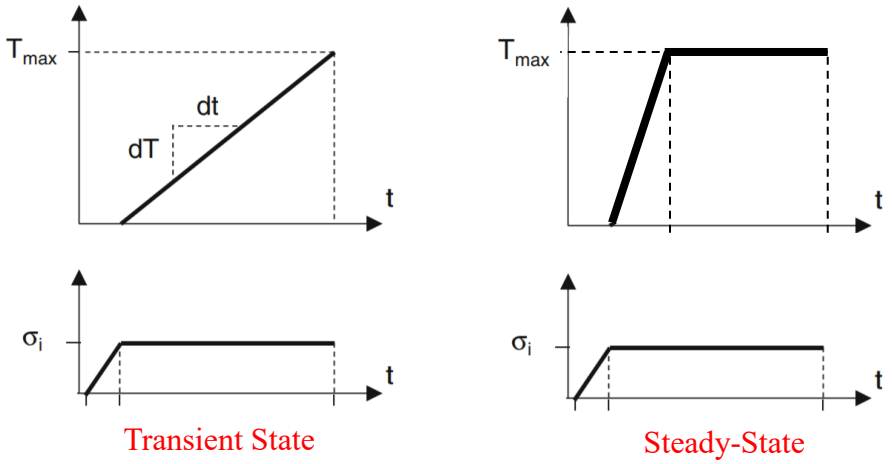


Figure 2.11 Testing methods for evaluating high-temperature creep of concrete

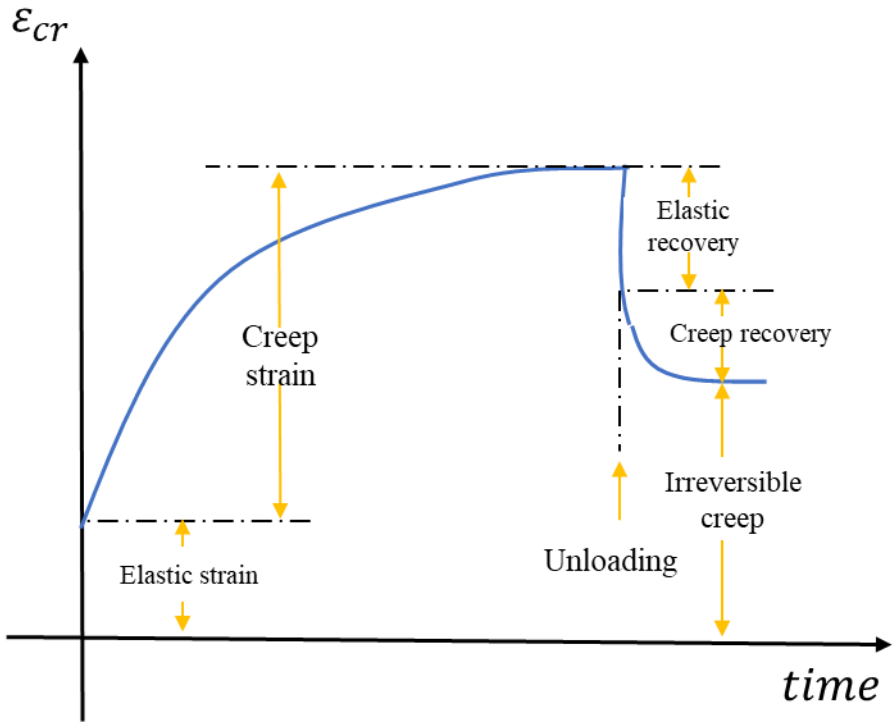


Figure 2.12 Creep behavior in concrete at ambient temperature

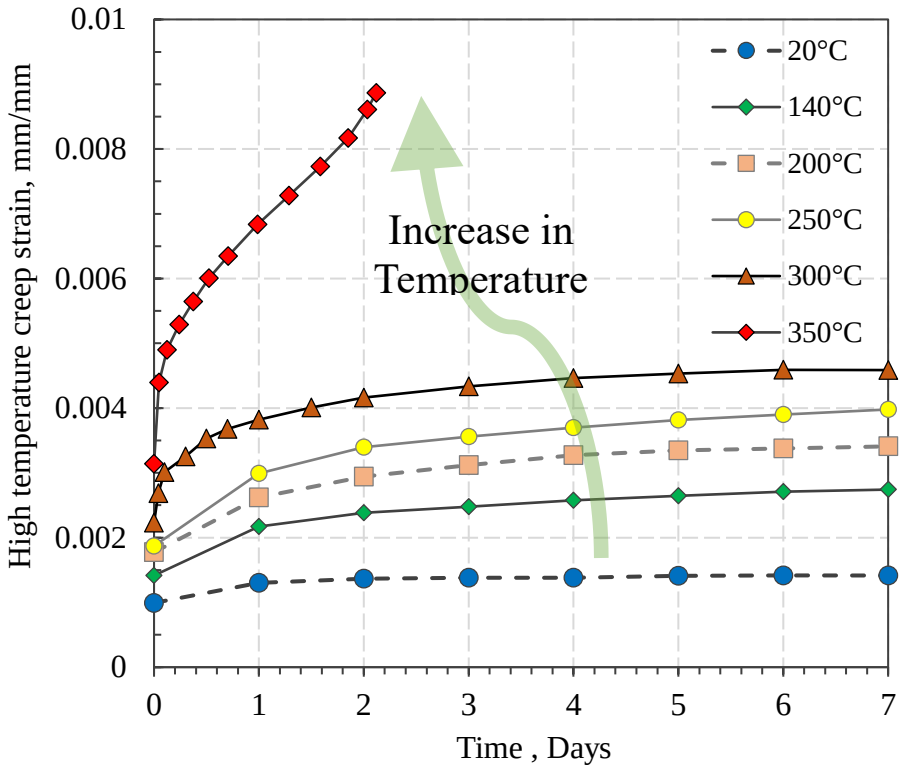


Figure 2.13 Effect of temperature on creep of concrete under steady-state of heating (Gross, 1975)

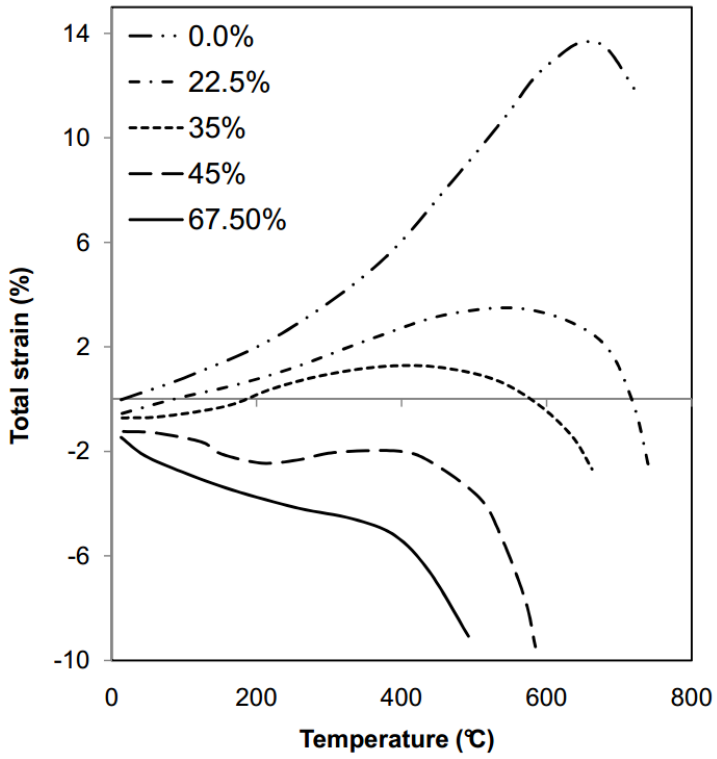


Figure 2.14 Total strain of concrete variation with temperature under different stress levels (Anderberg and Thelandersson, 1976)

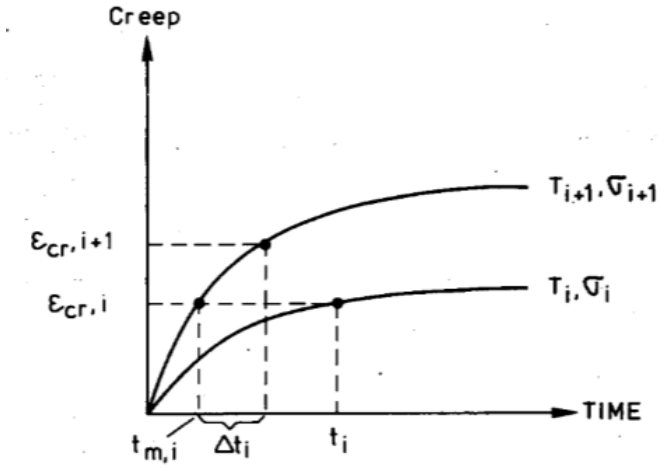


Figure 2.15 Principle of strain hardening for calculating creep strain (Anderberg and Thelandersson, 1976)

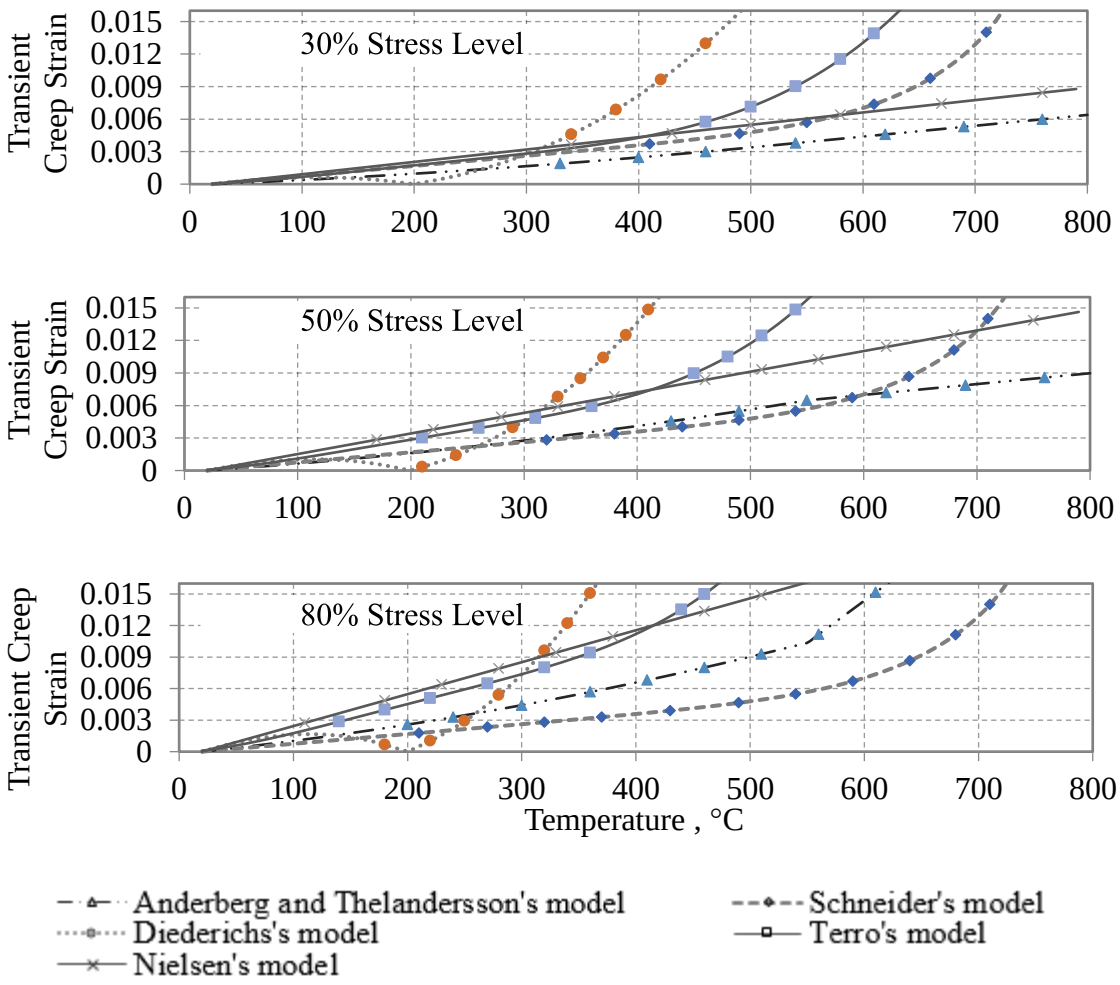


Figure 2.16 Predicted transient creep deformations in concrete at various temperatures for different stress levels.

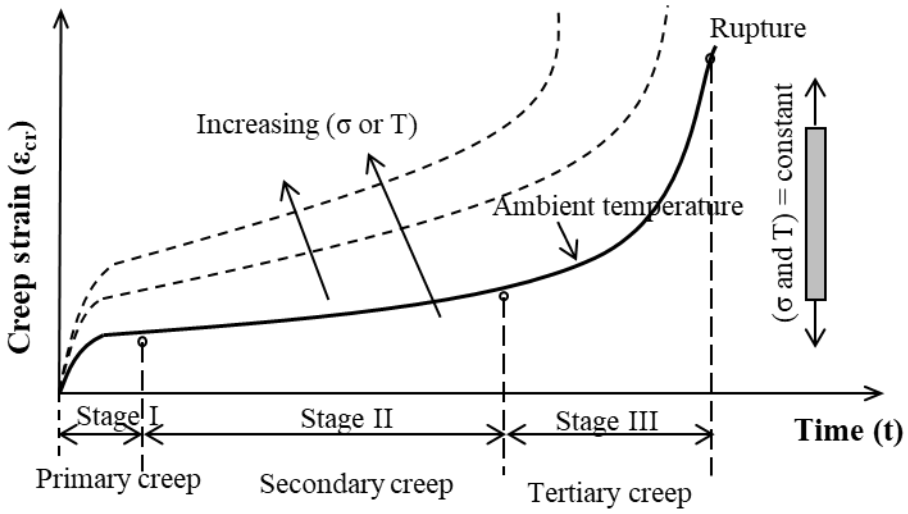


Figure 2.17 Classical creep response of steel (Kodur and Aziz, 2015)

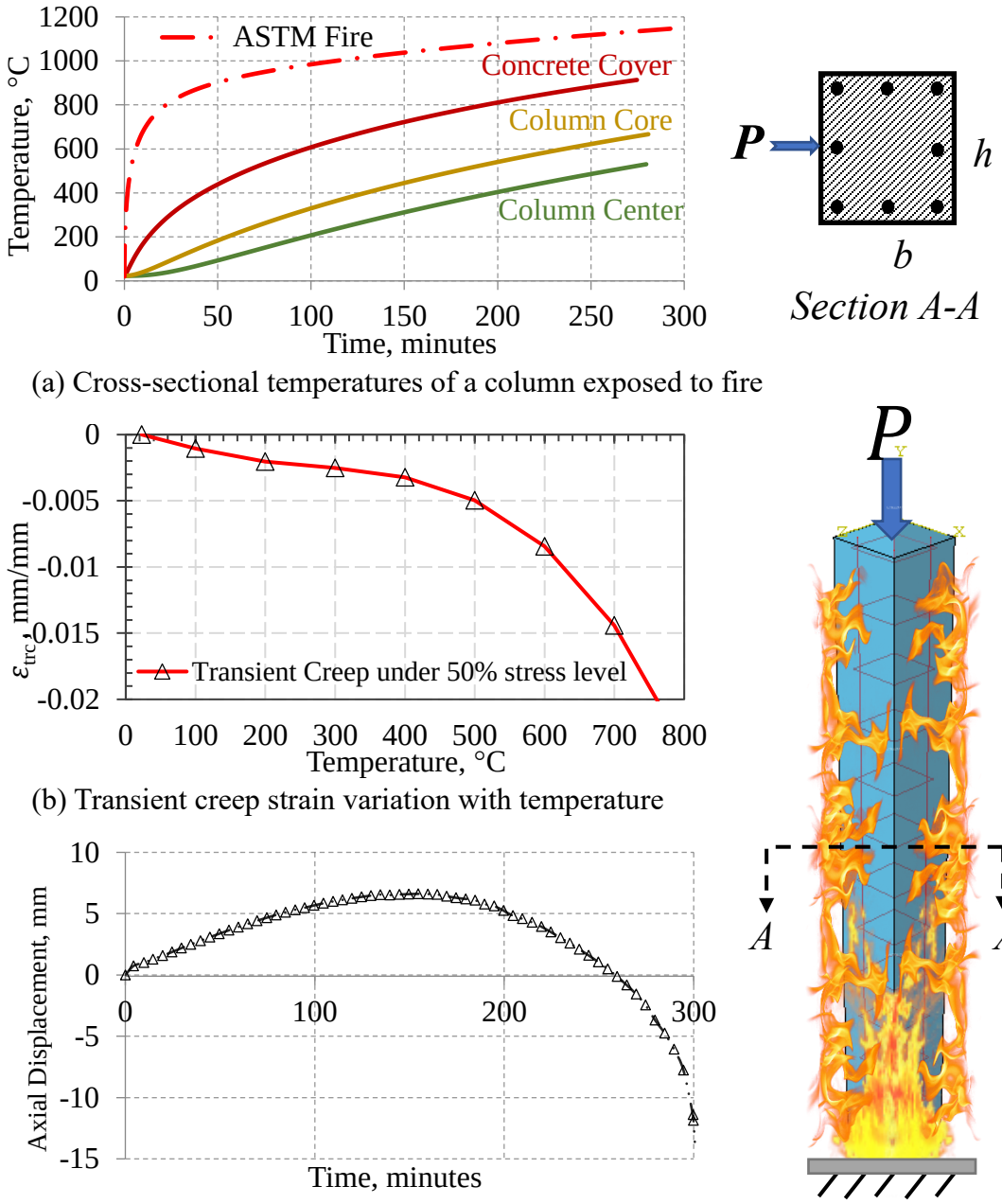


(a) Cross-sectional temperatures of a column exposed to fire

(b) Transient creep strain variation with temperature

(c) Axial displacement variation with time during fire

Figure 2.18 Influence of transient creep on response of reinforced concrete columns under fire conditions

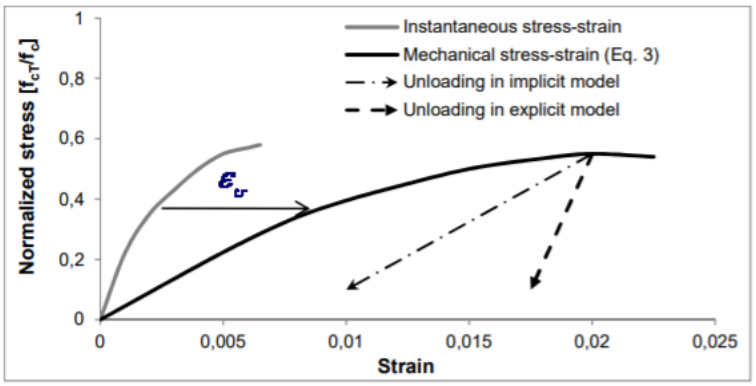


Figure 2.19 Strain components in the implicit and explicit models at 500°C (Gernay and Franssen, 2012)

# CHAPTER THREE

# 3. Transient Creep Experiments

## 3.1. General

The state-of-the-art review presented in Chapter 2 indicates that there have been a number of studies on quantifying creep effects in concrete at elevated temperatures. However, due to different techniques and test conditions adopted in measuring transient creep strain, large variation in the measured creep strains is present between various studies. Even to date, there is no standardized test procedure for measuring high-temperature creep in codes and standards and also there is a lack of equipment to measure transient creep. In addition, most of previous creep tests were conducted on conventional concretes under constant loading and transient heating conditions (Anderberg and Thelandersson, 1976; Khoury et al., 1985; Schneider, 1988).

In recent years, new types of concrete are being widely used in building construction. These new concrete types incorporate steel and polypropylene fibers to enhance mechanical properties and fire performance. Steel fibers enhance mechanical properties of concrete, while the presence of polypropylene (or nylon) fibers can minimize spalling in high-dense concretes under severe fire conditions (Lie and Kodur, 1996; Zeiml et al., 2006). For predicting realistic fire performance of structural members made of these new types of concrete, temperature-dependent creep strain is to be incorporated in the fire resistance analysis. Currently, there is lack of data and relations for temperature dependent creep strain in concretes incorporating fibers (Huismann et al., 2012; Bo Wu, Lam, Liu, Chung, and Ho, 2010; Yoon et al., 2017).

To quantify the development of transient creep in different concrete types under varying heating rates and stress levels, an experimental study was undertaken. A set of creep tests were conducted on four types of concrete; normal strength concrete (NSC), steel fiber reinforced

concrete (NSC-SF), high strength concrete (HSC), and high strength concrete with polypropylene fibers (HSC-PP) under different rates of heating and stress levels over 20°C to 750°C temperature range. Data generated from these tests is utilized to propose temperature-dependent creep relations that can be used for fire resistance evaluation of concrete structures.

## 3.2. Design of Creep Experiments

Transient creep experiments involve the application of simultaneous loading and heating on the specimen while monitoring variation in displacement. Such experiments can be carried out at the structural fire engineering laboratory at Michigan State University (MSU). Up to date, there is no clear standardized testing equipment nor a specific procedure for gauging transient creep strain in concrete at elevated temperatures. Limited recommendations are provided by RILEM (2007) to measure transient creep strain in concrete and no standard methods are provided by ASTM specifically for transient creep in concrete. In the preliminary design of transient creep experiments, the influential parameters to be varied during the experiments were determined as follows: temperature range, stress level, type of concrete, and rate of heating. For varying such parameter, the testing equipment along with the specimen shape and size, are ought to be carefully designed and selected. In this section, the preliminary design of experiments is presented, and difficulties associated with developing the applied testing equipment and procedure are discussed.

### 3.2.1. Test Matrix

Previous experimental studies on transient creep strain were mainly on conventional concrete and very limited studies exist on newer types of concrete including fiber reinforced concrete and high strength concrete. Furthermore, most of the previous studies were limited to low stress levels ($\alpha \leq 30\%$) and slow rates of heating (ROH $\leq 2$ °C/min). Due to these reasons, the test matrix included four concrete mixtures which were selected initially, based on lack of data, to

carry out the transient creep tests including a reference mix of normal strength concrete to compare with data in the literature. The concrete mix batches also included incorporating steel and polypropylene fibers in normal and high strength concretes to study their influence on transient creep strain.

Thus, the test matrix for creep experiments comprises four variables: temperature range, stress level, type of concrete, and rate of heating as shown in Table 3.1. A total of 100 concrete cylinders were cast from four concrete batches for both transient creep experiments and thermal and mechanical property tests. Transient creep experiments were to be conducted in the temperature range between 20 to 750°C under two different rates of heating. The stress level was proposed to be varied from 0% to 70%. Two concrete grades were selected; NSC and HSC, incorporating two types of fibers; steel and polypropylene. The size and shape of the specimens was selected to be standard cylinders of 75mm by 150mm (3" by 6") and 100mm by 200mm (4" by 8").

### 3.2.2. Test Equipment

Measuring deformations in concrete under elevated temperatures exposure is quit complex since displacement transducers and strain gauges are not designed to function at high temperatures and thus, cannot be attached directly to the specimen. Up to date, there is neither a standard testing equipment nor a procedure for gauging transient creep strain in concrete at elevated temperatures. Due to these reasons, researchers designed different testing equipment for measuring transient creep strain in concrete. These previously employed testing equipments in literature were comprised of a loading system to apply load on the specimen, a heating furnace, and a technique to capture deformations of the specimen. Similarly, in this study, the testing equipment should consist of these three components; a loading system, a heating furnace, and a technique for

measuring deformation. Thus, certain requirements are to be met by the testing equipment to carry out transient creep tests as summarized in the following bullet points:

- The testing equipment should include a loading system which is capable of applying load up to a maximum of 70% of the HSC specimens' ultimate strength to achieve the proposed stress levels. Then the loading system should be capable of holding this load constant on the specimens for prolonged durations (8+ hours).
- The testing equipment should include a furnace which can generate temperatures up to 800°C at selected heating rates. This furnace should also allow access to the specimens for applying load and measuring displacement.
- The testing equipment should include an apparatus to mechanically transfer the displacement of the specimen out of the furnace to allow for attachment of a displacement transducer.
- The testing equipment should include suitable instrumentation to capture the variation in load, temperatures, and deformations.

### 3.2.3. Selection of Instrumentation

Proper instrumentation is needed to monitor the variation in axial displacement of the specimen along with the level of applied loading and progression of temperatures within the specimen. Thus, the testing equipment should be instrumented with the following to measure the proposed variables:

- The equipment should be instrumented with load cells that have capacity higher than the proposed loads to be applied on the specimens. The load cell should be able to capture variation in applied loading with very high accuracy.

- The specimens and the equipment should be instrumented with thermocouples to monitor temperature progression at center and surface of the specimens, and at distinct locations within the testing equipment. The thermocouples should be capable of enduring high temperatures up to 800°C.
- The displacement transducers that will be employed to measure deformations should possess very high resolution to capture the small variation in concrete strain ($\leq \pm 0.0001$ mm/mm).

### 3.2.4. Preliminary Challenges in Testing

The biggest challenge faced in designing the transient creep experiments and testing equipment was determining the technique for measuring axial displacement of the specimen while it is being heated inside furnace. At the preliminary experiments, two different techniques were tested to measure axial displacement of the specimen. Both two techniques included devices that were not attached directly to the specimen. However, these employed techniques did not yield satisfactory results of axial displacement variation with time under exposure to elevated temperatures. Thus, a new technique was employed which included transferring the displacement of the specimen mechanically out of the heating furnace, so it can be gauged by displacement transducers.

Another challenge faced with measuring transient creep strain was the accuracy of the linear axial displacement transducers (LVDT) utilized for gauging the variation in displacement. The variation in transient creep strain is very small up to temperatures of around 400°C, and thus a very high-resolution LVDTs are to be used for measuring displacement. During the preliminary testing of specimens, LVDTs with different accuracy and stroke lengths were utilized. The LVDTs with the lowest noise in measured deformations of the specimen were selected to be employed.

The finalized experimental details which were utilized to generate the transient creep data in this study are discussed in detail in the following sections.

## 3.3. Experimental Details

For generating data on transient creep strain in different concrete types, a set of creep experiments were carried out at various temperature and stress levels. For undertaking these creep experiments, test equipment was specially designed and fabricated at Michigan State University. Details of the experimental regime followed in this study are outlined in the following sub-sections.

### 3.3.1. Test Specimens

For characterizing transient creep in different types of concrete, test specimens from four batch mixes of concrete, namely: NSC, NSC-SF, HSC, and HSC-PP, were prepared. These four concrete types are selected since they are widely used in building applications. Batch mix proportions for each of the four mixes are shown in Table 3.2. Two commercially available types of fibers: steel fibers (SF) and polypropylene fibers (PP) shown in Figure 3.1-a and b respectively are added to NSC and HSC batch mixes. Steel fibers are NOVOCON XR Type V meeting ASTM A820 specifications and having 38 mm length and 1.14 mm diameter with aspect ratio 34 and an estimated tensile strength between 966 to 1242 MPa. Polypropylene fibers are FORTA micro synthetic fibers made of 100% monofilament homopolymer polypropylene of a non-absorbent type. The physical properties of these polypropylene fibers are: length of 19mm, specific gravity of 0.91, melting point of 160°C, and tensile strength of 570-660MPa.

Twenty-five concrete cylinders of 76 mm diameter by 152 mm length were cast from each concrete mix for transient creep, as well as other mechanical property, tests. The specimens were cast in paper molds to facilitate easy installation of thermocouples in the cylinders and reduce

demolding labor. The casted concrete cylinders were demolded after 24 hours and stored in a curing room with humidity of 90% and temperature of 21°C for the first seven days. Following this, specimens were stored in the laboratory at ambient conditions of temperature and humidity. Cylinders from different concrete batch mixes were tested for measuring compressive strength on the $7^{th}$, $21^{st}$, $28^{th}$ day, and during creep tests to ensure that targeted design strength is achieved (shown in Table 3.1). Prior to casting, each concrete cylinder (mould) was instrumented with two Type-K Chromel-alumel thermocouples at mid-height center and surface of the specimen to monitor temperatures progression during the test.

### 3.3.2. Test Apparatus

For undertaking transient creep tests on concrete cylinders, a custom-built integrated heating furnace and loading equipment was designed and built inhouse. This equipment comprised of a heating furnace, hydraulic loading system, deformation measuring apparatus, and a data acquisition system. A schematic of the test set-up for transient creep test is shown in Figure 3.2. The electrical heating furnace consists of a cylindrical chamber with an inner diameter of 203 mm and a height of 305 mm. The furnace is programmable to automatically generate selected heating rates and holding times up to a temperature of 800°C. Three Type-K Chromel-alumel thermocouples are mounted inside the furnace to monitor temperature progression with time inside the furnace.

Two hydraulic jacks, each of 889 KN capacity, are utilized to apply load on the concrete cylinders. These hydraulic jacks have closing valves which allow load to be held constant for a long period of time during a strength test. Two load cells of 889 KN capacity are placed against 50 mm thick steel plate at each hydraulic jack rod to measure loading applied on to the test specimen. Figure 3.3 shows the test set up, electrical furnace, hydraulic jacks and their closing

valves. The steel cylinders, utilized to fabricate the loading shaft, are protected with fire insulation paste applied directly to steel and wrapped with ceramic fiber insulation sheets so as to limit the temperature rise in steel cylinders during elevated temperature exposure. The test specimen is placed inside the furnace between the fixed steel cylinders of the test set-up.

For monitoring axial deformations in heated concrete cylinders, a 12.7 mm hole is drilled through the loading steel shaft to the end of the top steel beam. This hole facilitates the passing of a fused quartz glass tube of inside diameter of 5 mm and outside diameter of 10 mm. Fused quartz glass was selected for measuring deformations due to its low thermal expansion coefficient, $0.5\times10^{-6}$ 1/°C and its low thermal conductivity, 1.4 W/m°C. This glass tube is placed on top of the concrete cylinder and a plate is attached to the other end to enable measuring of axial displacement by a linear variable differential transducer, LVDT, as shown in Figure 3.4. Two steel rings of 11 mm opening diameter are attached to the top and bottom shaft holes to reduce the inclination of the glass tube. This leaves a 0.5 mm clearance between the hole and the tube which minimize inclination of the glass tube. Temperatures at the ends of the quartz tube are monitored to calculate its expansion. However, the expansion of the quartz tube is very marginal due to low level of temperature, less than 200°C, that develop in most the tube.

To measure deformations during the test, a linear variable displacement transducer (LVDT) is placed against the plate on top of the glass tube. This LVDT has a stroke of ±38 mm with 0.0254 mm sensitivity. The load cells and LVDT are connected to a data acquisition system and a computer wherein load and displacement are recorded at ½ second intervals by averaging results of 10 recorded measurements.

Two data acquisition systems are utilized, one for recording temperatures and the other for load and displacement measurements. Temperature, axial displacement and applied loading were recorded at ½ second intervals.

### 3.3.3. Test Procedure

Limited recommendations that are given in RILEM (1998, 2007) standard for undertaking high-temperature creep tests is followed, while other relevant recommendations prescribed in ASTM standards, for room temperature creep tests, are slightly modified.

In each test, the concrete specimen was loaded with a pre-selected loading level. Then, the specimen was heated at a specified rate of heating until maximum target temperature, $T_{max}$ was reached, in the entire specimen, while maintaining the pre-applied load at a constant level. The heating for undertaking a transient creep test comprises of two phases; transient and steady-state phase as shown in Figure 3.5. The first phase is from the start of heating, $t_i$, to the time maximum temperature is attained in the center, $t_{max}$, of concrete cylinder. During this transient stage of heating, a thermal gradient develops within the cross section of the concrete cylinder (Figure 3.5). This is mainly due to the low thermal conductivity of concrete which slows down raise of temperatures from surface towards center of the cylinder. When temperatures at the surface of the concrete cylinder, $T_s$, reach near the maximum targeted temperature, $T_{max}$, the increase in the specimen's temperatures with time shifts from linear to a non-linear response until uniform temperature is reached throughout the specimen at time, $t_{max}$. Temperature at the point where the response changes from linear to a non-linear one is denoted as $T_s^*$ . RILEM recommends limits for $(T_{max} - T_s^*)$ based on the maximum targeted temperature, for instance, $(T_{max} - T_s^*) \leq 20$°C when $T_{max}$ = 750°C. When temperature at the specimen's surface reach, $T_s^*$ , the gap between temperatures at the specimen's surface, $T_s$ , and center, $T_c$, start to diminish till the two temperature

curves converge at $T_{max}$. The time from reaching a temperature of $T_s^*$ at the specimen's surface to reaching a uniform temperature, $T_{max}$, throughout the specimen is defined as the transitional thermal period, *TTP*. At the end of the *TTP* period, the transient phase of heating comes to an end. Then, the steady-state phase of heating starts from reaching a uniform temperature in the specimen until termination of the test. The time of the steady-state phase of heating is referred to in here as, the holding period, and this period ranges from 2 to 4 hours, depending on the target temperature (200 to 800°C) at which the creep test is undertaken.

In the creep tests, three primary parameters; namely: stress level, rate of heating, and holding period were varied. Stress level ranged from 0% to 70% of room temperature strength of the specimen to reflect the varying state of stress in most building applications during fire exposure. The two selected rates of heating for transient creep experiments were 4°C/min, and 6°C/min. The peak target temperature for transient creep tests was selected to be 750°C which provides transient creep strain history with time in the whole transient heating phase of the test. The holding period during the steady-state phase varied from 2 to 4 hours in order to measure steady-state creep strain during this period.

### 3.3.4. Measured Response Parameters

Three main response parameters were measured during each creep test; axial displacement, applied loading, and temperatures developed within the specimens (center and surface) as well as in the furnace. Measured parameters are recorded at a time interval of ½ minute throughout the test duration. Recorded load is utilized to calculate corresponding stress level on the specimen, whereas axial displacement values are utilized to deduce transient creep strain. Further, prior to the creep test, dimensions and weight of the specimens are measured to deduce density and mass loss before and after each transient test.

## 3.4. Results and Discussion

A total of 56 cylinders were tested to measure transient creep in four types of concrete; NSC, NSC-SF, HSC and HSC-PP. Under transient heating conditions, total strain developed in concrete comprises of three components; thermal strain ($\varepsilon_{th}$), mechanical strain ($\varepsilon_{me}$), and transient creep strain ($\varepsilon_{trc}$). Prior to heating, the mechanical strain ($\varepsilon_{me}$) due to applied loading was measured and subtracted from total strain. Thus, transient creep strain was evaluated as the difference between ($\varepsilon_{tot} - \varepsilon_{me}$) and free thermal strain ($\varepsilon_{th}$) as per RILEM recommendations for evaluating transient creep (2007), as shown in Figure 3.6. Thus, transient creep strain is deduced according to the following equation:

$$\varepsilon_{trc} = \varepsilon_{tot} - \varepsilon_{me} - \varepsilon_{th} \quad \text{.....[3.1]}$$

where $\varepsilon_{trc}$ is transient creep strain, and $\varepsilon_{tot}$ is the total strain of concrete under load and transient heating. The term, $\varepsilon_{me}$ is the load-induced (mechanical) strain, and $\varepsilon_{th}$ is the thermal (expansion) strain of concrete. Since deformation properties of concrete are significantly dependent on the heating level, stress level, and composition of the concrete mixture together with type of aggregate used, and the physicochemical reactions which occur in concrete when exposed to elevated temperatures, development of transient creep varies with concrete type, stress level, and rate of heating.

The RILEM assumption that total transient creep strain represents both basic creep strain and transient strain is adopted in here since it is impossible to differentiate between the two strains under transient heating and simultaneous loading. Both transient strain and creep strain get developed in concrete due to the same mechanisms of moisture loss and evaporation out of concrete, and thus, it is justified to combine these two strains under transient creep strain. Another reason to combine these two strains under one transient strain is that creep strain is a time

dependent strain whereas transient creep strain gets developed in relatively short time under fire conditions and has been referred to by some as short term creep (Torelli, Mandal, Gillie, and Tran, 2016).

### 3.4.1. Free Thermal Strain

Concrete, as a material, expands when subjected to elevated temperatures, but the extent of expansion is highly dependent on aggregate type, moisture content, dehydration, shrinkage, and microcracking caused by temperature-induced stresses (Kodur, 2014). Thermal expansion was measured in each concrete type without applying any axial load (i.e. stress level = 0%). Increase in thermal strain with temperature rise in each of the four concrete types is plotted in Figure 3.7. Thermal strain in concrete increases from zero at room temperature (20°C) to around 0.8% at 700°C. Thermal strain is minimal in concrete in the temperature range between 20°C to 320°C and the rate of expansion significantly increases beyond 320°C to about 700°C.

A comparison of measured thermal strain in four types of concrete shows that HSC undergoes higher expansion than NSC. HSC-PP experienced the highest thermal expansion of up to 1.0% at 700°C. The meltdown of polypropylene fibers in HSC-PP, in the temperature range between 160°C - 250°C, enables faster moisture flow out of concrete. This can result in developing shrinkage in the specimen that counteracts expansion. This reduces the rate of expansion in the temperature range 158°C - 227°C as can be seen in Figure 3.7, then the rate of expansion continues to increase from 250°C up to 700°C. Overall, type of concrete (NSC or HSC) and presence of fibers (SF or PP) affect level of thermal strain developed in the concrete (Kodur, 2014; Kodur and Sultan, 2003; Lie and Kodur, 1996).

### 3.4.2. Total Strain

The measured total strain in NSC, NSC-SF, HSC, and HSC-PP is plotted in figures 3.8 through 3.11 as a function of temperature at various stress levels. In case of NSC, total strain developed in concrete under transient heating conditions increase with rise in temperature and get amplified with the level of stress initially applied on the specimen. At stress levels below 20%, concrete experiences most expansion (thermal strain) from heating until transient creep dominates the strain response beyond 600°C. At stress levels above 20%, concrete undergoes gradual contraction till about 300°C, then the rate of contraction increases to temperatures of 700°C, mainly due to creep effects. After a steady-state of heating was reached in the specimens (see Figure 3.5), creep in concrete continued to increase until rupture.

In case of steel fiber reinforced concrete NSC-SF, total strain developed under transient heating conditions mostly follow similar trend as that of NSC, as shown in Figure 3.9. The main difference in NSC-SF concrete is the level undergone strain is slightly lower under stress levels of 30% and higher in the temperature range 20°C - 450°C. This can be attributed to the presence of steel fibers which minimize the effect of excessive microcracking in concrete. Steel fibers provide concrete with some level of confinement and prevent the propagation of cracks in the perpendicular direction to applied axial load through bridging effect. At temperatures above 450°C, however, steel fibers soften and can no longer prevent propagation of microcracks in concrete. At high stress levels ($\frac{\sigma}{f'_c} \geq 40\%$), an evident of increase in strain of NSC-SF occurs after 450°C and continues until failure of the specimen. Overall, strain response of NSC-SF specimens follows similar trends as in NSC but with slightly lower strain due to presence of steel fibers.

Results of total strain versus temperature for HSC show similar behavior as in NSC with slightly higher level of strain developing at the same stress level. Variation of strain with

temperature for HSC is plotted in Figure 3.10 for different stress levels. In case of plain HSC (without polypropylene fibers), tests could not be carried out beyond 500°C in the furnace due to the occurrence of explosive spalling. This happened on more than one specimen at temperatures below 500°C, and the total strain of the tested specimens is plotted in Figure 3.10.

In case of HSC-PP specimens, total strain developed under transient heating conditions follow similar trends as that of NSC, as shown in Figure 3.11, but with higher levels of strain at a given stress. The rate of transient creep increases in concrete between 200°C to 300°C when subjected to stress levels above 20% due to meltdown of polypropylene fibers. For both HSC and HSC-PP, the cement content is double that in NSC, and thus, a significant portion of transient creep originated from decomposition of cement hydrate components in these concretes at temperatures higher than 400°C. Thus, higher cement content combined with polypropylene fibers increases experienced total strain in HSC-PP as compared to that in NSC. For instance, HSC-PP strain at 60% stress level is almost double that measured in NSC for the same stress level at temperatures beyond 500°C.

### 3.4.3. Transient Creep Strain

Transient creep strain in concrete ($\varepsilon_{trc}$) is deduced by subtracting load-induced strain, ($\varepsilon_{me}$), and thermal strain, ($\varepsilon_{th}$), from the total strain ($\varepsilon_{tot}$), of concrete as outlined in Eq. 3.1 and Figure 3.6. Variation of transient creep strain in the four tested concrete types is plotted in figures 3.12 through 3.15 Transient creep strain in NSC increases with temperature and stress levels. At low stress levels below 20%, transient creep strain increases at a slow rate in 20°C - 500°C range, then creep strain increases at rapid pace. For stress levels of 30% or higher, transient creep strain develops at a higher rate in 20°C - 500°C, followed by rapid increase in 500°C - 700°C. For instance, at a stress level of 50%, magnitude of transient creep strain can reach up to 0.007 when

temperature reaches 600°C and can reach to 0.01 around 700°C (Figure 3.12). At stress level of 60% and higher, transient creep constitute most of the total strain when concrete temperatures exceed 500°C.

Evolution of transient creep in NSC-SF follow a similar trend as that in NSC, and transient creep strain increases with increasing temperature and stress as can be seen in Figure 3.13. The presence of steel fibers in NSC-SF leads to reduced transient creep strain up to temperatures of 400°C. Then the effect of steel fibers loses its impact above 450°C due to softening of steel fibers. The resulting creep strain in NSC-SF beyond 450°C is similar to that in NSC without steel fibers. Furthermore, the trends in transient creep strain in NSC-SF specimens is not as smooth as that in NSC due to presence of steel fibers. These steel fibers induce a combined effect of confinement and crack bridging in the concrete cylinder under compression until steel stiffness degrades significantly above 450°C. Beyond 450°C, transient creep strain in NSC-SF specimens is similar to that measured in NSC specimens.

HSC experienced explosive spalling in creep tests and thus complete response in the entire range could not be generated. The failure in these specimens was from spalling rather than creep dominant deformations as in the case of other concrete types. Thus, transient creep strain was measured in these specimens in the temperature range between 20°C - 400°C as can be seen in Figure 3.14. Variation of transient creep strain in HSC specimens with temperature follow similar trends as in NSC but with slightly higher strains for a given stress.

In case HSC-PP, transient creep strain follows similar trends as in NSC with higher experienced transient creep (see Figure 3.15). At low-stress levels ( $\frac{\sigma}{f'_c} \leq 20\%$), HSC-PP specimens experience minimal transient creep until temperature in the specimen exceed 500°C. At stress levels above 30%, however, a slight increase in the developed creep strains occur in the 200°C to

300°C range due to evaporation of polypropylene fibers followed by a decrease in transient creep development in the temperature range between 300°C to 450°C for stress levels of 30% to 50%. Then when temperature in concrete exceed 500°C, transient creep increases significantly (higher than that in NSC) due to the high cement content in HSC.

## 3.5. Effect of Critical Factors Governing Transient Creep

The above-generated creep test data can be utilized to study the critical factors governing transient creep strain evolution in concrete. The influence of temperature, stress level, rate of heating, and type of concrete on the extent of transient creep is evaluated.

### 3.5.1. Effect of Temperature and Stress Level

As shown in the previous section, temperature and stress level are the primary factors influencing the development of transient creep in concrete. Transient creep increases with increase in temperature and stress level. However, creep effects become dominant at a certain temperature for a given stress level. Creep critical temperature is determined for each stress level. This critical temperature is defined as the point in the strain-temperature domain at which transient creep exceeds 0.5% in concrete. In case of steel, this critical temperature is selected at the onset of tertiary creep (Kodur and Aziz, 2015). Due to the brittle failure nature of concrete, however, the onset of such tertiary creep is hard to capture in concrete.

Creep critical temperatures for the three concrete types are given in Table 3.3 for NSC, NSC-SF, and HSC-PP. The tested specimens of HSC without polypropylene experienced spalling at low temperatures, below 400°C. Since failure of HSC specimens is governed by spalling rather than transient creep, defining a critical temperature for HSC is not feasible. For the other concrete types, critical temperature is lower at higher stress levels, and increase with decreased stress level. The critical temperature in NSF-SF is higher between the studied types of concrete, while HSC-

PP have lower critical temperature for a given stress level. In all types of concrete, at stress level of 40% and higher, creep critical temperature is below 500°C.

### 3.5.2. Effect of Concrete Type

The trends from the above-generated test clearly indicate that HSC-PP experience higher transient creep strain than that of NSC and NSC-SF as can be seen in Figure 3.16 at any given temperature and stress level. At moderate levels of stress 30% and 40%, transient creep strain in HSC is slightly higher than what is experienced in NSC and NSC-SF. However, at high-stress levels of 50% and 60%, the magnitude of transient creep strain in HSC-PP is significantly higher than that in NSC and NSC-SF. Overall, higher extent of transient creep is experienced in high strength concretes when exposed to elevated temperature under constant loading (Huismann et al., 2012; Wu et al., 2010; Yoon et al., 2017).

This variation in transient creep strain between NSC and HSC can be attributed to the binder to water ratio in batch mix proportions. High strength concrete (HSC) contains higher cement content than normal strength concrete (NSC) as can be seen in Table 3.2, and higher packing density with less moisture content. As development of transient creep strain in NSC is mainly due to capillary moisture loss up to around 400°C, then physicochemical changes in the hydrated cement paste along with decomposition of C-S-H beyond 400°C permits evaporation of most of the chemically bound water which in turn amplify transient creep strain. Due to the higher cement content in HSC, transient creep strain increase significantly when temperatures exceed 400°C due to the generated transient creep portion from the decomposition of cement hydrates (Yoon et al., 2017).

### 3.5.3. Effect of Rate of Heating

Concrete specimens when heated at higher rates of heating develop larger thermal gradients (i.e. difference between center and surface temperatures) leading to higher thermal stresses and strains. When rates of heating are higher than 6 °C/min, effect of transient creep become much higher in concrete due to the development of large thermal gradients (Tao et al., 2013; Thelandersson, 1974; Torelli et al., 2016). However, rates of heating below 6 °C/min have been found to show little effect on transient creep of concrete due to the low induced thermal gradients in concrete. As the rate of heating increases, the rate of transient creep development increases. Although rapid rates of heating induce transient creep at a much higher rate, developed transient creep in concrete is higher under slow rates of heating for a given temperature and stress levels, but takes longer times to develop (Anderberg and Thelandersson, 1976; Khoury et al., 1985a; Schneider, 1976; Wu et al., 2010).

To illustrate the effect of heating rate on transient creep strain, transient creep strain for NSC under two different heating rates (4 and 6 °C/min) and subjected to same stress level of 60% are plotted in Figure 3.17-a and -b with respect to time and temperature, respectively. In the time domain, NSC specimen under low heating rate (4 °C/min) require 175 min to reach a maximum targeted temperature of 700°C as opposed to 115 minutes under 6 °C/min. Transient creep strain occurs at a slower rate (require a longer time to develop) under slow rates of heating as can be seen in Figure 3.17-a. However, under low rates of heating, magnitude of transient creep is slightly higher than that under rapid rates of heating for a given stress level when transient creep is plotted with respect to temperature as in Figure 16-b. Under the same stress level of 60%, the NSC specimens heated at 4 °C/min experienced slightly higher transient creep than that measured when specimens are heated at 6 °C/min for a given temperature as can be seen in Figure 3.17-b. Overall, the variation in transient creep under the two implemented rates of heating (4 and 6 °C/min) is

insignificant and rates of heating mainly influence the rate at which transient creep is developed in concrete.

## 3.6. Relations for Expressing Transient Creep

In recent years, a range of numerical approaches, including advanced analysis, is applied for evaluating fire resistance of concrete structures. In advanced analysis, a number of critical factors, including effect of transient creep, can be incorporated into fire resistance analysis so as to get reliable fire resistance predictions (Alogla and Kodur, 2018; Kodur and Alogla, 2016). For accounting creep effects in fire resistance analysis, temperature and stress dependent transient creep strain relations, specific to different concrete types is needed. Based on the data generated from creep tests, an empirical creep relation is developed to express transient creep strain in terms of temperature, stress level, and concrete type.

### 3.6.1. Formulation of Creep Relation

The total strain of concrete at elevated temperatures is assumed to comprise of three components; namely thermal, mechanical, and transient creep and is given as:

$$\varepsilon_{tot} = \varepsilon_{th} + \varepsilon_{me} + \varepsilon_{trc} \quad \text{..... [3.2]}$$

where $\varepsilon_{tot}$ is the total strain of concrete under load and transient heating, $\varepsilon_{th}$ is the thermal expansion strain of concrete, $\varepsilon_{me}$ is the load related mechanical strain, and $\varepsilon_{trc}$ is transient creep strain. Simplified relations for expressing thermal strain in different concrete types is well established in literature (Khaliq and Kodur, 2011; Lie and Kodur, 1996). Further, mechanical strain, $\varepsilon_{me}$, under elevated temperature exposure can be estimated utilizing existing $\sigma - \varepsilon$ relations for different concrete types. Thus, knowing total strain, transient creep strain can be deduced using Eq. [3.1]. The variation of deduced transient creep is plotted in figures 3.12 through 3.15 (Section 3.3.3) for the four types of concrete.

The variation of transient creep strain, shown in figures 11 to 14, is used to fit an empirical relation by nonlinear regression. This relation is expressed as a function concrete type and stress level, and temperature. Transient strain in this relation is linearly dependent on type of concrete and stress level and non-linearly dependent on temperature with a polynomial function, $f(T)$. Thus, transient creep strain in concrete is given as:

$$\varepsilon_{trc} = k \cdot \left(\frac{\sigma}{f'_c}\right) \cdot f(T) \qquad \text{.....[3.3]}$$

where *k* is a modification parameter to account for effect of concrete type on transient creep strain and is proposed to be 1.0 for NSC, 0.8 for NSC-SF and 1.05 for HSC, and HSC-PP to data of measured transient creep strain. Stress level in the proposed relation is represented by the term $\left(\frac{\sigma}{f'_c}\right)$ where $\sigma$ is stress to which the specimen is subjected and $f'_c$ is concrete strength. The temperature function, $f(T)$, in equation [3.3], is a quadratic function given as:

$$f(T) = -2.5 \times 10^{-10} \cdot T^3 + 2.0 \times 10^{-7} \cdot T^2 - 6.2 \times 10^{-5} \cdot T^2 + 0.002 \quad \text{.....[3.4]}$$

where temperature, *T*, is in Celsius, °C.

Predicted transient creep strain for NSC from equation [3.3] is plotted in Figure 3.18 as a function of temperature in 20°C - 800°C at various stress levels. As can be seen in Figure 3.18, the progression of transient creep strain is in three distinct stages, primary, secondary, and tertiary stages. In the primary stage, transient creep increases linearly up to 200°C, followed by a secondary stage during which transient creep increases in a nonlinear fashion between 200- 400°C. Beyond 400°C, transient creep strain increases rapidly till failure occurs in concrete and this is referred to as the tertiary stage of creep.

The formulated relation for transient creep strain in equation [3.3] was fitted to the experimental data by employing a non-linear regression analysis. Thus, transient creep data was

modeled by a quadratic function of temperature (non-linear) along with two other dependent variables; stress level and type of concrete. The difference between measured and predicted transient creep strain from the experiments and the proposed relations are compared and the difference in data at each temperature is calculated to be the residual error, e. Thus, the finalized version of the proposed relation was arrived at through minimizing the residual error for each stress level as well which consequently minimize the overall sum of residuals.

A summary of the calculated residual error is listed in Table 3.4. for different types of concrete. For each concrete type, the residual error is calculated for different stress levels as can be seen in Table 3.4.

### 3.6.2. Validation of Creep Relation

The validity of the above-proposed creep relation is established by comparing predicted transient creep strain values to previously reported creep test data as well as with other existing creep relations in the literature. Figure 3.19 shows a comparison of creep from the current creep relation with existing relations and creep data reported in tests in the literature.

As shown in Figure 3.19, the predicted creep strain from proposed creep relation, based on measured data in this study, match well with previous relations of Anderberg and Thelandersson (1976), and Schnider (1986) for NSC. The proposed relation for transient creep also yields similar trends in transient creep of both NSC and HSC-PP. The slight variation between different relations is due to different experimental data utilized to propose the relations. This variation in test conditions for generating experimental data can mainly be attributed to different techniques and conditions which are employed in producing experimental data as no standardized test procedure is in place. For HSC-PP, the proposed relation shows slightly lower transient creep strains than reported studies in the literature. However, the trends in transient creep strain are similar. Overall,

the proposed relation is capable of generating reliable transient creep strains in different types of concrete; NSC, NSC-SF, and HSC-PP.

## 3.7. Summary

In this chapter, experiments on the development of temperature-induced transient creep strain in different types of concrete are presented. To measure creep strain, concrete specimens were subjected to combined effects of heating and mechanical loading in the temperature range between 20°C to 750°C. The test variables included temperature, load level, rate of heating, strength of concrete and presence of fibers in concrete. Data from these tests indicate that transient creep strain constitutes a significant portion of total strain. Data also affirm that temperature range and stress level have significant influence on the magnitude of transient creep strain, specially at temperatures above 500°C and stress levels of 40% or more. However, rate of heating and presence of fibers in concrete have only a moderate influence on the generated transient creep. Presence of steel fibers in normal strength concrete slightly reduce the extent of transient creep strain, while the addition of polypropylene fibers to high strength concrete leads to higher transient creep strain. Finally, data generated in tests on transient creep strain was utilized to propose temperature and

stress dependent creep strain relations for different types of concrete. Such relations can be implemented in fire resistance evaluation of concrete members to account for transient creep strain.

Table 3.1 Test matrix for creep experiments on concrete

| Parameter | NSC Specimens | NSC-SF Specimens | HSC Specimens | HSC-PP Specimens |
|---|---|---|---|---|
| **Temperature Range** | 20 –750°C | 20 –750°C | 20 –400°C | 20 –750°C |
| **Stress Level** | 0 – 70% | 0 – 70% | 0, 30, and 50% | 0 – 60% |
| **Rate of Heating** | 4, and 6 °C/min | 4, and 6 °C/min | 4 °C/min | 4, and 6 °C/min |
| **Type of Fibers** | - | Steel | - | Polypropylene |
| **Specimen Size** | Cylinders 75mm×150mm (3” ×6”) and 100mm×200mm (4” ×8”) | | | |
| **Number of Specimens** | 25 | 25 | 25 | 25 |

Table 3.2 Batch proportions of concrete utilized for transient creep tests

| Components | NSC | NSC-SF | HSC | HSC-PP |
|---|---|---|---|---|
| Coarse Aggregate 3/8" Limestone, Kg/m$^3$ | 984.8 | 984.8 | 1088.3 | 1088.3 |
| Natural sand, Kg/m$^3$ | 929.7 | 929.7 | 640.7 | 640.7 |
| Cement, Kg/m$^3$ | 230.2 | 230.2 | 560.7 | 560.7 |
| Silica fume, Kg/m$^3$ | - | - | 41.5 | 41.5 |
| Fly Ash- Class C, Kg/m$^3$ | 76.5 | 76.5 | - | - |
| Water, Kg/m$^3$ | 153.6 | 153.6 | 150.7 | 150.7 |
| Superplasticizer, Kg/m$^3$ | 24.6 | 24.6 | - | - |
| Water reducer, Kg/m$^3$ | 6.1 | 6.1 | 71.8 | 71.8 |
| Accelerator, Kg/m$^3$ | 12.3 | 12.3 | - | - |
| Air content admixture, Kg/m$^3$ | 3.1 | 3.1 | - | - |
| Design Air content % | 2.0 | 2.0 | 0 – 3.0 | 0 – 3.0 |
| W/C ratio | 0.5 | 0.5 | 0.3 | 0.3 |
| Slump, mm | 101.6 | 127 | 101.6 | - |
| Steel fibers, Kg/m$^3$ | - | 41.5 | - | - |
| Polypropylene fibers, Kg/m$^3$ | - | - | - | 2.0 |
| $f'_c$ $^{7th}$ day | 17 | 17 | 58 | 55 |
| $f'_c$ $^{21st}$ day | 23 | 22 | 94 | 90 |
| $f'_c$ $^{28th}$ day | 29 | 29 | 111 | 100 |
| Test day | 31 | 32 | 115 | 104 |

Table 3.3 Critical temperatures for tested types of concrete at different stress levels

| **Stress Level %** | **Critical Temperatures, °C** | | |
|---|---|---|---|
| | NSC | NSC-SF | HSC-PP |
| 10 | 680 | 750 | 730 |
| 20 | 630 | 675 | 650 |
| 30 | 585 | 630 | 520 |
| 40 | 550 | 590 | 500 |
| 50 | 520 | 550 | 430 |
| 60 | 465 | 485 | 395 |
| 70 | 415 | 475 | NA |

Table 3.4 Residual error between predicted (proposed relation) and measured transient creep strain

| Stress Level % | Residual Error (e) | | | | | | |
|---|---|---|---|---|---|---|---|
| | NSC | | | | | | |
| | 100°C | 200°C | 300°C | 400°C | 500°C | 600°C | 700°C |
| 10 | 0.00029 | 0.00032 | 0.00032 | 0.00019 | 0.00022 | 0.00087 | 0.00390 |
| 20 | 0.00026 | 0.00038 | 0.00023 | 0.00013 | 0.00059 | 0.00097 | 0.00065 |
| 30 | 0.00057 | 0.00059 | 0.00023 | 0.00041 | 0.00064 | 0.00073 | 0.00027 |
| 40 | 0.00032 | 0.00041 | 0.00024 | 0.00030 | 0.00027 | 0.00007 | 0.00035 |
| 50 | 0.00059 | 0.00079 | 0.00024 | 0.00001 | 0.00010 | 0.00099 | 0.00182 |
| 60 | 0.00092 | 0.00119 | 0.00071 | 0.00015 | 0.00044 | 0.00202 | 0.00467 |
| 70 | 0.00039 | 0.00079 | 0.00019 | 0.00003 | 0.00032 | 0.00121 | 0.00351 |
| Stress Level % | NSC-SF | | | | | | |
| | 100°C | 200°C | 300°C | 400°C | 500°C | 600°C | 700°C |
| 10 | 0.00011 | 0.00015 | 0.00024 | 0.00005 | 0.00044 | 0.00124 | 0.00451 |
| 20 | 0.00028 | 0.00062 | 0.00060 | 0.00050 | 0.00002 | 0.00016 | 0.00070 |
| 30 | 0.00041 | 0.00071 | 0.00046 | 0.00006 | 0.00075 | 0.00052 | 0.00153 |
| 40 | 0.00064 | 0.00108 | 0.00064 | 0.00018 | 0.00061 | 0.00026 | 0.00424 |
| 50 | 0.00059 | 0.00085 | 0.00045 | 0.00070 | 0.00078 | 0.00088 | 0.00057 |
| 60 | 0.00042 | 0.00074 | 0.00046 | 0.00013 | 0.00075 | 0.00001 | 0.00109 |
| 70 | 0.00008 | 0.00038 | 0.00050 | 0.00011 | 0.00089 | 0.00146 | 0.00313 |
| Stress Level % | HSC-PP | | | | | | |
| | 100°C | 200°C | 300°C | 400°C | 500°C | 600°C | 700°C |
| 10 | 0.00014 | 0.00051 | 0.00079 | 0.00086 | 0.00103 | 0.00071 | 0.00022 |
| 20 | 0.00066 | 0.00088 | 0.00111 | 0.00097 | 0.00074 | 0.00230 | 0.00052 |
| 30 | 0.00030 | 0.00004 | 0.00045 | 0.00057 | 0.00146 | 0.00146 | 0.00054 |
| 40 | 0.00059 | 0.00072 | 0.00044 | 0.00022 | 0.00063 | 0.00004 | 0.00128 |
| 50 | 0.00077 | 0.00041 | 0.00042 | 0.00071 | 0.00093 | 0.00068 | 0.00097 |
| 60 | 0.00103 | 0.00079 | 0.00004 | 0.00098 | 0.00203 | 0.00124 | 0.00159 |

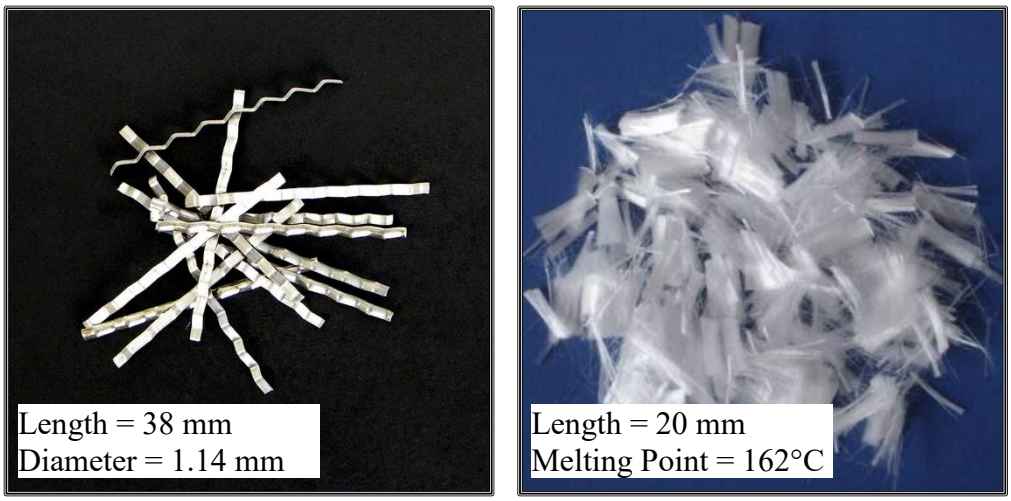


(a) Steel Fibers (b) Polypropylene Fibers

Figure 3.1 Type of steel and polypropylene fibers used in NSC and HSC specimens

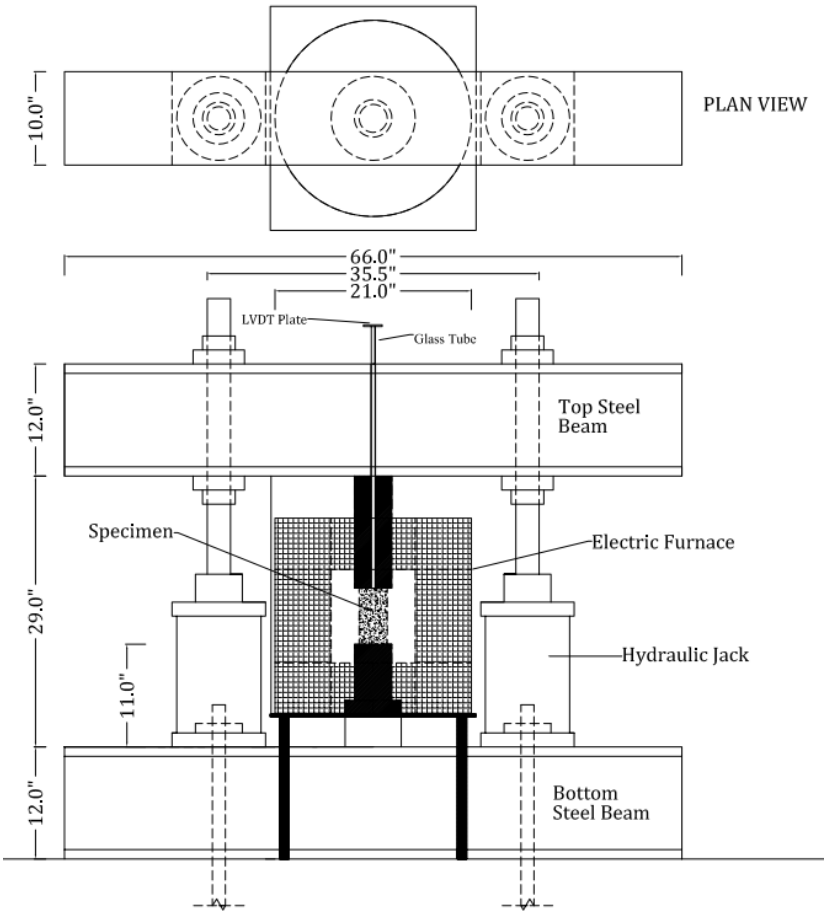


Figure 3.2 Schematic of specialized custom built test set-up for high-temperature transient creep tests

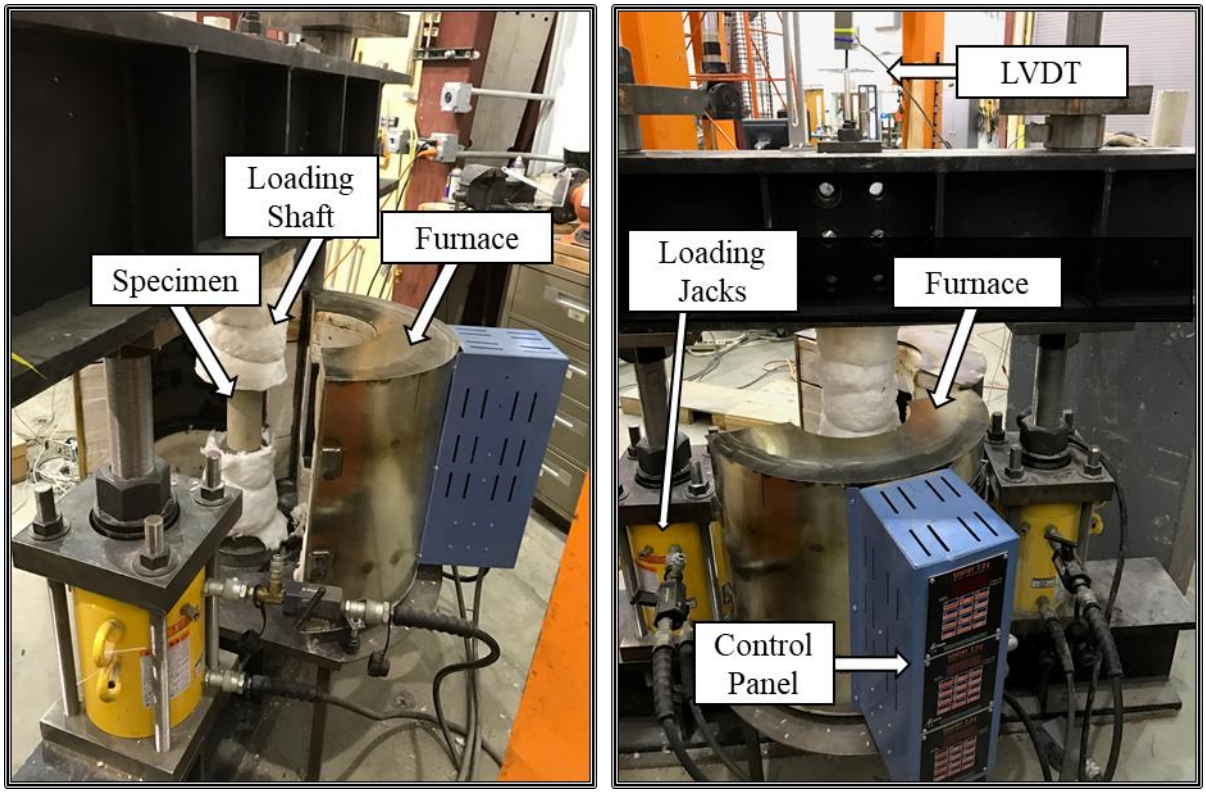


(a) Side view (b) Front view

Figure 3.3 Test set-up for undertaking transient creep tests

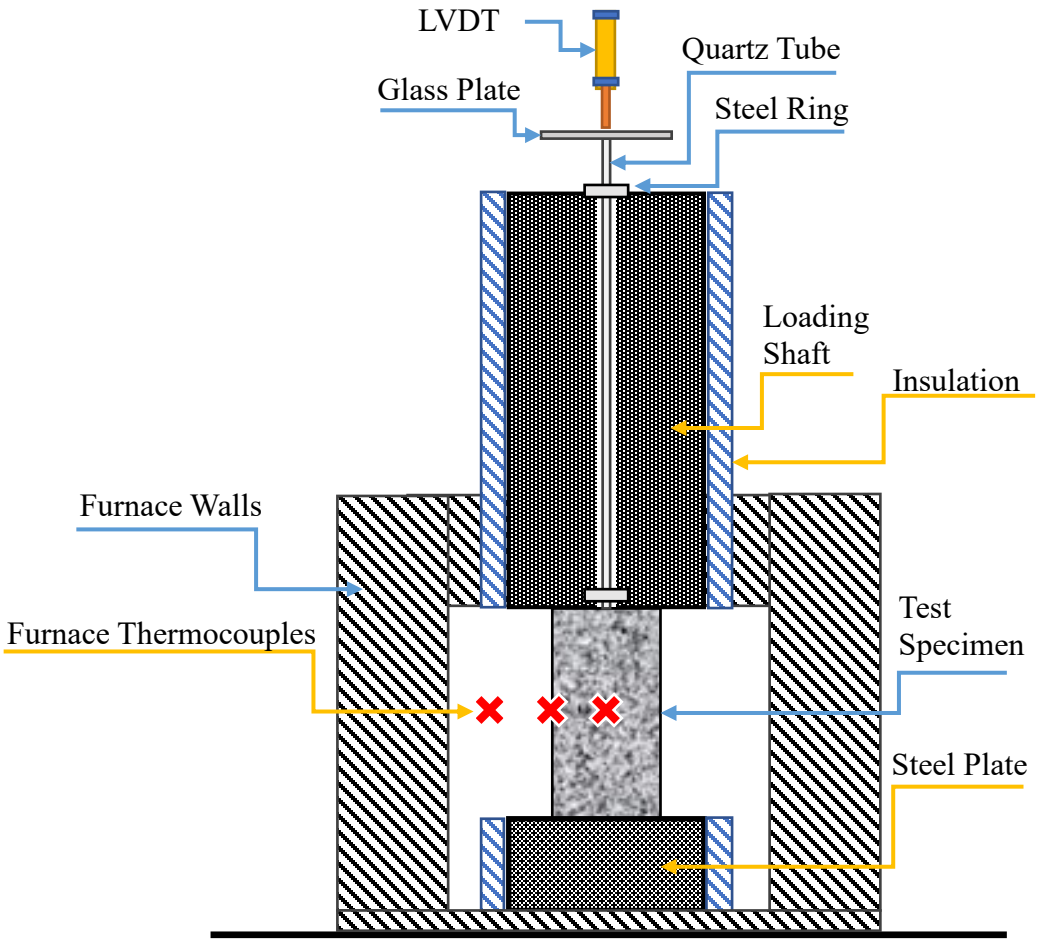


Figure 3.4 Apparatus for measuring axial displacement in test specimens

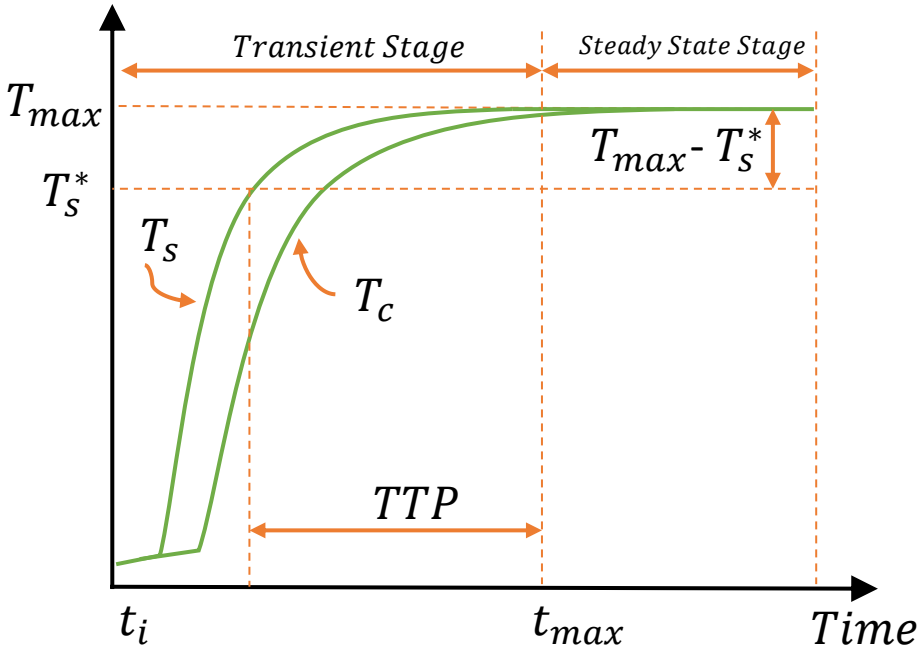


Figure 3.5 Temperature progression within a test specimen to be followed in transient creep tests as per RILEM standards

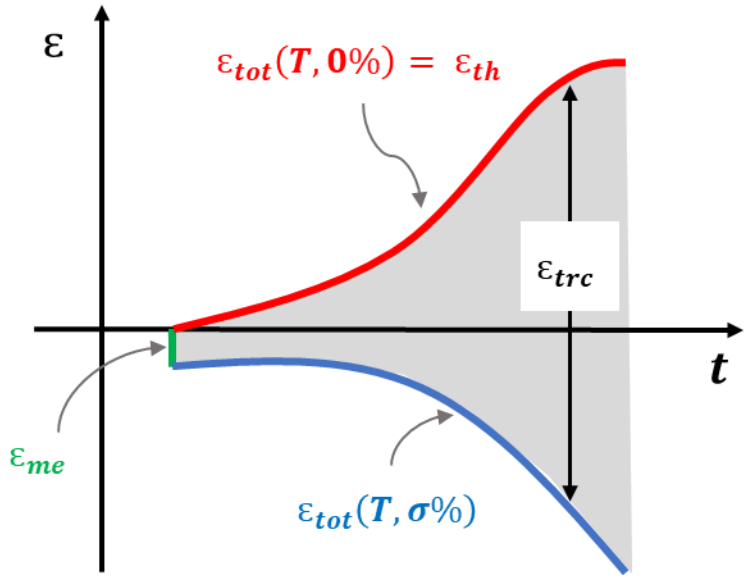


Figure 3.6 Calculating transient creep strain as per RILEM recommendations

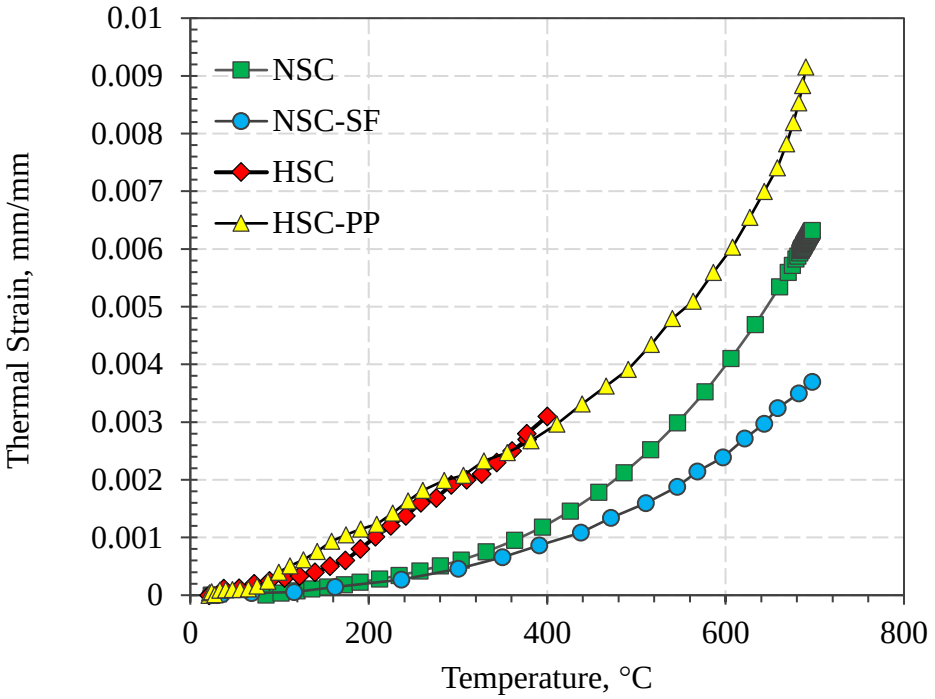


Figure 3.7 Variation of thermal expansion with temperature for different concretes

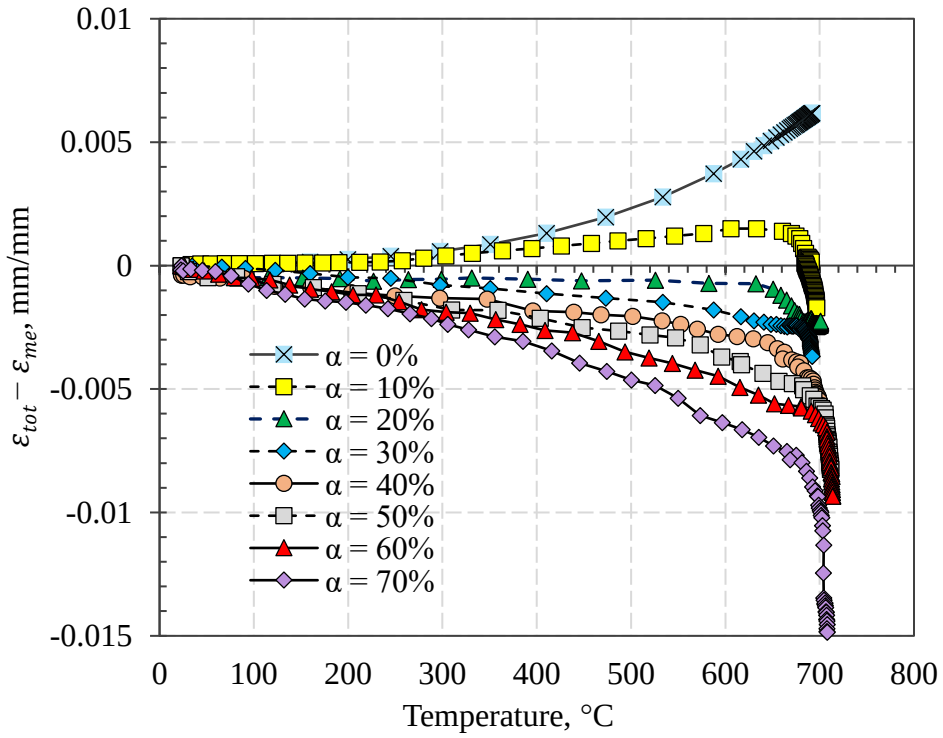


Figure 3.8 Total strain in NSC at various stress levels as a function of temperature

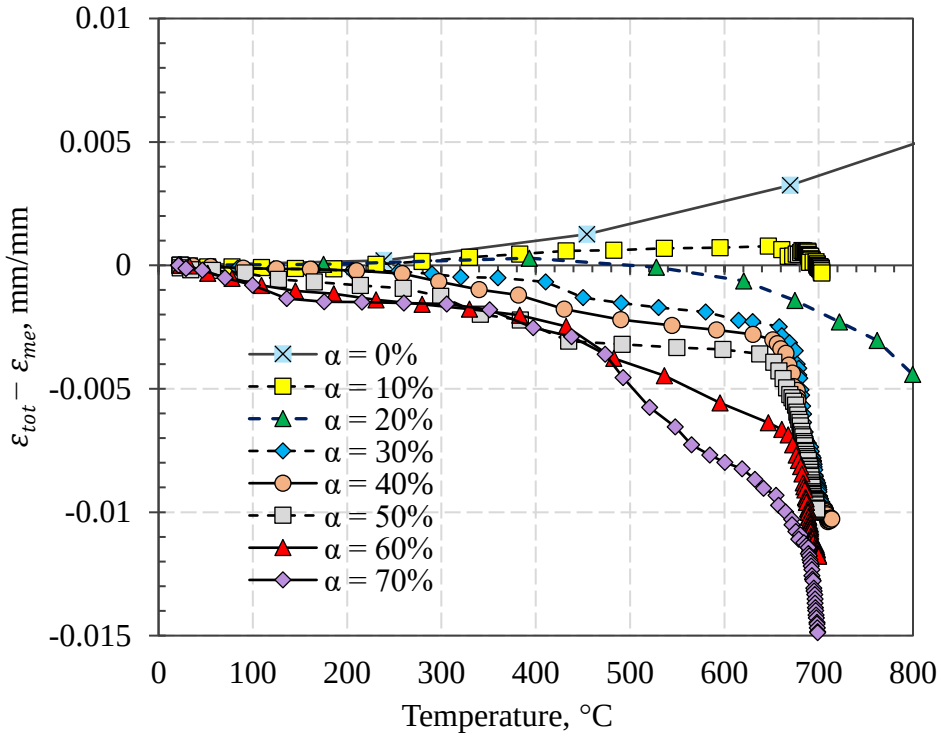


Figure 3.9 Total strain in NSC-SF at various stress levels as a function of temperature

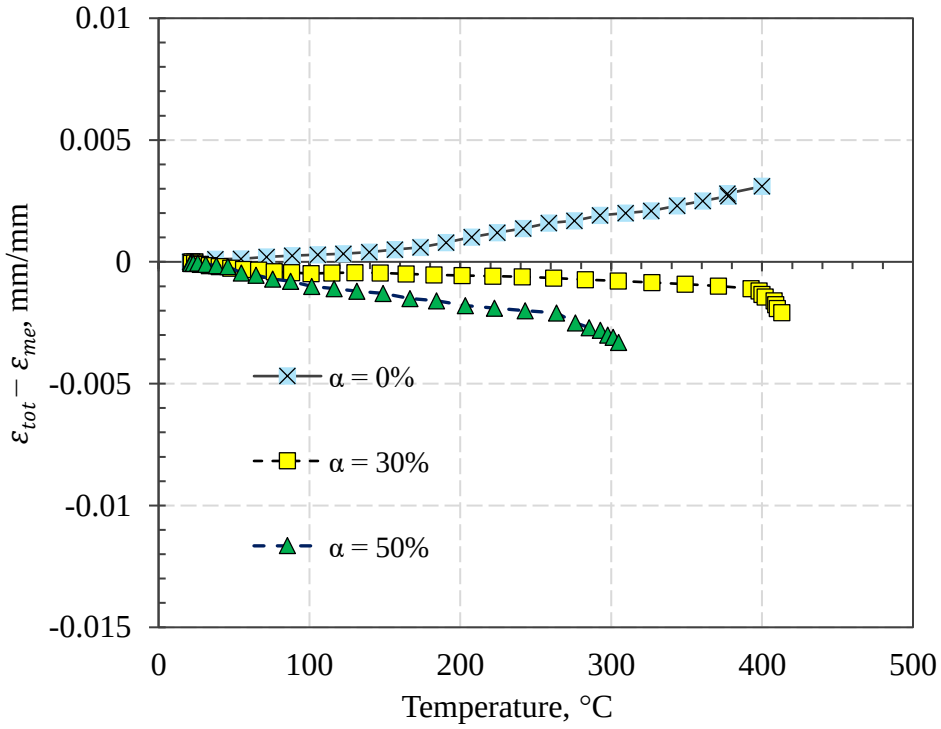


Figure 3.10 Total strain in HSC at various stress levels as a function of temperature

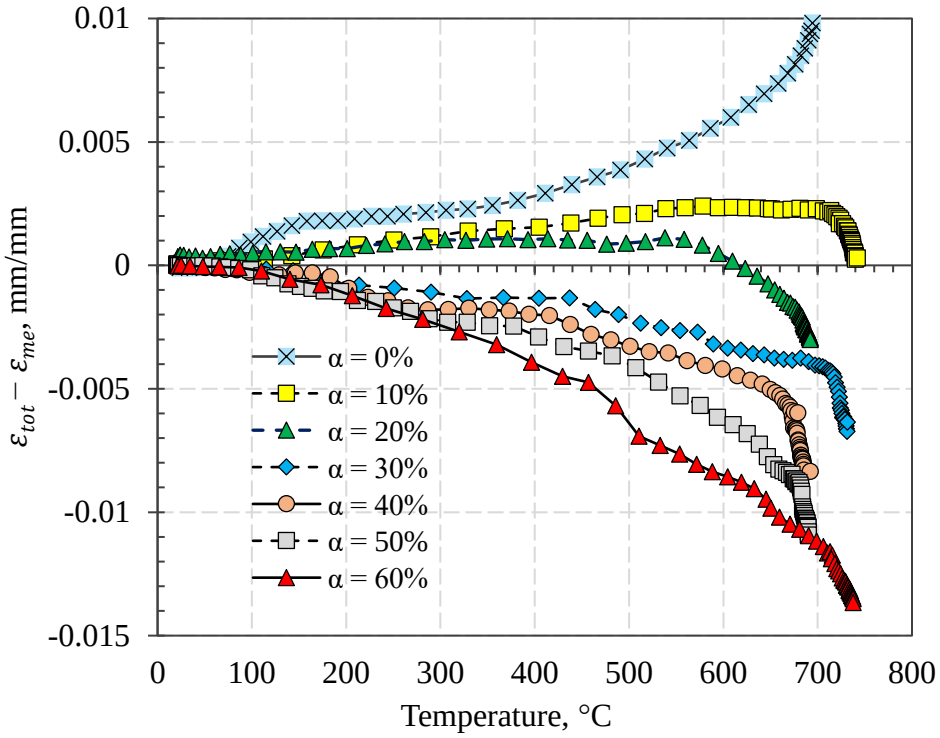


Figure 3.11 Total strain in HSC-PP at various stress levels as a function of temperature

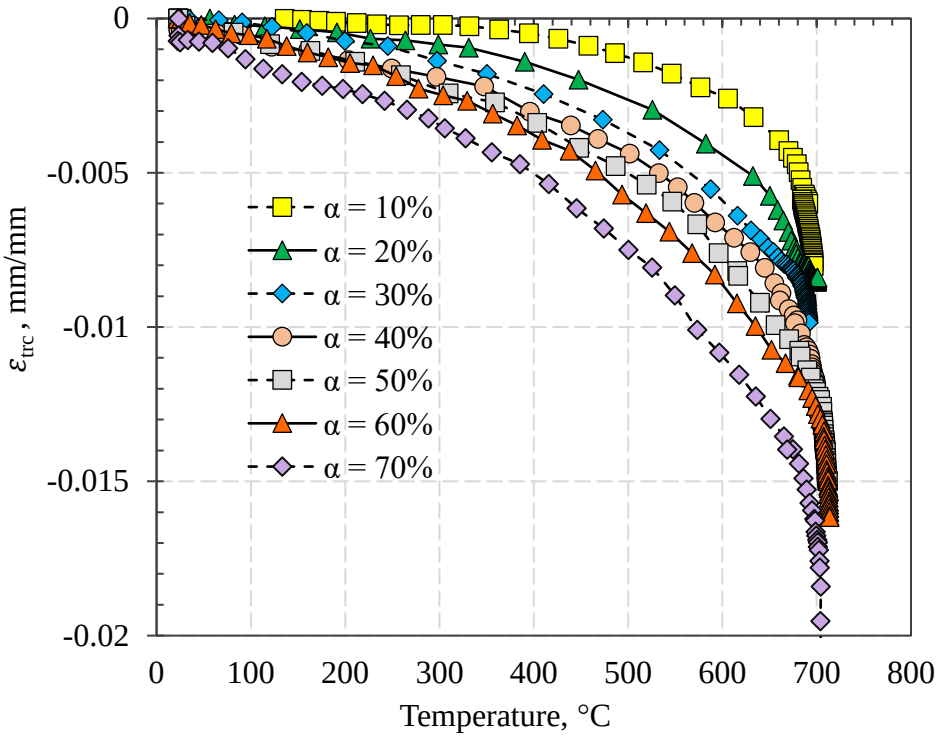


Figure 3.12 Transient creep strain in NSC as a function of temperature at various stress level

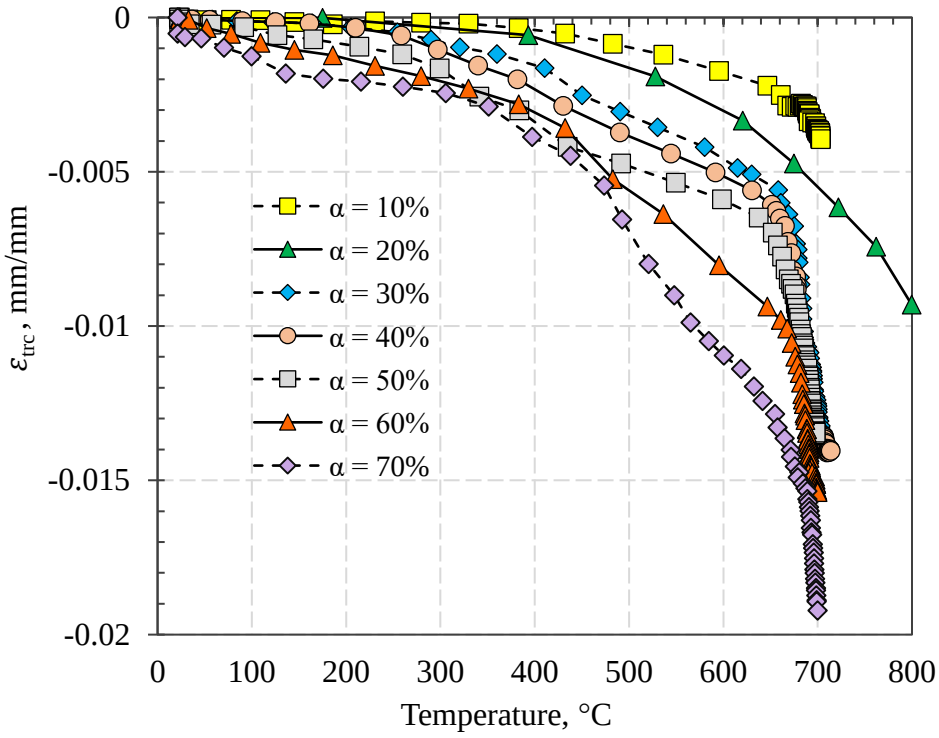


Figure 3.13 Transient creep strain in NSC-SF as a function of temperature at various stress level

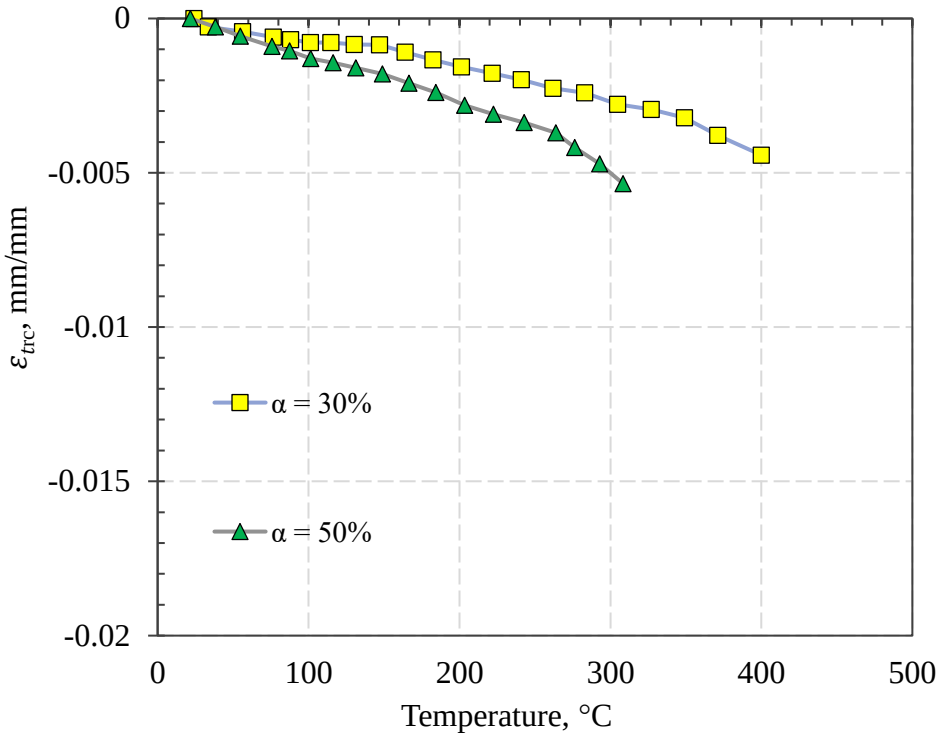


Figure 3.14 Transient creep strain in HSC as a function of temperature at various stress levels

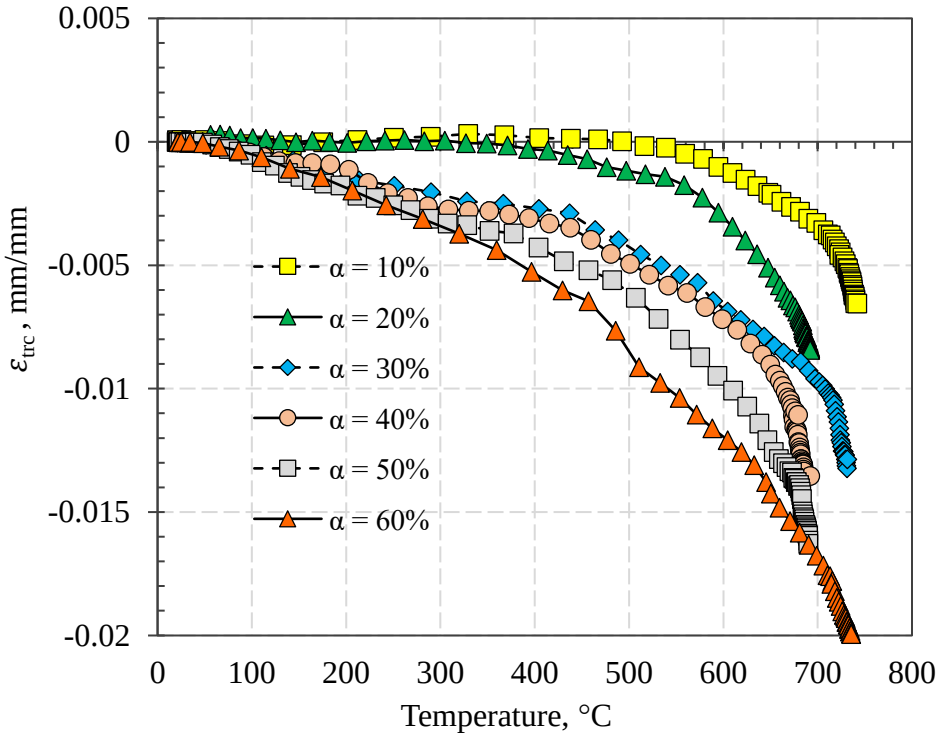


Figure 3.15 Transient creep strain in HSC-PP as a function of temperature at various stress levels

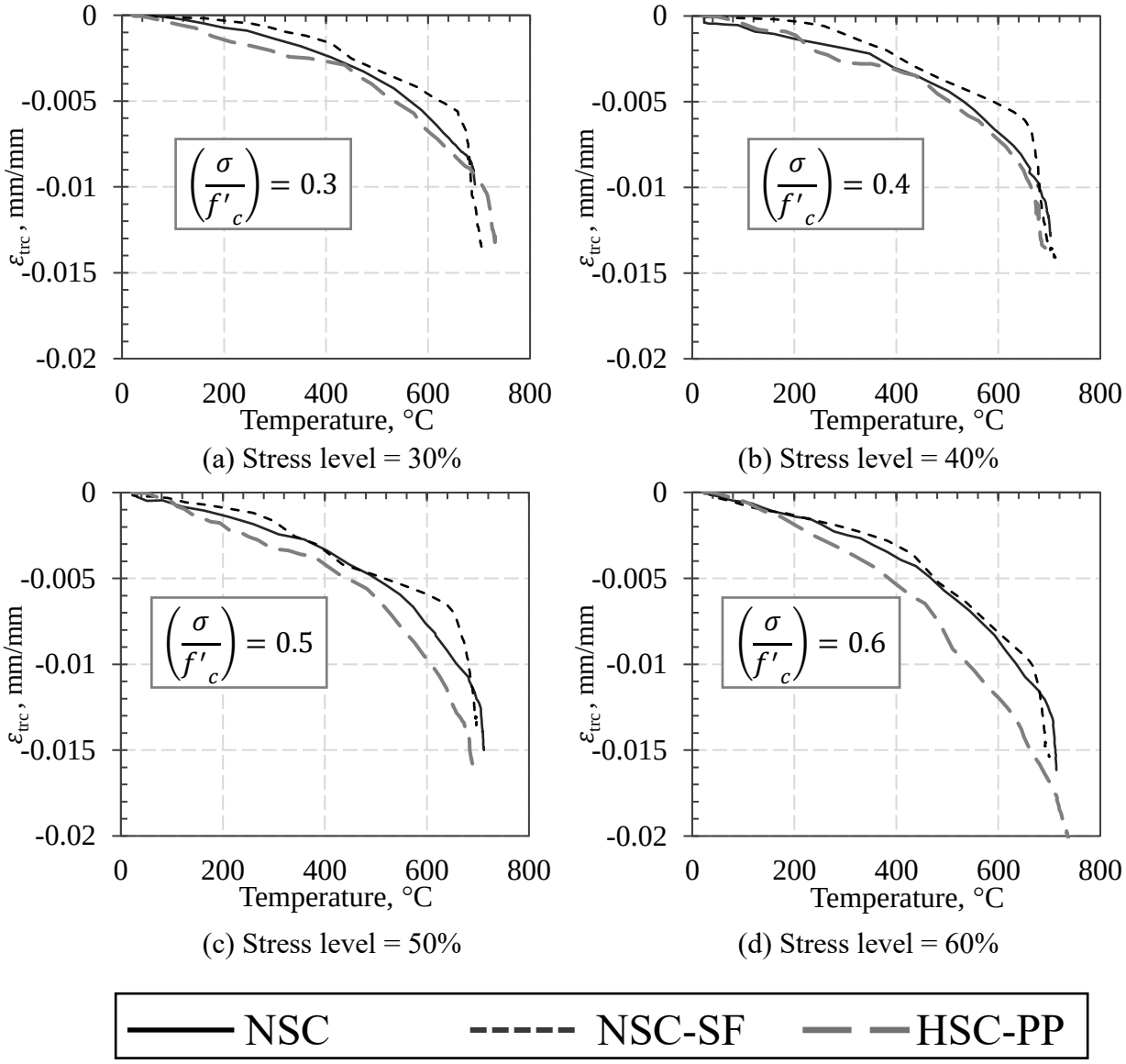


Figure 3.16 Effect of concrete type on transient creep strain of different concretes for various stress levels

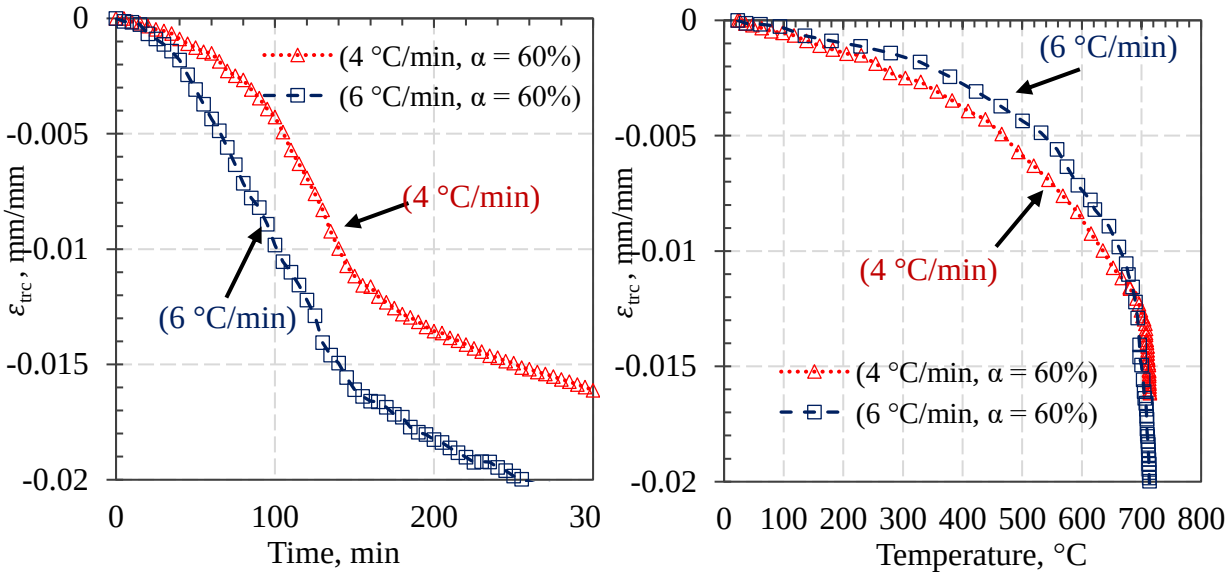


(a) Function of time (b) Function of temperature

Figure 3.17 Effect of heating rate on transient creep generation in NSC at stress level of 60%

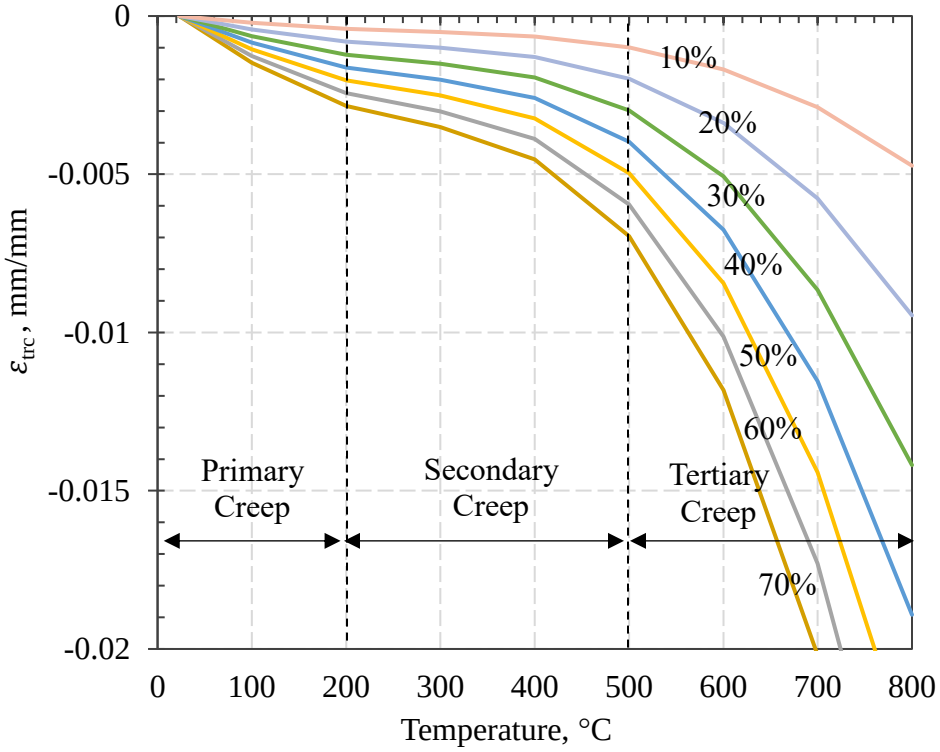


Figure 3.18 Proposed transient creep relation for NSC as a function of stress and temperature

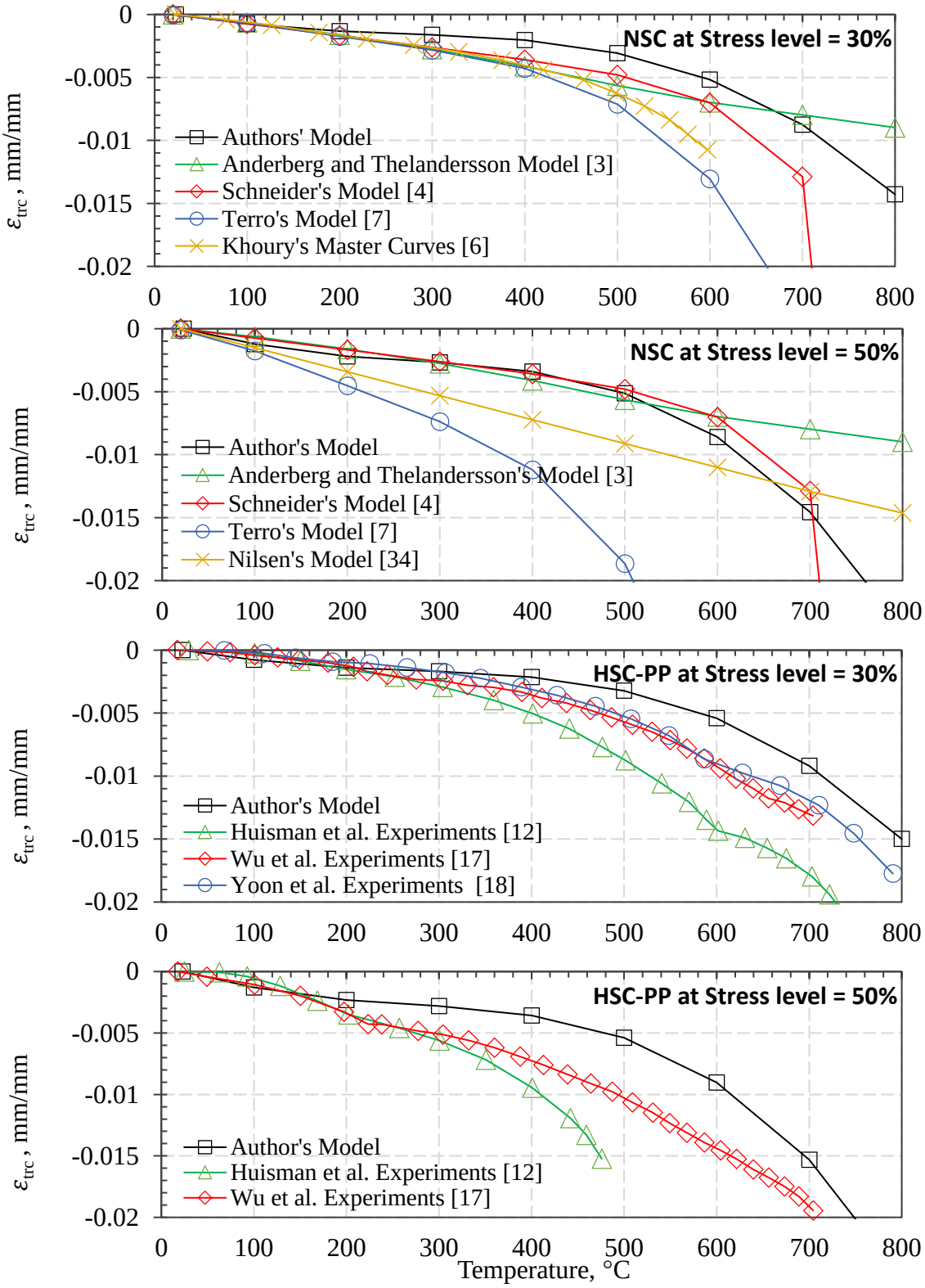


Figure 3.19 Comparison between proposed creep relation and previously published creep models and experiments for NSC and HSC-PP at different stress levels

# CHAPTER FOUR

# 4. Numerical Model

## 4.1. General

Fire resistance of structural members is still assessed mostly through prescriptive approaches, which are developed based on fire tests. There are numerous drawbacks on standard fire tests and hence reliable fire resistance cannot be generated. Further, the complexity involved in conducting fire tests together with scarcity of sophisticated fire testing facilities around the world, have highlighted the need for utilizing numerical modelling. In this study, a numerical modelling approach is applied to incorporate transient creep effects in evaluating behavior of RC columns under fire conditions. A three-dimensional numerical model is developed in the finite element program ABAQUS (2014) to trace the response of RC columns under different scenarios of fire exposure with explicitly accounting for high-temperature (HT) transient creep.

## 4.2. Development of Finite Element Model

Evaluating detailed response of concrete columns under fire conditions require the use of a finite element-based (FEM) computer software. The purpose of developing a numerical model is to study the creep effects in concrete columns under fire conditions, and then, quantify the influence of different parameters on transient creep strain in concrete columns. The developed model should account for high-temperature creep strains in evaluating fire resistance of concrete columns. Further, the model should account for changes in material property with temperature in the analysis to capture the fire-response of concrete columns correctly. Thus, the selection of the FEM computer software is to be carefully examined.

### 4.2.1. Selection of Finite Element Program

Several finite-element based computational software packages are available for undertaking thermo-mechanical engineering problems. Commercial programs such as ABAQUS, ANSYS, VULCAN and SAFIR are widely applied to simulate the response of structural members under fire conditions. In the current study, the general-purpose finite element program, ABAQUS, was selected to build the numerical model due to its various capabilities. This is due to the fact that ABAQUS can efficiently capture the response of different materials and can also account for high-temperature creep strains in analysis. ABAQUS provides users with built-in creep models which can be used to specify high-temperature transient creep in concrete columns under fire exposure. ABAQUS also offers various means to capture material and geometrical nonlinearities in thermo-mechanical problems and permits specifying temperature-dependent thermal and mechanical material properties. Further, the element library in ABAQUS is rich with options which can be used to simulate response of concrete and reinforcing steel.

Utilizing ABAQUS software, fire resistance can be carried out with incorporating transient creep strain in concrete columns. Further, other influencing parameters on fire resistance analysis of concrete columns can be considered in fire resistance analysis including material and geometrical nonlinearities, different fire scenarios, and loading conditions.

### 4.2.2. General Approach

When solving thermomechanical problems, thermal (heat transfer) and mechanical (structural) analysis can be either coupled or uncoupled depending on the type of problem. Coupled analysis is referred to as coupled temperature-displacement analysis whereas uncoupled analysis is typically divided into two consecutive stages of analysis: thermal and mechanical, and known as consequential thermo-mechanical analysis. Coupled temperature-displacement analysis is most

suitable for thermo-mechanical problems where temperature is strongly affected by load or deformation and the influence between temperature and displacement is reciprocal. For instance, metalworking problems can include considerable heating due to inelastic deformation or the metal which in turn significantly change the temperature and the property of the material. For thermo-mechanical problems where the influence of load and deformation on change in the material temperature is assumed to be insignificant, however, uncoupled temperature-displacement analysis can be applied. In evaluating fire response of structural members in incremental time steps, temperature distribution within the member is not significantly influenced by load nor by deformation in most cases.

Thus, fire resistance analysis of structural members can be carried out in two stages; namely; thermal and structural analysis and is to be carried out in various time increments, from start of fire exposure till failure or end of fire exposure. In thermal analysis, the distribution of temperatures within the structural member is generated at various nodes and stored as a function of fire exposure time (temperature history). These nodal temperatures predicted from thermal analysis are then applied as thermal loads for structural analysis. In the structural analysis, stresses and associated deformations resulting from considered effects of structural loading and high temperature (thermal) loading. Fire resistance analysis of structural members is generally carried out numerically according to the following steps:

- Selection of a fire exposure scenario (input time-temperature curve), geometry of the column, loading, etc.
- Components of the structural member are discretized into infinitesimal elements.
- Room temperature static structural analysis is performed on the structural members under applied loading to determine stresses and deformations.

- Thermal analysis: the distribution of cross-sectional temperatures is generated in the member.
- Structural analysis: apply the generated nodal temperature history as input for the fire resistance analysis.
- The fire resistance analysis is performed at incrementing time steps till failure occurs in the analyzed structural member.

The discussed general approach above is adopted in developing the numerical model for evaluating the fire response of concrete columns with accounting for creep strains in the analysis. Detailed analysis steps along with discretization of concrete columns and material models adopted in the analysis will be discussed in the subsequent sections.

### 4.2.3. Fire Exposure Scenarios

Typical fire scenarios implemented in fire resistance analysis can be grouped into two categories; namely, standard and realistic (design or natural) fire scenarios. Standard fire scenarios are specified fire temperatures variation with time (fire curves) in standards and codes. Fire scenarios such as ASTM E-119, and hydrocarbon, shown in Figure 4.1, are classified as standard fire scenarios. In design fires, on the other hand, variation in temperature with time is divided into two phases; heating and cooling. In the heating phase, temperature rise with time until reaching the maximum temperature of the fire, then the cooling phase start where fire temperatures cool down at a selected rate to room temperature as can be seen in Figure 4.1. Design fires require more parameters to be specified, such as fuel and ventilation, in order to determine rates of heating and cooling in the fire temperature-time curve. Fire scenarios F-90, F-120, and F-180 include a burning period as noted in minutes 90, 120, and 180 minutes, and a decay (cooling) phase. The temperature-

time curves for these fire scenarios including the decay phase is developed as per Eurocode 2 (2004) compartment fire characteristics.

Swedish fire curves and Eurocode 1 (Eurocode 1-2, 2002) parametric fire curves are two of the most popular examples of design (natural) fire scenarios. Further, for more realistic fire exposure scenarios, advanced computational fluid dynamics (CFD) models can be applied to determine the evolution of a fire in an enclosure with specified fuel and ventilation. However, utilizing such sophisticated approaches to predict fire temperatures is beyond the scope of this study. Thus, standard fire temperature-time curves together with design fire scenarios were selected in this study to compare with outcome of existing studies in the literature.

## 4.3. Incorporating Creep in ABAQUS

ABAQUS finite element software offers a number of creep models to account for long-term and short-term creep effects in various materials. Two of these creep models are implemented in the utilized numerical model in ABAQUS to account for temperature induced creep effects in evaluating fire response of RC columns. One is the Drucker-Prager creep model utilized for concrete transient creep and the second is CREEP power law utilized for reinforcing steel HT creep. Implementing these two creep models in the finite element model represents a new approach to account for transient creep in RC columns under fire exposure (Kodur and Alogla, 2016). Others have utilized different approaches to account for transient creep but not through this approach in ABAQUS (Sadaoui and Khennane, 2009; Gernay, 2011; Huang and Burgess, 2012; Gernay and Franssen, 2012). When performing viscoelastic analysis in ABAQUS, the total strain rate is assumed to be a linear summation of three strain components:

$$d\varepsilon = d\varepsilon^{el} + d\varepsilon^{pl} + d\varepsilon^{cr} \qquad \text{.....[4.1]}$$

where $d\varepsilon$ represents the total strain rate, which constitutes of elastic, plastic, and creep strains. The elastic and plastic concrete strains are input in the material module in ABAQUS in the form of constitutive material (concrete and steel) stress-strain relations for various temperatures. High-temperature creep strain in concrete and steel is input in the form of coefficients defining the two selected creep power laws.

Creep models in ABAQUS can be used in two forms: time hardening, and strain hardening. Time hardening form is used when the stress state is constant. Creep strain rate ($\dot{\varepsilon}_{cr}$) is written in this case as a function of time ($t$) and stress ($\sigma_s$) and is variant with temperature ($T$). The second form, strain hardening, is used for cases where stress is changing with time. Creep strain rate ($\dot{\varepsilon}_{cr}$) in this case is written as a function of creep strain ($\varepsilon_{cr}$) and stress ($\sigma_s$) and is variant with temperature ($T$). Both of these forms are integrated with respect to time during the analysis as:

$$\varepsilon_{cr} = \int_0^t \dot{\varepsilon}_{cr}(t, \sigma_s)\ dt \quad \text{.....[4.2]}$$

$$\varepsilon_{cr} = \int_0^t \dot{\varepsilon}_{cr}(\varepsilon_{cr}, \sigma_s)\ dt \quad \text{.....[4.3]}$$

Strain hardening form of creep is selected in the numerical model built in ABAQUS since HT creep develops at a very rapid pace within a short duration compared to that at ambient temperature. Thus, time hardening rule is irrelevant to transient creep problem from fire resistance analysis consideration. Both the Drucker-Prager creep model for concrete and the CREEP power law for steel have the same "strain hardening" form as in Eq. 4.3. The creep model for strain hardening in ABAQUS for both concrete and reinforcing steel is expressed as:

$$\dot{\varepsilon}_{cr} = (A\ (\sigma_s)^n[(m+1)^m\ \varepsilon_{cr}]\ ^m)^{\frac{1}{m+1}} \quad \text{.....[4.4]}$$

where $\dot{\varepsilon}_{cr}$ is the creep strain rate, $\sigma_s$ is the stress and $A$, $n$, and $m$ are user-defined creep material parameters specified as temperature dependent data. For concrete and reinforcing steel, HT creep versus stress curves are generated at different temperatures based on the available creep relations

in the literature (see Section 2.3.). Then the parameters *A*, and *n* are calculated by curve fitting of generated creep data to the creep power law in ABAQUS. The *A*, and *n* are to be taken as positive numbers and, $-1 < m \leq 0$ as per ABAQUS recommendations. By assuming $m = 0$, equation [4.4] reduces to:

$$\dot{\varepsilon}_{cr} = A\ (\sigma_s)^n \qquad \text{.....[4.5]}$$

Utilizing the presented creep relations in Section 2.3., a family of creep strain versus stress curves were generated for temperatures ranging from 20°C to 1000°C. The curve fitting of linear or parabolic material creep models was achieved by setting the power parameter, n, to 1 and 2 for each case, respectively. For each creep strain versus stress curve equation [4.5] is fitted based on the least square method and the corresponding parameter, *A*, is calculated. For instance, the curve for transient creep strain versus stress at 500°C, and based on Schneider's (1986) creep relation, is shown in Figure 4.2 along with fitted curve to predict the value of *A*.

The one-dimensional HT transient creep relation is transformed to the three-dimensional space in ABAQUS utilizing similar approach to the uniaxial stress-strain curves. The creep behavior in Drucker-Prager material model in ABAQUS is intimately tied to the plasticity behavior. ABAQUS adopts the notion that when the material reaches the plastic range, the generated creep surface, through definition of creep data and flow potential, should coincide with the yield surface. Consequently, the creep surfaces are defined by homogeneously scaling down the yield surface (ABAQUS, 2014). Thus, creep effects are included in the three-dimensional space for concrete through modifying the Drucker-Prager yield criteria. The yielding criterion for the linearly Drucker-Prager (DP) model for concrete is expressed as

$$d - tan\delta h - k = 0 \qquad \text{.....[4.6]}$$

where

$$d = f(K)\sqrt{J_2} = f(K)\sqrt{\frac{1}{6}[(\sigma_1 - \sigma_2)^2 + (\sigma_2 - \sigma_3)^2 + (\sigma_3 - \sigma_1)^2]} \quad \text{.....[4.7]}$$

$$h = \frac{-I\,1}{3} = \frac{-(\sigma_1+\sigma_2+\sigma_3)}{3} \quad \text{.....[4.8]}$$

and

$$f(K) = \frac{\sqrt{3}}{2}\left[1 + \frac{1}{K} - \frac{3\sqrt{3}}{2}\left(1 - \frac{1}{K}\right)\left(\frac{\sqrt[3]{J_3}}{\sqrt{J_2}}\right)^3\right] \quad \text{.....[4.9]}$$

In the above equations $\sigma_i$ represent the stress in the $i$ direction, constant $k$ represent the hardening or softening parameter that control the yielding surface and the development of subsequent yielding surfaces in the stress domain, and,$\delta$, friction angle, controls the slope of the yield surface, typically taken as 37° for concrete. The yield surface based on the DP criteria is plotted in Figure 4.3 in the stress domain along with subsequent yield surfaces based on the outlined equations above. The function $f(K)$, is an expression that combines the second and third invariants $J_2$, and $J_3$ while K is the factor which determine the shape of the yielding surface with its value ranging from 0.8 to 1.0 as shown in Figure 4.4. The flow rule in the DP criterion is governed by plastic potential function,$G$, as follows:

$$G = d - tan\beta h + constant \quad \text{.....[4.10]}$$

where $\beta$ represent the dilation angle of the material, and its value for concrete is around 31°. Thus, by adopting Drucker-Prager material model and with the knowledge of uniaxial compression stress-strain curves of concrete and corresponding parameters $\delta$, $\beta$, and $K$, three-dimensional response of concrete members can be traced. In the DP model, transient creep strain of concrete is specified as mentioned as a function of stress and temperature since it increases with rise in stress and temperature.

## 4.4. Analysis Details

Fire resistance analysis in the model is performed in a number of time steps, till failure of the column, using the sequentially coupled thermo-mechanical analysis procedure. In the thermal analysis, heat transfer analysis is performed in which the column is exposed to specified fire from four sides. The resulting nodal temperatures from the thermal analysis are input in the model for the structural analysis where the properties of constituent materials at variant temperatures are defined along with loading and boundary conditions. A flow chart illustrating the various analysis steps followed in the developed numerical model is shown in Figure 4.5. The model follows generally the thermo-mechanical approach for fire resistance analysis of structural members with explicitly accounting for HT creep strains in fire resistance analysis.

ABAQUS analysis was carried out at a maximum time step of 5 minutes, with "automatic incrementation" option selected to automatically reduce the time steps, towards the failure zone to minimize convergence problems. This "automatic incrementation" requires specifying a maximum, minimum, and initial time increments and the chosen input values in this study are 5 minutes, 1E-4 second, and 1 second, respectively. This allows ABAQUS to reduce the time step towards the failure stage of analysis to overcome convergence problems. Detailed analysis steps of the model are presented in the following sections of this chapter.

### 4.4.1. Thermal Analysis

To simulate the response of an RC column under fire conditions, temperature-dependent thermal properties of concrete and reinforcing steel are to be input into ABAQUS. The thermal properties include thermal conductivity, specific heat, and thermal expansion. The variation of thermal properties of concrete and reinforcing steel with temperature in the model follows relations specified in Eurocode 2 (2004). In thermal analysis, conductivity is assumed to be isotropic

temperature-dependent, and specific heat is assumed to be based on constant volume concept for both concrete and reinforcing steel. Thermal elongation for concrete and reinforcing steel is specified as temperature-dependent coefficient of thermal expansion. Heat transfer to the column from fire zone is simulated using convection and radiation, namely surface film condition and surface radiation.

After transfer of heat from fire to the column faces through convection and radiation, propagation of heat within the column is governed by conduction. The assumption of isotropic thermal conductivity in the developed model simplifies the governing differential equation for heat transfer through conduction within the column cross-section to:

$$\rho c_{(T)} \frac{dT}{dt} = \nabla . \left( k_{(T)} \nabla T \right) \quad \text{[4.11]}$$

where,

$k$ = conductivity,

$\rho$ = density,

$c$ = specific heat,

$T$ = temperature,

$t$ = time, and

$\nabla$ = is the *Laplacian operator*.

For the boundary equations which govern transfer of heat from fire to columns faces through convection and radiation in the thermal analysis, heat transfer is assumed to be as follow:

$$q_b = (h_{con} + h_{rad})(T - T_f) \quad \text{[4.12]}$$

where,

$h_{con}$= the coefficient of convective heat transfer,

$h_{rad}$ = the coefficient of radiative heat transfer, and is calculated as:

$$h_{rad} = 4\sigma\varepsilon\left(T^2 + T_f^2\right)(T + T_f) \quad [4.13]$$

where,

$T_f$ = temperature surrounding column's boundary (fire temperature),

$\sigma$ = Stefan-Boltzman constant,

$\varepsilon$ = emissivity factor which is related to exposed surface of structural member to the fire.

In addition to heat transfer properties, emissivity and convective factors, are input into the model. A pre-defined time-temperature fire curve is input as the reference temperature for heat transmission from fire source to exposed surfaces of RC member (column). A convection heat transfer coefficient, $h_{con}$ , of 25, 50, and 35 W/(m$^2$ °C), is utilized for surface film condition for building, hydrocarbon, and design fires, respectively. An emissivity, $\varepsilon$, of 0.7 and Stefan-Boltzmann radiation constant of $\sigma_s = 5.67\times10^{-8}$ W/(m$^2$ K$^4$) are utilized for radiative heat transfer.

In thermal analysis, heat flux and temperature gradient are related through Fourier's law of heat conduction as:

$$q = -k\nabla T \quad [4.14]$$

In Fourier's law, heat transfer is governed by the following equation on boundary of exposure (column faces):

$$k\left(\frac{\partial T}{\partial y}n_y + \frac{\partial T}{\partial z}n_z\right) = -q_b \quad [4.15]$$

where, $n_y$ and $n_z$ represent the components of the normal vector to the boundary in the plane of column's cross section. The term $q_b$ in Eq. [4.15] is dependent on the imposed boundary condition on columns faces. Two types of boundary equations are considered in thermal analysis as follow:

- On boundaries exposed to fire, the heat flux is given by the following equation:

$$q_b = -h_f(T - T_f) \quad [4.16]$$

- On unexposed boundaries, heat flux is governed by the following equation:

$q_b = -h_0(T - T_0)$……...[4.17]

where, $h_f$ and $h_0$ = coefficients of heat transfer on exposed and unexposed sides of the column, and $T_f$ and $T_0$ = temperatures at exposed and unexposed sides, respectively. Nodal temperatures of elements are then approximated by appropriate shape functions matrix (N) as follow:

$T = \{N\}^T . T_e$…….[4.18]

Following this, appropriate boundary conditions (Eq. 4.15) are applied to the heat transfer equation (Eq. 4.11), and discretization is performed as per Cook's (Cook et al., 2007):

$C_e^t \dot{T}_e + K_e^t T_e = Q_e$……..[4.19]

where, $C_e^t$ represent the specific heat matrix, $K_e^t$ represent the thermal matrix, i.e. the sum of conductivity and convection matrices. $Q_e$ represent the applied nodal thermal load and is comprised of the convective and radiative heat fluxes. And finally, $T_e$ is the nodal temperatures matrix.

In thermal analysis, distribution of temperatures within the concrete column is generated and stored as a function of fire exposure time (temperature history). Nodal temperatures predicted from thermal analysis are then applied as input for structural analysis. In the developed model, flow chart in Figure 4.5, the following summarize the steps undertaken in the thermal analysis part of fire resistance analysis:

- Start of thermal analysis, in which geometry, mesh size, and element types and numbers are defined. Discretization of the column is performed in the model based on the selected mesh properties and type of elements.
- Input the fire temperatures and boundary conditions for thermal analysis.

- The temperature-dependent thermal properties for concrete are input along with coefficients for convective and radiative heat transfer.
- The sectional temperatures in the concrete member are calculated based on heat transfer from fire source to the column's faces through convection and radiation.
- Then heat transfer is governed by conduction within the member.
- From thermal analysis, temperature history (temperature versus time) for total duration of fire exposure is calculated for the specified discretization of nodes and elements. Each node in the mesh consists of one degree of freedom (temperature).
- The temperature history of the column is then input in the structural sub-model along with geometry, boundary conditions, mesh size, and element types for structural analysis.

### 4.4.2. Structural Analysis

After generating the nodal temperatures in the column, structural analysis can be carried out to determine the structural response under fire conditions. Structural analysis in ABAQUS is performed based on the principle of virtual work in which the internal strain energy must satisfy the following equation:

$$\delta U = \delta V \quad \text{[4.21]}$$

where; U is strain energy and V is the external work exerted on the body. Variaition in this strain energy can be assessed according to:

$$\delta U = \int \{\delta \varepsilon\}\, \sigma\, dv \quad \text{[4.22]}$$

For concrete members subjected to fire exposure, the strain vector is the sum of three strain components; thermal ($\varepsilon_{th}$), mechanical ($\varepsilon_{me}$), and transient creep strain ($\varepsilon_{tcr}$).

$$\varepsilon = \varepsilon_{th} + \varepsilon_{me} + \varepsilon_{tcr} \quad \text{[4.23]}$$

Variation in exerted external work on the body ($\delta V$) due to applied forces at nodes ($F_e^n$) is computed assuming a variation in nodal displacement $\{\delta u\}$ acoording to:

$$\delta V = \{\delta u\}^T \{F_e^n\} \quad \text{.....[4.24]}$$

Nodal displacements ($u_e$) of the elements are related to the nodal displacement field by way of shape functions matrix ($N$) as:

$$u_e = \{N\}^T . u \quad \text{.....[4.25]}$$

This allow for rerwriting of the vritual work eqaution (Eq. 4.21) in matrix form as:

$$K_e u_e - F_e^{th} = F_e^n \quad \text{.....[4.26]}$$

where $K_e$ represent the element stiffness matrix, and $F_e^{th}$ is the element thermal load vector.

As shown in the model flowchart in Figure 4.5, the steps followed in structural analysis part of fire resistance can be summarized in the following:

- The temperature history of the column (from thermal analysis) is input in the structural sub-model along with geometry, boundary conditions, mesh size, and element types.
- The column is discretized for structural analysis based on specified mesh and elements properties.
- Assembly of the stiffness matrix, where temperature-dependent mechanical properties are input along with creep properties. In the followed approach Drucker-Prager creep model in ABAQUS was adopted for accounting for transient creep strain in concrete.
- Incorporating transient creep strain in the structural analysis as explained in Section 4.3.
- Based on the assembled stiffness matrix, stresses and strains in the concrete column can be calculated. At each node, six degrees of freedom are calculated representing forces and displacements in three dimensions x, y, and z.

- Based on the developed strains in the analyzed concrete column, axial displacement variation with time is calculated.
- Failure limit states are applied to determine failure using strength and displacement criteria. Displacement and rate of displacement failure limits for vertically loaded members, according to ISO834-1 (1999), are 0.01*h* mm and 0.003*h* mm/min where *h* is the height of the column in mm.
- Finally, the duration to the point at which the strength or deflection limit is exceeded represents the fire resistance of the column.

### 4.4.3. Discretization of Concrete Columns

For thermal analysis, reinforced concrete columns are discretized into two different sets of elements in three-dimensional space as shown in Figure 4.6. Concrete is discretized utilizing an 8-noded linear hexahedron heat transfer brick element, of type DC3D8, with linear geometric order. Steel reinforcement is discretized using a 2-noded linear heat transfer link of type DC1D2 with linear geometric order. Both these elements have temperature as the only active degree of freedom at each node. The external surface areas of the DC3D8 brick elements absorb heat through convection and radiation as the main heat transfer mechanisms. These 3-D elements are applicable to steady-state or transient thermal analysis.

For structural analysis in three-dimensional space, the RC column is discretized using two types of elements, namely, C3D8R, for concrete and, T3D2, for reinforcing steel as shown in Figure 4.6. C3D8R is a continum linear brick element capable of capturing cracking, crushing, creep, and large strains in concrete with 8-nodes and reduced integration. T3D2 is a 2-noded linear 3D truss element. Both these elements are of linear geometric order and have three degrees of freedom at each node; namely, three translations in x, y, and z directions.

The interaction between reinforcing steel and concrete is modeled utilizing embedded region constraint, i.e. defining reinforcement to be embedded in concrete as shown in Figure 4.6. A mesh (size) of 25 mm “cube” for concrete elements and 25 mm length “link” for reinforcing steel is selected for the analysis. The effect of geometric non-linearity is included in the analysis through an updated Lagrangian method, and Newton-Raphson based solution technique is utilized. A tolerance limit of 0.02 is selected as the convergence critieria in displacement norm.

During preliminary analysis, the mesh size adopted for concrete elements was varied to study the influence of mesh size on the predicted axial displacement in columns, as compared to measured axial displacement in fire tests. For concrete, the size of cubic elements was varied between 20 mm to 27 mm, and the steel reinforcement was varied similarly. The size of 25 mm elements produced the optimum results among the studied mesh sizes based on the results of the studied columns. Further, smaller mesh sizes, of 23 mm and less, lead to higher computational time. Thus, for optimization of results and consistency in the analysis, the elements size was unified in all studied columns (to 25 mm).

## 4.5. Material Properties at Elevated Temperature

Specific material property models are to be selected to generate temperature-dependent property data. This include thermal and mechanical property data together with data for transient creep strain. To generate such data for material property variation with temperature, available relations in codes of practice and literature can be utilized. However, a significant variation exists between various material constitutive laws at elevated temperature for both concrete and reinforcing steel. Further, current transient creep relations show slight variation as presented and discussed in Chapter 2. These variations in material property models slightly affect the predicted response of concrete columns under fire exposure and can change estimated fire resistance. Thus,

it is essential to decide on suitable material models in FEA that can accurately capture response of RC columns under fire conditions.

### 4.5.1. Thermal Property Relations

Thermal properties of concrete and reinforcing steel together with fire exposure scenario are what governs temperature distribution within concrete columns. These temperature-dependent thermal properties include thermal conductivity and specific heat for concrete and reinforcing steel. Temperature-dependent thermal properties specified in Eurocode 2 (2004) are applied in the developed model. The relations for temperature-dependent thermal properties are presented in Tables 4.1 and 4.2.

### 4.5.2. Mechanical Property Relations

To simulate the response of an RC column under fire conditions, temperature-dependent mechanical properties of concrete and reinforcing steel are to be input into ABAQUS. The mechanical properties comprise of density, poison's ratio, stress-strain relations, and creep strains. The mechanical properties which are most critical for fire resistance analysis in the developed model are temperature-dependent stress-strain constitutive relations and transient creep strain data. Transient creep strain variation with temperature is important since the model is intended to explicitly account for transient creep strain in reinforced concrete columns when exposed to fire. Based on the conducted experiments in Chapter 3, a set of transient creep data is generated for each tested type of concrete (NSC or HSC). Then the generated data is incorporated into the model to account for transient creep in concrete. Transient creep in concrete is explicitly accounted for in this developed numerical model through utilizing the Drucker-Prager material model available in ABAQUS.

Drucker-Prager is utilized for concrete since it can capture concrete compressive behavior and creep effects. In the Drucker-Prager model, transient creep strain of concrete is specified as a function of stress and temperature since it increases with rise in stress and temperature as discussed in Section 2.3. The measured transient creep data in Chapter 3 along with existing creep relations for NSC (Section 2.3) are utilized for generating transient creep strain for numerical modeling. Relations proposed by Schnider (1986), Nilsen (2002), and Terro (1998) are implemented in the developed model to study the influence of transient creep.

Concrete compressive stress-strain behavior has an elastic range, a nonlinear hardening range, and a softening range as shown in Figure 4.7. These stress-strain constitutive relations for concrete at various temperatures are summarized in Table 4.2. Reduction factors (temperature-induced degradation factors) associated with concrete constitutive relations to predict the strength of concrete at elevated temperatures, $f_{c,T}$ , together with the values of strain at maximum stress, $\varepsilon_{c1,T}$, and ultimate strain, $\varepsilon_{cu1,T}$, are summarized for various temperatures in Table 4.3. Concrete tensile behavior is expressed as a bilinear stress-strain curve, with tensile strength to be 10% of the compressive strength. Concrete tensile stress-strain curve includes the elastic range, and the post-cracking and softening range.

The temperature dependent stress-strain curves of reinforcing steel include a linear elastic range, a strain hardening range, and a softening range and follow relations presented in Eurocode 2 (2004) as shown in Figure 4.8. Stress-strain curve of reinforcing steel is linear up to the proportional limit, $f_{sp,T}$, then strain hardening range in stress-strain curve starts up to the maximum stress, $f_{sp,T}$. The softening range of the stress-strain curve in reinforcing steel is determined by the strain values of $\varepsilon_{st,T}$ , and $\varepsilon_{su,T}$. The characteristic values of these stress and strain curves at various temperatures is specified in Eurocode 2 (2004).

Explicit creep of reinforcing steel at high temperature is accounted for through CREEP power law option available in ABAQUS as discussed in Section 4.3, and this law parameters were calculated based on work of Williams-leir (1983). Similar to concrete, high-temperature creep in reinforcing steel is a function of stress and temperature.

## 4.6. Failure Limit States

Failure of RC columns in prescriptive based approach is evaluated based on critical temperature attained in reinforcing steel, specified as 593°C in ACI216R (2014), or through applying strength failure limit state. ISO834-1 (1999) also provides a displacement based failure criterion for evaluating failure of vertically loaded members such as columns in fire tests. Since transient creep effects; and thus deformations, can be significant in columns, failure during fire can be through limiting displacement. Therefore, applying displacement-based failure limit state to determine failure is critical for evaluating the realistic response of columns. Displacement and rate of displacement failure limits for vertically loaded members, according to ISO834-1 (1999), are $0.01h$ mm and $0.003h$ mm/min where $h$ is the height of the column in mm. However, it has been shown by Dumount et. al. (2016) that these displacement based criteria are more applicable to ductile members (steel members) and are unconservative for brittle structural members such as RC columns. Moreover, it has been shown from results of analysis that these displacement-based failure limits are unconservative when compared to actual fire test results on RC columns. Thus, a new displacement and rate of displacement-based approach is applied to evaluate failure of RC column in the current study. The displacement and rate of displacement at which the column failed in previous fire tests are selected as reference limits. For instance, if a column failed at a rate of displacement of $0.001h$ mm/min during its fire exposure instead of $0.003h$ (ISO834 limit), then the new selected limit in this approach becomes $0.001h$.

Thus, failure of an RC column in the analysis is evaluated at each time step by applying three failure criteria; displacement, displacement rate, and strength limiting criterion. In the displacement-based failure limit, at each time step of analysis, axial displacement or the rate of displacement of the column, as obtained from the numerical model, are compared with corresponding deflection limits. In the strength failure limit, a column is deemed to have failed when the reducing axial capacity of the column at that time step fall below the axial load present on the column. The duration to the point at which the strength or deflection limit is exceeded represents the fire resistance of the column.

## 4.7. Model Validation

The validity of the model is established by comparing fire response predictions generated from the numerical model with measured response parameters in fire tests on RC columns.

### 4.7.1. Selection of Columns

Five RC columns previously tested by Lie et al. (1984), Kodur et al. (2001), Raut and Kodur (2011) at National Research Council Canada, NRCC, and Michigan State University, MSU, are selected for numerical studies on the influence of transient creep strain. Detailed characteristics of these selected RC columns are listed in Table 4.4. The dimensions and material properties of these columns represent typical RC columns used in buildings and infrastructure.

For this validation, fire resistance analysis of two out of five analyzed RC columns, namely Column C2 and Column C3 (see Table 4.4), tested at the National Research Council of Canada, NRCC (Lie et al., 1984; Kodur et al., 2001), are presented in this section to establish the validity of the numerical model.

Column C2 and Column C3 has a capacity of 3371 KN, and 3598 KN, respectively, as per ACI 318 (2014). These two RC columns were subjected to 1067 KN and 930 KN load, and were

exposed to ASTM E119 (2014) standard fire conditions. Identical test conditions such as type of aggregate, fire scenario, reinforcement ratio, and concrete cover were simulated in the numerical analysis and progression of temperatures, axial displacement, and fire resistance are evaluated.

### 4.7.2. Thermal Response

As part of thermal response validation, measured and predicted temperatures on rebar and at distinct locations in concrete are compared in figures 4.9 and 4.10 for columns C2 and C3 respectively. The locations of thermocouples in rebar and concrete for each column are also shown in these figures. At the initial stages of fire exposure (in the first 50 minutes), temperatures in rebar and concrete increase gradually following the rise in fire temperatures. Then, the rate of temperature rise decreases slightly following the slower rate of increase in fire temperatures until failure of the column. As expected, measured and predicted temperatures in farther concrete layers from the exposed surface are lower than those at layers closer to the surface, due to lower thermal conductivity and higher specific heat of concrete. In Column C2, temperatures in the outer layers of concrete core exceed 500°C at 30 minutes prior to failure of the column as can be seen in Figure 4.9. Simultaneously temperature in reinforcement at this stage of fire, reaches around 500°C at which creep becomes predominant in steel.

The predicted cross section temperatures in Column C3, plotted in Figure 4.10 follow closely the measured temperatures during the fire test. At the initial stages of fire exposure, temperatures in rebar and outer layers of concrete cross section increase at a higher rate following the fire temperatures. However, the temperatures in the outer layers of concrete core of Column C3 do not reach 500°C till the last 30 minutes of fire exposure. During this late stage of fire, temperatures in reinforcing steel are high with values around 600°C. The slight variation between predicted and measured temperatures in Column C2 can be attributed to actual (general) thermal

properties of concrete and the ones utilized in the analysis. Overall, temperatures predicted in ABAQUS for both columns show a reasonable agreement with measured temperatures in fire tests.

### 4.7.3. Structural Response

As a part of structural response validation, measured axial displacement in columns C2 and C3 are compared with those predicted from ABAQUS. The measured and predicted displacement variation with time for C2 and C3 is shown in figures 4.11 and 4.12, respectively.

The axial displacement response for both columns can be grouped under three main stages; expansion, steady-state, and creep. In the first stage, till about 120 minutes of fire exposure, total displacement is mainly resulting from temperature-induced thermal expansion of constituent materials, concrete and steel, as a result of temperature rise. During this stage, concrete and reinforcing steel experience minimal material degradation due to lower temperatures of less than 300°C in outer layers of concrete core and 400°C in rebars. Axial displacement increases due to expansion of the column until it reaches to a point where expansion is fully developed.

In the second stage, thermal, mechanical, and transient creep strains contribute to axial displacement, and produce nearly a steady-state response. This steady-state response is attributed to increasing stiffness degradation in column and also due to effects of transient creep strain which offset much of thermal expansion. In the third stage, axial displacement response is dominated by increasing transient creep deformations and this changes the deformation state from expansion to contraction. This third “creep dominant” stage starts after about 150 minutes of fire exposure in C2 (see Figure 4.11). During this stage, cross-sectional temperatures (in concrete and rebar) in much of C2 rises above 500°C and this leads to significant creep strain. In the final 10 minutes of fire exposure, just prior to failure of C2, much of temperatures in concrete and rebar hover around 600°C, leading to further degradation of strength and stiffness properties of concrete and

reinforcing steel, and also producing high creep strains. This leads to "run-away" deformations leading to failure of the column. Axial displacement response in C3 follow similar trend as in C2 in stages 1 and 2, but there is a slight variation in response in stage 2. This slight variation in predicted response of C3 (see Figure 4.12) can be attributed to differences between actual expansion properties of concrete and that utilized in the analysis, taken from Eurocode 2 (2004).

The presented results of axial displacement in figures 4.11 and 4.12 are merely based on Eurocode 2 stress-strain curves which do not account for transient creep explicitly. Overall, the predicted axial displacement follow closely that measured during the fire tests for both columns. However, at the later stages when creep becomes dominant on the response, there is a significant difference in the progression of axial displacement between measured and predicted response.

### 4.7.4. Role of Transient Creep on Response of Columns

To illustrate the effect of accounting for high-temperature transient creep strains, axial displacements in fire exposed RC columns (columns C2, and C3) are plotted as a function of time for five analysis cases in figures 4.13 and 4.14 respectively. Fire resistance analysis was performed under five cases for the five analyzed columns. In Case 1, analysis was carried out without taking explicit creep into account. In Case 2, analysis was carried out with explicitly accounting for transient creep in concrete by incorporating data generated from the experimental part of this study in Chapter 3. In cases 3, 4, and 5, fire resistance analyses were carried out by taking high-temperature explicit creep into account as per Schneider (1986), Terro (1998), and Nilsen et al. (2002), respectively. For reinforcing steel, HT explicit creep was accounted for as per Williams-leir (1983). In Case 1, only partial creep effects in temperature-dependent stress-strain curves of concrete and reinforcing steel are incorporated. In Case 2, the generated creep data experimentally for NSC in Chapter 3 is utilized to account for transient creep in the model by calculating creep

parameters for ABAQUS creep laws as discussed in Section 4.3. Similarly, for the latter three cases, the generated data from creep relations in the literature for transient creep of concrete and reinforcing steel is curve fitted to creep power law models in ABAQUS, and the parameters of ABAQUS creep laws are calculated based on the least square method. These parameters are then inputted in the model to generate structural response by accounting for temperature induced creep.

For Column C2, the displacement response in Case 1, without accounting for HT transient creep, shows a good agreement with measured axial displacement till later stages of fire exposure, up to 150 minutes. Around 150 min into fire exposure, concrete and rebar temperatures in Column C2 surpass 500°C (Figure 4.9), and this will induce significant transient creep strains. Consequently, axial displacement predicted from Case 1 (without explicit creep) analysis underestimate HT transient creep strains and thus the predicted response deviates from measured displacement.

Axial displacement response in the four cases where creep was accounted for closely follow that of measured response during latter stages (creep stage) until failure of the column. Thus, the difference in axial displacement between Case 1, from analysis without including HT transient creep, and that measured in fire test is the result of underestimating temperature induced transient creep strain in concrete and rebar. This variation can be minimized when transient creep strains are specifically accounted for in the analysis as in cases 2 through 5. The slight variation in predicted axial displacements between these cases is due to the variations in high temperature creep strain that arise from the different creep relations (see Figure 2.16).

For Column C3, predicted axial displacement in Case 1, without accounting for HT transient creep, follow closely that of measured trend during the fire test in the first 100 minutes (see Figure 4.14). Predicted axial displacement from Case 1, then tend to slightly overestimate

measured deformation of C3, and this is attributed to the variation between actual and specified thermal elongation relations. In the last 60 minutes of fire exposure (creep stage), the difference between predicted and measured axial displacement becomes evident in Case 1 due to neglecting transient creep strains. In the four cases, where transient creep strain is explicitly included, axial displacement response predicted from the analysis shows good agreement with that measured in the test particularly for the last 60 minutes of the test where transient creep strains become dominant. Slight variations are observed in predicted axial displacements from cases 2, through 5 due to differences in different creep models.

The above set of analyses were reproduced by including the creep effects of concrete only and neglecting the creep in reinforcing steel bars. Results from these analyses indicated that the response of columns (with only creep in concrete) is very close to that of columns where creep effects from concrete and reinforcing steel is accounted for. This is mainly due to much smaller area of reinforcing steel as compared to the concrete in the column section. Thus, HT creep in reinforcing steel has no major impact on the axial displacement of the studied RC columns.

The presented trends clearly infer that transient creep influences the response of fire exposed concrete columns, particularly at latter stages of fire exposure. Further, stress-strain curves, specified in Eurocode and other standards, account for partial creep effects only. Neglecting full creep effects in fire resistance analysis results in an underestimation of deformations and lead to un-conservative fire resistance in column. For predicting the realistic response of fire exposed RC columns, full creep effects (including explicit creep) are to be accounted for in fire resistance analysis. The results also show that incorporating generated creep data for NSC in this study (Chapter 3) in the numerical model produce similar axial displacement trends as other cases where creep is accounted for through other existing relations for HT creep in

the literature. This is evident in Figure 4.13 and 4.14 between Case 2 of analysis and other cases where transient creep strain is accounted for.

### 4.7.5. Failure Modes and Times

Predicted fire resistance (failure time) for Column-2 from Case 1, without accounting for transient creep strains, is significantly overestimated. Without accounting for explicit creep in analysis, a fire resistance of 242 minutes is predicted for Column-1 as compared to 208 minutes measured during the fire test. This difference of 16% in failure time gets reduced when explicit creep effects are accounted for in analysis. For cases 2 through 5, analyses of Column-2, HT transient creep is accounted for explicitly, as per three different creep models. Calculated fire resistance in the column under these three cases are conservative with difference between predicted and measured failure time as low as 2% as shown in Table 4.5.

Predicted fire resistance (failure time) for Column-3 from Case 1, without accounting for transient creep strains, is also overestimated. Without accounting for explicit creep in analysis, a fire resistance of 298 minutes is predicted for Column-3 as compared to 278 minutes measured during the fire test. This difference in failure time is greatly reduced when transient creep strain is accounted for in the analysis as in cases 2 through 5. Fire resistance predicted without accounting for creep (Case 1) is un-conservative, while in cases 2 through 5, predicted fire resistances are conservative and closer to that measured in tests as shown in Table 4.5. The fire resistance and failure modes of the other three analyzed columns are also reported in Table 4.5. Among the five studied columns, only Column-1 (203mm×203mm) experienced buckling failure mode, whereas the other four columns failure mode was crushing compression.

## 4.8. Summary

This chapter introduces the development of a numerical model for tracing the response of concrete columns with explicitly incorporating transient creep strain in fire resistance analysis. Generated transient creep data in the experimental part of this Thesis (Chapter 3) was incorporated into the developed model to account for transient creep strain in fire resistance analysis of concrete columns. The numerical model, developed in commercially available finite element software ABAQUS, follows the consequential thermo-mechanical modeling approach. Thus, the model comprises of two sub-models, namely; thermal and structural. In addition to explicitly accounting for transient creep strain, the model also accounts for temperature-induced degradation in material property together with arising material and geometric nonlinearities. The model incorporated different loading combinations and fire scenarios to investigate the influence of transient creep strain on the response of concrete columns under fire conditions. The validity of the developed model was established through comparing numerically generated thermal and structural data with measured data from fire resistance tests on concrete columns. The validity of the model proves that it is capable of tracing the response of concrete columns under fire conditions. Further, incorporating transient creep strain in the model yields more precise and accurate results in terms of both predicted fire resistance and experienced axial displacement in the column. In the next chapter, the validated model will be applied to study the effect of critical parameters on the extent of transient creep in fire-exposed concrete columns.

Table 4.1 High-temperature thermal property relations for concrete

| | |
|---|---|
| Thermal conductivity (W/m K) | All types :<br>Upper limit*:*<br>$k_c = 2 - 0.2451\ (T / 100) + 0.0107\ (T / 100)^2$<br>*for* $20°C \leq T \leq 1200°C$<br>Lower limit:<br>$k_c = 1.36 - 0.136\ (T / 100) + 0.0057\ (T / 100)^2$<br>*for* $20°C \leq T \leq 1200°C$ |
| Thermal conductivity (W/m K) | Specific heat (J/kg C)<br>$c = 900$, *for* $20°C \leq T \leq 100°C$<br>$c = 900 + (T - 100)$, *for* $100°C < T \leq 200°C$<br>$c = 1000 + (T - 200)/2$, *for* $200°C < T \leq 400°C$<br>$c = 1100$, *for* $400°C < T \leq 1200°C$<br>Density change (kg/m$^3$)<br>$\rho = \rho(20°C)$ = *Reference density*<br>*for* $20°C \leq T \leq 115°C$<br>$\rho = \rho(20°C)\ (1 - 0.02(T - 115)/85)$<br>*for* $115°C < T \leq 200°C$<br>$\rho = \rho(20°C)\ (0.98 - 0.03(T - 200)/200)$<br>*for* $200°C < T \leq 400°C$<br>$\rho = \rho(20°C)\ (0.95 - 0.07(T - 400)/800)$<br>*for* $400°C < T \leq 1200°C$<br>***Thermal Capacity*** $= \rho \times c$ |

Table 4.2 Constitutive relations for concrete at elevated temperatures (EC2, 2004)

| | |
|---|---|
| Stress-strain relations | $$\sigma_c = \frac{3\varepsilon\ f'_{c,T}}{\varepsilon_{c1,T}\left(2+\left(\frac{\varepsilon}{\varepsilon_{c1,T}}\right)^3\right)}\ ,\varepsilon \le \varepsilon_{cu1,T}$$ For $\varepsilon_{c1(T)} < \varepsilon \le \varepsilon_{cu1(T)}$, Eurocode permits the use of both linear and nonlinear descending branch in the numerical analysis. **The parameters in this equation are listed in Table 4.3** |
| Thermal expansion | Siliceous aggregates: $\varepsilon_{th} = -1.8\times10^{-4}+9\times10^{-6}T+2.3\times10^{-11}T^3$ *for* $20°C \le T \le 700°C$ $\varepsilon_{th} = 14\times10^{-3}$ *for* $700°C < T \le 1200°C$ Calcareous aggregates: $\varepsilon_{th} = -1.2\times10^{-4}+6\times10^{-6}T+1.4\times10^{-11}T^3$ *for* $20°C \le T \le 805°C$ $\varepsilon_{th} = 12\times10^{-3}$ *for* $805°C < T \le 1200°C$ |

Table 4.3 Values of stress-strain relations parameters for normal strength concrete at high-temperatures (EC2, 2004)

| Temp. (˚C) | Normal Strength Concrete | | | | | |
|---|---|---|---|---|---|---|
| | Siliceous Aggregate | | | Calcareous Aggregate | | |
| | $\frac{f'_{c,T}}{f'_{c20}}$ | $\varepsilon_{c1,T}$ | $\varepsilon_{cu1,T}$ | $\frac{f'_{c,T}}{f'_{c20}}$ | $\varepsilon_{c1,T}$ | $\varepsilon_{cu1,T}$ |
| 20 | 1 | 0.0025 | 0.02 | 1 | 0.0025 | 0.02 |
| 100 | 1 | 0.004 | 0.0225 | 1 | 0.004 | 0.023 |
| 200 | 0.95 | 0.0055 | 0.025 | 0.97 | 0.0055 | 0.025 |
| 300 | 0.85 | 0.007 | 0.0275 | 0.91 | 0.007 | 0.028 |
| 400 | 0.75 | 0.01 | 0.03 | 0.85 | 0.01 | 0.03 |
| 500 | 0.6 | 0.015 | 0.0325 | 0.74 | 0.015 | 0.033 |
| 600 | 0.45 | 0.025 | 0.035 | 0.6 | 0.025 | 0.035 |
| 700 | 0.3 | 0.025 | 0.0375 | 0.43 | 0.025 | 0.038 |
| 800 | 0.15 | 0.025 | 0.04 | 0.27 | 0.025 | 0.04 |
| 900 | 0.08 | 0.025 | 0.0425 | 0.15 | 0.025 | 0.043 |
| 1000 | 0.04 | 0.025 | 0.045 | 0.06 | 0.025 | 0.045 |
| 1100 | 0.01 | 0.025 | 0.0475 | 0.02 | 0.025 | 0.048 |
| 1200 | 0 | - | - | 0 | - | - |

Table 4.4 Properties of selected columns for studying the effect of transient creep

| Column Name | Column C1 | Column C2 | Column C3 | Column C4 | Column C5 |
|---|---|---|---|---|---|
| Tested by | Raut and Kodur 2011 | Lie et al., 1984 | Kodur et al., 2001 | Kodur et al., 2001 | Lie et al., 1993 |
| Cross section, mm | 203×203 | 305×305 | 305×305 | 305×305 | 305×457 |
| Length, m | 3.810 | 3.810 | 3.810 | 3.810 | 3.810 |
| Concrete strength, $f'_c$, MPa | 51 | 36.1 | 40.2 | 40.2 | 42.5 |
| Longitudinal reinforcement | 4- 20 mm | 4- 25 mm | 4- 25 mm | 4- 25 mm | 6- 22 mm |
| Tie spacing, mm | 200 | 305 | 75 and 150 | 75 and 150 | 305 |
| Type of aggregate | Calcareous | Siliceous | Siliceous | Siliceous | Siliceous |
| Test load, KN | 280 | 1067 | 930 | 1500 | 1413 |
| Stress level % | 40 | 32 | 26 | 42 | 25 |
| Relative humidity % | 81.5 | 74 | 90 | 51 | 65 |
| Cover, mm | 50 | 48 | 48 | 48 | 48 |
| Test fire scenario | ASTM E-119 | | | | |
| Test FR, min | 183 | 208 | 278 | 204 | 396 |

Table 4.5 Comparison of predicted and measured fire resistances with and without transient creep

| Column Name | Fire Resistance (minutes) | | | | | |
|---|---|---|---|---|---|---|
| | Predicted from model | | | | | Measured |
| | Excluding explicit creep, Case 1 | Including explicit creep | | | | Fire Test |
| | | Case 2 (current study) | (Case 2- Schneider) | (Case 3- Terro) | (Case 4- Nilsen) | |
| Column C1 | 224 | 181 | 178 | 182 | 185 | 183 |
| Column C2 | 242 | 201 | 196 | 190 | 204 | 208 |
| Column C3 | 298 | 272 | 267 | 262 | 276 | 278 |
| Column C4 | 226 | 197 | 192 | 191 | 200 | 204 |
| Column C5 | 442 | 389 | 395 | 391 | 386 | 396 |

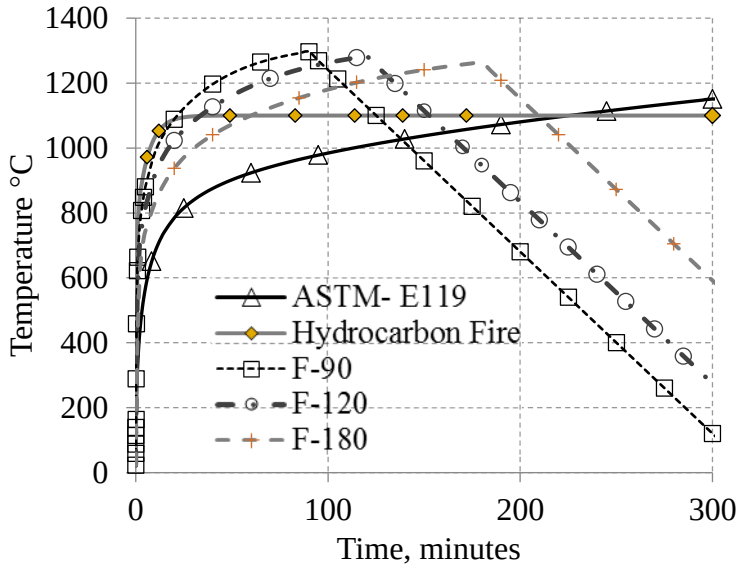


Figure 4.1 variation of temperature with time for standard (ASTM) and design fire (F-90, F-120, and F-180) scenarios

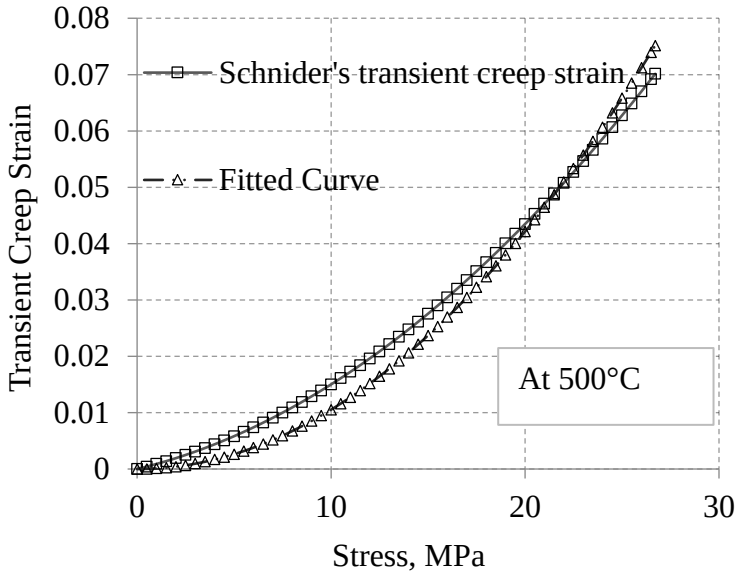


Figure 4.2 Comparison between generated transient creep strain of concrete as a function of stress and fitted curve to calculated parameters A, and n.

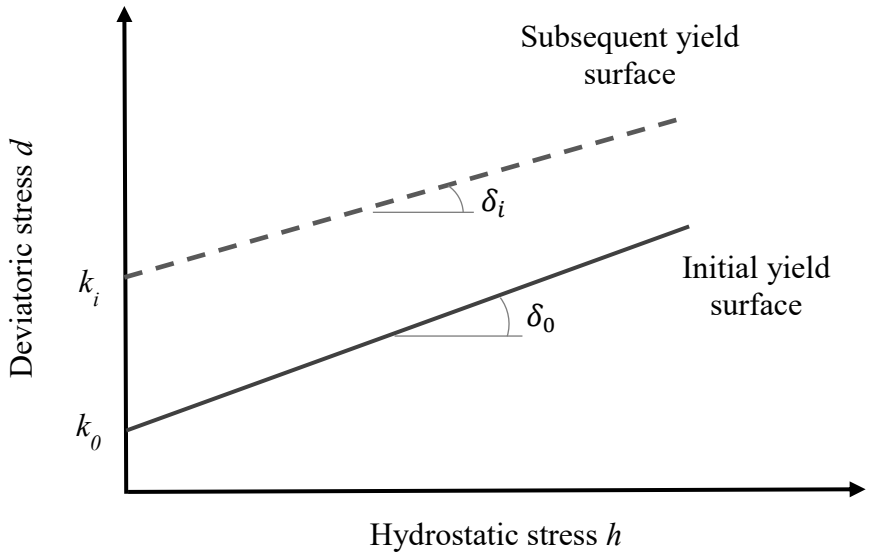


Figure 4.3 Yield surface based on Drucker-Prager model

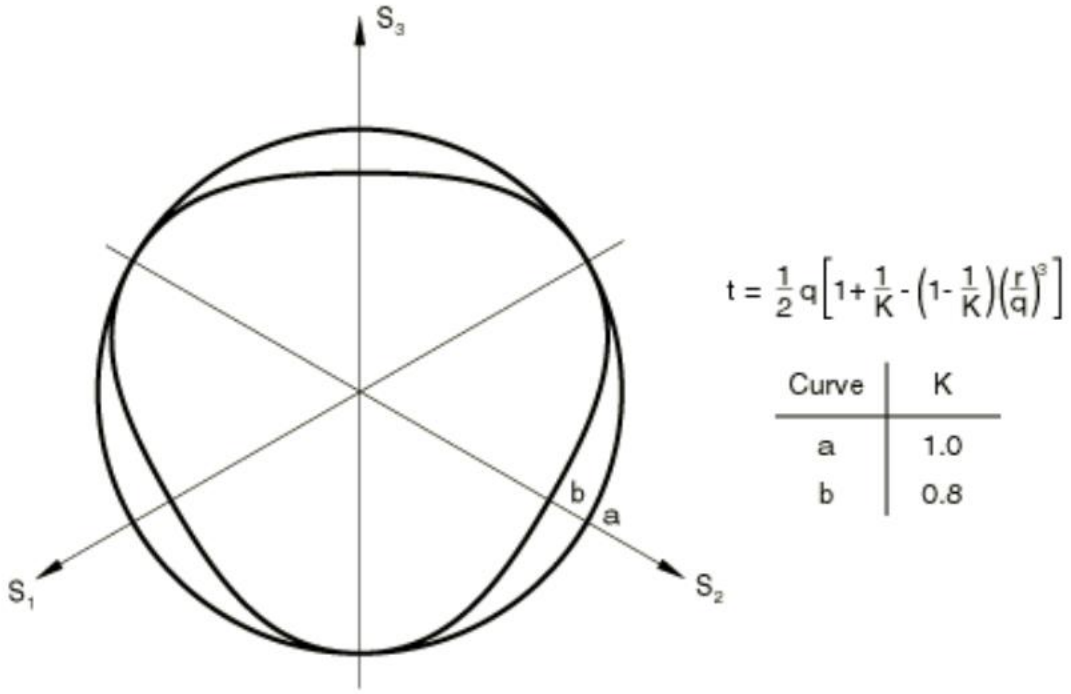


Figure 4.4 Yield surface in the Ducker-Prager model based on the selected shape factor value (ABAQUS, 2014)

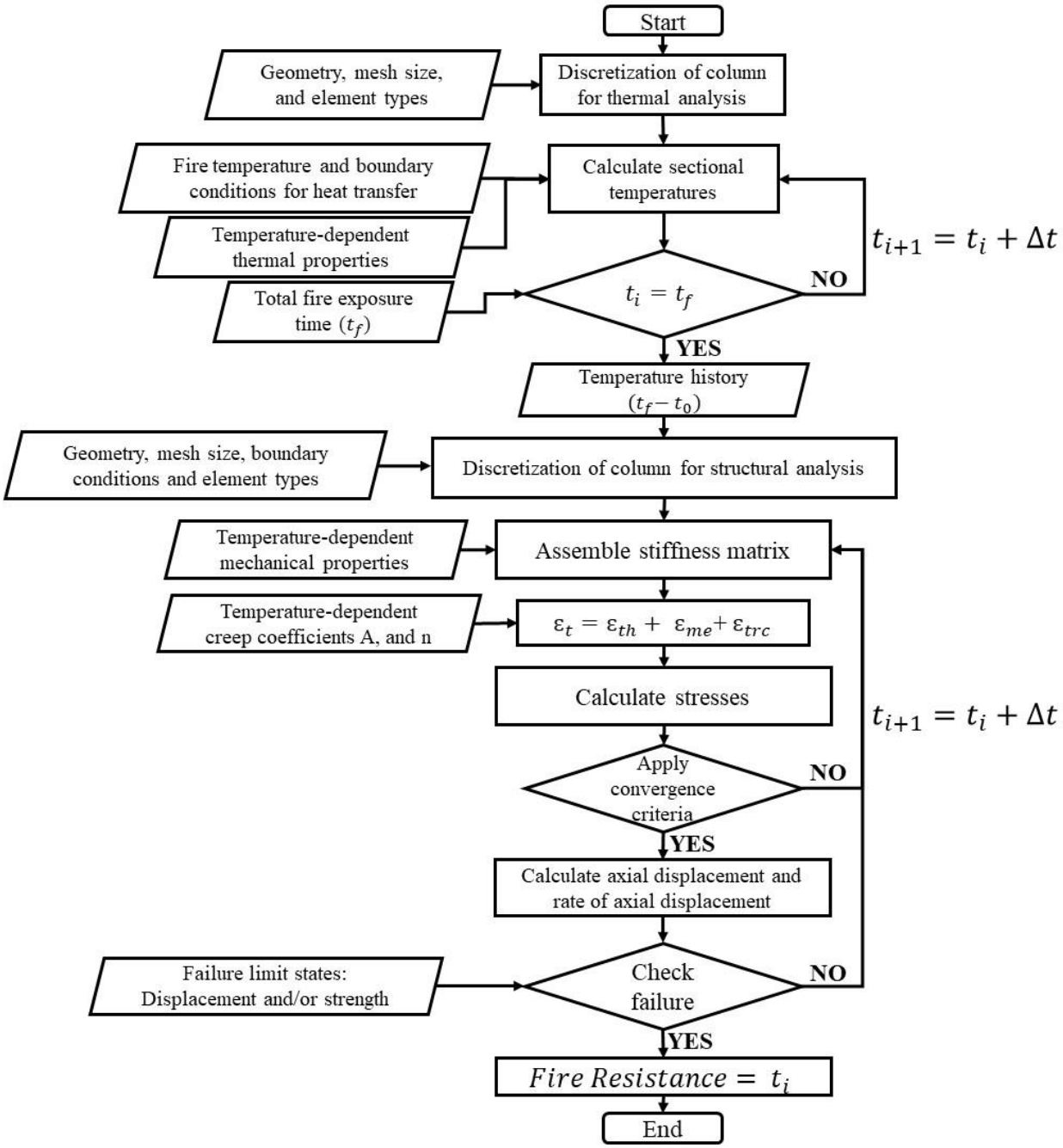


Figure 4.5 Flow chart illustrating steps in the numerical model for fire resistance analysis of RC columns by incorporating creep effects

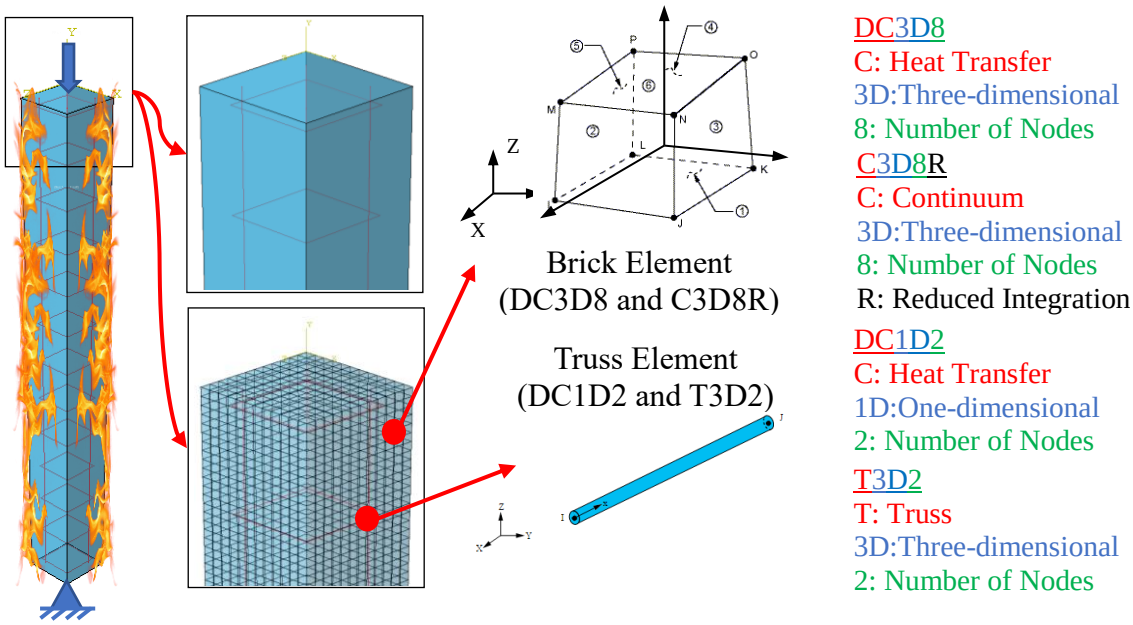


Figure 4.6 Discretization and element types for fire resistance analysis of RC columns

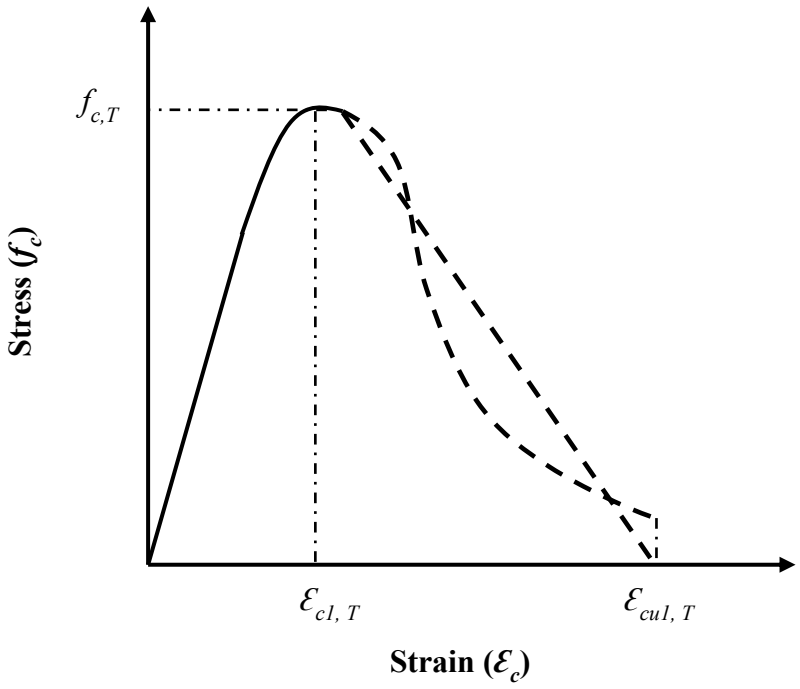


Figure 4.7 Stress-strain curves for concrete Eurocode 2 (2004)

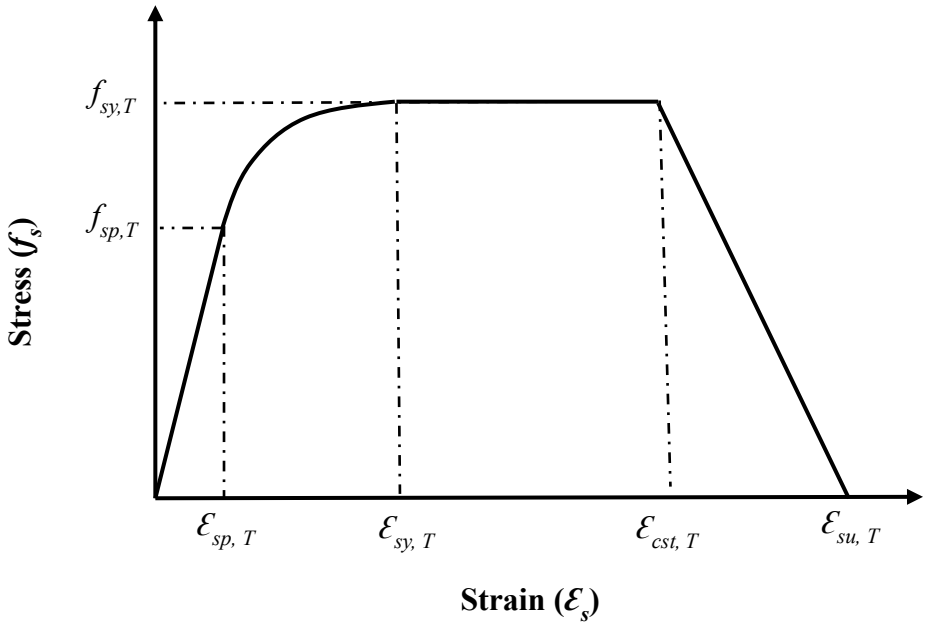


Figure 4.8 Stress-strain curves for reinforcing steel in Eurocode 2 (2004)

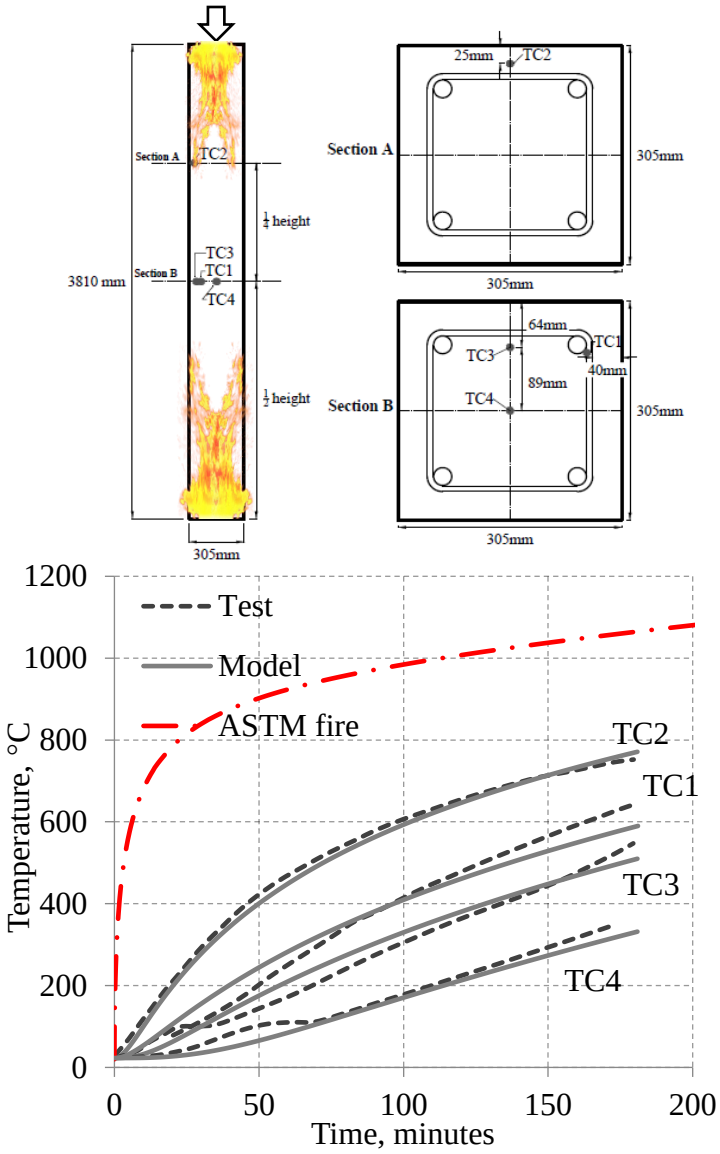


Figure 4.9 Measured and predicted temperatures for Column C2

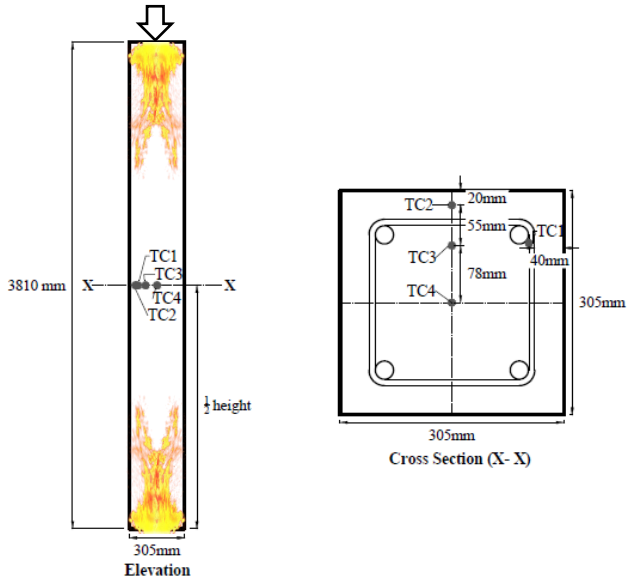


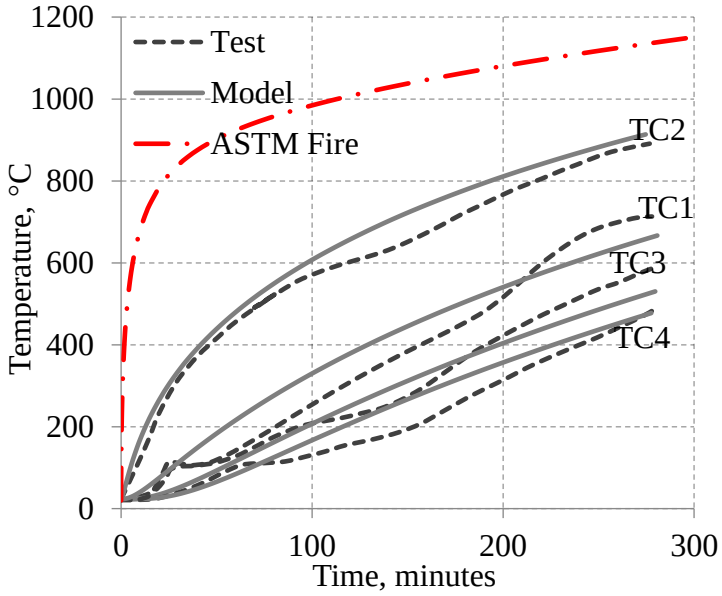


Figure 4.10 Measured and predicted temperatures for Column C3

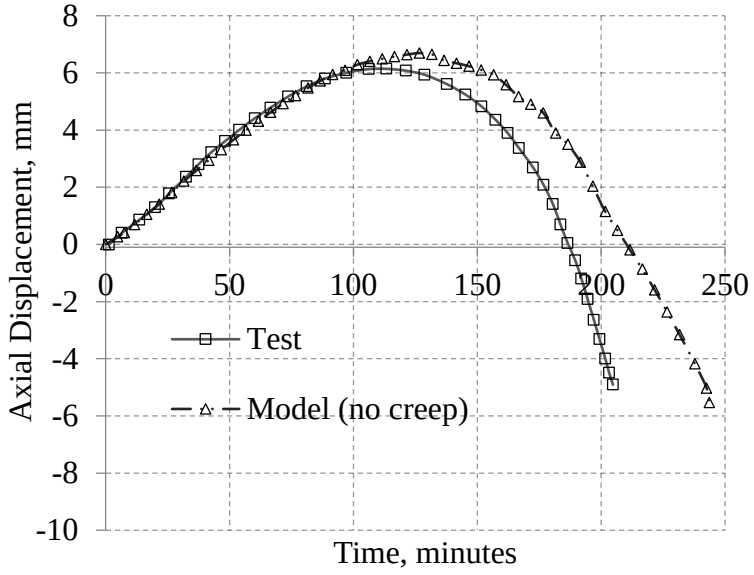


Figure 4.11 Comparison of predicted and measured axial displacement with time for Column C2

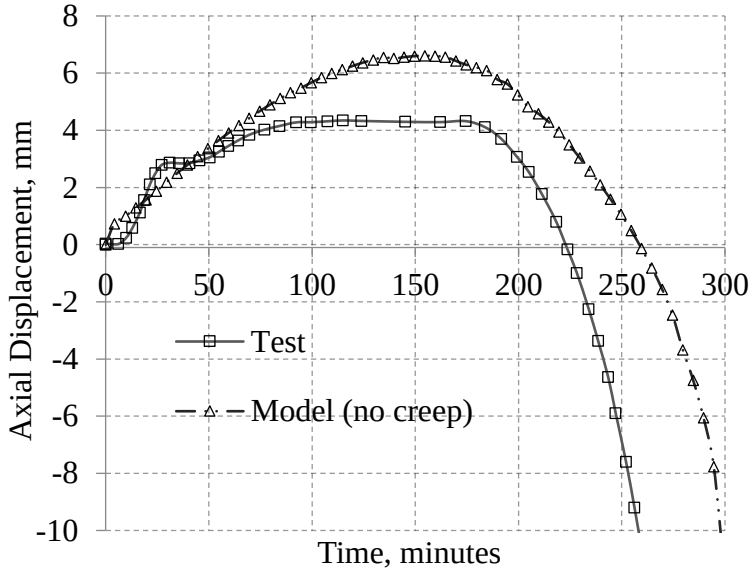


Figure 4.12 Comparison of predicted and measured axial displacement with time for Column C3

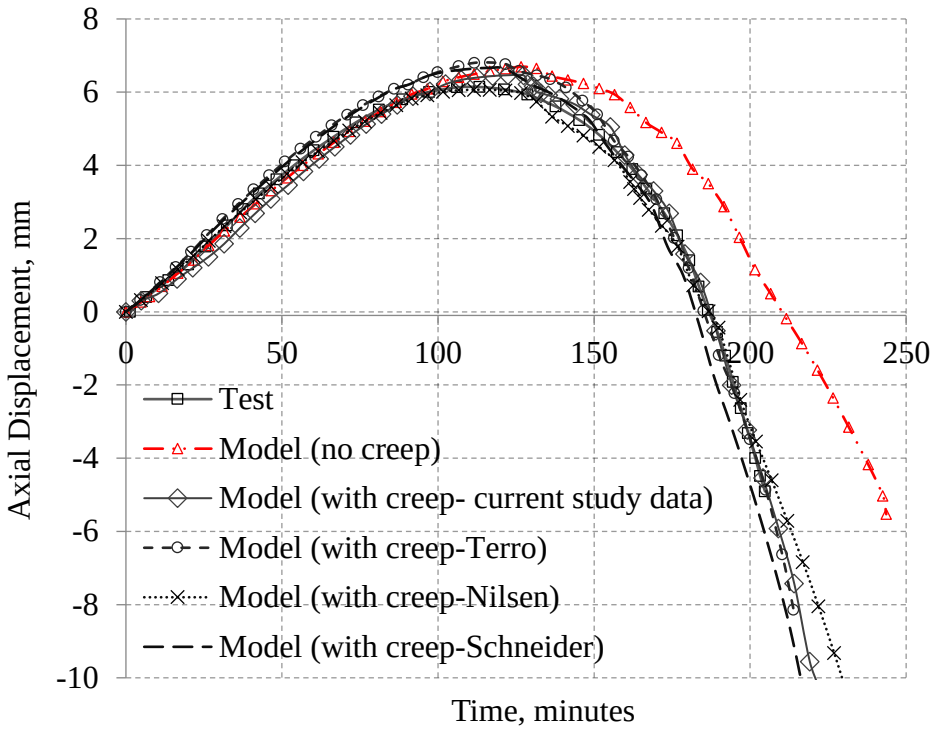


Figure 4.13 Effect of transient creep on axial displacement for Column C2

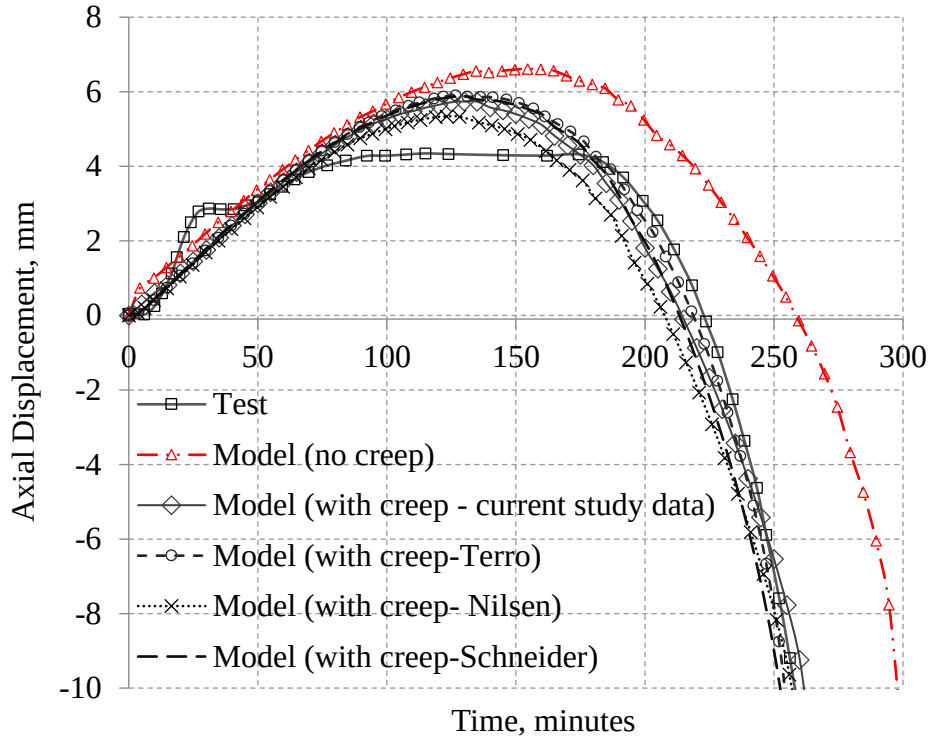


Figure 4.14 Effect of transient creep on axial displacement for Column C3

# CHAPTER FIVE

# 5. Parametric Studies

## 5.1. General

The validated model in Chapter 4, is applied to carry out several parametric studies on the effect of transient creep on the fire-response of RC columns under different conditions. Several factors can magnify the influence of transient creep on response of RC columns under fire. As discussed in Chapter 2, limited studies are available to study the extent of influence of critical factors on transient creep and thus on fire response of RC columns. Most previous studies were performed under standard fire scenarios with fire exposure from all four faces. However, in real fire incidents, columns in buildings can get exposed to different fire scenarios, in terms of fire severity and fire exposure sides (1-, 2-, or 3-sided). Moreover, the level of applied loading on a column can vary considerably depending on the loading condition. Finally, columns can be constructed with different types of concrete depending on design specifications. To study the influence of these varying parameters on transient creep effects in concrete columns, a set of parametric studies was carried out as per the outlined approach in Chapter 4.

## 5.2. Factors Influencing Transient Creep in Concrete Columns

The extent of transient creep developed during fire exposure is influenced by a number of factors such as temperature and stress levels, rates of heating, number of exposed faces, and concrete type. These factors are to be studied to quantify their influence on the experienced creep effects in concrete columns.

The extent of transient creep in a fire exposed concrete member mainly depends on cross-sectional temperatures in a concrete member. Thus, type of fire exposure (i.e. low, moderate or

severe fire intensity) influences the magnitude of transient creep deformations. Under moderate fire, such as standard ASTM E-119 fire (2014), rate of heating and peak fire temperatures attained in a member are lower than what is experienced under severe fires, such as hydrocarbon ASTM E1529 (2014) or severe design fires, as can be seen in Figure 5.1. The time-temperature ( *t-T* ) plot in Figure 5.1 resulting from exposure to severe design fire (F-90, F-120, and F-180) is calculated as per Eurocode 2 (2004) recommendations for design fires with burning periods of 90, 120, and 180 minutes and is compared with *t-T* curves of standard and hydrocarbon fire exposures. Under such rapid rates of heating, as encountered in severe fires, concrete columns are prone to deterioration and accelerated failure due to effects of high thermal gradients developed within the section. These high thermal gradients induce dominant transient creep strains leading to high levels of deformations in concrete columns, and thus, cause early than that under standard (ASTM E-119) fire exposure, currently used in fire resistance evaluation of concrete members. Therefore, incorporating transient creep strains generated under such severe fires, explicitly in fire resistance analysis, is critical for predicting realistic fire response of columns.

Load (stress) level to which the RC column is subjected during a fire play a major role in determining the extent of transient creep strain developed in a column. Load level is defined as the ratio of applied loading on a column to its calculated capacity at room temperature. Creep in concrete is typically evaluated at various stress level, ratio of applied stress on a concrete specimen to its strength at room temperature. An increase in stress level by 10% - 20% can lead to a significant rise in transient creep in concrete (Colina and Sercombe, 2004; Huismann et al., 2012; Khoury et al., 1985b). Owing to the fact that transient creep increases with higher stress levels, columns subjected to higher loads will experience higher transient creep effects given all other conditions of fire exposure are identical (Kodur and Alogla, 2016). In current codes of buildings,

fire resistance in structural elements is often evaluated under a critical stress level of 50%. A stress level of 50% is implemented because of the high probability that during fire incidents much of live loads are evacuated or burned. Under such high stress level, concrete experience significant transient creep strains, and the influence of variant load levels is of interest to this study.

Type of concrete in columns can have an influence on the structural response under fire conditions. Different concrete types (NSC, HSC etc) exhibit distinctive mechanical behavior at elevated temperatures, and therefore, this variation in material behavior can influence the fire response of concrete columns. Moreover, transient creep strain in concrete at elevated temperatures is significantly dependent on the batch proportions and water content in the concrete mix. Creep tests on different types of concrete showed that normal strength concrete possesses a different response from that of high strength concrete (Chapter 3). Further, fiber-reinforced concrete shows slight variation in deformation response from that of concrete without fibers as demonstrated in Chapter 3. NSC reinforced with steel fibers showed slightly lower deformations under transient heating than that of NSC without fibers. Similarly, HSC with and without polypropylene fibers showed higher undergone deformations under transient heating conditions than that of NSC or NSC-SF. Due to the above-mentioned differences between concrete types in terms of mechanical properties and deformation response under elevated temperature exposure, effect of transient creep on concrete columns is evaluated with respect to different concrete types. Three different concrete types are chosen to evaluate influence of transient creep strain on response of concrete columns.

Thermal gradients resulting from different sides of exposure can influence the level of transient creep in concrete columns. In case of columns subjected to four side heating, thermal gradients are symmetric but under 1-, 2-, or 3-side heating asymmetric thermal gradients will

develop in the column. These asymmetric thermal gradients can lead to temperature-induced eccentricity and produce biaxial bending in the column (Raut and Kodur 2011), leading to early failure of a column. The extent of transient creep generated under asymmetric thermal gradients has not been studied in the literature.

In real fire incidents, there is always a cooling phase that follows the heating phase of a fire. The presence of such cooling phase complicates treatment of creep phenomenon in fire resistance analysis since no guidance is given in current codes of practice for accounting creep in fires with cooling phase. Eurocode 2 (2004) stress-strain relations does not take into account effects of cooling phase on transient creep for two main reasons. First, most of the deformations experienced during the heating period of fire exposure is plastic (permeant), and thus irrecoverable (Gernay and Franssen, 2012). Second, implicit consideration of transient creep in EC2 stress-strain relations permits recovery of transient creep strain during the cooling phase of the fire even though transient creep only occur at first time heating (Khoury et al. 1985). Thus, utilizing EC2 stress-strain relations for fire resistance analysis of RC columns under fire with cooling phase can result in underestimation of experienced shortening (contraction) in RC columns during the heating phase of the fire. Further, implicit consideration of transient creep permits reversibility of transient creep (during cooling phase).

## 5.3. Parametric Study on Effect of Transient Creep on Columns Behavior

Based on the literature review presented in Chapter 2, there is lack of understanding on the influence of transient creep strain on response of concrete columns under fire exposure. Further, the influence of some of the critical parameters on the extent of creep deformations in concrete columns is not well established in literature. Influence of transient creep on response of concrete columns under fire exposure can be amplified by variation in various parameters such as

temperature, stress level, etc. Thus, in the following sections, RC columns are analyzed under different varying parameters.

### 5.3.1. Selection of Columns

Seven RC columns previously tested by Lie et al. (1984), Kodur et al. (2001), Raut and Kodur (2011) at National Research Council Canada, NRCC, and Michigan State University, MSU, are selected for numerical studies on the influence of transient creep strain. Detailed characteristics of these selected RC columns are listed in tables 5.1 and 5.2. The dimensions and material properties of these columns represent typical RC columns used in buildings and infrastructure.

### 5.3.2. Range of Parameters

The range of variation in the studied parameters is tabulated in Table 5.3. RC columns are analyzed under five different varying parameters; fire severity, stress level, concrete type, axisymmetric thermal gradients, and cooling phase. To highlight the effect of variation of these parameters on fire performance of columns, fire resistance analysis is performed under two cases for each scenario; with transient creep and without transient creep.

### 5.3.3. Analysis Procedure

Fire resistance analysis is carried out on selected columns using a sequentially coupled thermo-mechanical analysis procedure as outlined in Chapter 4. In the thermal analysis, heat transfer analysis is performed in which the column is exposed to specified heating from one to four sides depending on the selected fire exposure type and scenario. The resulting nodal temperatures from the thermal analysis are then inputted in the model for the structural analysis where the properties of constituent materials at variant temperatures based on concrete type are defined along with loading and boundary conditions. Transient Creep of concrete is specified in terms of stress level and temperature for different concrete types. The proposed transient creep relation in Chapter

3 is utilized for generating transient creep strain for generating creep data for different types of concrete.

Analysis in ABAQUS was carried out at a maximum time step of 5 minutes, with "automatic incrementation" option selected to automatically reduce the time steps, towards the failure zone to minimize convergence problems. This "automatic incrementation" requires specifying a maximum, minimum, and initial time increments and the chosen input values in this study are 5 minutes, 1E-4 second, and 1 second, respectively.

To simulate the response of an RC column under fire conditions, temperature-dependent thermal properties of concrete and reinforcing steel is to be input into ABAQUS. The thermal properties include thermal conductivity, specific heat, and thermal expansion. The variation of thermal properties of concrete and reinforcing steel with temperature follow relations specified in Eurocode 2 (2004). In thermal analysis, conductivity is assumed to be isotropic temperature-dependent, and specific heat is assumed to be based on constant volume concept for both concrete and reinforcing steel. Thermal elongation for concrete and reinforcing steel is specified as temperature-dependent coefficient of thermal expansion, as per EC2.

In addition, heat transfer properties; emissivity convective and radiative factors, are input in to the model. A pre-defined time-temperature fire curve is input as the reference temperature for heat transmission from fire source to exposed surfaces of RC member (column). A convection heat transfer coefficient, $\alpha_c$, of 25, 50, and 35 W/(m$^2$ °C), is utilized for surface film condition for building, hydrocarbon, and design fires, respectively. An emissivity factor, $\varepsilon$, of 0.7 and Stefan-Boltzmann radiation constant of $\sigma_s = 5.67\times10^{-8}$ W/(m$^2$ K$^4$) are utilized for radiative heat transfer.

In the conducted parametric studies, reinforced concrete columns are discretized into two different sets of elements for thermal analysis in three-dimensional space as shown in Figure 5.2 and outlined in Chapter 4.

### 5.3.4. Generated Response Parameters

In each carried out analysis case, a number of response parameters are generated from fire resistance analysis on a column. In this parametric studies, the main response parameters generated for evaluating the extent of transient creep in concrete columns are fire resistance and axial displacement response. Thus, the evaluation of the extent of creep is mainly assessed based on these two response parameters.

## 5.4. Effect of Varying Creep Parameters on Fire Resistance

To evaluate the influence of transient creep on response of concrete columns; two analysis scenarios are carried out on each column, namely: with and without accounting for transient creep in analysis. Response parameters generated in the analysis are utilized to quantify the effect of various parameters on transient creep, and thus on fire resistance of the column.

### 5.4.1. Fire Severity

Fire exposure on columns can be categorized under two types: standard or design (realistic) fire scenarios. Standard fire scenarios, such as ASTM E-119 and ISO 834, are expressed in terms of temperature-time relations in which temperatures rise rapidly in the first few minutes and then continue to increase with time for the remaining duration of fire exposure. However, in real or design fire scenarios, fire temperature increases to a peak, then cool down to room temperature. The fire growth characterization and its decay are dependent on many factors such as compartment's dimensions, fuel load, fuel type and ventilation.

To evaluate the creep effects under varying fire exposure scenarios; fire resistance analysis is carried out on columns C1 to C5 by exposing the columns separately to hydrocarbon (HC) and standard ASTM E-119 fire. The analysis was carried out under two cases; with and without accounting for explicit transient creep. Thus, four analysis cases were carried out on each column, namely; (Case 1): standard ASTM E-119 fire exposure with transient creep, (Case 2): standard ASTM E-119 fire exposure without transient creep, (Case 3): hydrocarbon fire with transient creep, and (Case 4): hydrocarbon fire without transient creep.

Under HC fire exposure, temperature increase more rapidly than under ASTM E-119 standard fire as shown in Figure 5.1. This high rate of heating under hydrocarbon fire exposure induces higher thermal gradients in the column in much shorter times than what is typically experienced in concrete columns under ASTM E-119 fire exposure. Cross-sectional temperatures predicted under hydrocarbon fire exposure in comparison with predicted temperatures under standard ASTM E-119 fire are plotted in Figure 5.3-a and -b, for columns C4 and C5, respectively. The outer layers of concrete section experience higher temperatures under hydrocarbon fire than that experienced under exposure to standard ASTM fire. For instance, temperature at 25mm from the exposed surface is at least 200°C higher under hydrocarbon fire than that under standard ASTM fire at the majority of the fire exposure time. However, temperatures at the central core of the column are very close under the two fire scenarios due to slower heat transfer to the core resulting from concrete's high specific heat and low thermal conductivity.

Thus, hydrocarbon fire exposure induces higher thermal gradients on the column's cross section than what is experienced under standard ASTM building fire, particularly at the early stage of exposure as shown in Figure 5.4. for column C4. Influence of thermal gradients is more profound under hydrocarbon due to the high difference between maximum and minimum

temperatures as compared to thermal response under ASTM fire exposure. These thermal gradients induce significant differential transient creep strains between the edges and the interior core of the section (based on the thermal gradient shape) and consequently apply additional stresses on the column section. Differential stresses in the section due to thermal gradients exert a bending moment that is higher during early stages of hydrocarbon fire exposure since the difference in temperatures between edge and center of the interior core is the highest (see Figure 5.4). With incrementing time of fire exposure, difference in thermal gradients reduce between the two fire scenarios due to the convergence of the fire temperatures in these two fires (as can be seen in Figure 5.1.).

A summary of results, in the form of failure times (or fire resistance), is presented for all five columns in Table 5.4. For illustrating the effect of transient creep on column response, axial displacement response is plotted for the four analysis cases in figures 5.5 and 5.6 for columns C4 and C5 respectively. Similar axial displacement trends are predicted under hydrocarbon fire and standard ASTM E-119 fire, but deformations occur at a much faster rate in stage 3, under HC fire exposure due to the higher heating rates. Axial displacement variation with time under fire can be grouped under three stages: early-expansion stage, short steady-state stage, and creep-dominant stage. Expansion under hydrocarbon fire is slightly higher than under standard fire due to the rapid exposure to high temperature at an early stage of fire (see Figure 5.1.). The steady-state stage in axial displacement of RC columns is much shorter under exposure to hydrocarbon fire than under standard fire. Further, transient creep effects under HC fire onset at earlier times than under standard ASTM E-119 fire and produces higher axial deformations. This combined with degradation in stiffness leads to lower fire resistance of RC columns under hydrocarbon fires than under standard ASTM E-119 fire.

For column C4, of size 305mm×305mm, axial displacement response under Case 1 (i.e. accounting for transient creep strain) follow closely that of measured response in fire test as can be seen in Figure 5.5. However, in Case 2, when transient creep is not accounted in fire resistance analysis, predicted axial displacement deviates from that measured in the fire test at later stages of exposure due to non-inclusion of transient creep effects. Similarly, predicted axial displacement for column C4 under hydrocarbon fire exposure under cases 3 and 4 of analysis compare well with each other till the onset of the creep dominant stage, i.e. at around 70 minutes into the fire. At this stage, temperatures in the outer zones of the column's core already reached 500°C (see Figure 5.4-a), and the influence of transient creep strain becomes evident. Further, the difference between predicted axial displacements with and without transient creep increased under hydrocarbon fire (i.e. cases 3 and 4) as compared to that under standard fire (i.e. cases 1 and 2) as can be seen in Figure 5.5. This infer that transient creep has more influence under hydrocarbon or severe fire than under standard fire due to higher fire exposure temperatures (see Figure 5.1).

Similar axial displacement response is predicted for Column C5, of size 305mm×457mm, as shown in Figure 5.6 for both ASTM E-119 and hydrocarbon fire scenarios. Under hydrocarbon fire scenario in cases 3 and 4, axial displacement variation with time of column C5 are in good agreement until the start of the creep dominant stage at around 230 minutes. After this time predicted axial displacement under Case 4 are lower than that from Case 3 due to non-inclusion of transient creep effects explicitly in the analysis.

Overall, analysis results from five analyzed columns show similar behavior in each of the four selected cases. The effect of transient creep is higher under severe or hydrocarbon fire than that under standard fire due to rapid rate of heating and higher exposure temperatures. When transient creep strain is neglected, axial displacement is underestimated, and failure time is overestimated.

However, when transient creep is explicitly accounted in the analysis, predicted axial displacements and failure times (fire resistance) were closer to the measured deformations and fire resistance obtained in the fire tests.

### 5.4.2. Stress Level

Transient creep at high temperatures is primarily a function of sectional temperature and stress level as shown in Figure 5.7. At higher stress and temperature level, transient creep strain increases and constitutes a significant part of total strain in concrete. This is also evident from the failure times of the columns analyzed under standard ASTM E-119 fire as tabulated in Table 5.5. As applied loading level increases on a column, failure under fire exposure occur faster, given all other parameters are similar. For the five analyzed columns, the influence of stress level on extent of creep effects can be quantified by evaluating the difference between predicted fire resistance with and without accounting for creep. As stress level increases, the difference between predicted fire resistance increases. Columns C1, C4 and C5, have different characteristics and test conditions and the effect of stress level is not evident. Columns C2 and C3, have the same cross-sectional size, concrete strength, reinforcement configuration, and aggregate type, but were analyzed under different levels of loading to evaluate the effect of stress level on transient creep. During fire exposure, column C2 was subjected to a load equivalent to 50% of its capacity, while column C3 was subjected to a load level of 80%. Creep effects were explicitly accounted for in fire resistance analysis. As expected, column C3, under higher load level, failed at 204 minutes of fire test, whereas failure time of column C2 in test was 278 minutes.

Transient creep strain under stress level of 80% is much higher than creep generated under stress level of 50% (as can be seen in Figure 5.7). When concrete is heated, free physical water evaporates and as heating continues, chemically bounded water within C-S-H eventually

evaporates causing dehydration of C-S-H and creating more porous microstructure. The porous microstructure in concrete is more prone to be crushed and consolidated under higher stress levels leading to rise in transient creep that results from rapid pore structure collapse. This high sensitivity of stress level to transient creep strain is to be taken into consideration, through explicit temperature dependent creep models, in evaluating response of concrete columns under fire conditions, specially at higher levels of loading.

For the two analyzed columns C2 and C3, failure times from fire resistance analysis performed under ASTM E-119 fire scenario with and without accounting for transient creep showed different failure times as shown in Table 5.5. The difference in fire resistance between analysis cases, with and without transient creep, increased in column C3 due to higher applied stress level. Thus, with increase in stress level, the influence of transient creep in RC columns gets amplified, as expected. Thus, for columns with higher stress levels (above 50%), accounting for transient creep in fire resistance analysis is critical.

### 5.4.3. Type of Concrete

Type of concrete (NSC, HSC, or HPC) influences the mechanical properties at elevated temperatures including the level of undergone transient creep strain as illustrated in Chapter 3. To account for transient creep in fire resistance analysis of concrete columns made of different types of concrete, specific creep data for each type of concrete is needed. Thus, the generated creep data in Chapter 3 for normal strength concrete with steel fibers (NSC-SF), and high strength concrete with polypropylene fibers (HSC-PP), was incorporated into the developed model in Chapter 4 to study transient creep effects in concrete columns constructed with these two types of concrete.

For evaluating the fire resistance of steel fiber-reinforced concrete columns and high-strength concrete columns with polypropylene fibers, suitable material property variation with

temperature should be implemented in the analysis. Thus, thermal and mechanical properties at elevated temperatures for steel fiber-reinforced concrete from Lie and Kodur (1996) are adopted. For high strength concrete with polypropylene fibers, thermal and mechanical properties at elevated temperature are adopted from Khaliq and Kodur (2011).

For evaluating the effect of transient creep strain in NSC-SF and HSC-PP columns, two previously tested concrete columns (C6 and C7) under fire conditions were selected for fire resistance analysis according to the developed model. These two columns were previously tested under fire conditions and detailed characteristics are presented in Table 5.2. Column C6 was made of steel fiber reinforced concrete, whereas Column C7 was constructed with high strength concrete containing polypropylene fibers. The two columns were tested under standard ASTM-E119 fire, and measured axial displacement and fire resistance is reported in Kodur et al. (2003).

To highlight the effect of accounting for transient creep in analysis, each of the two columns is analyzed under two different scenarios: with and without accounting for transient creep in analysis. Then the predicted axial displacement along with failure times are compared with the reported data in fire tests.

Prior to evaluating the structural response of the columns under these two scenarios, thermal response predicted from the model for the two columns is compared to that measured during the fire tests in figures 5.8 and 5.9, for columns C6 and C7, respectively. The generated thermal response indicate that the model is capable of accurately predicting the thermal response of the two columns with marginal difference that can be attributed to the variation between actual and assumed thermal properties of concrete.

For Column C6, steel fiber reinforced concrete, axial displacement variation with time is plotted in Figure 5.10. Axial displacement response under the two analysis cases; with and without

considering transient creep explicitly, show similar transient creep effects as was illustrated for normal strength concrete without fibers. At later stages of the fire (creep stage) the difference between axial displacement predicted from the two cases increases as temperature increases within the column. The predicted fire resistance from the case, where transient creep is accounted, for column C6 was 243 minutes (Fire resistance from test = 239 minutes). When transient creep is not accounted for in the fire resistance analysis, the predicted fire resistance was 265 minutes as shown in Table 5.5.

Similarly, for Column C7, HSC with polypropylene fibers, the predicted axial displacement under the two studied scenarios is plotted in Figure 5.11. Axial displacement under the two scenarios match well with the measured axial displacement during the fire test till temperature in the concrete core rise to high levels after 150 minutes of fire exposure (Figure 5.9). At this stage of fire exposure, the predicted axial displacement without accounting for transient creep strain underestimate the experienced strains at exposure temperatures and result in unconservative predictions. The predicted fire resistance with accounting for creep explicitly was 279 minutes for Column C7, whereas when creep is not accounted fire resistance predicted was 311 minutes.

Overall, transient creep effects in steel fiber reinforced concrete and high strength concrete with polypropylene fibers is similar to that in normal strength concrete. Neglecting transient creep strain in these concrete types result in underestimated deformations and unconservative failure time. From the results of these two columns C6 andC7, high strength concrete with polypropylene fibers experience higher levels of transient creep effects as compared to steel fiber reinforced concrete. The difference in the axial displacement and fire resistance of the two analyzed cases is higher in Column C7 than in Column C6. It was shown in Chapter 3 that transient creep strain is

higher in high strength concrete than in normal strength concrete. Thus, accounting for transient creep strain in fire resistance analysis is more critical for concrete columns made of high strength concrete with polypropylene fibers than in NSC or NSC-SF columns.

### 5.4.4. Asymmetric Thermal Gradients

Concrete columns in buildings are prone to fire exposure from 1-, 2-, 3-, or 4-sides depending on the location of burning, location of columns, and how they are embedded with walls in a building. For instance, corner columns (without walls) of a building can get exposed to fire from two sides, whereas interior columns exposure to fire can be from 1-, 2-, 3- or 4-sides depended on how columns are integrated with walls. Under 1-, 2-, or 3-side fire exposure, RC columns can experience significant asymmetrical thermal gradients as shown in Figure 5.12, and this can magnify the effects of high-temperature transient creep. To isolate the effect of thermal gradients on high-temperature transient creep, response of concrete columns is evaluated under different set of gradients resulting from varying fire exposure scenarios. Typical axial displacement response predicted under hydrocarbon fire and different sides of exposure is shown in Figure 5.13 for column C2. For each fire exposure scenario, the response is predicted with and without accounting for transient creep to show its influence on axial displacement.

For fire exposure on 1- or 2-(adjacent) sides of a column, axial displacement response can be characterized by expansion followed by long steady-state behavior as shown in Figure 5.13. Under 1-side exposure to hydrocarbon fire, the majority (more than 2/3) of the column cross-section is still below 300°C for more than four hours. High heat capacity and low thermal conductivity of concrete hinder heat transfer to as much as half of the column's cross-section, and limit temperature induced transient creep effects for fire exposure up to 4 hours. Although columns under 1-side exposure are subjected to uniaxial bending, degradation in strength and stiffness of

the column is minimal due to the slow rise in sectional temperatures (Raut and Kodur, 2011). Similarly, under 2-adjacent side exposure, column C2 survived exposure to hydrocarbon fire, due to low temperatures experienced in most of the cross section even though the column was subjected to biaxial bending (Raut and Kodur, 2011). Predicted axial displacements with and without creep under 1- and 2-adjacent side exposure are similar until late stages of fire exposure, where transient creep start dominating the deformation pattern. At this stage, columns show a slight variation in axial displacement with and without creep but still can survive fire for long durations (more than 4 hours) as was the case for column C2 (305mm×305mm). Thus, results from the analysis clearly show that fire resistance under 1- and 2-adjacent side exposure is quite high for the analyzed columns and the effect of transient creep is not evident due to lower temperatures developed in most of the columns cross section for up to four hours into fire exposure.

However, under 3-side exposure, transient creep influence is evident and neglecting creep strains can result in underestimation of axial displacement and thus overestimation of fire resistance as shown in Figure 5.13 for column C2. This trend is similar for columns C1, C2, and C5 and the fire resistance values for these columns is tabulated in Table 5.7. Predicted failure times vary greatly between cases with and without transient creep in the case of exposure to hydrocarbon fire from 3 sides. Fire resistance without accounting for transient creep effects in these columns (C1, C2, and C5) indicate that these columns can withstand hydrocarbon fire for extended durations. However, when transient creep is explicitly accounted in fire resistance analysis, these columns failed within considerably shorter durations as listed in Table 5.7.

These trends infer that when exposure to fire is from 3- and 4- sides, accounting for transient creep effects have a significant influence on predicted fire resistance. Further, results from the analysis show 3-side exposure as worst case scenario with the highest influence of

transient creep strain on axial displacement (as can be seen in Figure 5.13) and predicted fire resistance (listed in Table 5.7). Under 3-side exposure, columns are subjected to a uniaxial bending induced by the shape of thermal gradient present on the section. Moreover, induced transient creep strain under 3-sides exposure can increase the uniaxial bending moment induced by asymmetrical thermal gradients. For Column C2, axial displacement at failure was -10 mm without transient creep under exposure to hydrocarbon fire from 3 sides. When transient creep is accounted for explicitly, failure occur at a displacement of -15 mm (50% increase). In the case of 4-side exposure, without transient creep effects, displacement at failure was -12 mm whereas including transient creep explicitly increased displacement at failure to -17 mm (40% increase).

### 5.4.5. Cooling Phase

To study the effect of transient creep strain on response of RC columns in cases where the cooling phase is present, three severe fire scenarios with cooling phase are selected, as shown in Figure 5.1. Fire scenarios F-90, F-120, and F-180 include a burning period as noted in minutes 90, 120, and 180 minutes, and a decay (cooling) phase. The temperature-time curves for these fire scenarios including decay phase are developed as per EC2 compartment fire characteristics. In the case of three design and hydrocarbon fires, temperature increases at a steep rate of heating exceeding 180 °C/min during the first 5 minutes. The decay (cooling) phase in these three selected severe fire scenarios (F-90, F-120, and F-180) is where transient creep strain treatment becomes complex. Moreover, exposure to such severe fires, with temperatures surpassing 500°C early in the fire, can induce significant transient creep strains in columns during the burning (heating) phase of the fire itself.

In fire resistance analysis, transient creep is explicitly included in the heating phase of these fires and excluded during the cooling phase. Thus, during heating phase of the fire, EC2 stress-

strain relations along with explicit transient creep, as well as thermal (expansion) strain are input into analysis as concrete strain. In the cooling phase of the fire, the explicit transient creep part is excluded in analysis to produce more realistic results since transient creep only get generated during first time heating (Khoury et al. 1985). The constitutive model for concrete and rebar in cooling phase of natural fires are based on Eurocode 2 specifications in which thermal damage is induced through decreasing compressive strength and increasing deformability. During the cooling phase, the Eurocode 2 mechanical property relations are adapted without changes for rebar, and with a reduction in strength by 10% for concrete for each temperature. Further, during the cooling phase, explicit transient creep is excluded in analysis since its irrecoverable, and thermal expansion strain is assumed to be partially recoverable. In Figure 5.14, axial displacement is plotted for column C1 under each fire scenario (F-90, F-120, and F-180) with and without considering transient creep explicitly in the heating phase of fire.

The influence of neglecting transient creep is highest under exposure to F-180 fire which has 180 minutes burning period, followed by a 225 minutes cooling phase. When the burning period is reduced to 2 hours (as in F-120) and with a cooling phase of 225 minutes, accounting for transient creep also significantly alters predicted axial displacement. However, when the burning period is reduced to 90 minutes, followed by a 230 minutes of cooling phase, the response is less influenced by transient creep than under F-120 and F-180 fires. This is evident in the predicted axial displacement trends for column C1, shown in Figure 5.14, and failure times of analyzed columns as listed in Table 5.8.

Axial displacement, without explicitly considering transient creep, predicted under severe fire exposure with a cooling phase show lower contraction (shortening) in columns than axial displacement predicted with explicitly accounting for transient creep (see Figure 5.14). For

instance, Column C1 under F-180 fire exposure, experienced contraction of -30 mm when transient creep is accounted for, whereas the contraction was -12 mm when transient creep is neglected. Further, recovery (i.e. rebound from contraction to expansion) of axial displacement in the cooling phase of fire only occur in cases where transient creep is implicitly considered. Under exposure to F-120 fire, contraction in axial displacement for Column C1 reach to around -15 mm whereas in the case without transient creep, contraction recovers as in Figure 5.14. Fire resistance analysis performed on five columns without accounting for transient creep showed that columns can withstand severe fires F-120 and F-180 without failure. However, in cases where transient creep is considered explicitly, failure occured in columns C2 and C5 under F-120 and F-180 (see Table 5.8). Thus, for severe design fire exposure with longer burning periods (2 hours and more) followed by a cooling phase of about 4 hours, transient creep effects have significant influence. Therefore, accounting for transient creep strain in fire resistance analysis of RC columns under such severe fires is critical for predicting realistic failure times. Thus, not accounting for transient creep explicitly underestimates permanent axial deformation (contraction) in the column and can produce unrealistic response during the cooling phase.

## 5.5. Summary

The influence of critical factors on transient creep and fire response of RC columns was quantified under five different varying parameters; fire severity, stress level, concrete type, axisymmetric thermal gradients, and cooling phase. To highlight the effect of variation of these parameters on fire performance of columns, fire resistance analysis was evaluated with transient creep and without transient creep for each column. Then the extent of creep effect in a column under five selected fire exposure scenarios was assessed by comparing undergone axial displacement and predicted fire resistance generated from the two analysis cases. Severity of the

fire highly influences the rate at which creep deformations occur in a concrete column. Columns analyzed under hydrocarbon fire developed creep strains at early stages as compared to columns analyzed under standard ASTM E119 fire. Increase in applied loading level on a column also amplifies the extent of experienced transient creep strain under fire exposure. Type of concrete also have an influence on the extent of transient creep in fire exposed concrete columns due to differences in concrete properties based on their type (NSC, HSC, FRC). In addition, axisymmetric thermal gradients developed in concrete columns due to exposure from 1-, 2- , or 3-sides can magnify the creep effects if not accounted. Finally, for realistic response during the cooling phase of a fire, transient creep is to be accounted explicitly in fire resistance analysis of concrete columns.

Table 5.1 Properties of selected columns for parametric studies on the effect of transient creep

| Column Name | **C1** | **C2** | **C3** | **C4** | **C5** |
|---|---|---|---|---|---|
| **Tested by** | Raut and Kodur 2011 | Kodur et al., 2001 | Kodur et al., 2001 | Lie et al., 1984 | Lie et al., 1993 |
| Cross section, mm | 203×203 | 305×305 | 305×305 | 305×305 | 305×457 |
| Length, m | 3.350 | 3.810 | 3.810 | 3.810 | 3.810 |
| End Conditions * | P-F | P-F | P-F | P-F | P-F |
| Concrete strength, $f'_c$, MPa | 51 | 40.2 | 40.2 | 36.1 | 42.5 |
| Rebar yield stress, $f_y$, MPa | 420 | 354 | 354 | 443 | 414 |
| Longitudinal reinforcement | 4- 20 mm | 4- 25 mm | 4- 25 mm | 4- 25 mm | 6- 22 mm |
| Tie spacing, mm | 200 | 75 and 150 | 75 and 150 | 305 | 305 |
| Type of aggregate | Calcareous | Siliceous | Siliceous | Siliceous | Siliceous |
| Test load, KN | 280 | 930 | 1500 | 1067 | 1413 |
| Stress level % | 40 | 54 | 87 | 85 | 67 |
| Relative humidity % | 81.5 | 90 | 51 | 74 | 65 |
| Mix moisture content % | 6 | 10 | 10 | 6 | 6 |
| Cover thickness, mm | 50 | 48 | 48 | 48 | 48 |
| Test fire scenario | ASTM E-119 | | | | |
| Failure time in test, min | 183 | 278 | 204 | 208 | 396 |

* P; Pined, F: Fixed

Table 5.2 Properties of selected fiber-reinforced columns for parametric studies on the effect of concrete type

| Column Name | **C6 - SFRC** | **C7 - PFRC** |
|---|---|---|
| **Tested by** | Kodur et al., 2003 | Kodur et al., 2003 |
| Cross section, mm | 305×305 | 305×305 |
| Length, m | 3.810 | 3.810 |
| End conditions * | P-F | P-F |
| Concrete strength, $f'_c$, MPa | 89 | 86 |
| Rebar yield stress, $f_y$, MPa | 420 | 420 |
| Longitudinal reinforcement | 4- 25 mm | 4- 25 mm |
| Tie spacing, mm | 75 and 150 | 75 and 150 |
| Type of aggregate | Siliceous | Siliceous |
| Test load, KN | 1800 | 1800 |
| Stress level % | 54 | 54 |
| Cover thickness, mm | 48 | 48 |
| Fiber type | Steel | Polypropylene |
| Fiber quantity, $kg/m^3$ | 42 | 1 |
| Test fire scenario | ASTM E-119 | |
| Failure time in test, min | 239 | 271 |

* P; Pined, F: Fixed

Table 5.3 Range of variation in studied parameters for transient creep extent in columns

| Parameter | Range of Variation | Cases | Columns Analyzed |
|---|---|---|---|
| Fire Severity | ASTM E119 | With and without creep effects | C1 |
| | | | C2 |
| | Hydrocarbon | | C3 |
| | | | C4 |
| | | | C5 |
| Stress Level | 40 | With and without creep effects | C1 |
| | 50 | | C2 |
| | 60 | | C3 |
| | 70 | | C4 |
| | 80 | | C5 |
| Type of Concrete | NSC | With and without creep effects | C2 |
| | NSC-SF | | C6 |
| | HSC-PP | | C7 |
| Number of Exposed Sides | 1- side | With and without creep effects | C1 |
| | 2- sides | | C2 |
| | 3- sides | | C4 |
| | 4-sides | | C5 |
| Cooling Phase | No cooling phase | With and without creep effects | C1 |
| | 90 minutes cooling phase | | C2 |
| | 120 minutes cooling phase | | C4 |
| | 180 minutes cooling phase | | C5 |

Table 5.4 Influence of fire severity on transient creep effects in fire exposed concrete columns

| Parameter | Column | Size, mm (in) | Applied Load, KN (Kips) | Fire Scenario | Exposed faces | Fire Resistance (min) | | | Failure Mode |
|---|---|---|---|---|---|---|---|---|---|
| | | | | | | With Creep | No Creep | Difference | |
| Fire Severity | C1 | 203×203 (8×8) | 280 (63) | Hydrocarbon | 4 | 127 | 139 | 12 | Displacement |
| | C2 | 305×305 (12×12) | 930 (209) | | 4 | 183 | 263 | 80 | |
| | C3 | 305×305 (12×12) | 1500 (337) | | 4 | 125 | 151 | 26 | |
| | C4 | 305×305 (12×12) | 1067 (240) | | 4 | 126 | 157 | 31 | |
| | C5 | 305×457 (12×18) | 1413 (318) | | 4 | 236 | 269 | 33 | |

Table 5.5 Influence of stress level on transient creep effects in fire exposed concrete columns

| Parameter | Column | Size, mm (in) | Applied Load, KN (Kips) | Fire Scenario | Stress Level | Fire Resistance (min) | | | Failure Mode * |
|---|---|---|---|---|---|---|---|---|---|
| | | | | | | With Creep | No Creep | Difference | |
| Stress Level | C1 | 203×203 (8×8) | 280 (63) | ASTM E-119 | 40 | 182 | 224 | 42 | D |
| | C2 | 305×305 (12×12) | 930 (209) | | 54 | 276 | 298 | 22 | S |
| | C3 | 305×305 (12×12) | 1500 (337) | | 87 | 191 | 226 | 35 | S |
| | C4 | 305×305 (12×12) | 1067 (240) | | 85 | 204 | 242 | 38 | S |
| | C5 | 305×457 (12×18) | 1413 (318) | | 67 | 391 | 442 | 51 | S |

* S: Strength, D: Displacement

Table 5.6 Influence of type of used concrete on transient creep in fire exposed concrete columns

| Parameter | Column | Size, mm (in) | Applied Load, KN (Kips) | Fire Scenario | Type of Fibers * | Fire Resistance (min) | | | Failure Mode |
|---|---|---|---|---|---|---|---|---|---|
| | | | | | | With Creep | No Creep | Difference | |
| Concrete type | C2 | 305×305 (12×12) | 930 (209) | ASTM E-119 | - | 276 | 298 | 22 | Displacement |
| | C6 | 305×305 (12×12) | 1800 (405) | | SF | 243 | 265 | 22 | |
| | C7 | 305×305 (12×12) | 1800 (405) | | PP | 279 | 311 | 31 | |

* SF: steel fibers, PP: polypropylene fibers

Table 5.7 Influence of thermal gradients on transient creep effects in fire exposed concrete columns

| Parameter | Column | Size, mm (in) | Applied Load, KN (Kips) | Fire Scenario | Exposed faces | Fire Resistance (min) | | | Failure Mode* |
|---|---|---|---|---|---|---|---|---|---|
| | | | | | | With Creep | No Creep | Differ-ence | |
| Thermal Gradients | C1 | 203×203 (8×8) | 280 (63) | Hydrocarbon | 2-adj | NF | NF | - | NF |
| | C1 | 203×203 (8×8) | 280 (63) | | 3 | 144 | NF | - | D |
| | C2 | 305×305 (12×12) | 930 (209) | | 2-adj | NF | NF | - | NF |
| | C2 | 305×305 (12×12) | 930 (209) | | 3 | 216 | 323 | 107 | S |
| | C5 | 305×305 (12×12) | 1413 (318) | | 2-adj | NF | NF | - | NF |
| | C5 | 305×457 (12×18) | 1413 (318) | | 3 | 256 | NF | - | NF |

* NF: No failure, S: Strength, D: displacement

Table 5.8 Influence of cooling phase on transient creep effects in fire exposed concrete columns

| Parameter | Column | Size, mm (in) | Applied Load, KN (Kips) | Fire Scenario | Fire Resistance (min) | | | Failure Mode * |
|---|---|---|---|---|---|---|---|---|
| | | | | | With Creep | No Creep | Differ-ence | |
| Severe Fires with Cooling Phase | C1 | 203×203 (8×8) | 280 (63) | F-90 | NF* | NF | - | NF |
| | C1 | 203×203 (8×8) | 280 (63) | F-120 | 138 | NF | - | D |
| | C2 | 305×305 (12×12) | 930 (209) | F-90 | 233 | NF | - | D |
| | C2 | 305×305 (12×12) | 930 (209) | F-120 | 194 | NF | - | D |
| | C2 | 305×305 (12×12) | 930 (209) | F-180 | 189 | 203 | 14 | D |
| | C5 | 305×457 (12×18) | 1413 (318) | F-180 | 282 | NF | - | D |

* NF: No failure, D: Displacement

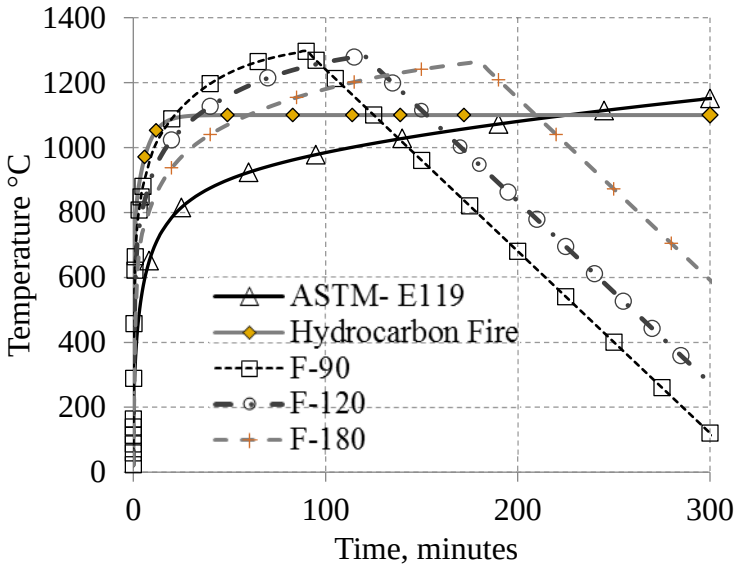


Figure 5.1 Variation of temperature with time for selected fire scenarios

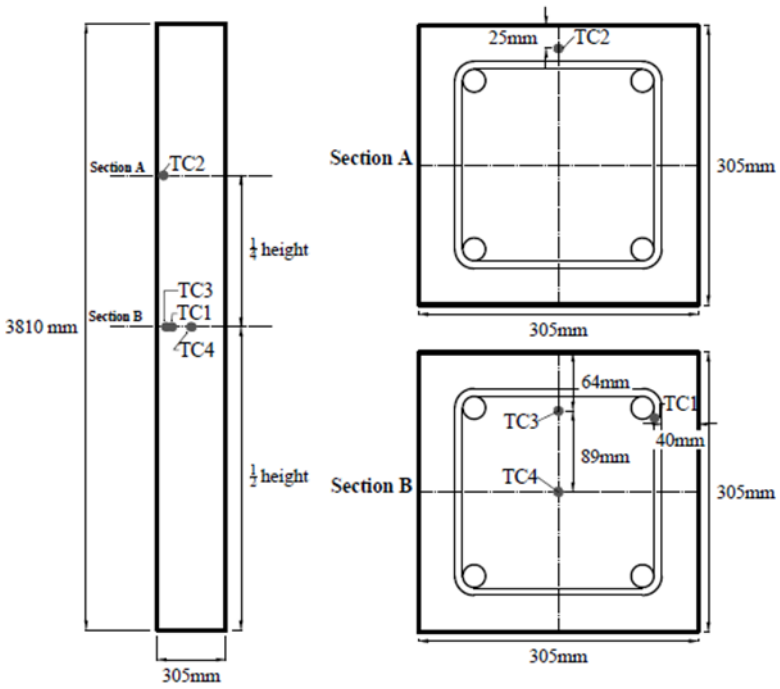


(a) Column Elevation (b) Cross Section

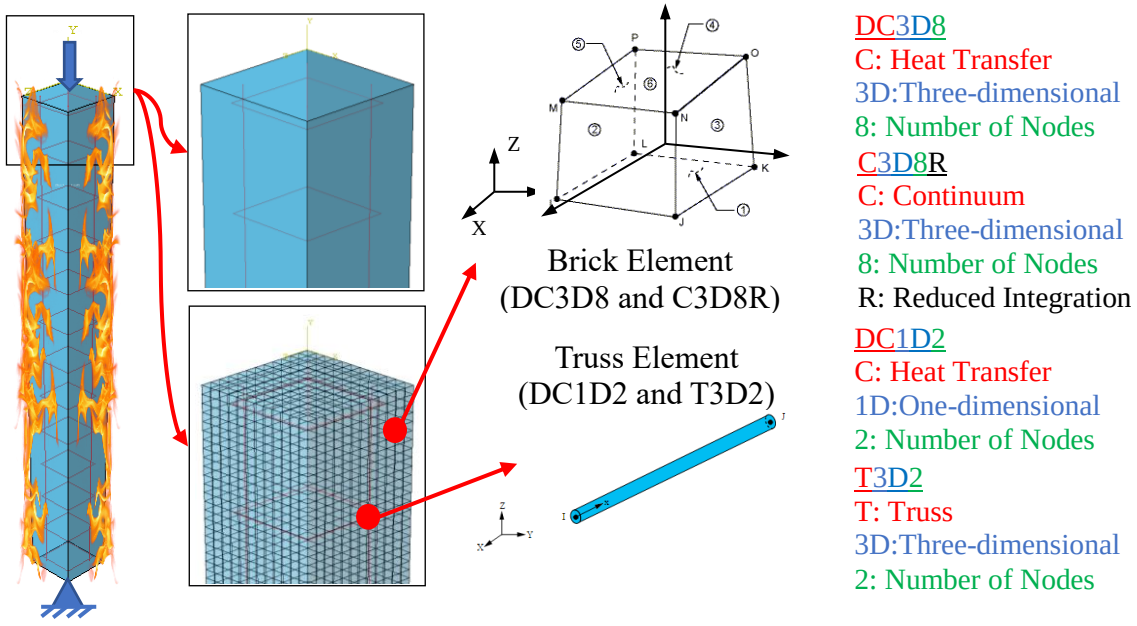


(c) Column Discretization (d) Element Details

Figure 5.2 Discretization of RC column for fire resistance analysis

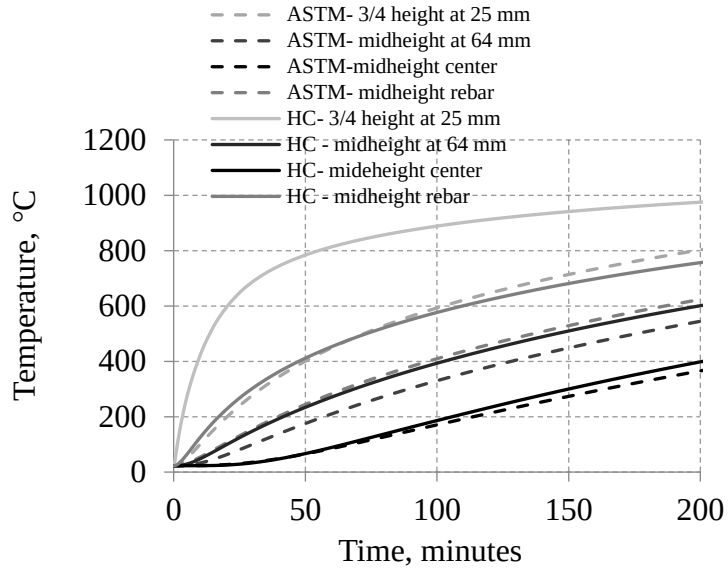


(a) Predicted Temperatures for C4

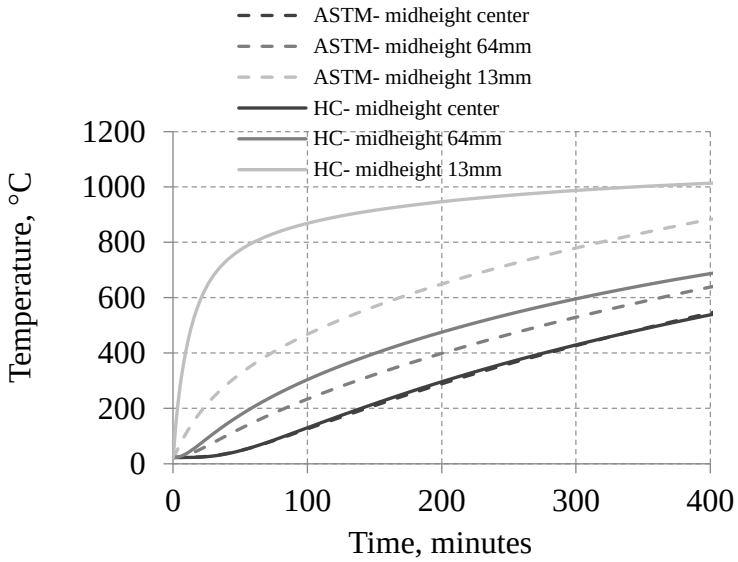


(b) Predicted Temperatures for C5

Figure 5.3 Cross sectional temperatures in C2 and C5 under standard ASTM- E119 and hydrocarbon fires

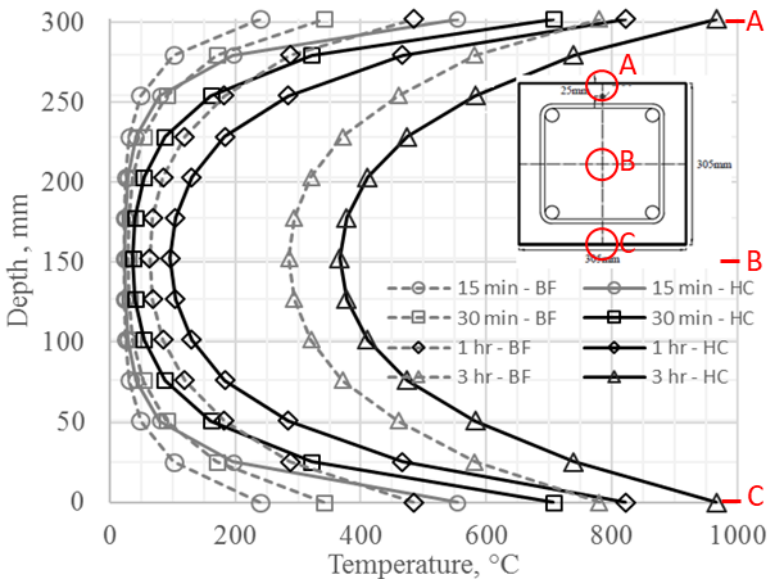


Figure 5.4 Thermal gradients at mid-height section of Column C4 for standard ASTM E-119 (BF) and hydrocarbon (HC) fires at different times of fire exposure

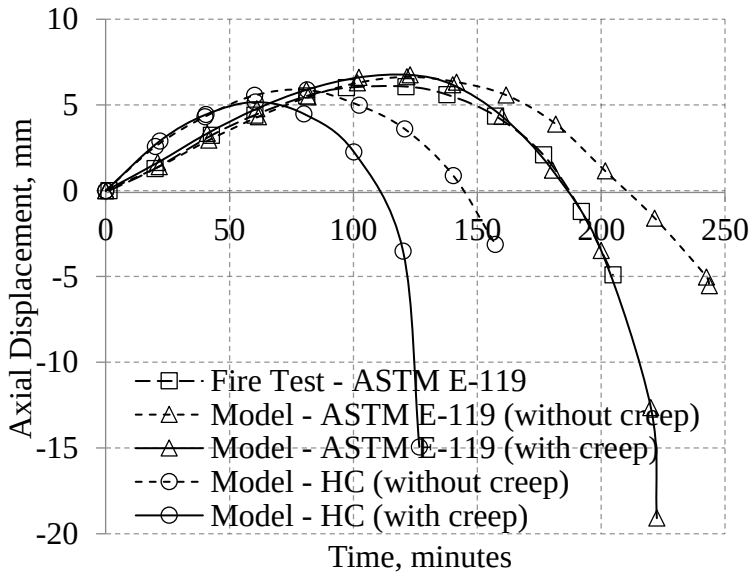


Figure 5.5 Effect of transient creep on axial displacement response of Column C4 under hydrocarbon (HC) and standard ASTM fire

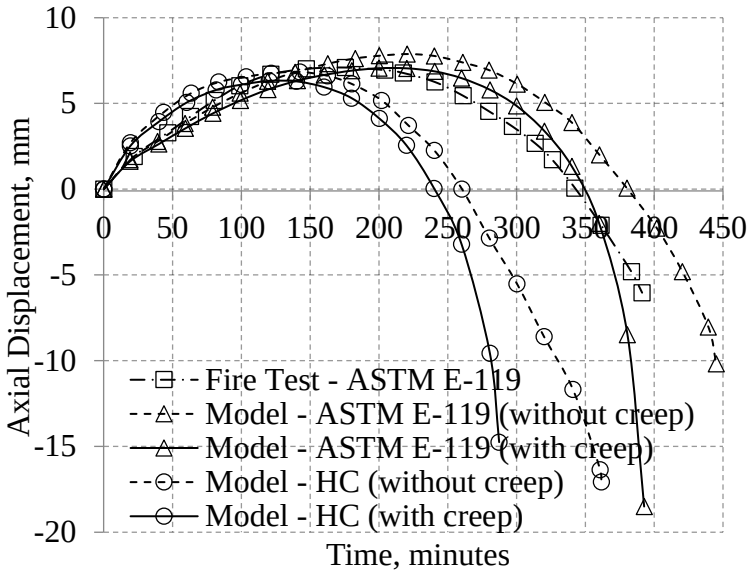


Figure 5.6 Effect of transient creep on axial displacement response of Column C5 under hydrocarbon (HC) and standard ASTM fire

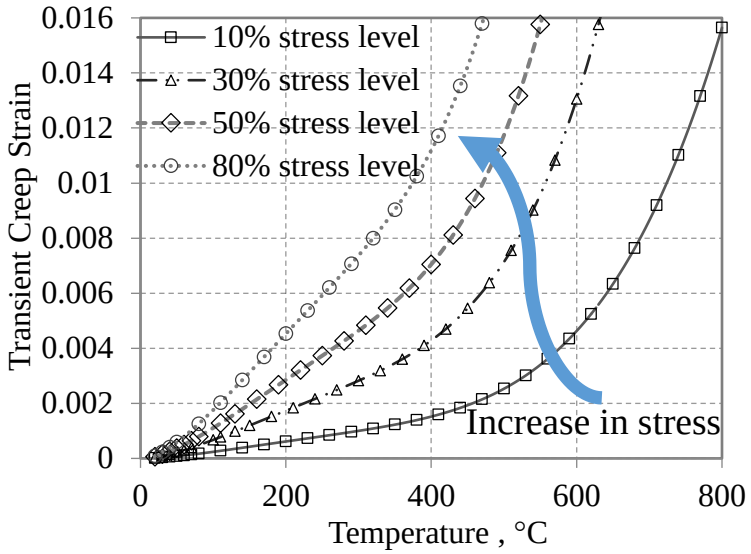


Figure 5.7 Transient creep as a function of temperature and stress level

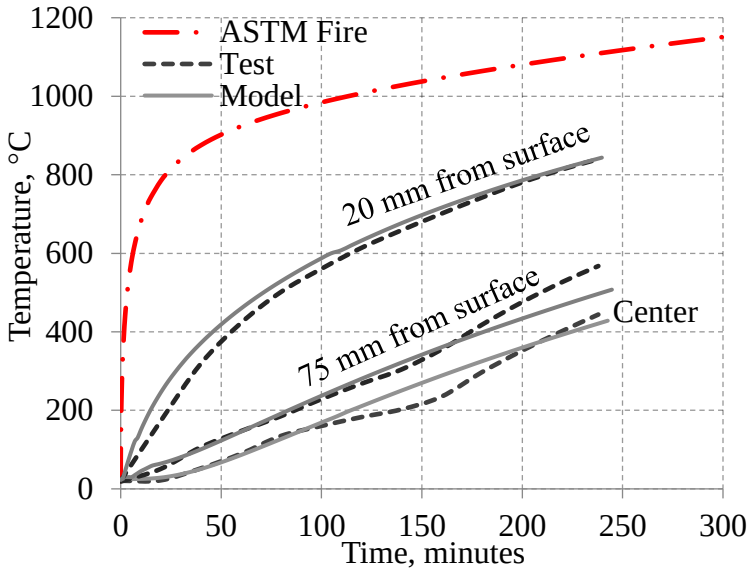


Figure 5.9 Measured and predicted temperatures for Column C6

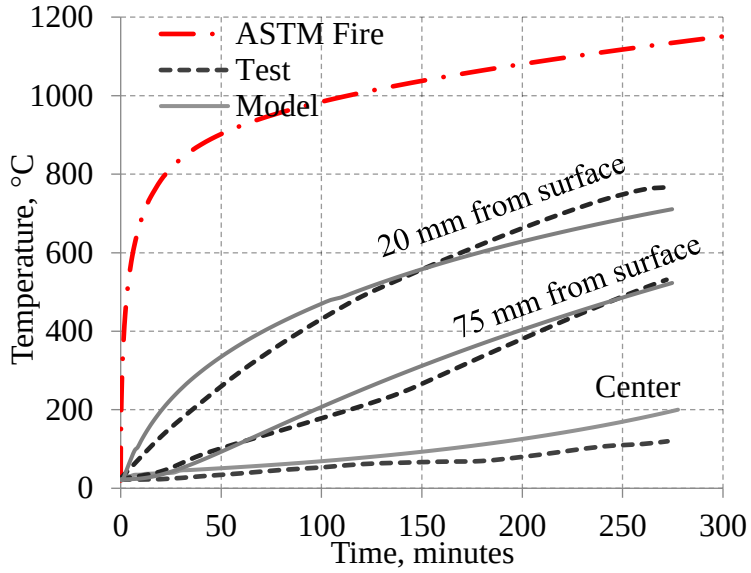


Figure 5.8 Measured and predicted temperatures for Column C7

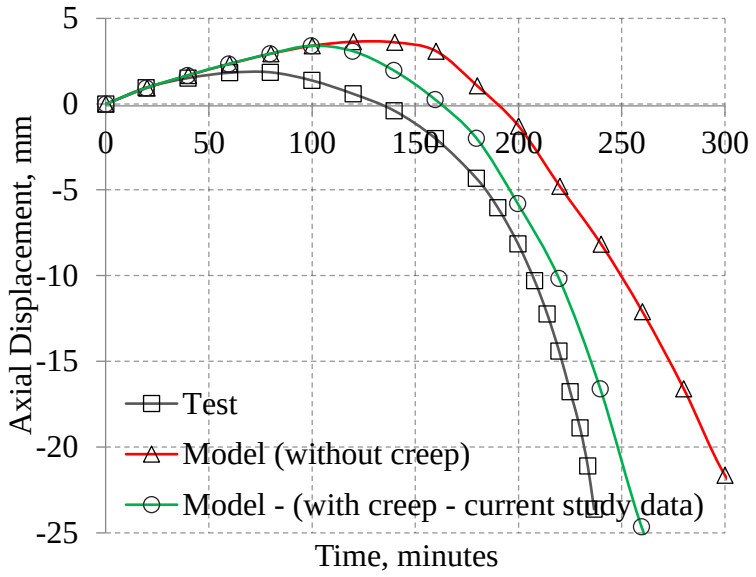


Figure 5.10 Effect of transient creep in steel fiber reinforced concrete Column C6

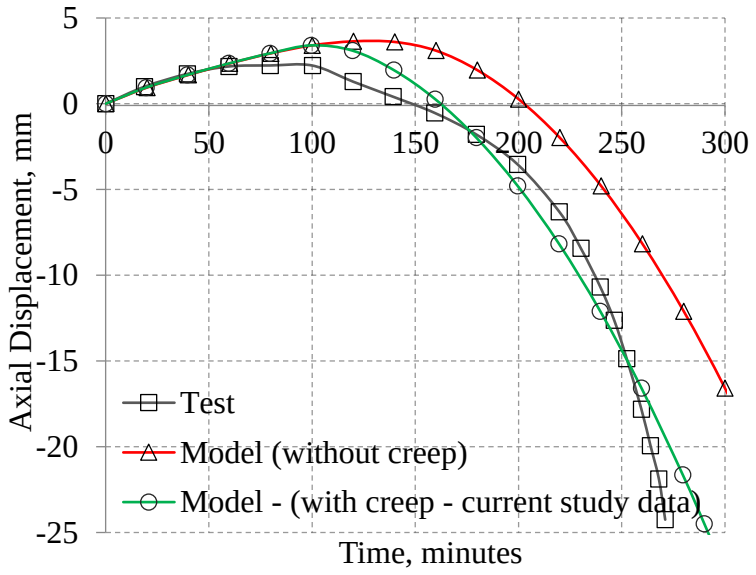


Figure 5.11 Effect of transient creep in HSC Column C7 made of polypropylene fiber reinforced concrete

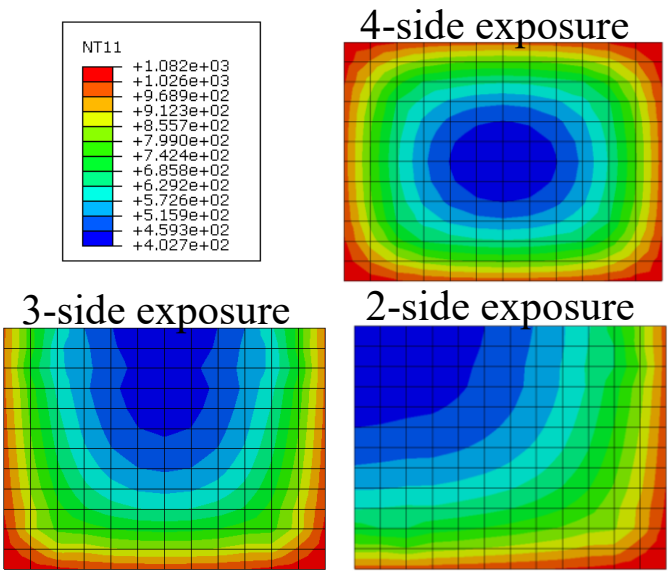


Figure 5.12 Effect of number of exposed sides of the column on the shape of the thermal gradient

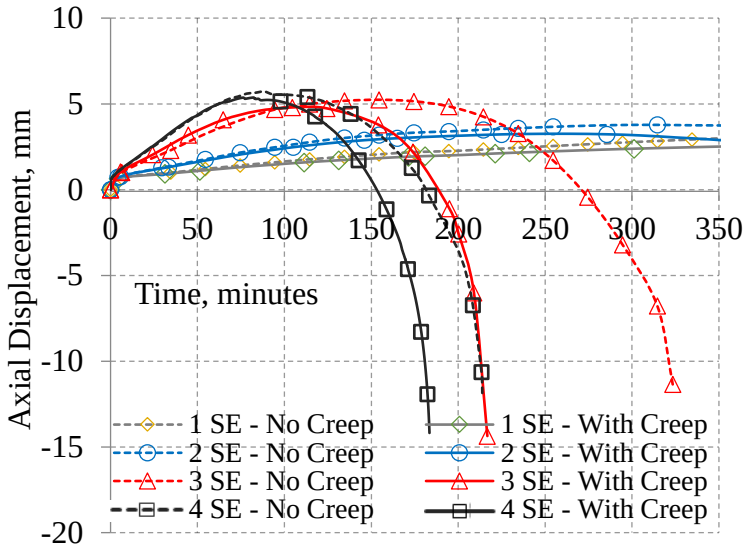


Figure 5.13 Effect of different sides of exposure (SE) on axial displacement of Column C2 under hydrocarbon fire

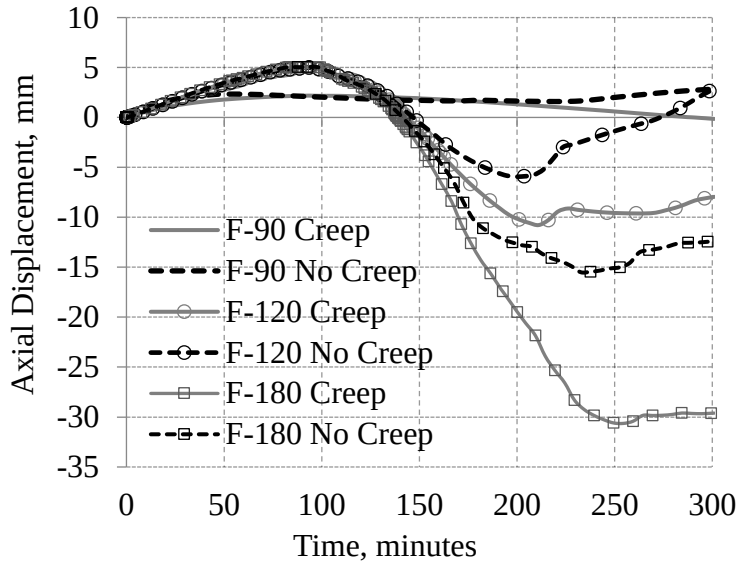


Figure 5.14 Effect of cooling phase of fire on axial displacement response of Column C1

# CHAPTER SIX

# 6. Design Recommendations

## 6.1. General

Structural members can develop significant creep strain in later stages of fire exposure and thus are susceptible to early failure due to high-temperature creep strains. In reinforced and prestressed concrete members, transient creep strain of concrete can form a significant portion of total strain at elevated temperatures and thus needs to be fully accounted for in fire resistance analysis. Despite the adverse effects of transient creep on fire response of concrete columns, very limited guidelines and recommendations are available on treatment of high-temperature creep in evaluating fire resistance of concrete members.

Fire resistance of concrete members is mostly evaluated through prescriptive-based approaches as specified in ACI 216.1-14 (2014) or Eurocode 2 (2004). Even in current rational approaches for evaluating fire resistance transient creep effects are not specifically accounted for in concrete members. Further, advanced analysis procedures incorporating stress-strain relations for concrete at elevated temperatures, as specified in ASCE manual (1992) and Eurocode 2 (2004), only account for partial transient creep strain implicitly. However, this implicit consideration does not take into account much of the high-temperature creep developed just prior to failure of a fire exposed member. This is especially true when concrete temperatures reach 500°C and creep strains dominate the deformation response. In fact, Eurocode 2 (2004) states that "creep effects are not explicitly considered" in the stress-strain relations, and recommends to explicitly account for creep effects in carrying out advanced fire resistance analysis of RC structures. However, there are no specific guidelines for the explicit treatment of creep strains under fire conditions.

Thus, current calculation methods for evaluating fire resistance of concrete columns based on these stress-strain relations lack full extent of transient creep (Gernay and Franssen, 2012; Kodur and Alogla, 2016; Sadaoui and Khennane, 2009). This problem is more prominent in columns due to the fact that columns, unlike flexural member (beams, slabs), are compression members and full portion of the concrete (section) is utilized in resisting loading. In most cases of beams and slabs, concrete in compressive zone contribute to resisting load but this portion of concrete is a small part of the overall section and is often not directly exposed to fire. Thus, transient creep effects arising from concrete is much smaller in flexural members.

Further, limited approaches are available to account for transient creep strain when carrying out advanced fire resistance analysis of concrete columns. These approaches, as the one outlined in Chapter 4, are often complex and involve high level of calculations. Due to complexity associated with such approaches, fire resistance analysis incorporating high-temperature explicitly is typically carried out only for research purposes and in rare cases for design.

To overcome these limitations related to accounting transient creep effects in fire resistance analysis of concrete columns, design recommendations are presented in this chapter. Specifically, guidance is given on when temperature-induced creep strains are to be included in fire resistance analysis of concrete structures. Such recommendations can be implemented in the evaluation of fire resistance of concrete columns specifically in cases where transient creep is most likely to dominate the deformation response under fire exposure.

## 6.2. Evolution of Creep

Creep at ambient temperature is a time-dependent deformation phenomenon that results in additional plastic deformation in concrete under sustained loading over a prolonged period. With the accumulation of creep deformations over time (years), creep effects start to influence the

structural member under sustained loading and ambient conditions. Creep strain, at elevated temperatures, however, develops at a much rapid rate depending on the stress level and temperature range. Above 500°C, creep effects get amplified and dominate the deformation response of concrete.

Under fire exposure, concrete members get exposed to transient heating where concrete develop transient creep strain. This transient creep strain forms a significant portion of total strain in concrete at elevated temperatures and gets highly amplified with increase in temperature and stress level. Total strain experienced in concrete under such transient heating conditions is plotted in Figure 6.1-a. If no load is applied on concrete while under transient heating, the developed strain is a pure thermal strain (expansion). At stress level of 10%, total strain of concrete under transient heating is not significantly affected by transient creep as shown in Figure 6.1-a. However, at stress levels of 30% and higher, transient creep strain can form a significant part of total strain in concrete at 400°C or above. As shown in Figure 6.-b, transient creep strain at stress levels of 30, 50 and 70% of room temperature strength constitute to most of the deformations experienced in concrete. This causes the total strain of concrete under transient heating to shift from expansion (positive) to contraction (negative) as shown in Figure 6.1.

Since this transient creep strain constitutes a big part of total strain in concrete, it dominates the deformation response of concrete members when exposed to prolonged fire exposure. Failure of concrete columns, for instance, is highly susceptible to be governed by transient creep strain when exposed to fire. To illustrate the creep effects on the fire response of RC columns, variation of axial deformation with fire exposure time for a concrete column is plotted in Figure 6.2. In general, axial displacement response during fire exposure can be grouped under three main stages; expansion, steady-state, and creep. In the first stage, total deformation is mainly resulting from

temperature-induced thermal expansion of constituent materials, concrete and steel, due to temperature rise. During this stage, concrete and reinforcing steel experience minimal material degradation due to lower sectional temperatures below 300°C in outer layers of concrete core and 400°C in rebars. Axial deformation gradually increases due to expansion of the column until it reaches to a point where expansion is fully developed.

In the second stage, thermal, mechanical, and transient creep strains contribute to axial deformation. This nearly steady-state response in this stage is attributed to counteracting of expansion effect from stiffness degradation in column due to raising in sectional temperatures, as well as development of effects of transient creep strain. In the third stage, axial displacement response is completely dominated by increasing transient creep strain and the high transient strains lead to transferring the deformation state from expansion to contraction. The contraction phase of the column continues until its failure. During this stage, cross-sectional temperatures (in concrete and rebar) in much of the section rises above 500°C and this produce high levels of creep strain, ultimately leading to "run-away" deformations and thus failure of the column.

Although transient creep strain dominates the deformation response in concrete columns at later stages of fire exposure, it is often overlooked when evaluating their fire resistance. In fact, fire resistance of concrete members, in general, is currently evaluated through prescriptive-based approaches as specified in ACI 216.1-14 (2014) or Eurocode 2 (2004) in which transient creep effects are not fully accounted. These codes provide simplified approaches for design of structural members and evaluation of their fire resistance. In addition, Eurocode 2 recommend use of advanced analysis with accounting for creep strain but fail to provide guidelines on cases where such kind of analysis is recommended leaving the choice to designers. Further, advanced analysis that involves only the use of stress-strain relations for concrete at elevated temperatures, as

specified in ASCE manual (1992) and Eurocode 2 (2004), only account for partial transient creep strain. Thus, current calculation methods for evaluating fire resistance of concrete members based on these stress-strain relations lack full extent of transient creep and can result in overestimation of fire resistance, as was shown for columns in this Thesis.

## 6.3. Limitations of Implicit Creep in Stress-Strain Models

Fire resistance evaluation of concrete columns incorporates appropriate constitutive stress-strain relations to describe the mechanical behavior of both concrete and reinforcing steel. In advanced fire resistance analysis, including the use of finite element-based programs, creep strains at elevated temperatures are often accounted for implicitly through these constitutive models (stress-strain relations). In this section, limitations inherent to consideration of high-temperature creep implicitly in concrete stress-strain models are discussed.

As demonstrated in Chapters 4 and 5, the Eurocode 2 (2004) stress-strain relations fail to capture full transient creep effects in concrete under certain scenarios of fire exposure. To further illustrate the limitations of implicit creep in constitutive models, ASCE and EC2 constitutive models are compared with a transient stress-strain response derived from transient creep experiments presented in Chapter 3.

Utilizing data generated from transient experiments, stress-strain response under transient heating can be plotted up to the highest stress level applied during transient experiments (70% or $\frac{f'_{c,T}}{f'_{c,(20℃)}}$ = 0.7). Each point along the stress-strain curve can be determined through three parameters; stress, strain, and temperature. However, for the complete stress-strain response, the remaining part of the stress-strain curve (from stress level of 70% to failure) is to be assumed. This remaining part of the stress-strain curve can be determined for different temperatures through two other points. One is the point of maximum stress, or the strength at elevated temperatures, $f'_{c,T}$ ,

and the corresponding strain at peak stress, $\varepsilon_{c0,T}$ . The second point is at ultimate strain, $\varepsilon_{cu,T}$ and zero stress (end of the descending branch of the curve). Therefore, the generated response for comparison under transient heating conditions is derived up to the point where maximum stress level was applied during transient experiments (70% or $\frac{f'_{c,T}}{f'_{c,(20°C)}}$ = 0.7).

The comparison between the two stress-strain models and transient stress-strain response for temperatures ranging from ambient to 700°C is shown in figures 6.3 and 6.4. For 20-300°C, plotted in Figure 6.3, derived transient stress-strain response compares well with the stress-strain response from both codes (ASCE and EC2). However, above 300°C, the generated transient stress-strain response shows higher stiffness (i.e. lower strain values for the same stress level) as shown in Figure 6.4 for temperatures 400-700°C. As temperature in concrete increase, the difference in elastic modulus at elevated temperatures, $E_{c,T}$ , between transient response and steady-state response increases.

The reason for the higher concrete stiffness under transient heating is that concrete is loaded before heating start. When concrete specimens are heated to a certain temperature before testing for stress-strain response, as in the steady-state method or unstressed method, degradation in stiffness is already induced before loading. The reduction in stiffness in these stress-strain models is also in part due to implicit accounting of transient creep in these models at elevated temperature. Accounting for creep strain implicitly in concrete stress-strain response was first suggested by Collins and Mitchell (1987) in which the strain at peak stress is increased from $(\varepsilon_{c0})$ to $(\varepsilon_{c0} + \Delta\varepsilon_{cr})$ where $\Delta\varepsilon_{cr}$ is creep strain at maximum stress. The same principle is applied in concrete stress-strain response at elevated temperatures by shifting the strain at peak stress, $\varepsilon_{c0,T}$ , by a selected creep strain magnitude, $\Delta\varepsilon_{trc,T}$ . Thus, shifting the strain at maximum stress to a higher value cause a reduction in the slope of the elastic range of response as shown in Figure 6.5. In this

figure, a comparison between stress-strain response with and without increasing strain at peak stress by $\Delta\varepsilon_{trc,T}$ to account for creep implicitly. The increase in strain at peak stress by $\Delta\varepsilon_{trc,T}$ reduce concrete elastic modulus, E, and increase the range of the elastic response in concrete.

Thus, implicit accounting for transient creep in stress-strain relations can be misleading under certain scenarios of fire exposure, as shown in Chapters 4 and 5. The limitations inherent to this implicit transient creep consideration can be summarized in the following:

- Implicit stress-strain relations do not consider the order of heating and loading regime and the various possible paths of stress and temperature (i.e. heating then loading, loading then heating, or simultaneous heating and loading).
- Considering transient creep strain implicitly does not account for the irreversibility of transient creep since it only develops at first time heating and is not repeatable upon reheating.
- In the cooling phase of a fire, implicit consideration of transient creep strain does not exclude transient creep from the total experienced strain.
- Implicit consideration of transient creep through shifting the strain at peak stress results in reducing the actual elastic modulus at temperatures higher than 400°C.
- Upon unloading, consideration of transient creep implicitly results in underestimated unloading stiffness and overestimated plastic strains.

## 6.4. Treatment in Fire Resistance Analysis

Evaluating fire resistance of concrete members can be performed according to simplified approaches and advanced ones. Thus, treatment of creep effects in fire resistance analysis can be grouped under three scenarios, creep effects not critical in fire resistance analysis, implicit

consideration to creep through stress-strain relations, and finally explicit consideration to transient creep in fire resistance analysis.

### 6.4.1. Scenarios where Creep is not Critical

In many scenarios of fire exposure, creep effects might not govern the failure of the concrete member. In fact, fire resistance evaluation is currently mostly based on simplified approaches in which transient creep strain is not accounted. These approaches are widely applied for evaluating fire resistance of concrete members. In this section, the cases of fire exposure on concrete members where creep is not critical to be accounted in fire resistance analysis are summarized in the following:

- When failure of the concrete member is more likely to be governed by strength failure limit. Under strength failure limit, degraded capacity of the concrete member is compared to the applied loading. Thus, the calculated degraded capacity does not get affected significantly by considering creep.
- When temperature in the concrete member does not reach 400°C under service stress levels, effect of transient creep strain on fire resistance analysis of concrete members can be minimal.

### 6.4.2. Scenarios where Implicit Creep is Sufficient

In certain scenarios of fire exposure, accounting for high-temperature creep implicitly in fire resistance analysis is sufficient to predict a realistic fire response of concrete members. In this section, the scenarios of fire exposure on concrete members where creep is not needed to be accounted explicitly in fire resistance analysis are summarized in the following:

- When temperature in the concrete member does not exceed 400°C under service stress levels, effect of transient creep strain on fire resistance analysis of concrete members can be minimal.
- In flexural members (beams and slabs), when the exposure to fire from the bottom and temperature in the concrete compressive zone does not reach creep critical temperature. If the compressive zone does not reach creep critical temperature, then concrete only develops primary creep which only has slight effects if neglected in fire resistance analysis.
- In lightly loaded concrete columns, where applied loading is much lower than degrading capacity of the column (stress level < 30%). Under low stress levels (stress level < 30%), developed transient creep in concrete is insignificant to be explicitly considered in fire resistance analysis and implicit consideration is sufficient.

### 6.4.3. Scenarios where Creep is to be Considered Explicitly

Due to the complexity associated with accounting for high-temperature creep in fire resistance analysis of structural members, one of this Thesis objectives is to provide recommendations on cases where creep is critical in concrete members. Based on the parametric studies presented in Chapter 5, explicit accounting for transient creep in fire resistance analysis can be critical in certain cases of fire exposed concrete columns. Thus, in this section, scenarios, where creep can be significant in concrete columns, are first highlighted in order to determine where advanced analysis is highly recommended. Then, general scenarios on concrete members where creep can become dominant under fire exposure are discussed.

As discussed, transient creep strain is mainly a function of stress and temperature. Thus, certain scenarios of fire exposure impose higher temperature on concrete columns than others. In

Figure 6.6, temperatures at the edge of a square concrete column (305mm by 305mm) are plotted under three different scenarios of fire exposure, namely; ASTM E-119, hydrocarbon and design fire with 2 hours burning, F-120. Temperatures below 400°C are considered to be creep safe temperatures, where only marginal creep is developed in the concrete column. Temperatures above 400°C, on contrast, are considered to be creep critical temperatures where significant creep can be developed in the column. As shown in Figure 6.6, severity of the fire control the time at which such high temperatures are attained in the columns core, and hence, induce creep strains at a faster rate than standard ASTM E119 fire. The extent of developed creep in concrete members, in general, can be classified under three categories; minor, moderate and severe based on experienced temperature and stress level. As shown in Table 6.1., the categories are given for different temperature ranges based on applied stress level on the member. As stress level increases, the severity of creep increases even at low temperatures. At high temperatures (> 500°C), creep extent is significant even under low stress level as shown in Table 6.1.

In order to simplify determining cases of concrete columns where creep can be critical, recommendations based on stress and temperature are provided in Table 6.2 as time at which creep become dominant in concrete columns of different sizes under two standard scenarios of fire exposure, ASTM- E119 standard fire and hydrocarbon fire. This can be referred to as time after which creep deformations are dominant in concrete columns. For all studied column sizes, increase in applied stress level lowers the time at which transient creep become dominant on the deformation response. Since temperatures under hydrocarbon fire exposure raise more rapidly than under ASTM-E119, it takes shorter times for transient creep to become dominant in concrete columns under hydrocarbon fire exposure. These recommendations are given for column sizes analyzed in current studies. For other column sizes, similar times can be determined based on

temperatures in the column section reaching to creep critical temperatures as in Table 6.3 in the core of the column. These creep critical temperatures refer to the temperature at which creep become dominant in concrete and are provided for studied concrete types (NSC, NSC-SF, and HSC-PP).

The concept of utilizing creep critical temperatures can also be extended to be applied on fire exposed concrete members, specifically, members under compression loading (walls, post-tensioned slabs, etc.). If concrete in the structural member reaches to creep critical temperature, then transient creep strain is more likely to dominate the deformation response. Thus, in fire resistance analysis, it is recommended to account for transient creep when temperatures reach to critical creep levels for a given stress level, as specified in Table 6.3.

In addition to the influence of temperature and stress level, type of concrete influences the extent of transient creep strain developed during fire conditions. As in Table 6.3, high strength concrete with polypropylene fibers (HSC-PP) experienced the highest transient creep among the studied concretes. Similarly, normal strength concrete with steel fibers (NSC-SF) experienced lower transient creep than conventional concrete up to a temperature of around 400°C. Thus, for cases where transient creep is dominant in fire exposed concrete members, the concrete type can increase or reduce the demand for explicitly accounting for transient creep.

Number of exposure sides of the column to fire was shown to be critical in accounting for transient creep strain in fire resistance analysis (see Chapter 5). Under exposure to fire from two or three sides, additional stress and bending moment can be exerted on the column depending on the shape of the developed thermal gradients. Under such asymmetric thermal gradients, columns can be subjected to biaxial moment which could trigger creep deformations in heated portion of the cross section. Thus, under such scenarios of fire exposure, transient creep is recommended to

be explicitly considered in fire resistance analysis. For other concrete members, the type of fire exposure and the exposed area of the member, might also be influential in accounting for transient creep in fire resistance analysis.

Overall, under certain scenarios of fire exposure, creep effects can govern the failure of a concrete member and in such cases transient creep is to be explicitly accounted for in fire resistance analysis. Recommendations to account for transient creep explicitly in fire resistance analysis are given based on these critical scenarios. The recommendations can be grouped into two categories: general recommendations for concrete members, and specific recommendations for concrete columns under fire conditions. Then a summary of the developed approach (in the current study) for accounting for transient creep explicitly is presented in the subsequent sections.

For concrete members in general, the following are scenarios where explicit accounting of transient creep strain become critical:

- When extent of creep in concrete members can be severe, as specified in Table 6.1. Under minor and moderate creep effects, implicit consideration of creep in stress-strain response at elevated temperature can be sufficient.
- When temperature in a concrete member exceed “creep critical temperature” as specified in Table 6.3 for different types of concrete and under different levels of applied stress.
- When concrete is subjected to loading and unloading since implicit consideration of transient creep underestimate concrete stiffness and overestimate plastic strain.

For concrete columns, based on the studies carried out in this Thesis, it is highly recommended to account for transient creep in fire resistance analysis of concrete columns under the following scenarios:

- When temperature in the core of a concrete column exceeds creep critical temperature as specified in Table 6.3 for different types of concrete under various stress levels. At such critical temperatures, creep dominate the deformation response and influence the predicted fire resistance if not accounted.
- For analyzed column sizes in the current study, transient creep becomes dominant after specified times in Table 6.2. Thus, for concrete columns exposed to standard ASTM E119 or hydrocarbon fire longer than specified times in Table 6.2, transient creep is highly recommended to be explicitly accounted in fire resistance analysis.
- For highly loaded columns, with stress level of 40% and more, high-temperature creep strains are recommended to be explicitly accounted in fire resistance analysis.
- For columns made of high strength concrete with polypropylene fibers, accounting for transient creep in fire resistance analysis is more critical than in NSC columns. Thus, it is recommended to explicitly account for transient creep when evaluating fire resistance of high strength concrete columns enhanced with polypropylene fibers.
- For columns constructed with steel fiber reinforced concrete, transient creep is recommended to be accounted for explicitly when temperature in a column's core exceed 450°C under service stress levels (30% to 70%).
- Under exposure from two or three sides, transient creep is recommended to be explicitly accounted for in fire resistance analysis of concrete columns since it highly affects the deformation response.
- If a cooling phase is considered in fire resistance analysis of a concrete column, it is highly recommended to explicitly account for transient creep in analysis.

- For slender concrete columns, as specified in ACI 318-14 (2014), accounting for high-temperature creep explicitly in fire resistance is recommended since slender columns are more susceptible to buckling than short columns.

A summary of the above-mentioned scenarios for treatment of transient creep in fire resistance analysis of concrete members is grouped in to three categories; namely creep is not critical, creep implicitly, and creep explicitly. (see Table 6.4)

## 6.5. Approach for Incorporating Creep Explicitly in Advanced Analysis

### 6.5.1. General

Advanced fire resistance analysis where creep calculations are to be considered explicitly is to be performed utilizing finite element programs such as ANSYS and ABAQUS. As in the case of FE model in Chapter 4, fire resistance evaluation can be performed according to the general sequential thermo-mechanical approach. In this approach, creep can be explicitly accounted for through built-in creep models available in FEM programs, or through developing subroutines specifically for accounting explicit creep. In this section, the general approach to account for transient creep explicitly in fire resistance evaluation in this Thesis is summarized and outlined.

### 6.5.2. Numerical Model

Fire resistance analysis of concrete columns in is to be undertaken through a two-step formulation; thermal and structural analysis. In thermal analysis, temperature distribution within the concrete column is generated and stored as a function of fire exposure time (temperature history). Nodal temperatures predicted from thermal analysis are then applied as an input for structural analysis. In the structural analysis, stresses and associated deformations resulting from exposure to fire are calculated based on temperature-dependent material properties. The following steps summarize the general procedure typically adopted in this approach:

- Selection of a fire exposure scenario (input time-temperature curve), geometry of the column, loading, boundary conditions, etc.
- Discretization of concrete and reinforcing steel in the concrete column into infinitesimal elements.
- Thermal analysis: the distribution of cross-sectional temperatures is generated in the column based on specified temperature-dependent thermal properties.
- A static structural analysis at room temperature is performed on the concrete column under applied loading to determine stresses and deformations.
- Structural analysis: the generated nodal temperature history is applied as an input for the fire resistance analysis. Explicit high-temperature creep is accounted in this step of the analysis.
- Fire resistance analysis is performed at incrementing time steps till failure occurs in the column.

Accounting for transient creep strain in this approach is performed in the structural analysis step of fire resistance evaluation. When inputting stress-strain data in numerical analysis, it is specified weather transient creep is accounted explicitly or implicitly. For explicit accounting of transient creep, a mean for incorporating transient creep data in numerical analysis is needed.

In the numerical model presented in Chapter 4, transient creep is incorporated in analysis through the use of the Drucker-Prager creep model available in ABAQUS. A detailed flow chart illustrating the steps followed in this numerical model is shown in Figure 6.6. The highlighted portion of the flowchart in red is where transient creep is incorporated into fire resistance analysis in this model. Thus, if transient creep is recommended to be explicitly accounted for in fire resistance analysis of concrete columns, this approach can be applied. The steps followed in the

outline approach in Figure 6.6 follow the general approach of thermo-mechanical analysis and can be summarized as:

- Start of thermal analysis where geometry, mesh size, element types and number of nodes are defined. Discretization of the column is carried out based on the selected mesh properties and type of elements.
- Input the fire temperature-time curve and boundary conditions for thermal analysis. The sectional temperatures in the concrete member are calculated based on heat transfer from the fire source to the column's faces through convection and radiation. Then the heat of transfer is governed by conduction within the column. The temperature-dependent thermal properties for concrete and reinforcing steel are input along with coefficients for convective and radiative heat transfer.
- From the thermal analysis, temperature history (temperature variation with time) for total duration of fire exposure is calculated for the specified discretization of nodes and elements. Each node in the mesh consists of one degree of freedom (temperature).
- The temperature history of the column is then inputted in the structural sub-model along with geometry, boundary conditions, mesh size, and element types.
- The column is discretized for structural analysis based on the specified mesh and elements properties.
- Assembly of the stiffness matrix, where temperature-dependent mechanical properties are input along with creep properties. In the followed approach Drucker-Prager creep model in ABAQUS was adopted for accounting for transient creep strain in concrete. However, other approaches can be applied such as utilizing user-defined subroutines for specifying constitutive relations in ABAQUS.

- Using the assembled stiffness matrix, stresses and strains in the concrete column can be calculated. At each node, six degrees of freedom are calculated representing forces and displacements in three dimensions x, y, and z.
- Based on the developed strains in the analyzed concrete column, axial displacement variation with time is calculated.
- Failure limit state are applied to determine fire resistance using strength and displacement criteria. Displacement and rate of displacement failure limits for vertically loaded members, according to ISO834-1 (1999), are $0.01h$ mm and $0.003h$ mm/min where $h$ is the height of the column in mm. In the displacement-based failure limit, at each time step of the analysis, axial displacement or the rate of displacement of the column, as obtained from the numerical model, are compared with corresponding deflection limits. In the strength failure limit, a column is deemed to have failed when the reducing axial capacity of the column at that time step fall below the axial load present on the column.
- Finally, the duration to the point at which the strength or deflection limit is exceeded represents the fire resistance of the column.

In the approach outlined above, explicit treatment of creep requires input of creep relations (models) for concrete and reinforcing steel. Recommendations for these creep relations are given below.

### 6.5.3. Relations for Incorporating Creep Explicitly

After narrowing down the scenarios of fire exposure where transient creep can be critical in fire resistance evaluation of concrete members, advanced analysis where high-temperature creep is explicitly accounted can be undertaken. To perform such type of analysis, explicit relations

expressing creep strain as a function of temperature and stress level are needed for concrete and reinforcing steel.

The developed relation for transient creep strain in Chapter 3 (Section 3.6) can be utilized to explicitly account for transient creep in fire resistance evaluation of concrete members. Further, the relation is based on experiemnts conducted on different concrete types and, thus, can be used accordingly. Transient creep strain is expressed in this relation as:

$$\varepsilon_{trc} = k \cdot \left(\frac{\sigma}{f'_c}\right) \cdot f(T) \qquad \text{.....[6.1]}$$

where *k* is a modification parameter to account for the effect of concrete type on transient creep strain and is proposed to be 1.0 for NSC, 0.8 for NSC-SF and 1.05 for HSC, and HSC-PP. For other concrete types, the modification factor, *k*, can be determined experimentally following the outlined procedure in Chapter 3. Stress level in the proposed relation is represented by the term $\left(\frac{\sigma}{f'_c}\right)$ where $\sigma$ is stress to which the specimen is subjected and $f'_c$ is concrete strength. The temperature function, $f(T)$, in equation [6.1], is a quadratic function given as:

$$f(T) = -2.5 \times 10^{-10} \cdot T^3 + 2.0 \times 10^{-7} \cdot T^2 - 6.2 \times 10^{-5} \cdot T^2 + 0.002 \quad \text{.....[6.2]}$$

where temperature, *T*, is in Celsius, °C.

Predicted transient creep strain for NSC from equation [6.2] is plotted in Figure 6.7 as a function of temperature in 20°C - 800°C at various stress levels. As can be seen in Figure 6.7, the progression of transient creep strain is in three distinct stages, primary, secondary, and tertiary stages. In the primary stage, transient creep increases linearly up to 200°C, followed by a secondary stage during which transient creep increases in a nonlinear fashion between 200- 400°C. Beyond 400°C, transient creep strain increases rapidly till failure occurs in concrete and this is referred to as tertiary stage of creep.

In addition to the presented relation above, other relations provided in Chapter 2 (Section 2.3) can be utilized to generate temperature-dependent transient creep for NSC. For HSC-PP the presented above relation can be adopted as well as the one proposed by Wu et. al (2010), presented in Section 2.3.2.5.

For reinforcing steel creep strain at elevated temperature, as shown in the literature review presented in Section 2.4, there is lack of relations specific on the grades of steel utilized for reinforcement in concrete structures. However, creep models developed for steel yield satisfactory results for creep strain due to the similarity in creep mechanisms. In the numerical model in Chapter 4, temperature-dependent creep data provided by Williams-leir (1983) are incorporated. In addition, creep models such as the one proposed by Harmathy (1967) can be adopted to generate high-temperature creep data for reinforcing steel. However, for cases where stress is variant under fire exposure, Harmathy's model have been shown to mis-capture creep response in steel structural members (Kodur, Dwaikat, and Fike, 2010). Thus, when concrete members are subjected to variant state of stress, such creep models might not be applicable.

### 6.5.4. Failure Limit States

Failure of RC members in prescriptive based approach is evaluated based on critical temperature attained in reinforcing steel, specified as 593°C in ACI216R (2014), or through applying strength failure limit state. ISO834-1 (1999) also provides displacement based failure criterion for evaluating failure of vertically loaded members such as columns in fire tests. Since transient creep effects; and thus deformations, can be significant in columns, failure during fire can be through limiting displacement. Therefore, applying displacement-based failure limit state to determine failure is recommended for evaluating realistic response of columns. Displacement and rate of displacement failure limits for vertically loaded members, according to ISO834-1

(1999), are 0.01*h* mm and 0.003*h* mm/min where *h* is the height of the column in mm. However, it has been shown by Dumount et. al. (2016) that these displacement based criteria are more applicable to ductile members (steel members) and are unconservative for brittle structural members such as RC columns. Moreover, it has been shown from fire resistance analyses performed as part of this study on columns that these displacement-based failure limits are unconservative when compared to actual fire test results on RC columns.

Thus, a displacement and rate of displacement-based approach is to be used in evaluating failure of RC columns. The displacement and rate of displacement at which the column fails in previous fire tests are selected as reference limits. For instance, if a column failed at a displacement of 0.004*h* mm during the fire test instead of 0.01*h* (ISO834 limit), then the new selected limit in this approach becomes 0.004*h*. Based on numerical studies undertaken in this Thesis, failure is more likely to occur when axial displacement exceeds 0.004*h* mm in concrete columns. This value is much lower than what is specified in ISO834 (0.01*h* mm). Thus, it is recommended to use a displacement limit of 0.004*h* for concrete columns.

## 6.6. Summary

To overcome limitations related to accounting transient creep effects in fire resistance analysis of concrete members, design recommendations are presented in this chapter. Specifically, guidance is given on when temperature-induced creep strains are to be included in fire resistance analysis of concrete columns. Recommendations on scenarios where incorporating creep in evaluation of fire resistance of concrete members are given. In addition, general recommendations are given for cases where accounting creep strains is critical in evaluating fire resistance of concrete members.

The proposed recommendations are mainly related to temperature and stress levels attained during exposure of concrete members to fire. Based on creep critical temperature at a given stress level, times, when transient creep strain becomes dominant in concrete columns, are presented based on two scenarios of fire exposure, ASTM E-119 and hydrocarbon fire. If concrete columns are exposed to fire for a duration longer than the times provided in Table 6.2., transient creep is recommended to be accounted explicitly in fire resistance analysis. These temperatures are given for concrete columns of three different sizes based on attained temperatures in the column's core during exposure to fire under the two selected scenarios. Similarly, for concrete members, recommendations are given to account for creep strains when temperature in concrete exceed creep critical temperature.

Furthermore, specific recommendations are given for treatment of transient creep in fire resistance analysis of concrete columns based on results of parametric studies. Concrete columns under exposure from 2- or 3- sides might be more critical when it comes to accounting for creep strains in fire resistance evaluation. Finally, under exposure to fires with cooling phase, recommendations were given to account for transient creep explicitly in fire resistance analysis of concrete members. This is due to the fact that transient creep is irreversible and only occur during first-time heating.

Table 6.1 Extent of creep in concrete members based on temperature and stress level

| Temperature / Stress Level | 20-300°C | 300-500°C | > 500°C |
|---|---|---|---|
| 30 | Minor | Minor | Moderate |
| 40 | Minor | Moderate | Severe |
| 50 | Minor | Moderate | Severe |
| 60 | Moderate | Severe | Severe |
| 70 | Moderate | Severe | Severe |

Table 6.2 Time in minutes until transient creep deformation become dominant in concrete columns under different fire exposure scenarios

| Fire Exposure | ASTM E-119 Scenario | | | Hydrocarbon Scenario | | |
|---|---|---|---|---|---|---|
| Size, mm / Stress Level | 203×203 | 305×305 | 305×457 | 203×203 | 305×305 | 305×457 |
| 30 | 140 | 180 | 200 | 120 | 170 | 180 |
| 40 | 130 | 170 | 190 | 110 | 140 | 170 |
| 50 | 120 | 150 | 180 | 100 | 120 | 150 |
| 60 | 110 | 130 | 160 | 90 | 110 | 130 |
| 70 | 100 | 120 | 150 | 80 | 100 | 120 |

Table 6.3 Creep critical temperatures for different concrete types at different stress levels

| Stress Level % | Critical Temperatures, °C | | |
|---|---|---|---|
| | NSC | NSC-SF | HSC-PP |
| 10 | 680 | 750 | 730 |
| 20 | 630 | 675 | 650 |
| 30 | 585 | 630 | 520 |
| 40 | 550 | 590 | 500 |
| 50 | 520 | 550 | 430 |
| 60 | 465 | 485 | 395 |
| 70 | 415 | 475 | - |

Table 6.4 Treatment of creep in fire resistance analysis under different scenarios of fire exposure

| Creep not critical | Implicit Creep | Explicit Creep |
|---|---|---|
| • When failure is evaluated based on strength criteria<br>• When temperature in concrete members does not reach 400°C<br>• Simplified analysis | • When temperature in concrete members does not exceed 400°C<br>• In flexural members when fire exposure is only at the bottom surface and compressive zone is at the top<br>• In lightly loaded concrete columns or beams (stress level < 30%)<br>• Require advanced analysis<br>• Creep built in stress-strain relations | • Under severe fire exposure conditions such as hydrocarbon fire and high stress levels<br>• When temperature in concrete members exceed critical creep temperature as specified in Table 6.3<br>• For concrete columns; specifically, under severe fire exposure and high stress levels<br>• For concrete columns under exposure from 2 or three sides only<br>• When cooling phase of the fire is considered<br>• Require advanced analysis |

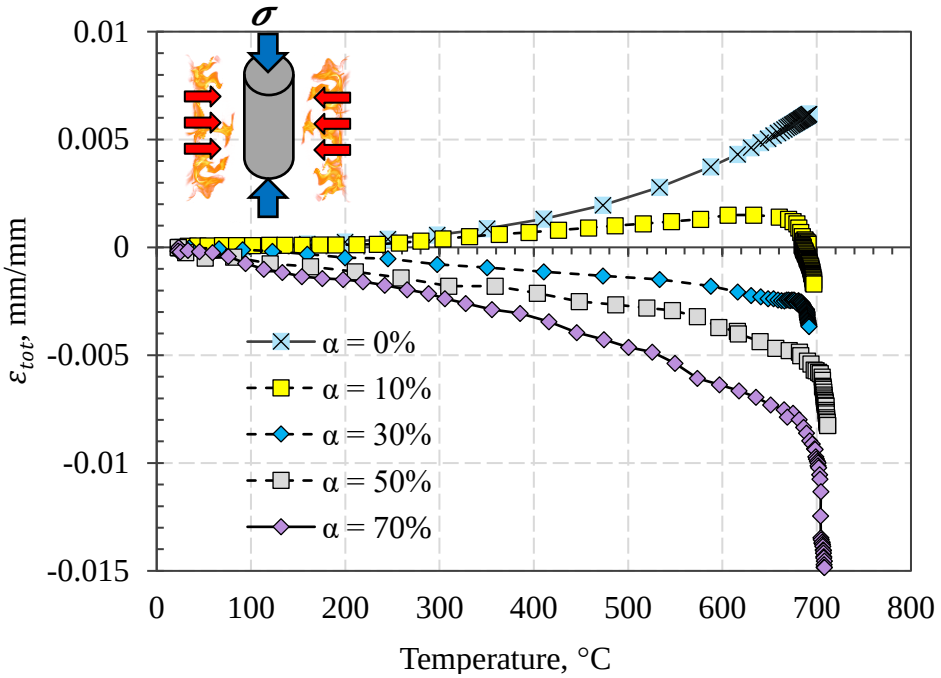


(a) Total strain in concrete under transient heating as a function of temperature at various stress level

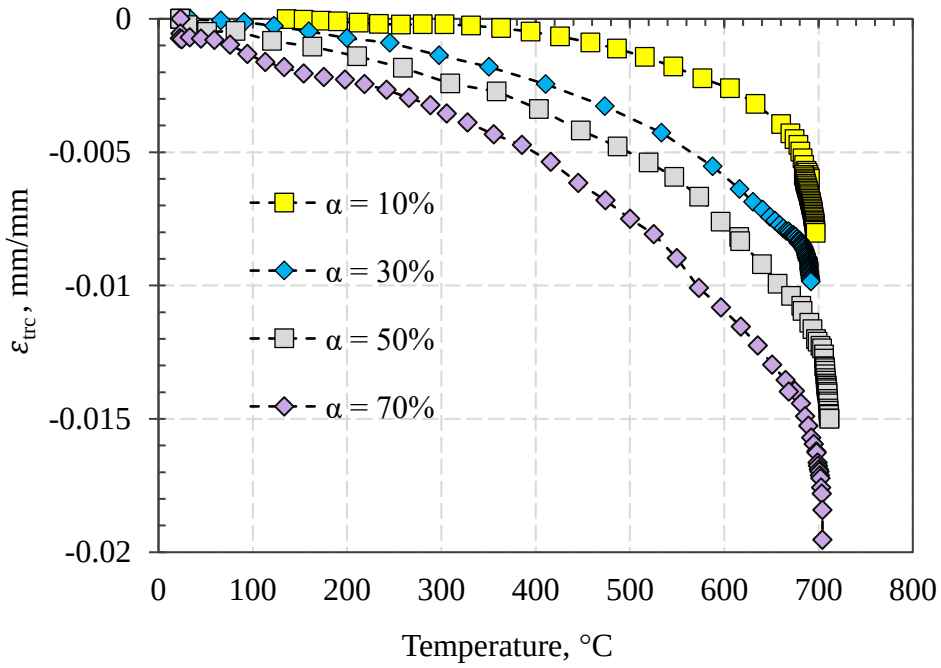


(b) Transient creep strain in concrete as a function of temperature at various stress level

Figure 6.1 Evolution of transient creep strain in concrete

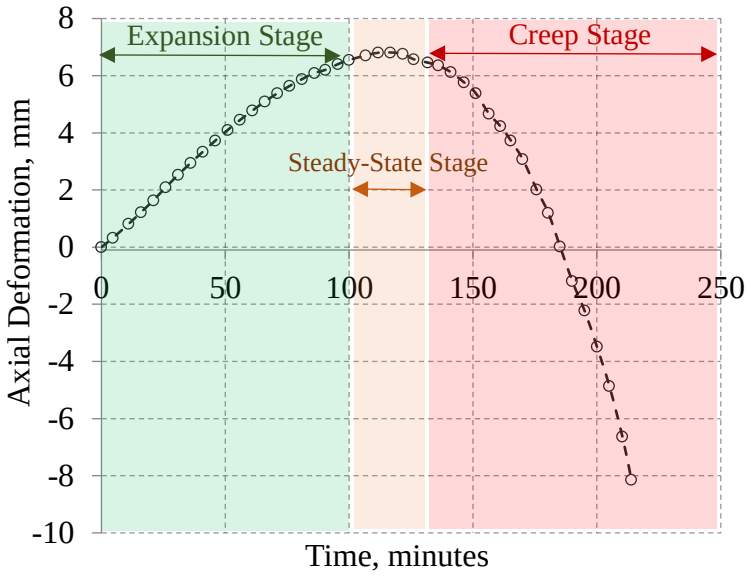


Figure 6.2 Axial displacement variation in a fire exposed concrete column with and without accounting for transient creep strain

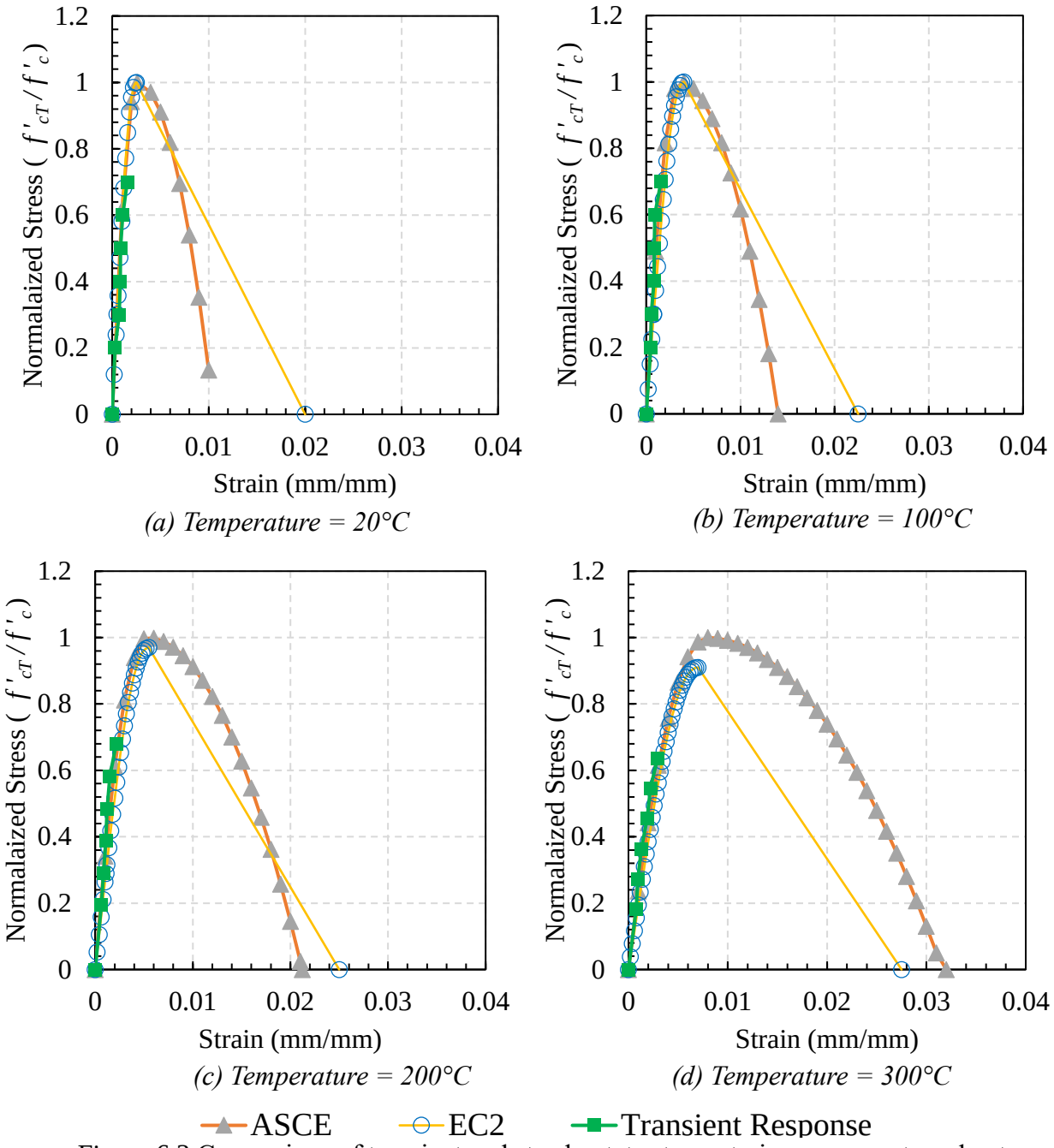


Figure 6.3 Comparison of transient and steady-state stress strain response at moderate temperatures (20-300°C)

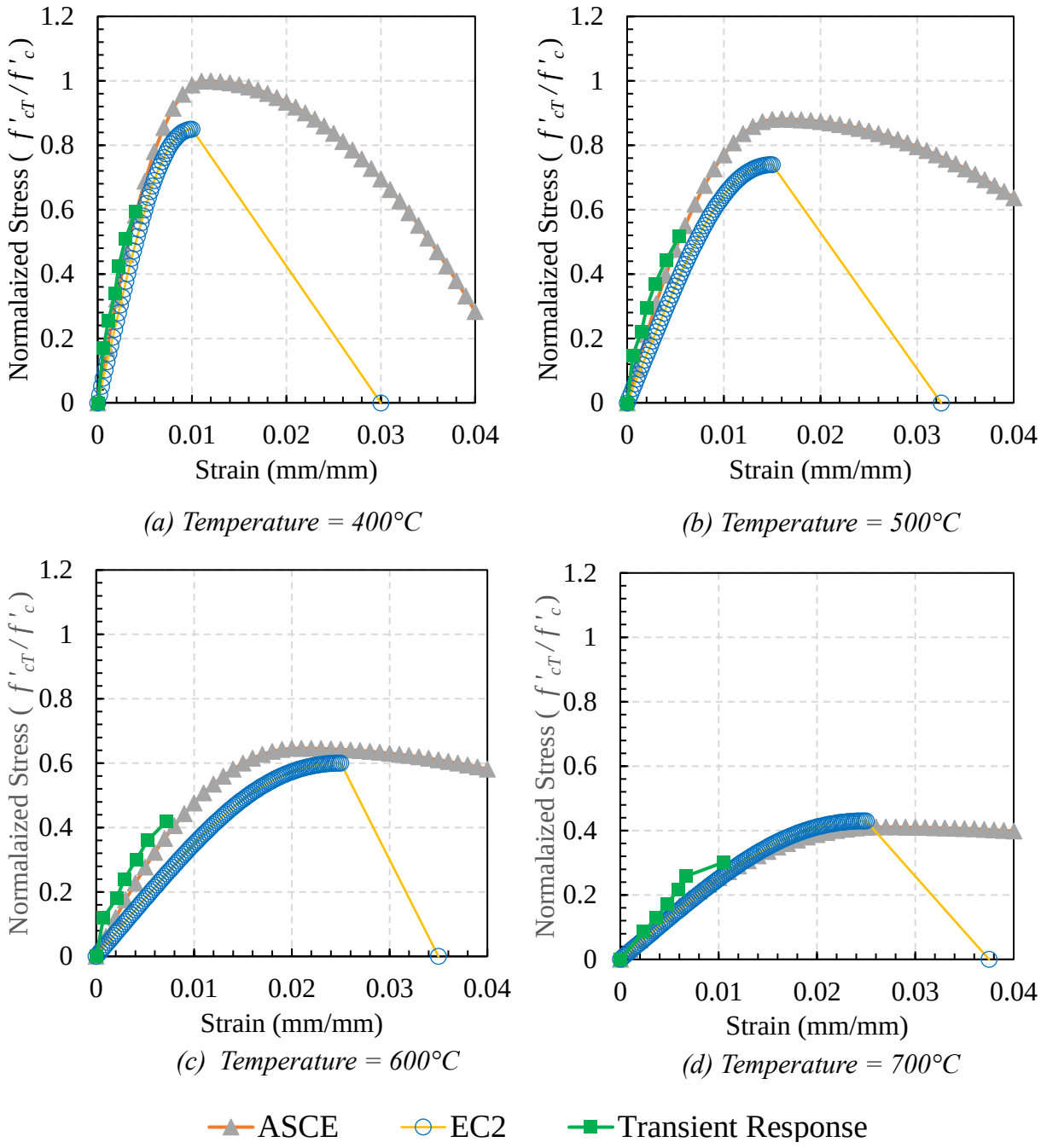


Figure 6.4 Comparison of transient and steady-state stress strain response at high temperatures (400-700°C)

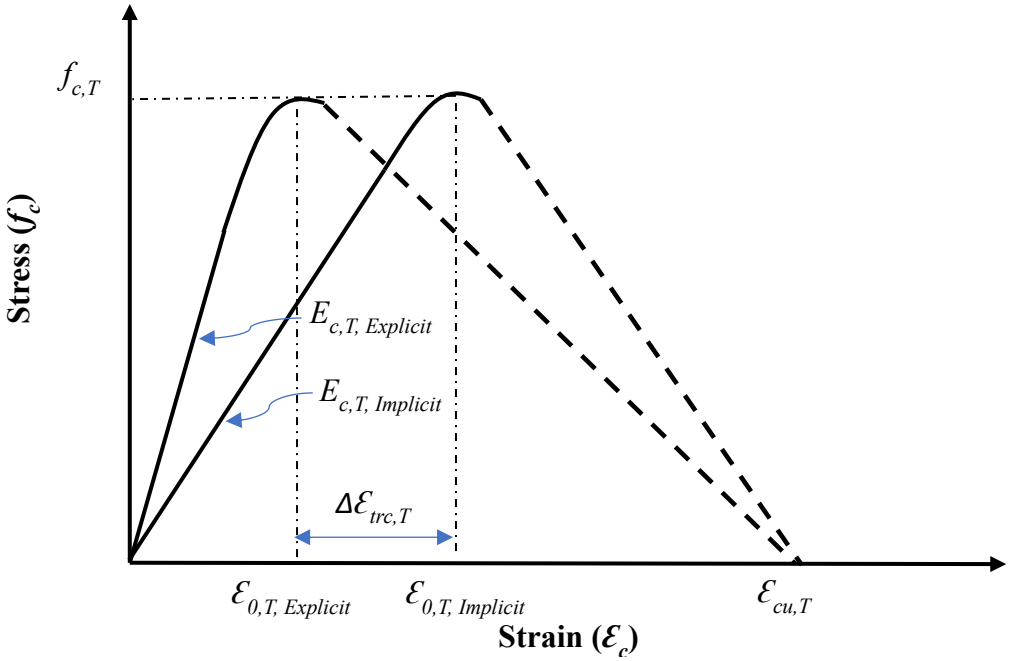


Figure 6.5 Difference between implicit and explicit consideration of transient creep in stress-strain constitutive models

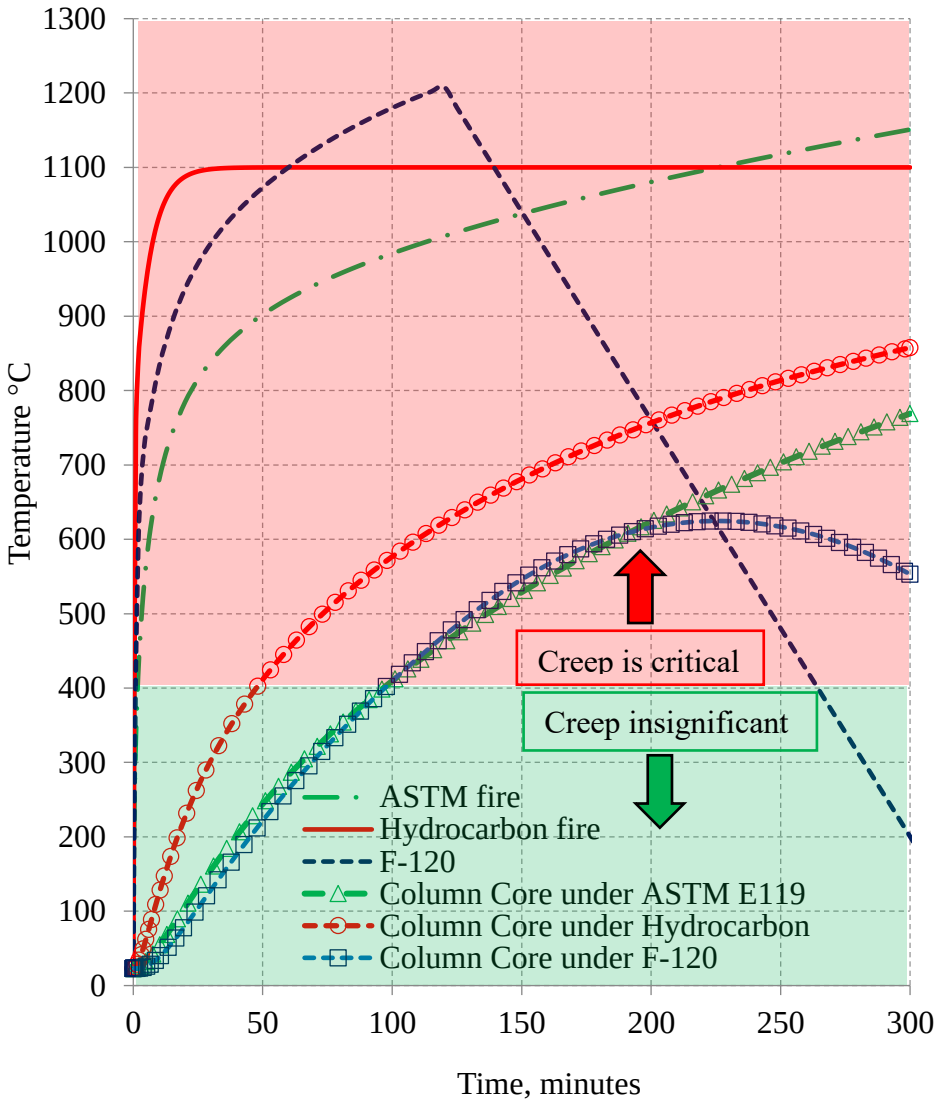


Figure 6.6 Temperature at the edge of the core in a concrete column (305×305mm$^2$) under exposure to different fire scenarios (ASTM E119, Hydrocarbon, and F-120)

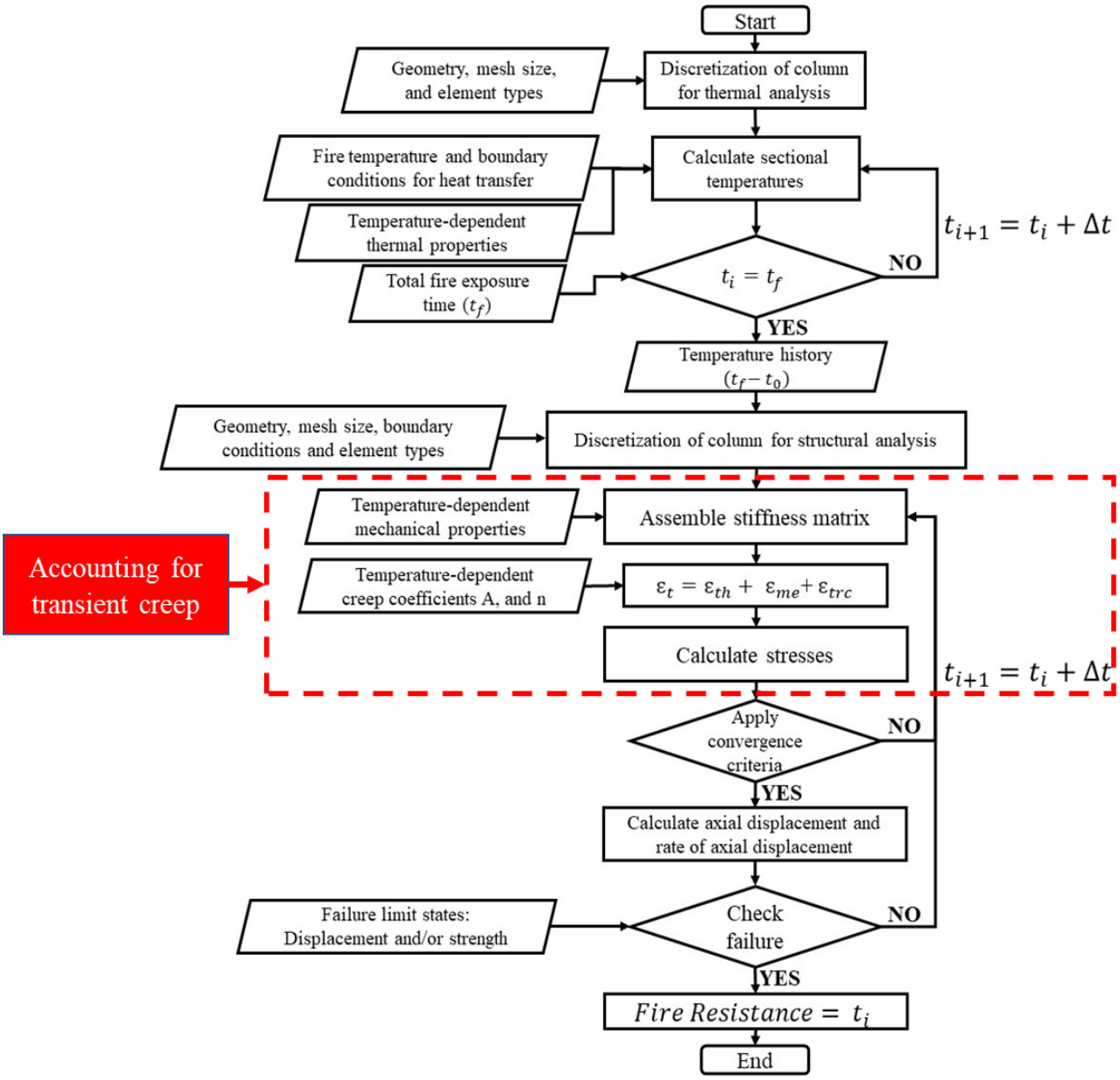


Figure 6.7 Flow chart illustrating steps in fire resistance analysis of RC columns by incorporating creep effects

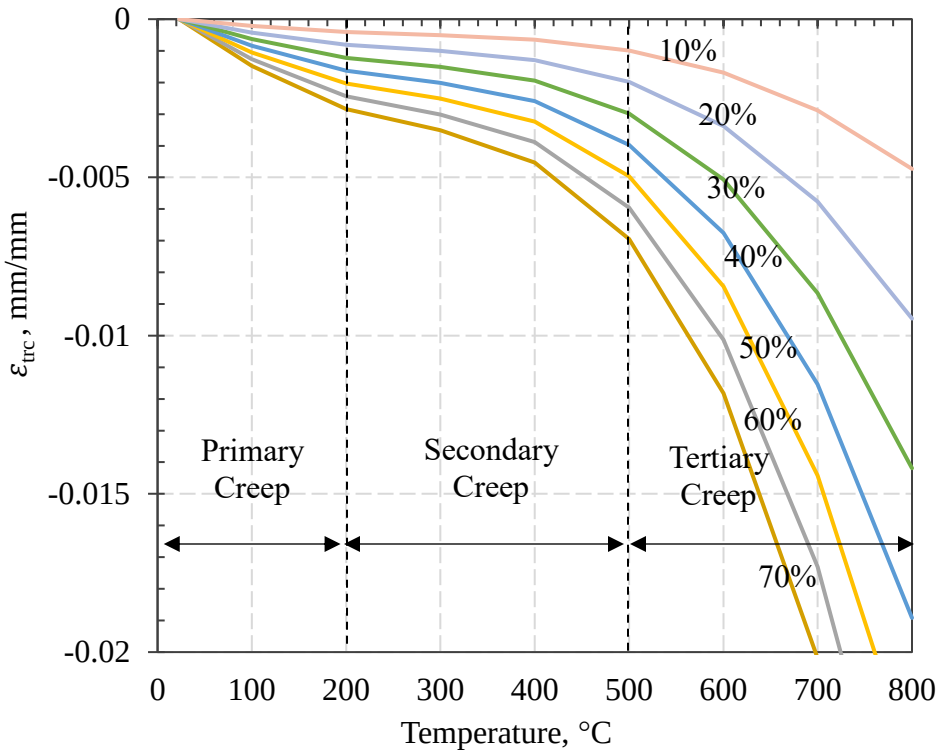


Figure 6.8 Explicit transient creep relation for NSC as a function of stress and temperature

# CHAPTER SEVEN

# 7. Conclusions

## 7.1. General

The effect of temperature-induced creep on the response of concrete columns is studied to develop a fundamental understanding of the behavior of concrete columns under fire conditions. Limited studies exist on the evolution of temperature-induced creep strain at elevated temperatures as well as its effect on the response of concrete columns under fire conditions. The lack of data on creep in concrete can be attributed to the complexity associated with capturing (measuring) creep strains in concrete at elevated temperature at both material and structural levels, and also to the introduction of new types of concrete in recent years. To overcome this gap, transient creep experiments were carried out on four types of concrete, namely: normal strength concrete (NSC), normal strength reinforced with steel fibers (NSC-SF), high strength concrete (HSC), and high strength concrete containing polypropylene fibers (HSC-PP). The generated transient creep strain data is utilized to propose empirical relations expressing creep strain as a function of temperature in different concrete types.

To incorporate transient creep strain in fire resistance analysis of reinforced concrete columns, a finite element based numerical model was developed in ABAQUS. In this model creep effects are explicitly accounted in fire resistance analysis. The proposed creep relations were incorporated into the model explicitly in evaluating the response of concrete columns under fire conditions. The validity of the model was established by comparing response predictions generated from the numerical model with measured response parameters in fire tests on RC columns. The validated model was applied to evaluate the influence of different parameters on the extent of transient creep effects in concrete column under various fire exposure scenarios. In these numerical

studies, the influence of various parameters was studied including fire severity, stress level, type of concrete, asymmetric thermal gradients, and cooling phase.

The numerical model developed in this study utilizes the finite element-based program, ABAQUS, for incorporating transient creep strain in fire resistance analysis. Such an analysis is quite complex and requires advanced analysis skills, which may not be viable for design of structures. To facilitate creep analysis in design of structures, recommendations are made on when "creep is critical", and also on how to account for transient creep strain in fire resistance analysis of concrete members.

## 7.2. Key Findings

Based on the information developed in this Thesis, the following key findings can be drawn:

1- There is lack of understanding pertaining to influence of transient creep strain on fire response of concrete structural members under fire conditions. This is mainly due to lack of high-temperature creep data and to the complexity in incorporating temperature induced creep strains in fire resistance analysis. Creep data, as well as associated creep relations available in the literature for transient creep of concrete have a considerable variation due to different test conditions, test procedures, including varying rates of heating, and stress levels adopted in previous test programs.

2- Temperature and stress levels have a dominant influence on the extent of creep generated in concrete at elevated temperatures. Temperature-induced creep strain is minimal till about 400°C and then get amplified in 400°C-800°C depending on stress level, with higher stress level leading to higher creep strain. Creep effects in a material become dominant beyond a certain temperature for a given stress level and this

temperature is termed as creep critical temperature. The creep critical temperature is lower for higher stress levels and increases with reduction in stress level.

3- Type of concrete, specifically the presence of fibers (i.e. fiber reinforced concrete), has a moderate influence on the extent of creep strain generated at elevated temperatures. Under similar conditions, normal strength concrete with steel fibers experiences lower creep strains than that in plain normal strength concrete, while high strength concrete with polypropylene fibers experience much higher creep strain.

4- The evolution of high-temperature creep in concrete members is influenced by the combined effect of temperature, stress, and rate of heating apart from type of concrete. Although rapid rates of heating lead to faster increase in transient creep strain in concrete, slower rates of heating, that take longer times to reach creep critical temperature levels, produce higher creep strain.

5- The proposed creep relations expressing transient creep strain in terms of stress level and temperature take into account type of concrete, and hence when incorporated explicitly in advanced fire resistance analysis can lead to reliable evaluation of fire resistance concrete structural members.

6- The proposed numerical model, built in ABAQUS, is capable of explicitly accounting for temperature induced creep strains in concrete and reinforcing steel in predicting thermal and structural response of fire exposed RC columns. This model also accounts for varying fire loading and restraint conditions as well as temperature-induced degradation in properties of materials, and associated material and geometric nonlinearities.

7- Temperature-induced transient creep strain has a significant influence on the resulting axial displacements in RC columns, specifically at latter stages of fire exposure. Neglecting such transient creep effects explicitly in fire resistance evaluation of concrete members, in RC columns, can lead to underestimation of axial displacements and, thus, overestimation of failure time or fire resistance.

8- The main factors that influence the extent of creep in fire exposed concrete columns are fire scenario (temperature levels), thermal gradients, stress level, and type of concrete. Asymmetrical thermal gradients, developed from 1-, 2- or 3-side exposure, can induce large transient creep effects in a concrete column, especially when the columns are subjected to eccentric loading. Transient creep strain increases with increase in applied stress level, and thus, heavily loaded columns undergo much higher deformations at a faster rate leading to lower fire resistance (failure time). Finally, accounting for transient creep explicitly in fire resistance analysis of RC columns during the cooling phase of a fire is critical to predict realistic response of columns.

## 7.3. Future Work

The work presented in this Thesis advanced an understanding on the effect of transient creep on response of concrete columns under fire conditions and also provided much needed data on transient creep for different concrete types. However, there is much scope for further research in the area of temperature induced creep effects to close many knowledge gaps. The following are a few of the key recommendations for future research in this area:

- The experimental work in this Thesis provided much needed data for transient creep in HSC, HSC-PP, and NSC-SF, and its treatment in fire resistance analysis of RC columns. However, new types of concrete are continuously emerging and are used in

building applications where fire resistance is a key consideration. Data on transient creep, with associated relations, are needed for these new types of concrete including ultra-high-performance concrete (UHPC), Self-consolidating concrete (SCC), and high-performance concrete (HPC).

- The scope of this Thesis covered most of the scenarios where transient creep can be dominant on the deformation response of concrete columns. However, the sizes of the studied columns represent typical columns in building applications, and RC columns of larger sizes such as in bridges are to be studied further to evaluate creep effects. Further, in bridges, the fire exposure resulting from car accidents, for instance, often occur in a localized area of the column. Thus, the influence of transient creep on the response of columns under such scenarios is to be addressed.
- This Thesis specifically looked at the role of creep in reinforced columns. Other concrete compression members (for instance, concrete walls and post-tensioned slabs) might have the same trends in behavior as that of concrete columns in which transient creep strain dominate the deformation response under later stages of fire exposure. Research in this area is needed to evaluate the influence of transient creep effects on the fire response of such concrete members.
- Concrete flexural members (beams and slabs) under specific configurations (i.e. continuous beam, beam-column, etc.) can be subjected to compressive stresses in the lower part of the cross section (compressive zone at bottom of the section). In such scenarios, the compressive zone of the section can suffer high-temperature increase from fire, and, thus, is prone to developing high levels of transient creep. Further

research is needed to determine if transient creep strain needs to be explicitly considered under such scenarios of fire exposure in concrete flexural members.

## 7.4. Research Impact

Reinforced concrete columns are primary load carrying members in buildings and need to satisfy fire resistance requirements, as specified in codes. The current prescriptive approaches, as well as simplified approaches for evaluating fire resistance, neglect temperature-induced transient creep strain completely. Even in advanced analysis procedures wherein stress-strain relations of concrete and steel are incorporated, creep effects are not fully accounted. In addition, fire ratings of concrete columns are mainly based on strength failure criteria. Nonuse of displacement-based failure criterion in fire resistance evaluation lead to underestimation of transient creep effects and lead to inaccurate estimation of axial displacement of RC columns under fire, and consequently un-conservative prediction of fire resistance or failure times.

The current research was aimed at developing a rational analysis approach for accounting transient creep strain explicitly in fire resistance analysis of RC columns. Such assessment of transient creep in RC columns under fire helps in developing a fundamental understanding of the subject and determining the cases of fire exposure where creep effects are critical. Based on this advanced analysis, the effect of varying parameters and conditions of fire exposure under which creep effects dominate was evaluated. Accordingly, failure of RC columns can be governed by transient creep under higher stress levels and severe fire scenarios. For instance, in hydrocarbon fire exposure, transient creep strain plays a critical role in determining failure times in a column. Thus, neglecting transient creep effects or only partially accounting for it in fire resistance analysis can lead to an inaccurate assessment of fire performance.

For accounting for creep in fire resistance analysis, this research developed transient creep relations for different concrete types including NSC, NSC-SF, HSC, and HSC-PP. Incorporating these creep relations (based on concrete type, stress level, and temperature range) in fire resistance analysis explicitly can lead to better assessment of fire resistance in concrete structures made of these types of concrete.

# APPENDIX

# Appendix A Constitutive Stress-Strain Response of Concrete at Elevated Temperatures from ASCE and EC 2

Two of the widely available stress-strain relations for concrete at elevated temperatures are: ASCE (1992) manual relations, and Eurocode 2 (2004). In this Appendix, a summary of these constitutive models for concrete is presented.

## A.1. ASCE Constitutive Model

The American Society of Civil Engineers in its Structural Fire Protection manual provide temperature-dependent stress-strain model to describe the mechanical behavior of concrete at elevated temperatures. The ASCE constitutive model is given in Table A.1, and generated stress-strain response at elevated temperature from this model is shown in Figure A.1 for various temperatures. A stress-strain curve is plotted for each respective temperature ranging from 100°C to 800°C. The stress-strain response according to ASCE manual includes an elastic linear range, a non-linear hardening (ascending) range, and a nonlinear softening (descending) branch. As temperature increase, concrete experience high degradation in strength and stiffness (more than 80% loss in strength at 800°C) and undergo large ultimate strains of up to 0.08 beyond 700°C.

## A.2. Eurocode 2 Constitutive Model

Eurocode 2 part 2.1 provide a constitutive model describing the mechanical behavior of concrete at elevated temperatures as shown in Figure A.2. The Eurocode model is widely used for evaluating fire resistance of concrete structural members. In this model, the stress-strain response consists of a linear elastic range, a hardening non-linear range, and allow for both linear and non-linear descending branch. The main parameters to generate stress-strain response according to Eurocode model are strength at elevated temperature, $f'_{c,T}$ , strain at peak stress, $\varepsilon_{c1,T}$, and ultimate

strain, $\varepsilon_{c1u,T}$. Values of these parameters for computing the stress-strain response are specified in Eurocode as shown in Table A.2 for both normal and high strength concretes.

The generated stress-strain response based on Eurocode model is plotted in Figure 6.3 for various temperatures ranging from 100°C to 1000°C. As temperature increase, degradation in stiffness and strength increase and concrete undergo higher strains. At temperatures above 500°C, concrete softens dramatically which result in higher ultimate strain and much lesser stiffness and strength. Up to temperatures of 500°C, concrete is assumed to lose only 25% of its room temperature strength. However, when temperatures reach 800°C, 75% of concrete strength at room temperature is lost.

Table A.1 Constitutive laws for concrete stress-strain at elevated temperatures

| | |
|---|---|
| | **ASCE Structural Fire Protection Manual (1992)** |
| Stress-Strain Relations for NSC | $$\sigma_c = \begin{cases} f'_{c,T}\left[1-\left(\dfrac{\varepsilon - \varepsilon_{max,T}}{\varepsilon_{max,T}}\right)^2\right], \varepsilon \le \varepsilon_{max,T} \\ f'_{c,T}\left[1-\left(\dfrac{\varepsilon_{max,T} - \varepsilon}{3\,\varepsilon_{max,T}}\right)^2\right], \varepsilon > \varepsilon_{max,T} \end{cases}$$ $$f'_{c,T} = \begin{cases} f'_c, & 20℃ \le T \le 450℃ \\ f'_c\left[2.011 - \dfrac{2.353(T-20)}{1000}\right], & 450℃ < T \le 874℃ \\ 0, & T > 874℃ \end{cases}$$ $$\varepsilon_{max,T} = 0.0025 + (6.0T + 0.04T^2) \times 10^{-6}$$ |
| | **Eurocode 2 (2004)** |
| Stress-Strain Relations for NSC and HSC | $$\sigma_c = \frac{3\,\varepsilon\, f'_{c,T}}{\varepsilon_{c1,T}\left(2+\left(\dfrac{\varepsilon}{\varepsilon_{c1,T}}\right)^3\right)}, \varepsilon \le \varepsilon_{cu1,T}$$ For $\varepsilon_{c1,T} < \varepsilon \le \varepsilon_{cu1,T}$, the Eurocode allows the use of either linear or nonlinear descending branch up to the specified value of $\varepsilon_{cu1,T}$ The parameters in Eurocode model are presented in Table 6.2. |

Table A.2 Parameters values for the stress-strain relations for NSC and HSC at elevated temperatures

| Temp. ˚F | Temp. ˚C | NSC | | | | | |
|---|---|---|---|---|---|---|---|
| | | Siliceous Agg. | | | Calcareous Agg. | | |
| | | $\frac{f'_{c,T}}{f'_{c,(20℃)}}$ | $\varepsilon_{c1,T}$ | $\varepsilon_{cu1,T}$ | $\frac{f'_{c,T}}{f'_{c,(20℃)}}$ | $\varepsilon_{c1,T}$ | $\varepsilon_{cu1,T}$ |
| 68 | 20 | 1 | 0.0025 | 0.02 | 1 | 0.0025 | 0.02 |
| 212 | 100 | 1 | 0.004 | 0.0225 | 1 | 0.004 | 0.023 |
| 392 | 200 | 0.95 | 0.0055 | 0.025 | 0.97 | 0.0055 | 0.025 |
| 572 | 300 | 0.85 | 0.007 | 0.0275 | 0.91 | 0.007 | 0.028 |
| 752 | 400 | 0.75 | 0.01 | 0.03 | 0.85 | 0.01 | 0.03 |
| 932 | 500 | 0.6 | 0.015 | 0.0325 | 0.74 | 0.015 | 0.033 |
| 1112 | 600 | 0.45 | 0.025 | 0.035 | 0.6 | 0.025 | 0.035 |
| 1292 | 700 | 0.3 | 0.025 | 0.0375 | 0.43 | .025 | 0.038 |
| 1472 | 800 | 0.15 | 0.025 | 0.04 | 0.27 | 0.025 | 0.04 |
| 1652 | 900 | 0.08 | 0.025 | 0.0425 | 0.15 | 0.025 | 0.043 |
| 1832 | 1000 | 0.04 | 0.025 | 0.045 | 0.06 | 0.025 | 0.045 |
| 2012 | 1100 | 0.01 | 0.025 | 0.0475 | 0.02 | 0.025 | 0.048 |
| 2192 | 1200 | 0 | - | - | 0 | - | - |

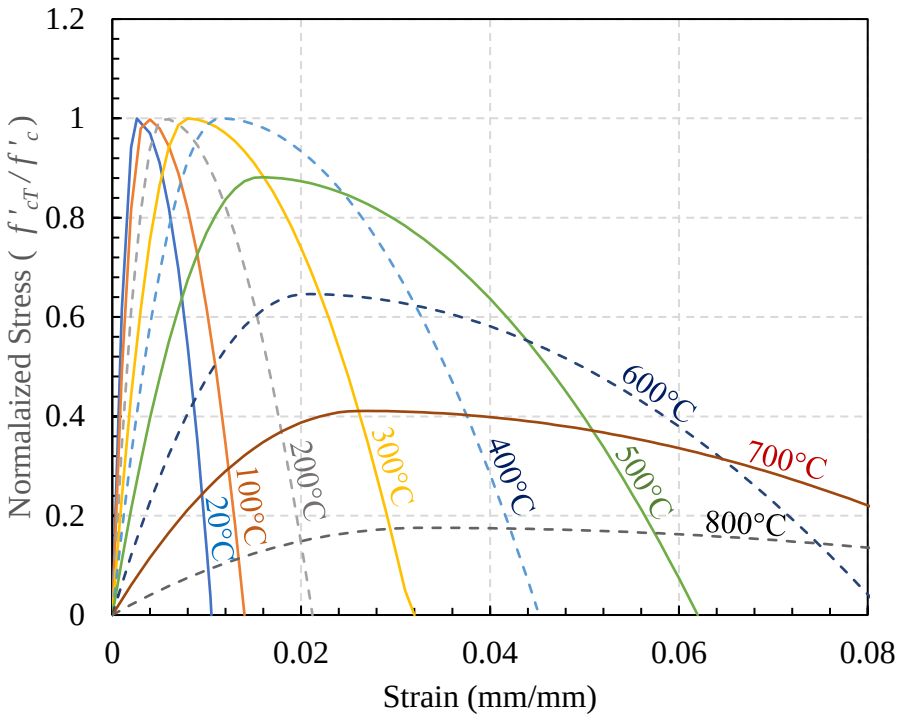


Figure A.1 ASCE stress-strain response at elevated temperatures

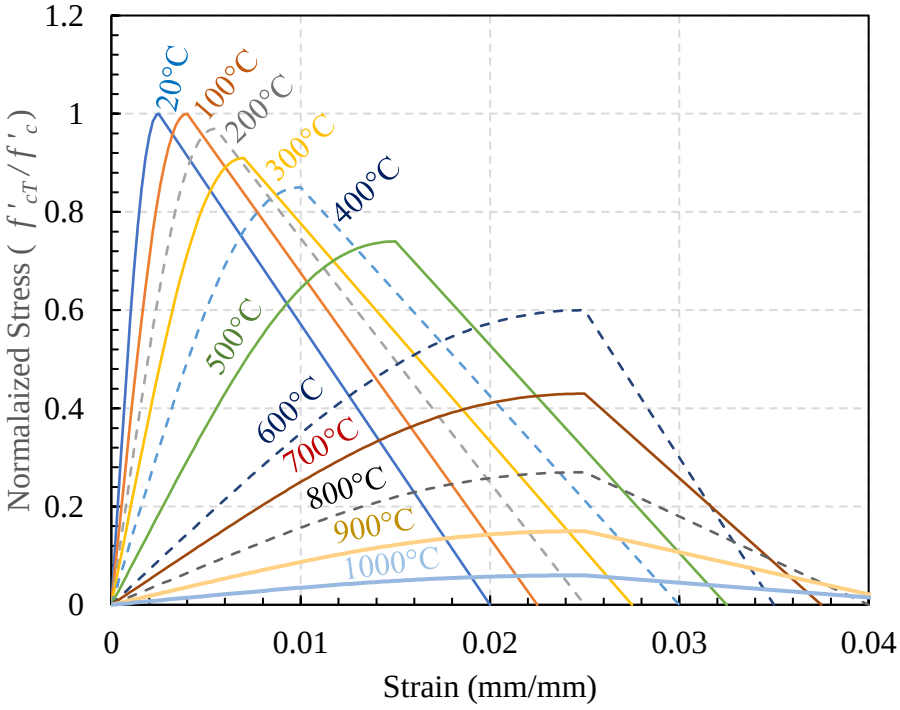


Figure A.1 Eurocode stress-strain response at elevated temperatures

# REFERENCES

## REFERENCES


ABAQUS, Dassault Systèmes. (2014). *ABAQUS Documentation* (6.14). Providence, RI.

ACI 216.1-14 Code Requirements for Determining Fire Resistance of Concrete and Masonry Assemblies. (2014). ACI.

Aldea, C. M., Franssen, J. M., and Dotreppe, J. C. (1997). *Fire test on normal and high strength reinforced concrete columns* (No. NIST SP 919) (pp. 109-124 pp). Gaithersburg, MD.

Ali, F. A., O'Connor, D., and Abu-Tair, A. (2001). Explosive spalling of high-strength concrete columns in fire. *Magazine of Concrete Research*, *53*(3), 197–204. https://doi.org/10.1680/macr.2001.53.3.197

Ali, F., Nadjai, A., Silcock, G., and Abu-Tair, A. (2004). Outcomes of a major research on fire resistance of concrete columns. *Fire Safety Journal*, *39*(6), 433–445. https://doi.org/10.1016/j.firesaf.2004.02.004

Alogla, S., and Kodur, V. K. R. (2018). Quantifying transient creep effects on fire response of reinforced concrete columns. *Engineering Structures*, *174*, 885–895. https://doi.org/10.1016/j.engstruct.2018.07.093

American Concrete Institute. (2014). *Building code requirements for structural concrete and commentary (ACI 318-14)* (Vol. ACI 318-14).

Anderberg, Y., and Thelandersson, S. (1976). Stress and deformation characteristics of concrete at high temperatures. 2. Experimental investigation and material behaviour model. *Bulletin of Division of Structural Mechanics and Concrete Construction, Bulletin 54*.

ASCE. (1992). *Structural Fire Protection*. (T. T. Lie, Ed.). New York: American Society of Civil Engineers. https://doi.org/10.1061/9780872628885

ASTM E05 Committee. (2014). *Test methods for fire tests of building construction and materials*. ASTM International.

ASTM E1529- 14a. (n.d.). *Standard Test Methods for Determining Effects of Large Hydrocarbon Pool Fires on Structural Members and Assemblies*.

Bažant, Z. P., and Jirásek, M. (2018). *Creep and Hygrothermal Effects in Concrete Structures*. Springer Netherlands.

Bažant, Z. P., and Kaplan, M. F. (1996). *Concrete at High Temperatures: Material Properties and Mathematical Models*. Longman.

Bazant, Zdenek P. (1975). Theory of creep and shrinkage in concrete structures: A precis of recent developments. *Mechanics Today*, *2*, 1–93.

Bazant, ZDENEK P. (1995). Creep and damage in concrete. *Materials Science of Concrete IV*, 355–389.

Bazant, Zdenek P., Cusatis, G., and Cedolin, L. (2004). Temperature effect on concrete creep modeled by microprestress-solidification theory. *Journal of Engineering Mechanics*, *130*(6), 691–699.

Bazant, Zdenek P., and Prasannan, S. (1989a). Solidification theory for concrete creep. I: Formulation. *Journal of Engineering Mechanics*, *115*(8), 1691–1703.

Bazant, Zdenek P., and Prasannan, S. (1989b). Solidification theory for concrete creep. II: verification and application. *Journal of Engineering Mechanics*, *115*(8), 1704–1725.

Beitel, J., and Iwankiw, N. (2005). Historical Survey of Multistory Building Collapses Due to Fire. *Fire Protectrion Engineering*, (27), 42.

Benmarce, A., and Guenfoud, M. (2015). Experimental behaviour of high-strength concrete columns in fire. *Magazine of Concrete Research*. https://doi.org/10.1680/macr.2005.57.5.283

Bratina, S., Čas, B., Saje, M., and Planinc, I. (2005). Numerical modelling of behaviour of reinforced concrete columns in fire and comparison with Eurocode 2. *International Journal of Solids and Structures*, *42*(21–22), 5715–5733. https://doi.org/10.1016/j.ijsolstr.2005.03.015

Canada, G. of C. N. R. C. (2017, March 16). User manual for SAFIR: a computer program for analysis of structures at elevated temperature conditions - NRC Publications Archive - National Research Council Canada.

Carette, G. G., E. Painter, K., and Malhotra, V. M. (1982). Sustained high temperature effect on concretes made with normal Portland cement, normal Portland cement and slag, or normal Portland cement and fly ash., *4*, 41–51.

Chan, Y. N., Peng, G. F., and Anson, M. (1999). Residual strength and pore structure of high-strength concrete and normal strength concrete after exposure to high temperatures. *Cement and Concrete Composites*, *21*(1), 23–27. https://doi.org/10.1016/S0958-9465(98)00034-1

Colina, H., and Sercombe, J. (2004). Transient thermal creep of concrete in service conditions at temperatures up to 300 C. *Magazine of Concrete Research*, *56*(10), 559–574.

Collins, M., and Mitchell, D. (1987). *Prestressed concrete basics*. Ottawa (ON, Canada): Canadian Prestress Concrete Institute.

Cook, R. D., Malkus, D. S., Plesha, M. E., and Witt, R. J. (2007). *Concepts and Applications of Finite Element Analysis*. USA: John Wiley & Sons, Inc.

Dumont, F., Wellens, E., Gernay, T., and Franssen, J.-M. (2016). Loadbearing capacity criteria in fire resistance testing. *Materials and Structures*, *49*(11), 4565–4581. https://doi.org/10.1617/s11527-016-0807-7

Dwaikat, M. B., and Kodur, V. K. R. (2009). Hydrothermal model for predicting fire-induced spalling in concrete structural systems. *Fire Safety Journal*, *44*(3), 425–434. https://doi.org/10.1016/j.firesaf.2008.09.001

Eurocode 1-2. (2002). *EN 1991-1-2: Eurocode 1: Actions on structures - Part 1-2: General actions - Actions on structures exposed to fire* (The European Union Per Regulation).

Eurocode 2. (2004). *EN 1992-1-2: Eurocode 2: Design of concrete structures - Part 1-2: General rules - Structural fire design*.

Franssen, J.-M., and Dotreppe, J.-C. (2003). Fire Tests and Calculation Methods for Circular Concrete Columns. *Fire Technology*, *39*(1), 89–97. https://doi.org/10.1023/A:1021783311892

Fu, Y.-F., Wong, Y.-L., Poon, C.-S., Tang, C.-A., and Lin, P. (2004). Experimental study of micro/macro crack development and stress–strain relations of cement-based composite materials at elevated temperatures. *Cement and Concrete Research*, *34*(5), 789–797. https://doi.org/10.1016/j.cemconres.2003.08.029

Furumura, F., Abe, T., and Shinohara, Y. (1995). Mechanical properties of high strength concrete at high temperatures. *High Performance Concrete; Material Properties and Design; Prodeedings of the Fourth Weimar Workshop on High Performance Concrete; Material Properties*, 237–254.

Gao, W. Y., Dai, J.-G., Teng, J. G., and Chen, G. M. (2013). Finite element modeling of reinforced concrete beams exposed to fire. *Engineering Structures*, *52*, 488–501. https://doi.org/10.1016/j.engstruct.2013.03.017

Georgali, B., and Tsakiridis, P. E. (2005). Microstructure of fire-damaged concrete. A case study. *Cement and Concrete Composites*, *27*(2), 255–259. https://doi.org/10.1016/j.cemconcomp.2004.02.022

Gernay, T., and Franssen, J.-M. (2012). A formulation of the Eurocode 2 concrete model at elevated temperature that includes an explicit term for transient creep. *Fire Safety Journal*, *51*, 1–9. https://doi.org/10.1016/j.firesaf.2012.02.001

Gernay, Thomas. (2011). Effect of Transient Creep Strain Model on the Behavior of Concrete Columns Subjected to Heating and Cooling. *Fire Technology*, *48*(2), 313–329. https://doi.org/10.1007/s10694-011-0222-0

Gernay, Thomas, and Franssen, J.-M. (2011). A Comparison Between Explicit and Implicit Modelling of Transient Creep Strain in Concrete Uniaxial Constitutive Relationships.

Gillen, M. (1981). Short-term creep of concrete at elevated temperatures. *Fire and Materials*, *5*(4), 142–148. https://doi.org/10.1002/fam.810050403

Gross, H. (1975). High-temperature creep of concrete. *Nuclear Engineering and Design*, *32*(1), 129–147.

Han, C.-G., Hwang, Y.-S., Yang, S.-H., and Gowripalan, N. (2005). Performance of spalling resistance of high performance concrete with polypropylene fiber contents and lateral confinement. *Cement and Concrete Research*, *35*(9), 1747–1753. https://doi.org/10.1016/j.cemconres.2004.11.013

Harmathy, T., and Stanzak, W. (1970). Elevated-Temperature Tensile and Creep Properties of Some Structural and Prestressing Steels. *Fire Test Performance*. https://doi.org/10.1520/STP44718S

Harmathy, T. Z. (1967). A Comprehensive Creep Model. *Journal of Basic Engineering*, *89*(3), 496–502. https://doi.org/10.1115/1.3609648

Hassen, S., and Colina, H. (2006). Transient thermal creep of concrete in accidental conditions at temperatures up to 400 C. *Magazine of Concrete Research*, *58*(4), 201–208.

Hatt, W. K. (1907). Notes on the effect of time element in loading reinforced concrete beams. *Proceedings of ASTM*, *7*, 421–433.

Huang, S.-S., and Burgess, I. W. (2012). Effect of transient strain on strength of concrete and CFT columns in fire – Part 2: Simplified and numerical modelling. *Engineering Structures*, *44*, 389–399. https://doi.org/10.1016/j.engstruct.2012.05.052

Huismann, S., Weise, F., Meng, B., and Schneider, U. (2012). Transient strain of high strength concrete at elevated temperatures and the impact of polypropylene fibers. *Materials and Structures*, *45*(5), 793–801. https://doi.org/10.1617/s11527-011-9798-6

ISO 834. (1999). *Fire-resistance tests -- Elements of building construction -- Part 1: General requirements* (1)

JOHANSEN, R., and BEST, C. H. (1962). *Creep of concrete with and without ice in the system* (RILEM Bulletin No. 16) (pp. 47–57).

Kalifa, P., Menneteau, F.-D., and Quenard, D. (2000). Spalling and pore pressure in HPC at high temperatures. *Cement and Concrete Research*, *30*(12), 1915–1927. https://doi.org/10.1016/S0008-8846(00)00384-7

Khaliq, W, and Kodur, V. (2011). High Temperature Properties of Fiber Reinforced High Strength Concrete. *ACI Special Publication: Innovations in Fire Design of Concrete Structures*, (279), 3.1-3.42.

Khaliq, W., and Kodur, V. K. R. (2011). Effect of High Temperature on Tensile Strength of Different Types of High-Strength Concrete. *ACI Materials Journal*, *108*(4).

Khaliq, Wasim. (2012). *Performance characterization of high performance concretes under fire conditions* (Ph.D.). Michigan State University, East Lansing, Michigan, USA.

Khaliq, Wasim, and Kodur, V. (2011). Thermal and mechanical properties of fiber reinforced high performance self-consolidating concrete at elevated temperatures. *Cement and Concrete Research*, *41*(11), 1112–1122. https://doi.org/10.1016/j.cemconres.2011.06.012

Khaliq, Wasim, and Kodur, V. (2012). High Temperature Mechanical Properties of High-Strength Fly Ash Concrete with and without Fibers. *Materials Journal*, *109*(6), 665–674. https://doi.org/10.14359/51684164

Khoury, G. A., Dias, W. P., and Sullivan, P. J. E. (1986). Deformation of concrete and cement paste loaded at constant temperatures from 140 to 724 c. *Materials and Structures*, *19*(2), 97–104.

Khoury, Gabriel A., Grainger, B. N., and Sullivan, P. J. (1985a). Strain of concrete during first heating to 600 C under load. *Magazine of Concrete Research*, *37*(133), 195–215.

Khoury, Gabriel A., Grainger, B. N., and Sullivan, P. J. (1985b). Transient thermal strain of concrete: literature review, conditions within specimen and behaviour of individual constituents. *Magazine of Concrete Research*, *37*(132), 131–144.

Kim, G.-Y., Kim, Y.-S., and Lee, T.-G. (2009). Mechanical properties of high-strength concrete subjected to high temperature by stressed test. *Transactions of Nonferrous Metals Society of China*, *19*, s128–s133. https://doi.org/10.1016/S1003-6326(10)60260-9

Ko, J., Ryu, D., and Noguchi, T. (2011). The spalling mechanism of high-strength concrete under fire. *Magazine of Concrete Research*, *63*(5), 357–370. https://doi.org/10.1680/macr.10.00002

Kodur, V. K. R. (2014). Properties of concrete at elevated temperatures. *ISRN Civil Engineering*, *2014*, e468510. https://doi.org/10.1155/2014/468510

Kodur, V. K. R., and Aziz, E. M. (2015). Effect of temperature on creep in ASTM A572 high-strength low-alloy steels. *Materials and Structures*, *48*(6), 1669–1677. https://doi.org/10.1617/s11527-014-0262-2

Kodur, V. K. R., and Alogla, S. M. (2016). Effect of high-temperature transient creep on response of reinforced concrete columns in fire. *Materials and Structures*, *50*(1), 27. https://doi.org/10.1617/s11527-016-0903-8

Kodur, V. K. R., Cheng, F. P., Wang, T. C., Latour, J. C., and Leroux, P. (2001). Fire resistance of high-performance concrete columns. National Research Council of Canada (NRCC.

Kodur, V. K. R., Cheng, F.-P., Wang, T.-C., and Sultan, M. A. (2003). Effect of strength and fiber reinforcement on fire resistance of high-strength concrete columns. *Journal of Structural Engineering*, *129*(2), 253–259.

Kodur, V. K. R., Dwaikat, M., and Fike, R. (2010). High-Temperature Properties of Steel for Fire Resistance Modeling of Structures. *Journal of Materials in Civil Engineering*, *22*(5), 423–434. https://doi.org/10.1061/(ASCE)MT.1943-5533.0000041

Kodur, V. K. R., and Dwaikat, M. M. S. (2010). Effect of high temperature creep on the fire response of restrained steel beams. *Materials and Structures*, *43*(10), 1327–1341. https://doi.org/10.1617/s11527-010-9583-y

Kodur, V. K. R., Dwaikat, M. M. S., and Dwaikat, M. B. (2008). High-temperature properties of concrete for fire resistance modeling of structures. *ACI Materials Journal*, *105*(5), 517–527.

Kodur, V. K. R., and Harmathy, T. Z. (2002). *Properties of Building Materials* (3rd Edition). P.J. DiNenno, National Fire Protection Agency, Quincy, MA.

Kodur, V. K. R., and Sultan, M. A. (2003). Effect of temperature on thermal properties of high-strength concrete. *Journal of Materials in Civil Engineering*, *15*(2), 101–107. https://doi.org/10.1061/(ASCE)0899-1561(2003)15:2(101)

Kodur, V. K. R., and Mcgrath, R. (2003). Fire Endurance of High Strength Concrete Columns. *Fire Technology*, *39*(1), 73–87. https://doi.org/10.1023/A:1021731327822

Kodur V., and Khaliq W. (2011). Effect of Temperature on Thermal Properties of Different Types of High-Strength Concrete. *Journal of Materials in Civil Engineering*, *23*(6), 793–801. https://doi.org/10.1061/(ASCE)MT.1943-5533.0000225

Li, L., and Purkiss, J. (2005). Stress–strain constitutive equations of concrete material at elevated temperatures. *Fire Safety Journal*, *40*(7), 669–686.

Li, M., Qian, C., and Sun, W. (2004). Mechanical properties of high-strength concrete after fire. *Cement and Concrete Research*, *34*(6), 1001–1005. https://doi.org/10.1016/j.cemconres.2003.11.007

Lie, T. T. (1993). Method to calculate the fire resistance of reinforced concrete columns with rectangular cross section. *ACI Structural Journal*, *90*(1), 52–60. https://doi.org/10.14359/4210

Lie, T. T., and Celikkol, B. (1991). Method to Calculate the Fire Resistance of Circular Reinforced Concrete Columns. *Materials Journal*, *88*(1), 84–91.

Lie, T. T., and Kodur, V. K. R. (1996). Thermal and mechanical properties of steel-fibre-reinforced concrete at elevated temperatures. *Canadian Journal of Civil Engineering*, *23*(2), 511–517. https://doi.org/10.1139/l96-055

Lie, T. T., Lin, T. D., Allen, D. E., and Abrams M.S. (1984). *Fire resistance of reinforced concrete columns* (NRCC 23065 No. 1167). Ottawa: National Research Council Canada.

Lie, T. T., and Woolertoon, J. L. (1988). *Fire Resistance of RC Columns* (Test Results). National Research Council Canada.

Lin, W.-M., Lin, T. D., and Powers-Couche, L. J. (1996). Microstructures of fire-damaged concrete. *ACI Materials Journal*, *93*(3).

Malhotra, H. (1982). *Design of fire-resisting structures*. London: Surrey University Press.

Mehta, P. K., and Monteiro, P. J. (2006). *Concrete: microstructure, properties, and materials* (Vol. 3). McGraw-Hill New York.

Morovat, M., Lee, J., Engelhardt, M., Taleff, E. M., Helwig, T., and Segrest, V. (2012). Creep properties of ASTM A992 steel at elevated temperatures. *Advanced Materials Research*, *446*, 786–792. https://doi.org/10.4028/www.scientific.net/AMR.446-449.786

Nasser, K. W., and Lohtia, R. P. (1971). Mass concrete properties at high temperatures. In *ACI Journal Proceedings* (Vol. 68). ACI.

Nasser, Karim W., and Neville, A. M. (1965). Creep of concrete at elevated temperatures. In *ACI Journal Proceedings* (Vol. 62). ACI.

Nielsen, C. V., Pearce, C. J., and Bićanić, N. (2002). Theoretical model of high temperature effects on uniaxial concrete member under elastic restraint. *Magazine of Concrete Research*, *54*(4), 239–249. https://doi.org/10.1680/macr.2002.54.4.239

Noumowe, A. (2005). Mechanical properties and microstructure of high strength concrete containing polypropylene fibres exposed to temperatures up to 200 °C. *Cement and Concrete Research*, *35*(11), 2192–2198. https://doi.org/10.1016/j.cemconres.2005.03.007

Raut, N., and Kodur, V. (2011). Response of High-Strength Concrete Columns under Design Fire Exposure. *Journal of Structural Engineering*, *137*(1), 69–79. https://doi.org/10.1061/(ASCE)ST.1943-541X.0000265

Raut, N., and Kodur, V. (2011). Response of Reinforced Concrete Columns under Fire-Induced Biaxial Bending. *Structural Journal*, *108*(5), 610–619. https://doi.org/10.14359/51683218

RILEM. (1998, June). RILEM TC 129-MHT: Test methods for mechancial properties of concrete at high temperatures. Recommendations: Part 7: Transient Creep for service and accident conditions. *Materials and Structures, 31*, 290–295.

RILEM Technical Committee 200-HTC. (2007). Recommendation of RILEM TC 200-HTC: mechanical concrete properties at high temperatures—modelling and applications: Part 2: Stress–strain relation. *Materials and Structures*, *40*(9), 855–864. https://doi.org/10.1617/s11527-007-9286-1

Sadaoui, A., and Khennane, A. (2009). Effect of transient creep on the behaviour of reinforced concrete columns in fire. *Engineering Structures*, *31*(9), 2203–2208. https://doi.org/10.1016/j.engstruct.2009.04.005

Sadaoui, A., and Khennane, A. (2012). Effect of Transient Creep on Behavior of Reinforced Concrete Beams in a Fire. *Materials Journal*, *109*(6), 607–616.

Schaffer, E. L. (1992). *Structural Fire Protection*. American Society of Civil Engineers, ASCE.

Schneider, U. (1976). Behaviour of concrete under thermal steady state and non-steady state conditions. *Fire and Materials*, *1*(3), 103–115.

Schneider, U., Schneider, M., and Franssen, J.-M. (2008). Consideration of nonlinear creep strain of siliceous concrete on calculation of mechanical strain under transient temperatures as a function of load history. In *Proceedings of the Fifth International Conference Structures in Fire*. Retrieved from http://orbi.ulg.ac.be/handle/2268/15084

Schneider, Ulrich. (1986). Modelling of concrete behaviour at high temperatures. In *Design of Structures Against Fire* (pp. 53–69). Aston University, Birmingham, UK: Elsevier applied science publishers.

Schneider, Ulrich. (1988). Concrete at high temperatures—a general review. *Fire Safety Journal*, *13*(1), 55–68.

Shin, K.-Y., Kim, S.-B., Kim, J.-H., Chung, M., and Jung, P.-S. (2002). Thermo-physical properties and transient heat transfer of concrete at elevated temperatures. *Nuclear Engineering and Design*, *212*(1), 233–241. https://doi.org/10.1016/S0029-5493(01)00487-3

Sideris Kosmas K. (2007). Mechanical Characteristics of Self-Consolidating Concretes Exposed to Elevated Temperatures. *Journal of Materials in Civil Engineering*, *19*(8), 648–654. https://doi.org/10.1061/(ASCE)0899-1561(2007)19:8(648)

Tao, J., Liu, X., and Taerwe, L. (2013). Transient strain of self-compacting concrete loaded in compression heated to 700°C. *Materials and Structures*, *46*(1–2), 191–201. http://dx.doi.org/10.1617/s11527-012-9894-2

Terro, M. J. (1991). *Numerical modeling of thermal and structural responses of reinforced concrete structures in fire* (PhD dissertation). Department of Civil Engineering, Imperial College.

Terro, M. J. (1998). Numerical modeling of the behavior of concrete structures in fire. *ACI Structural Journal*, *95*(2), 183–193.

Thelandersson, S. (1974). Mechanical behaviour of concrete under torsional loading at transient, high-temperature conditions. *Bulletin of Division of Structural Mechanics and Concrete Construction, Bulletin 54*, *46*, 83.

Thienel, K.-C., and Rostasy, F. S. (1996). Transient creep of concrete under biaxial stress and high temperature. *Cement and Concrete Research*, *26*(9), 1409–1422.

Torelli, G., Mandal, P., Gillie, M., and Tran, V.-X. (2016). Concrete strains under transient thermal conditions: A state-of-the-art review. *Engineering Structures*, *Complete*(127), 172–188. https://doi.org/10.1016/j.engstruct.2016.08.021

Wei, Y., Au, F. T. K., Li, J., and Tsang, N. C. M. (2016). Effects of transient creep strain on post-tensioned concrete slabs in fire. *Magazine of Concrete Research*, 1–10. https://doi.org/10.1680/jmacr.15.00266

Williams-leir, G. (1983). Creep of structural steel in fire: Analytical expressions. *Fire and Materials*, *7*(2), 73–78. https://doi.org/10.1002/fam.810070205

Williamson, R. B. (1972). Solidification of Portland cement. *Progress in Materials Science*, *15*(3), 189–286. https://doi.org/10.1016/0079-6425(72)90001-1

Wu, B., Lam, E. S. S., Liu, Q., Chung, W. Y. M., and Ho, I. F. Y. (2010). Creep behavior of high-strength concrete with polypropylene fibers at elevated temperatures. https://doi.org/10.14359/51663581

Wu, Bo, Lam, E. S.-S., Liu, Q., Chung, W. Y., and Ho, I. F. (2010). Creep Behavior of High-Strength Concrete with Polypropylene Fibers at Elevated Temperatures. *Materials Journal*, *107*(2), 176–184. https://doi.org/10.14359/51663581

Yoon, M., Kim, G., Kim, Y., Lee, T., Choe, G., Hwang, E., and Nam, J. (2017). Creep behavior of high-strength concrete subjected to elevated temperatures. *Materials*, *10*(7). https://doi.org/10.3390/ma10070781

Youssef, M. A., and Moftah, M. (2007). General stress–strain relationship for concrete at elevated temperatures. *Engineering Structures*, *29*(10), 2618–2634.

Zeiml, M., Leithner, D., Lackner, R., and Mang, H. A. (2006). How do polypropylene fibers improve the spalling behavior of in-situ concrete? *Cement and Concrete Research*, *36*(5), 929–942. https://doi.org/10.1016/j.cemconres.2005.12.018